Stony Brook University

Morphometric Variation in the Appendicular Skeleton of Recent and Prehistoric Humans

A Dissertation Presented

by

Danielle Frances Royer

to

The Graduate School

in Partial Fulfillment of the

Requirements

for the Degree of

Doctor of Philosophy

in

Anthropology

(Physical Anthropology)

Stony Brook University

August 2009

Stony Brook University

The Graduate School

Danielle Frances Royer

We, the dissertation committee for the above candidate for the

Doctor of Philosophy degree, hereby recommend

acceptance of this dissertation.

Frederick E. Grine – Dissertation Advisor
Professor, Departments of Anatomical Sciences and Anthropology

John G. Fleagle – Chairperson of Defense
Professor, Department of Anatomical Sciences

William L. Jungers
Professor and Chair, Department of Anatomical Sciences

Osbjorn M. Pearson
Department of Anthropology, University of New Mexico

This dissertation is accepted by the Graduate School

Lawrence Martin
Dean of the Graduate School

Abstract of the Dissertation

Morphometric Variation in the Appendicular Skeleton

of Recent and Prehistoric Humans

by

Danielle Frances Royer

Doctor of Philosophy

In

Anthropology

(Physical Anthropology)

Stony Brook University

2009

The study of phenotypic variation can help elucidate the various influences that have shaped within-population morphometric diversity within *Homo sapiens*, and provides another line of evidence to complement molecular and craniometric research on human evolution. Moreover, because modern skeletal samples frequently provide a framework for interpreting diversity and taxonomic relationships in the fossil record, it is imperative to test assumptions concerning the magnitude and pattern of past and present-day skeletal variability, since inequalities may contribute to serious biases. The primary aim of this dissertation is to broaden our understanding of phenotypic diversity in the postcranial skeleton of select modern and prehistoric *H. sapiens* groups. This is accomplished through univariate comparisons of the magnitude of morphometric variability in the major long bones of the appendicular skeleton 1) between recent

African populations, 2) between recent African populations and prehistoric samples from the terminal Pleistocene and early Holocene, 3) between modern African populations and samples of early *H. sapiens* from the Middle Stone Age (MSA) and early Upper Paleolithic (EUP), and 4) between MSA and EUP fossil samples.

This dissertation demonstrates equal relative variation among recent African populations, although some sex-specific samples exhibit significant differences in the magnitude of appendicular variation. African populations from the terminal Pleistocene and early Holocene are characterized by an equal magnitude and pattern of appendicular variation relative to recent Africans. In contrast, both MSA and EUP fossil samples exhibit an elevated magnitude of variation throughout the appendicular skeleton compared to recent and prehistoric populations, demonstrating that modern diversity substantially underestimates the early diversity of our lineage. However, the MSA sample, which spans over 100,000 years, is not more variable than the EUP sample which spans less than 15,000 years. These results suggest that time averaging alone is insufficient to account for the increase of variation documented in the fossil samples. Furthermore, the reduction of diversity to present-day levels appears to be bracketed between the end of the early Upper Paleolithic and the terminal Pleistocene at approximately 14,000 years BP. This dissertation also tested the accuracy of metric and non-metric methods for classifying sex from fragmentary pelvis remains in modern Africans. The most reliable method, discriminant analysis, is used to diagnose the sex of prehistoric humans, including the first formal diagnosis for Omo I, the earliest *H. sapiens* fossil currently known. The unambiguous female diagnosis for Omo I suggests that at least some of the greater diversity documented in the past may reflect stronger sexual dimorphism.

Table of Contents

List of Figures……...ix
List of Tables……...xi
Acknowledgments…….....xiv
Chapter 1 – Introduction……1
Goals of the Dissertation……..6
Chapter 2 – Data Collection Methods and Skeletal Samples…….....9
Skeletal Measurements……....9
Measurement Error and Reliability…….....10
Data Transformation and Analysis: An Overview…….....14
Skeletal Samples……15
Reference Samples: Rationale for Choice……16
Recent Africans: Zulu……18
Recent Africans: Kikuyu……18
Recent Africans: Nilotic Ugandans…….....19
Archaeological Africans: Khoe-San……..20
Archaeological Africans: Sudanese……...22
Archaeological Africans: Taforalt……23
Early *Homo sapiens* Fossils……...24
Middle Stone Age Sample……26
Early Upper Paleolithic Sample……37
Figures……46
Tables……47
Chapter 3 – A Test of Methods for Determining Sex Using Fragmentary Os Coxae……...……61
Introduction……61
Goals……..61
Determining Sex from Skeletal Remains……...62
Skeletal Samples……....67
Method: Testing the Accuracy of the Visual Method……...68
Preauricular Surface Character……..69
Composite Arch Character……..…71
Greater Sciatic Notch Character……72
Sacroiliac Complex: Final Diagnosis…….……74
Results: Accuracy of the Visual Method……...74
Discussion: Utility of the Visual Method…….…….....75
Method: Testing the Accuracy of Discriminant Function Analysis…..…77
Assumptions…….…….....79
Os Coxae Variables: Form versus Shape……..…….....80

Stepwise Procedure…….....81
Determining Accuracy……...82
Results: Accuracy of Discriminant Function Analysis……..83
Accuracy of Form DFA…….……....83
Accuracy of Shape DFA……86
Discussion: Utility of Discriminant Function Analysis ….....91
Conclusions: Comparison of the Methods……94
Figures……96
Tables……...106
Chapter 4 – Classifying Sex in Prehistoric Humans Using Fragmentary Os Coxae……..117
Introduction……..117
Skeletal Samples……..117
Methods……....118
Results…….……122
Classification of Sex: Archaeological Samples……...122
Classification of Sex: Early *H. sapiens* Fossils……...123
Discussion: Utility of the Methods……..125
Archaeological Samples……...125
Early *H. sapiens* Fossils……...129
Omo I……...131
Qafzeh 9……...132
Skhūl 4…….133
Grotte des Enfants 4…….133
Grotte des Enfants 5…….134
Nazlet Khater 2……135
Paviland 1…….135
Skhūl 5…….136
Barma Grande 2……...137
Cro-Magnon 1……..138
Cro-Magnon 4315……139
Grotte du Cavillon 1…….139
Mladeč 21…….140
Conclusions……..141
Figures……...143
Tables……...158
Chapter 5 – Morphometric Variation in the Appendicular Skeleton: Testing the Assumption of Equality Among Recent Sub-Saharan Africans……..173
Introduction……..173
Goals……173
Assumption of Equality of Variation in Modern Humans……...174

Sources of Variation in Modern Humans……176
Skeletal Samples……..179
Methods: Equality of Relative Variation…….180
Hypotheses……...186
Results……...190
Equality of Variation Between Females……..190
Equality of Variation Between Males……..193
Equality of Variation Between the Sexes……194
Equality of Variation Between Populations…….197
Discussion: The Assumption of Equality……199
Conclusions……..207
Figures……..210
Tables……...239
Chapter 6 – Morphometric Variation in the Appendicular Skeleton of Prehistoric Humans……..270
Introduction……..270
Goals……270
Variation in Early *H. sapiens*……...271
Measurements……..278
Skeletal Samples……..278
Methods: Testing for Differences in Relative Variation……..280
Hypotheses……...280
Results……..284
Equality of Variation Between the Zulu and Archaeological Samples……285
Excess Variation in MSA and EUP Fossils Compared to Modern Humans……...287
Excess Variation in MSA Compared to EUP *H. sapiens*……293
Discussion……293
Variability in the Terminal Pleistocene and Holocene ……...293
Variability in Early *H. sapiens* versus Modern Humans…….294
Interpreting the Elevated Variation in the Past……...…….298
Implications for Paleontological Studies…….305
Conclusions……..306
Figures……..308
Tables……...323
Chapter 7 – Summary and Conclusions…….....354
Classification of Sex Using Fragmentary Os Coxae……354
Appendicular Variation in Recent Sub-Saharan Africans……...358
Appendicular Variation in Prehistoric Humans...……360
Conclusions……..364

References Cited……..……..365
Appendix 1 – Measurement List and Data Collection Protocols……....392
Photographic Protocol for the Os Coxae…….401
Appendix 2 – Summary Statistics for the Skeletal Samples……..……403
Humerus……...404
Ulna……..411
Radius……..418
Os Coxae..……423
Femur……...427
Tibia…….433

List of Figures

Figure 2.1 – Size, shape and form changes……46
Figure 2.2 – Omo I postcranial skeleton……46
Figure 3.1 – Preauricular surface of the os coxae……..96
Figure 3.2 – Scoring the PS1 sub-character……...96
Figure 3.3 – Scoring the PS2 sub-character……...97
Figure 3.4 – Scoring the PS3 sub-character……...97
Figure 3.5 – Majority score of the PS character……98
Figure 3.6 – Scoring the composite arch character……98
Figure 3.7 – Scoring the SN1 and SN2 sub-characters……..99
Figure 3.8 – Scoring the SN3 sub-character and SN majority score……...100
Figure 3.9 – Final sex diagnosis of the sacroiliac complex……100
Figure 3.10 – Form: Discriminant scores of the Zulu…….……101
Figure 3.11 – Form: Discriminant scores of the Kikuyu……..……...101
Figure 3.12 – Form: Discriminant scores of the pooled Africans……102
Figure 3.13 – Shape: Discriminant scores of the Zulu……102
Figure 3.14 – Shape: Discriminant scores of the Kikuyu……103
Figure 3.15 – Shape: Discriminant scores of the pooled Africans……..103
Figure 3.16 – Modified Shape: Discriminant scores of the Zulu……104
Figure 3.17 – Modified Shape: Discriminant scores of the Kikuyu……104
Figure 3.18 – Modified Shape: Discriminant scores of the pooled Africans…...105
Figure 4.1 – MSA early *H. sapiens* os coxae……...…143
Figure 4.2 – EUP early *H. sapiens* os coxae……144
Figure 4.3 – Omo I os coxae……145
Figure 4.4 – Qafzeh 9 os coxae……....146
Figure 4.5 – Skhūl 4 os coxae……..147
Figure 4.6 – Grotte des Enfants 4 os coxae……148
Figure 4.7 – Grotte des Enfants 5 os coxae……149
Figure 4.8 – Nazlet Khater 2 os coxae……150
Figure 4.9 – Paviland 1 os coxae……151
Figure 4.10 – Skhūl 5 os coxae……152
Figure 4.11 – Barma Grande 2 os coxae……..153
Figure 4.12 – Cro-Magnon 1 os coxae……154
Figure 4.13 – Cro-Magnon 4315 os coxae……...…155
Figure 4.14 – Grotte du Cavillon 1 os coxae……...156
Figure 4.15 – Mladeč 21 and 22 os coxae……...157
Figure 5.1 – Humerus variability in females……...210
Figure 5.2 – Ulna variability in females……..211
Figure 5.3 – Radius variability in females……...212

Figure 5.4 – Femur variability in females……213
Figure 5.5 – Tibia variability in females……..214
Figure 5.6 – Humerus variability in males……...215
Figure 5.7 – Ulna variability in males..……...216
Figure 5.8 – Radius variability in males..……217
Figure 5.9 – Femur variability in males..…….218
Figure 5.10 – Tibia variability in males….……..219
Figure 5.11 – Humerus variability between the sexes…….220
Figure 5.12 – Ulna variability between the sexes..…….221
Figure 5.13 – Radius variability between the sexes..……...…222
Figure 5.14 – Femur variability between the sexes..……...223
Figure 5.15 – Tibia variability between the sexes….……..224
Figure 5.16 – Plots of PC1 versus PC2 for the humerus…….225
Figure 5.17 – Plots of PC1 versus PC2 for the ulna……226
Figure 5.18 – Plots of PC1 versus PC2 for the radius…….227
Figure 5.19 – Plots of PC1 versus PC2 for the femur……..228
Figure 5.20 – Plots of PC1 versus PC2 for the tibia…….……...229
Figure 5.21 – Comparison of humerus ISD and CV……230
Figure 5.22 – Comparison of ulna ISD and CV……...231
Figure 5.23 – Comparison of radius ISD and CV……232
Figure 5.24 – Comparison of femur ISD and CV……233
Figure 5.25 – Comparison of tibia ISD and CV……..234
Figure 5.26 – Global comparison of appendicular CV among females……...235
Figure 5.27 – Global comparison of appendicular CV among males……..237
Figure 6.1 – Humerus variability in recent and archaeological Africans…….....308
Figure 6.2 – Ulna variability in recent and archaeological Africans…….....309
Figure 6.3 – Radius variability in recent and archaeological Africans…….....310
Figure 6.4 – Femur variability in recent and archaeological Africans…….....311
Figure 6.5 – Tibia variability in recent and archaeological Africans…….....312
Figure 6.6 – Humerus variability in fossil and modern humans…….....313
Figure 6.7 – Humerus variability in fossil and pan-African humans……...314
Figure 6.8 – Ulna variability in fossil and modern humans…….....315
Figure 6.9 – Ulna variability in fossil and pan-African humans…….....316
Figure 6.10 – Radius variability in fossil and modern humans…….....317
Figure 6.11 – Radius variability in fossil and pan-African humans……318
Figure 6.12 – Femur variability in fossil and modern humans…….....319
Figure 6.13 – Femur variability in fossil and pan-African humans…….320
Figure 6.14 – Tibia variability in fossil and modern humans…….....321
Figure 6.15 – Tibia variability in fossil and pan-African humans……...322

List of Tables

Table 2.1 – Number of morphometric variables per element……47
Table 2.2 – Measurement error paired *t*-test results……..48
Table 2.3 – Average percent error for each variable…….50
Table 2.4 – Intra-observer technical error of measurement……...52
Table 2.5 – Coefficient of reliability…….…….54
Table 2.6 – Composition of reference samples……..56
Table 2.7 – Early *H. sapiens* fossil samples……..57
Table 2.8 – Inventory of Omo I elements……..58
Table 2.9 – Inventory of Levantine early *H. sapiens*…….58
Table 2.10 – Inventory of early Upper Paleolithic *H. sapiens*……...…59
Table 3.1 – Accuracy of the visual method…….106
Table 3.2 – Accuracy of the PS character……106
Table 3.3 – Accuracy of the CA character……...107
Table 3.4 – Accuracy of the SN character……...107
Table 3.5 – Pelvis variables used in the discriminant function analysis……..108
Table 3.6 – *T*-test results: sex differences in pelvis form……108
Table 3.7 – Form: cross-validated classification results……..109
Table 3.8 – Form: functions applied to other samples…….110
Table 3.9 – *T*-test results: sex differences in pelvis shape……...111
Table 3.10 – Shape: cross-validated classification results……...112
Table 3.11 – Shape: functions applied to other samples……..113
Table 3.12 – *T*-test results: sex differences in pelvis modified shape…….114
Table 3.13 – Modified shape: cross-validated classification results……115
Table 3.14 – Modified shape: functions applied to other samples……..116
Table 4.1 – Measurements for fossil os coxae sexed using DFA.....158
Table 4.2 – Measurements for fossils with insufficient data for DFA…….159
Table 4.3 – Chi-square results: archaeological samples……..160
Table 4.4 – *T*-test results: Khoe-San sex and time samples…….160
Table 4.5 – *T*-test results: Sudanese sex and random samples……161
Table 4.6 – *T*-test results: Taforalt sex and random samples……...162
Table 4.7 – Fossil classification results using shape variables and the pooled African sample…….163
Table 4.8 – Fossil classification results using shape variables and the Kikuyu sample…….164
Table 4.9 – Fossil classification results using shape variables and the pooled African sample…….165
Table 4.10 – Fossil classification results using form variables and the pooled African sample…….166

Table 4.11 – Fossil classification results using form variables and the Zulu sample……..167
Table 4.12 – Fossil classification results using form variables and the Kikuyu sample…….168
Table 4.13 – Fossil classification results using the visual method……..169
Table 4.14 – Comparison of fossil sex assignments……170
Table 4.15 – Summary of early *H. sapiens* sex classification…….171
Table 5.1 – Composition of the recent human skeletal samples……..…239
Table 5.2 – FK results for the humerus: equality between females…….239
Table 5.3 – FK results for the ulna: equality between females…….....240
Table 5.4 – FK results for the radius: equality between females…….....241
Table 5.5 – FK results for the femur: equality between females…….....242
Table 5.6 – FK results for the tibia: equality between females…….....243
Table 5.7 – Levene's test results: equality between females……...244
Table 5.8 – FK results for the humerus: equality between males..……..245
Table 5.9 – FK results for the ulna: equality between males..…….....246
Table 5.10 – FK results for the radius: equality between males..…….....247
Table 5.11 – FK results for the femur: equality between males..…….....248
Table 5.12 – FK results for the tibia: equality between males..…….....249
Table 5.13 – Levene's test results: equality between males..……..250
Table 5.14 – *T*-test and FK results for the humerus: equality between sexes…..251
Table 5.15 – *T*-test and FK results for the ulna: equality between sexes…….253
Table 5.16 – *T*-test and FK results for the radius: equality between sexes……..255
Table 5.17 – *T*-test and FK results for the femur: equality between sexes.....257
Table 5.18 – *T*-test and FK results for the tibia: equality between sexes.....259
Table 5.19 – *T*-test and Levene's test for PC1 scores between the sexes……261
Table 5.20 – Correlation between size and PC scores among the Zulu……...262
Table 5.21 – Correlation between size and PC scores among the Kikuyu……..263
Table 5.22 – FK results for the humerus: equality between populations..……...264
Table 5.23 – FK results for the ulna: equality between populations..…….265
Table 5.24 – FK results for the radius: equality between populations..……...266
Table 5.25 – FK results for the femur: equality between populations..……...267
Table 5.26 – FK results for the tibia: equality between populations..…….268
Table 5.27 – Levene's test results: equality between populations..…….269
Table 6.1 – Composition of skeletal samples……..323
Table 6.2 – Humerus FK results: archaeological samples versus Zulu……...324
Table 6.3 – Ulna FK results: archaeological samples versus Zulu……...…...326
Table 6.4 – Radius FK results: archaeological samples versus Zulu……...328
Table 6.5 – Femur FK results: archaeological samples versus Zulu……...330
Table 6.6 – Tibia FK results: archaeological samples versus Zulu…….332
Table 6.7 – Humerus FK results: fossil samples versus Zulu……..334

Table 6.8 – Humerus FK results: fossil samples versus Khoe-San…….335
Table 6.9 – Humerus FK results: fossil samples versus pan-African……..336
Table 6.10 – Ulna FK results: fossil samples versus Zulu……...337
Table 6.11 – Ulna FK results: fossil samples versus Khoe-San……..338
Table 6.12 – Ulna FK results: fossil samples versus pan-African……...339
Table 6.13 – Radius FK results: fossil samples versus Zulu……...340
Table 6.14 – Radius FK results: fossil samples versus Khoe-San……...341
Table 6.15 – Radius FK results: fossil samples versus pan-African……342
Table 6.16 – Femur FK results: fossil samples versus Zulu……343
Table 6.17 – Femur FK results: fossil samples versus Khoe-San……344
Table 6.18 – Femur FK results: fossil samples versus pan-African……345
Table 6.19 – Tibia FK results: fossil samples versus Zulu……..……346
Table 6.20 – Tibia FK results: fossil samples versus Khoe-San……..……347
Table 6.21 – Tibia FK results: fossil samples versus pan-African……..348
Table 6.22 – Humerus FK results: MSA versus EUP……...349
Table 6.23 – Ulna FK results: MSA versus EUP…….350
Table 6.24 – Radius FK results: MSA versus EUP…….351
Table 6.25 – Femur FK results: MSA versus EUP……..352
Table 6.26 – Tibia FK results: MSA versus EUP……....353
Table A2-1 – Humerus summary statistics……..404
Table A2-2 – Ulna summary statistics…….411
Table A2-3 – Radius summary statistics…….418
Table A2-4 – Os coxae summary statistics……..423
Table A2-5 – Femur summary statistics……..427
Table A2-6 – Tibia summary statistics……433

Acknowledgments

Working on a doctorate often seems like a very lonely endeavor. Yet looking back over the six years of my graduate career, it is clear to me that I was never alone. Along the way, many people and organizations provided much motivation, encouragement and support – whether academic, emotional, or financial – thereby contributing in one way or another to the completion of this dissertation. In case I didn't say it before: Thank You!

During the proposal and grant-writing stages of my doctoral research, I benefited tremendously from a Doctoral Fellowship from the Social Sciences and Humanities Research Council of Canada. The dissertation itself involved nearly eight months of data collection at 22 institutions (and one person's home) in eleven different countries, a feat which would have been impossible without the generous financial support of several funding agencies. A National Science Foundation Dissertation Improvement Grant (NSF BCS 0726115), a Wenner-Gren Dissertation Fieldwork Grant and a Leakey Foundation General Research Grant all contributed the funds that turned my dissertation proposal into reality. As a Canadian studying in the United States, I consider myself extremely fortunate to have received support from the country of my birth as well as the country in which I chose to complete my graduate work. I hope that such opportunities continue to be available for students in all fields regardless of nationality.

During an eight month-long data collection trip, I had the pleasure of studying original fossil remains and human skeletons in many institutions. Fossils are rare, irreplaceable and often fragile links to the past. While it may be tempting to keep them under lock and key, such protectionism can hamper scientific investigations. I extend a heartfelt thank you to all the curators and staff who kindly allowed me to study the specimens entrusted into their care, and

provided facilities in which to work: Dr. Fawsi Ibrahim, Director of the Rockefeller Museum (Jerusalem, Israel), and Dr. Alegre Savariego, Curator of the Israeli Antiquities Authority, for allowing me to view the remarkably complete (but almost fully class-encased) Skhūl 4 fossil; Dr. Yoel Rak of Tel Aviv University for access to fossils from Qafzeh, as well as providing casts of Skhūl 4; Dr. Charles Ibingira (Makerere University School of Medicine, Kampala, Uganda) for use of the Galloway Osteological Collection, with special thanks to Duncan who brought the specimens to me each day and to Yakobo Nviiri, my unofficial assistant; Dr. I. Farah and the Ministry of Education, Science and Technology of Kenya for permission to study the paleontology and osteology collections at the National Museums of Kenya in Nairobi, and Dr. Ogeto Mwebi for facilitating access to the Kikuyu skeletons at NMK, with special thanks to David Chege for good conversations in the lab as well as organizing the specimen boxes (*after* I was gone, but it's a start); Dr. John Fleagle and Mamitu Yilma, Director of the National Museum of Ethiopia, for granting me permission to measure the Kibish postcranial material, with special thanks to Solomon Yirga and Dr. Shannon McPherron for helping me navigate NME and Addis; Ms. N. Pather and Ruth for their assistance with the Dart Collection, and Dr. Bernhard Zipfel for granting me access to the Tobias Fossil Collection at the University of the Witwatersrand; Dr. Sarah Wurz, Curator of Pre-Colonial Archaeology at the Iziko South African Museum in Cape Town, and Dr. Hilary Deacon for permission to study the Khoe-San skeletons and the Klasies River material; Dr. David Morris of the McGregor Museum (Kimberley, South Africa) for access to the Riet River Khoe-San skeletons and what remains of the Border Cave fossils; Dr. James Brink, Head of the Florisbad Quaternary Research Station (National Museum, Bloemfontein), for allowing me to study additional Khoe-San specimens and providing on-site housing; Rob Kruszynski for facilitating my visit to the Natural History Museum in London to study Skhūl 9 and Kabwe, and for

calming me down when my laptop inexplicably stopped working that morning; Dr. John Taylor and Dr. Rebecca Redfern for permission to measure the Jebel Sahaba specimens in the Wendorf Collection at the British Museum; Dr. Mercedes Okumura for granting me access (on two separate occasions) to the large collection of Kerma skeletons in the Duckworth Laboratory, University of Cambridge, with special thanks to Fred and Sandra for generously allowing me to stay with them during my first visit to Cambridge; Dr. Marina Sapelli Ragni, Superintendant for Archaeology in Liguria, and the staff of the Museo dei Balzi Rossi for facilitating my study of the Barma Grande triple burial, with special thanks to Roberta Salmi for kindly translating our correspondence (if only you had been with me in Ventimiglia!); Dr. Patrick Simon, Director of the Musée d'Anthropologie préhistorique (Monaco) for permission to study the Grotte des Enfants fossils; Dr. Derek Siveter and Eliza, Oxford University Museum of Natural History, for access to the Paviland 1 casts and closing down part of the exhibition hall so that I could take the measurements; Dr. Philippe Mennecier, Curator of Anthropology at the Musée de l'Homme, for allowing me to study the original Cro-Magnon and Grotte de Cavillon fossils; Professor H. de Lumley and Amélie Vialet of L'Institut de paleontologie humaine for access to the Qafzeh fossils and Taforalt Collection, with special thanks to Stéphanie Renault and Louisa Aoudia for answering questions about the collection and letting me back inside IPH after lunch every day; Dr. Bruno Maureille and Dr. Isabelle Crevecoeur for facilitating my study of the Nazlet Khater specimen at the l'Université de Bordeaux 1; Dr. Maria Teschler-Nicola for access to the Mladeč fossils at the Natural History Museum in Vienna; Dr. David Hunt, National Museum of Natural History, for permission to use the Terry Collection; Olivia Herschensohn for facilitating my visit to the Peabody Museum of Archaeology and Ethnology at Harvard University to study the other Skhūl fossils as well as

the Egyptian skeletons used for my pilot study, and Dr. Jason Ur and Heather for letting me stay with them.

I consider myself extremely privileged to have worked under the supervision of Fred Grine. Fred taught me much about human evolution, helped me navigate through my first grant submission (and rejection), then through the messy bureaucracy of several successful grants as well the intricacies of my first publication, and tirelessly corrected my writing when it was clear that I had been thinking in French. But he also reminded me along the way that it was OK to have fun, taught me how to select the ideal strip of biltong and how to drive stick shift, took me on a lovely driving tour of the Cape, welcomed me into his home-away-from-home in Cambridge, and together we figured out how to play roulette – and win! I'll always cherish the memory of Fred walking me down the aisle during the reenactment of my wedding. Fred, you have been the best academic father a girl could have – thank you!

Many others at Stony Brook and beyond also contributed directly to this dissertation. My committee members, John, Bill and Ozzie, all gave generously of their time, providing many useful comments, suggestions, as well as motivation during all stages of the doctorate. In particular, I thank John Fleagle who first got me interested in early *H. sapiens* and allowed me to work on the Omo Kibish material. I firmly believe that I entered IDPAS in 2003 with the best possible cohort. I can't imagine making it through 1st year and beyond without them: Mat and Liz (oh how far we've come from that cramped 6th floor office and Chapin!), Andrea (our Gmail chats made data collection *so* much easier!), Wendy (who would have thought we'd both end up in NYC?!), Kerry (who would have thought we'd both end up married!), and Alice (come back safe – the tumbleweeds paper needs to be published!). Happy Hour in Anatomy, fondue parties and countless nights spent at the Corner with Aryeh, Andrea, Andy & Sarah, Anne, Biren, Chris, Clara, David, Doug, Liz, Mat, wine and a movie with my favourite

housemate Sarah, and long lunches/coffee breaks with Mat definitely made my stay on Long Island substantially more pleasant than it would otherwise have been.

I have often envied fellow students who come from academic families where everyone has an intimate understanding of academic life because I commonly felt as though I was speaking a different language when trying to discuss daily life with my family. Yet even though biological anthropology, fieldwork, research, and the ultimate goal of being a professor were entirely foreign to them, my family has always been supportive of my dreams and aspirations. In particular, my mother Suzanne and sister Liane provided unconditional support during my time in graduate school, readily sharing my joy and listening to my concerns throughout the ups and downs of this journey. It was an honor to have them in the audience during my defense. And it makes me smile to think that my mother is finally able to say that her daughter is a professor, and not just a 29 year old student!

There is no doubt in my mind that this dissertation would not have been completed at this time were it not for the motivation, encouragement, support and love provided so freely by my husband. David allowed me the luxury of not working during the last spring and summer semesters, which certainly facilitated the period of intense analysis and writing that has defined my life over the last few months. But it is his unshakable belief in me and my abilities that actually propelled me forward day-to-day, and allowed me to dare to look beyond graduate school. I am so fortunate to have found a loving partner with an independent and inquisitive yet silly mind, combined with enough of a sense of adventure to join me in the next stage of life.

Chapter 1

Introduction

Recent years have seen major improvements in the cost and efficacy of collecting, sequencing and analyzing of vast amounts of genetic data from humans around the globe (Mielke et al., 2006). A common goal of many molecular studies is to assess levels and patterns of diversity within populations (e.g., Schmitt, 1995; Castri et al., 2009; Coia et al., 2009). On the other hand, metric and non-metric morphological data are rarely considered in terms of intra-population variability. The primary utility of skeletal data tends to be in defining differences between populations, rather than offering insights onto the population itself. This focus on differences between populations is clearly necessary for forensic applications (e.g., Howells, 1995; Scheuer, 2002), permits an understanding of the influence exerted on the skeleton by a range of environmental, climatic, or behavioral factors (e.g., Ruff, 1994; Pearson, 2000a; Ruff et al., 2006), and is critical in delimiting the boundaries of our species (e.g., Day and Stringer, 1982; Kidder et al., 1992; Pearson, 1997), an important step for reconstructing fossil relationships and *H. sapiens* evolution (e.g., Trinkaus et al., 2003; White et al., 2003; Grine et al., 2007). However, the focus on between-population differences at the expense of within-population differences, despite long-standing evidence demonstrating that most of human genetic diversity is contained within populations than between them (Lewontin, 1972), may in part reflect a legacy of racial and typological thinking across the discipline (Edgar and Hunley, 2009; Relethford, 2009).

One application of morphology to reflect intra-population variability stems from efforts to find morphological support for the genetic claim that populations from sub-Saharan Africa are more diverse than non-Africans. This patterning in modern human diversity, initially suggested from studies of mtDNA (Cann et al., 1987), has now been confirmed across numerous aspects of the genome (as reviewed by Pearson, 2004; Weaver and Roseman, 2008), in addition to receiving support from studies of craniometric diversity (Relethford, 1994; Relethford and Harpending, 1994; Lahr, 1996; von Cramon-Taubadel and Lycette, 2008; Betti et al., 2009; Gunz et al., 2009; Relethford, 2009). These studies propose that the greater diversity of within African populations likely reflects the longer history of *H. sapiens* on this continent compared to other parts of the globe, and is not simply caused by larger effective population size in Africa compared to elsewhere for much of human history (Templeton, 1993; Harpending, 1996; Relethford, 1999; Relethford and Jorde, 1999). The sequential decrease in within-population diversity as distance from Africa increases (Harpending and Rogers, 2000; Betti et al., 2009) is consistent with an African origin for our species, and fits the pattern of variation predicted by the Recent Out of Africa (ROA) model for human origin (Stringer and Andrews, 1988). Furthermore, recent fossil discoveries such as the ca. 156 ka BP cranial fossils from Herto, Ethiopia (White et al., 2003), and the application of new radiometric dating techniques in the Kibish Formation of Ethiopia (McDougall et al., 2005), providing a secure age of ca. 195 ka BP for the Omo Kibish fossils (Leakey, 1969; Pearson et al., 2008b), confirm that the earliest record of *H. sapiens* is found in Africa.

At the other end of the spectrum, the Multiregional (MR) model provides an alternative but equally extreme view on human origins. MR predicts the lack of a consistent temporal pattern for the appearance of modern humans across the globe, a widespread distribution of transitional fossils contributing to a global pattern of regional continuity, leading to a pattern of marked differences between

populations in peripheral regions of the *H. sapiens* range, while elevated variation is expected in the center of the range (Wolpoff et al., 1994; Wolpoff et al., 2000; Thorne and Wolpoff, 2003). The clear signal of temporal primacy for *H. sapiens* in Africa noted above, and the absence of evidence for regional continuity in Eurasia (Lahr, 1994; Lahr and Foley, 1998; Pearson, 2000b; Trinkaus, 2007), where humans from different areas are morphologically much more similar to one another than with their respective antecedents (except perhaps Australasia - see Lahr, 1996), provides little support for the MR model. If Africa is indeed the center of the range, then the pattern of higher genetic and craniometric diversity among Africans described above can also fit the MR model.

As observed by Trinkaus (2005), the strict ROA and MR models are both contradicted by the available genetic and paleontological data, and the debate framed only by these two polarized views should be considered intellectually dead. Molecular and skeletal data support the origin of *H. sapiens* in Africa sometime prior to 100,000 years ago (Cann et al., 1987; Disotell, 1999a; Pearson, 2004; Weaver and Roseman, 2008), but the contribution of local populations to modern diversity cannot be ignored. As suggested by the Assimilation model, humans may have variably absorbed local populations while dispersing out of Africa (Smith et al., 2005; Smith, 2006), although the exact degree of admixture is debated and may be beyond the resolution afforded by both morphological and molecular data (Stringer, 1994; Duarte et al., 1999; Relethford, 2001; Satta and Takahata, 2002; Pearson, 2004; Serre et al., 2004; Trinkaus, 2007).

In addition to potential contributions from local antecedent populations, the modern human gene pool has also been shaped by a complex history of migrations from Africa, and reflects the influence of population contractions and expansions both within and outside of Africa. Based on fossil, archaeological and climatic evidence from Africa, Lahr and Foley (1998) suggested that human populations may have differentiated within Africa, such that multiple dispersals

from already differentiated populations, possibly using different routes (Mellars, 1996; Stringer, 2000; Walter et al., 2000), could account for the patterning of modern diversity. A scenario of multiple dispersals, including the possibility of back migrations to Africa, is also supported by genetic evidence (Templeton, 2002; von Cramon-Taubadel and Lycette, 2008). Iterative dispersals from Africa by *H. sapiens* could have been triggered by periods of rapid global climate change during the Late Pleistocene (Ambrose, 1998; Lahr and Foley, 1998; Gamble et al., 2004; Carto et al., 2009).

For example, the temporary collapse of thermohaline circulation in the Atlantic Ocean, caused by the cooling and desalinization of the North Atlantic due to the sudden addition of meltwater from surges of icebergs and ice sheets instability, can lead to rapid cooling in northern regions and increasing aridity in Africa (Heinrich, 1988). This episodic process, known as a Heinrich Event, causes dramatic shifts in the global climate on a very rapid timescale (100 – 500 years, followed by rapid warming), and when these events are superimposed on the general pattern of increasing aridity associated with global cooling in much of the Late Pleistocene, they could have caused substantial parts of North, West and East Africa unsuitable for human habitation (Carto et al., 2009). Heinrich Events have been documented at least eight times during the Late Pleistocene (at ca. 105 ka, 85 ka, 65 ka, 45 ka, 38 ka, 30 ka, 22 ka, and 16 ka BP), and could have caused major population bottlenecks, the temporary isolation of the remaining populations in refugia (both within Africa, and later, outside of Africa), and the rapid climatic release and warming following this or other similar events may have provided a stimulus for repeated human dispersals (Lahr and Foley, 1998; Forster, 2004; Gamble et al., 2004; von Cramon-Taubadel and Lycette, 2008; Carto et al., 2009). Other more unique events such as the roughly 70 ka BP super-eruption of Mount Toba in Sumatra and the ensuing volcanic winter may have also contributed to global climate change on a rapid scale, and caused

genetic bottlenecks that contributed to the pattern of diversity observable today (Ambrose, 1998).

Presently, the available craniometric and molecular evidence provides support for a more complex view of human evolution, in which the ancestral human population in Africa was subjected to episodic fluctuations in local effective population size and temporary isolation, leading to some differentiation between African populations mitigated by patterns of gene flow during periods of climatic release and population expansions (Excoffier, 2002; Marth et al., 2003; Harding and McVean, 2004; Wakeley, 2004; Manica et al., 2007; Gunz et al., 2009). In addition, multiple dispersals out of Africa (and possible back into Africa) from this structured metapopulation (Templeton, 2002; von Cramon-Taubadel and Lycette, 2008; Gunz et al., 2009), variable rates of admixture with local populations (Trinkaus, 2007), the influence of additional demographic factors such as bottlenecks and expansions (Harpending and Rogers, 2000; Marth et al., 2003; Watkins, 2003), and potential sociocultural factors leading to a sex-biased contribution to gene flow (Disotell, 1999b; Destro-Bisol et al., 2004; Wood et al., 2005; Coia et al., 2009) across the burgeoning worldwide human population, must all be considered to account for the pattern of diversity in *H. sapiens* today.

The complex model for modern human evolution described above has clearly benefited from a consideration of both molecular and morphological data. Reassuringly, the bones and genes are generally in agreement. The genetic underpinning for this complex metapopulational scenario has been compiled from multiple aspects of the genome, including various aspects of nuclear DNA, mtDNA and the Y-chromosome (see review in Weaver and Roseman, 2008). In contrast, most of the morphological data brought to bear on issues of *H. sapiens* evolution and patterns of modern diversity are more limited in scope, reflecting solely the size and shape of the skull (Relethford, 1994; Relethford and

Harpending, 1994; Manica et al., 2007; Betti et al., 2009; Gunz et al., 2009), but see Pearson (2000b) for an exception. The postcranial skeleton has not been completely ignored in later hominin research. However, studies of Late Pleistocene postcranial morphology have been primarily concerned with identifying skeletal differences between modern humans and Neandertals or other archaic hominins, differences believed to reflect speciation, local adaptations following ecogeographic patterning, or behavioral contrasts between taxa (e.g., Trinkaus, 1983, 1992; Churchill et al., 1996; Holliday, 1997; Yokley and Churchill, 2006). Yet the magnitude and pattern of intra-population postcranial variability among past and present humans remain poorly understood.

Goals of the Dissertation

The main goal of this dissertation is to contribute to a better understanding of intra-population postcranial diversity within the human lineage. Modern humans are frequently used as reference samples to help reconstruct taxonomic and/or phenetic relationships between hominin fossils, and to investigate diversity in the fossil record. Given the complexity of factors known to have shaped modern diversity, our assumptions regarding modern and past skeletal variation, whether implicit or not, would benefit from explicit testing. Specifically, this dissertation compares the magnitude and pattern of appendicular morphometric variation between modern and prehistoric populations from Africa, and between modern and early *H. sapiens*.

Chapter 2 outlines the appendicular measurements recorded on the modern, prehistoric and fossil skeletal samples that form the basis of this study, and also provides a reliability study to assess the contribution of measurement error to sample variation. Reliable methods to diagnose sex from skeletal remains are necessary in order to understand the role of sexual dimorphism on levels of

variability within any population. Chapter 3 therefore provides a test of one non-metric and one metric method for the diagnosis of sex using fragmentary os coxae in two modern human populations from sub-Saharan Africa. The methods developed in this chapter are then employed in Chapter 4 to refine the diagnosis of sex in samples of early *H. sapiens*, as well as other prehistoric humans from the terminal Pleistocene and Holocene.

As noted above, modern African populations exhibit greater diversity than non-Africans. However, the equality of variation in the appendicular skeleton between African populations has yet to be tested. In Chapter 5, this assumption is directly tested using univariate and multivariate comparisons of variability in the major long bones between a selection of modern African populations. In light sex-specific contributions to human diversity at the genomic level, Chapter 5 also tests for the equality of morphometric variation in the appendicular skeleton among the sexes between populations; that is, females *versus* females, and males *versus* males from different African populations. Finally, the relationship between sexual dimorphism and level of morphometric variability is explored through comparisons of variability between the sexes among populations.

As noted above, the study of skeletal variability can provide insights into past genetic diversity and the evolutionary forces and demographic processes that have shaped the evolution of our species. Chapter 6 evaluates the morphometric variability in the appendicular skeleton of prehistoric human populations, including early *H. sapiens*, to help elucidate the nature of the biological transition to modernity. First, Chapter 6 tests whether prehistoric humans from the terminal Pleistocene to Holocene of Africa exhibit an equal magnitude of variation relative to modern Africans, as expected based on the results of genetic and craniometric studies of modern diversity. The results of these analyses will help to determine whether modern African levels of variation extended into the terminal Pleistocene and early Holocene. Furthermore, these comparisons provide a context in which

to evaluate the influence of time averaging on variability within a sample. That is, do samples of archaeological origin spanning several thousand years necessarily exhibit increased variability?

Secondly, Chapter 6 evaluates the claim that the diversity of living humans underestimates the variability present among penecontemporaneous humans during the Late Pleistocene by directly testing whether early *H. sapiens* fossils from the Late Pleistocene of Africa, the Levant, and Europe exhibit an excess of morphometric variation relative to modern humans. Few studies have directly compared the magnitude of phenotypic variation between the earliest representatives of our species and living populations, and none have considered variability in the postcranial skeleton, despite the indirect evidence for greater skeletal variability in the past provided by numerous studies. Understanding the magnitude and patterning of postcranial variation in the past may shed light on the nature of human evolution, and may provide an additional line of evidence to compliment molecular and craniometric studies. Furthermore, documenting and comparing intra-population variability also has serious implications for paleoanthropological studies since numerous analytical methods implicitly employ a framework of variation equality.

Chapter 2

Data Collection Methods and Skeletal Samples

Skeletal Measurements

Morphometric variables were selected to reflect the size and shape of the major long bones of the appendicular skeleton (humerus, ulna, radius, femur, and tibia), in addition to the os coxae. In selecting variables, particular emphasis was placed on capturing the size and shape of articular surfaces since these skeletal parts are frequently found isolated in archaeological and fossil contexts. This permits a separate analysis of joints in cases where complete elements are not available. Measurements of the os coxae were included specifically to evaluate their utility in determining the sex of specimens. In total, 109 variables were recorded on six elements; the number of measurements recorded per element is listed in Table 2.1. The complete list of morphometric variables recorded in this study is presented in Appendix 1 along with a description of measurement protocols. All linear measurements (n = 108) were taken directly on the specimens using digital sliding calipers (Mitutoyo model CD-6”CX: resolution = 0.01 mm, accuracy = ± 0.02 mm) with direct input of data via SPC cable, osteometric board or tape measure as appropriate.

One angular measurement (PEL11, average sciatic notch angle) was taken from digital photographs using Sigma Scan Pro 5.0©. Following the protocol outlined in Appendix 1, the sciatic notch angle of each individual was measured from photographs on three separate occasions, and the average of these assays

was employed (PEL11). To assess the precision of measuring the sciatic notch angle in this manner, the absolute deviation of each individual measurement from the mean of the three assays was computed, providing the mean deviation for each individual. Next, the percent deviation of the assays was computed:

$$\% \text{ Deviation} = \left(\frac{\text{Mean Deviation}}{\text{Assay Mean}}\right) \times 100$$

Individuals exhibiting greater than 3% difference between measurements were measured another three times. The average sciatic notch angle (PEL11) was computed for each individual once less than 3% difference was observed between measurements. In addition to the metric variables, seven non-metric characters of the pelvis were scored. Since these features pertain specifically to the sex determination portion of this study, they are described in Chapter 3.

Measurement Error and Reliability

In any morphometric study, it is important to appreciate that the overall variance documented in a sample does not strictly represent the true biological variance. This is because other factors, namely measurement and instrument error, may also contribute to the observed variation. Variance can be partitioned in the following way:

$$V_t = V_b + V_{e1} + V_{e2} + V_{e3}$$

where V_t = total variance observed, V_b = true biological variance, V_{e1} = variance due to intra-observer measurement error, V_{e2} = variance due to inter-observer measurement error, and V_{e3} = variance due to instrument error (Ulijaszek and Lourie, 1994). Sliding calipers are the main instrument employed in this study; they are accurate to 0.01 ± 0.02 mm, thereby minimizing variance due to instrument error. This source of error is further limited by using the same

equipment throughout the length of the study. Inter-observer measurement error (V_{e2}) is minimized because the author measured most of the specimens herself. However, as will be discussed in greater detail below, a limited amount of data for the European early Upper Paleolithic fossil sample were taken from the literature because the original specimens were unavailable for study. The incorporation of these data may influence variation within this sample. To assess the contribution of inter-observer error to sample variation, one would ideally compare select measurements recorded by the present author with those recorded for the same specimens by the researchers from which published data are employed. This is problematic because the sources of published data utilized here often do not report measurements taken by those workers for other fossils measured in this dissertation. Thus, the contribution of inter-observer error to variation within the European early Upper Paleolithic sample cannot be assessed.

To estimate intra-observer measurement error, all morphometric variables were recorded twice on a sample of five randomly selected African American adult individuals from the Terry Collection (National Museum of Natural History, Washington DC). For each linear variable, the initial and repeat measurement trial occurred on different days, and the data were recorded in separate spreadsheets to prevent bias. In the case of the sciatic notch angle, two sets of os coxae photographs were taken on separate days, allowing the angle to be measured from different images.

For each variable, % Error was computed to assess the difference between the initial and repeat measurement of each individual:

$$\%\ \text{Error} = \frac{(\,|\ \text{initial measurement} - \text{repeat measurement}\ |\,)}{\text{initial measurement}} \times 100$$

The average % Error across the five individuals was calculated for each variable, and a paired *t*-test was performed in SPSS 11.0© to statistically assess the

difference between the two measurement trials. As reported in Table 2.2, the paired *t*-test identified eight variables which present significant differences between trials: HUM14, HUM22, ULN10, RAD11, PEL3, FEM6, and FEM12. As Table 2.3 demonstrates, the variables also show a large range of average % Error, further suggesting that some variables may be unreliable. Yet if a threshold of acceptable error is set conservatively at 3%, it is apparent that the majority of variables, including the eight listed above, have low error. Indeed, only eleven variables exceed this threshold of acceptable error: HUM7, HUM8, HUM9, HUM10, HUM19, ULN16, ULN17, ULN18, RAD8, FEM14, and TIB8 (Table 2.3). The high % Error exhibited by these measurements suggests that they may be unreliable and should be used with caution. Of the eleven variables with high error, more than half were designed to capture the dimensions of muscle attachment sites which tend to be more poorly defined compared to articular surfaces. For example, length and breadth of the deltoid tuberosity (HUM9 and HUM10 respectively), and breadth of the pectoralis major insertion site (HUM8) on the humerus each have high % Error. Other variables with high % Error define bony features that may be difficult to measure accurately due to uneven articular surfaces (e.g., FEM14: patellar notch width, and TIB8: medio-lateral diameter of the medial tibial condyle), non-distinct articular borders (e.g., HUM19: olecranon fossa breadth, and ULN16: radial notch breadth), or unclear orientation (e.g., ULN18: antero-posterior diameter of the proximal ulnar shaft).

In order to achieve a more refined assessment of measurement error, the technical error of measurement (TEM) is estimated for each morphometric variable as follows:

$$TEM = \sqrt{\frac{(\sum D)^2}{2N}}$$

where D = the absolute difference between the initial and repeat measurement for each individual, and N = the number of individuals measured (Ulijaszek and Lourie, 1994). Since the TEM is reported in the unit of the original measurement (millimeters in all cases except for sciatic notch angle, which is measured in degrees), it provides an indication of the impact of intra-observer error on each variable. As shown in Table 2.4, many of the variables selected here have TEMs well below 1.0 mm, suggesting that the contribution of intra-observer error to sample variation is low. Frisancho (1990) reports reference TEM values for anthropometrics of living humans, yet as with % Error, no guidelines for TEM currently exist for skeletal metrics.

However, TEM values can be used to evaluate the usefulness of the variables by computing a coefficient of reliability (R):

$$R = 1 - [(\text{TEM})^2/(\text{V})^2]$$

where V = the total variance between individuals, including measurement error (Ulijaszek and Lourie, 1994). R ranges from 0 to 1, and indicates what proportion of variance between individuals in a sample is free of measurement error. For example, an R of 0.99 demonstrates that 99% of the variance in the sample is attributed to factors other than measurement error. As a guide, Ulijaszek and Lourie (1994) recommend that R be greater than 0.95 in most cases. As shown in Table 2.5, the majority of variables selected for this study exhibit high reliability with R values greater than 0.95, although seventeen variables exhibit R values lower than the recommended threshold. Of these, several also exhibited high % Error (HUM7, HUM8, HUM10, HUM19, ULN16, ULN18, and RAD8) or significant differences (HUM22 and RAD11) between measurement trials, while additional variables were identified in which true biological variation may be masked by high measurement error.

To minimize the influence of measurement error on sample variation, while preserving sufficient variables to undertake this study, ten variables with an *R* lower than 0.90 were eliminated: HUM7, HUM8, HUM10, HUM16, HUM22, ULN16, RAD4, RAD11, RAD12, and PEL4. The humerus dataset is the most affected, losing five variables. While this will limit comparisons of the magnitude of variation between articular and muscle attachment surfaces in the humerus, twenty morphometric variables remain, which is enough to capture the morphological variability of this element.

Data Transformation and Analysis: An Overview

A combination of univariate and multivariate methods are employed to provide a clearer understanding of differences in the magnitude and pattern of morphometric variation between groups of modern and past peoples. To simplify the description of the diverse methods employed herein, the specific procedural details and assumptions for each method will be addressed in the relevant chapter.

This dissertation considers morphological differences in both the size and shape of appendicular long bones. As depicted in Figure 2.1, size and shape may change together, thereby creating a new form, or they may change independently of one another (Richtsmeier et al., 1992). The linear measurements collected for this study capture the form of appendicular element because they contain both size and shape details. To facilitate the interpretation of shape differences alone in certain aspects of this study, some type of size-adjustment must be employed to eliminate or control for differences in scale between specimens. The geometric mean (GM), which is the *n*th root of the product of the *n* variables in a particular dataset, can be used to represent the size of each specimen (Mosimann, 1970). Using this new size variable, shape variables are created by computing a ratio of each raw variable (Y) and the geometric mean (GM) of all the variables in that

particular dataset (Mosimann, 1970; Darroch and Mosimann, 1985). These Mosimann shape ratios are dimensionless and scale-free variables that can facilitate the interpretation of shape changes (Corruccini, 1987; Jungers et al., 1995). The size variable (i.e., the GM) can make use of all available measurements for an element (e.g., all ten linear variables of the pelvis), or it may be created from a few select measurements believed to appropriately represent the size of the element or region under consideration (e.g., acetabular width and posterior acetabuluar ischial length of the pelvis). The specific shape ratios employed in this dissertation will be described in the revelant sections as appropriate, and the new shape variables will be distinguished from the form variables (i.e., the raw data) by a lowercase 's' in front of the variable name (e.g., sHUM1).

Raw measurements are used to create the shape variables, although the resulting shape variables may be log-transformed as necessary. Similarly, in the analyses of form the raw data may be transformed using the natural log in order to help promote a normal distribution, a requirement for most parametric statistical tests (Sokal and Rohlf, 1995). Such transformations will be specified in each subsequent chapter as appropriate.

Skeletal Samples

For all samples employed in this study, morphometric variables and non-metric pelvic characters were recorded preferentially on the left side. If the left element was missing, damaged or pathological, the right side was substituted. In some instances, elements from both sides were unavailable, leading to some variation in sample size between elements within each sample. This is especially notable in the archaeological and fossil samples where preservation is more variable between specimens. When available, curatorial records were used to

select individuals of adult age (≥ 20 years). When age-at-death was unrecorded, adult status was determined on the basis of third molar eruption and/or epiphyseal fusion of long bones. Curatorial details and population background specific to each sample are described below. Univariate summary statistics by element for each sample are provided in Appendix 2.

Reference Samples: Rationale for Choice

The osteometrics described above were collected for skeletons drawn from six African populations: three recent populations (Zulu, Kikuyu, and Nilotic Ugandans), and three archaeological groups (Khoe-San, Sudanese and Moroccans). The recent samples comprise known-sex, known-age individuals with secure tribal affiliations. Thus, geographic variation is tightly controlled within these samples, and each can be divided into known-sex sub-samples. Additionally, individuals in each recent sample lived more or less contemporaneously in the 20th century, and many were likely from the same generation. Thus, temporal variation is also heavily limited within the recent samples. In contrast, the archaeological samples are drawn from a wider time span and provide a window onto variation through time in different African populations. Geographic variation is still controlled within the archaeological samples, however, these samples do not provide a known record of sex. Each archaeological sample is assumed to comprise a combination of males and females, and this dissertation will estimate the distribution of sex by applying sex determination methods (see Chapter 4). Together, the six reference samples employed in this study provide different models for comparing and understanding morphometric variation in early *H. sapiens* because they have the potential to capture magnitude and pattern of variation stemming from different sources.

In this study, sample choice was intentionally limited to heat-adapted populations because they are argued to represent the most appropriate models for understanding variation in fossil *H. sapiens*. Studies have proposed that the closest phenetic affinity of many early *H. sapiens* lies with heat-adapted peoples such as modern Africans and Australian Aborigines (e.g., Pearson, 2000). This may be because many aspects of human morphology, including limb proportions, body size, and body shape, are known to be ecogeographically patterned. For example, modern tropical peoples typically share a linear or nilotic body build (e.g., Ruff, 1991; Ruff, 1994; Ruff, 2000). Studies have reconstructed similar linear physiques for early *H. sapiens*, including specimens from Israel and Ice Age Europe (Holliday, 1997, 1999, 2002). Therefore, limiting the samples to heat-adapted populations helps to control for the potential effects of ecogeographic adaptation on morphometric variation in the postcranial skeleton. In an ideal sampling strategy, samples would be drawn from a global distribution of heat-adapted populations, including African populations but also Australian Aborigines and other tropical groups. Unfortunately, an insufficient number of skeletons from native Australians and other island populations were available for study, and sampling was restricted to African groups.

However, for the purposes of this study, limiting samples to African populations is justified based on the distribution of biological variation within and between living populations. In a study of cranial morphology and various genetic markers, Relethford (1994) found that the magnitude of living human intrapopulation variation exceeded that of interpopulation variation. Thus, the African groups included here should adequately sample modern human within population skeletal variation.

Recent Africans: Zulu

A total of 42 individuals (n = 20 females, n = 22 males) were randomly chosen from skeletons in the Raymond A. Dart Collection, University of the Witwatersrand (Johannesburg, South Africa). All skeletons are derived from cadavers used by the medical school. Records provide reliable information on the sex and age-at-death of each individual, as well as tribal affiliation, and were used to randomly select specimens. The individuals range in age from 22 to 96 years old, died between 1935 to 1962, and belong to the Zulu ethnic group. The Zulu derive from the agriculturalist Nguni people, and are part of the Bantu linguistic group believed to have migrated into South Africa roughly 1,000 years ago (Nurse et al., 1985). Genetic analyses attest to some admixture between the Zulu and the Khoe-San, the indigenous inhabitants of South Africa (Nurse et al., 1985).

Recent Africans: Kikuyu

A total of 40 individuals (n = 12 females, n = 16 males, and n = 12 of indeterminate sex) were selected from the Modern Human Collection in the Division of Osteology, National Museum of Kenya (Nairobi, Kenya). These skeletons are the remains of members of the Kikuyu tribe killed between 1952 and 1959 during the Kenya Emergency when the Mau Mau rebelled against British colonial rule. The bodies were exhumed by Dr. Morris Rogoff, then chief pathologist for Her Majesty's police, and used as evidence against the Mau Mau. As with the Zulu, the Kikuyu are agriculturalists that belong to the Bantu linguistic group (Oschinsky, 1954; Goldthorpe and Wilson, 1960).

The Division of Osteology catalogue contains personal details such as name, sex, tribal affiliation, injuries sustained, and location of exhumation for many of the individuals. The initial sampling strategy devised for this collection

relied on these details to randomly select specimens. However, inconsistencies and duplications in the catalogue, as well as unexplained corrections to the records and the overall disorganized nature of the collection resulted in osteometrics being recorded for twelve specimens of indeterminate (or rather, unreliable) sex, thereby reducing the sample size of the sex-specific Kikuyu samples.

Recent Africans: Nilotic Ugandans

A total of 33 individuals (n = 5 females, n = 26 males, n = 2 unknown sex) were selected from the Galloway Osteological Collection, Department of Anatomy, Makerere University (Kampala, Uganda). The Galloway Collection comprises over 300 skeletons of unclaimed patients from Mulago Hospital who died between the 1940s and early 1970s. Tribe, sex, age-at-death, and cause of death are recorded for each individual. Uganda is an ethnically and linguistically diverse country with more than a dozen main tribes as well as many smaller ones (Oschinsky, 1954; Goldthorpe and Wilson, 1960), many of which are represented in the Galloway Collection. In the southern half of the country, tribes speaking Bantu languages dominate, while Nilo-Hamitic-Sudanic languages are spoken mainly in the north. In order to control for geographic variation while maintaining a suitably large sample size, only individuals attributed to the non-Bantu tribes of northern Uganda were sampled: the Acholi (n = 4), Lango (n = 9), Lugbara (n = 7), Madi (n = 3), and Teso (also called Etesot) (n = 10), with roughly equal distribution among the Nilotic (Acholi + Lango), Nilo-Hamitic (Teso) and Sudanic (Lugbara + Madi) main tribal groups. Early to mid-20th century anthropologists also divided the tribes of the Nilo-Hamitic-Sudanic linguistic group (including those sampled here) into morphological groups based on the distribution of metric and non-metric bodily features, with broad overlap

between the linguistic and morphological groups: Hamitomorphs, Nilotomorphs, and Nilohamitomorphs (see Oschinsky, 1954 and work reviewed therein). Although these groups differ in certain physical aspects such as skin color, facial proportions and hair texture, they share many physical features that likely reflect underlying similarities of the skeleton including tall stature, small relative sitting height, and the relatively long upper and lower extremities associated with a linear or Nilotic physique. Therefore, it seems appropriate to lump these individuals together for the purpose of the present study.

Unfortunately, the Galloway Collection comprises a substantially greater representation of males than females, especially among the Nilotic tribes. This creates an unequal distribution of sex in the Ugandan sample employed in the present study. Moreover, the record of sex in the catalogue was changed without explanation in two cases; these two individuals ('unreliable' females) are excluded from the known-sex sub-samples, further limiting the size of the female sample, but they are included in the total Ugandan sample. In some instances, the female sample size is further reduced due to missing elements, possibly due the use of the skeletal collection by medical students.

Archaeological Africans: Khoe-San

A total of 98 Khoe-San skeletons were measured from three collections in South Africa: $n = 50$ from Iziko, South African Museum (Cape Town), $n = 30$ from the National Museum at Bloemfontein (Florisbad Quaternary Research Station), $n = 18$ from the McGregor Museum (Kimberley). Sex is unrecorded for these specimens, but it will be estimated using discriminant function classification of the pelvis (see Chapter 4). The preservation of the Khoe-San material varies widely between specimens depending on the context from which it was recovered, resulting in variable sample size across elements. The minimum sample size for

the Khoe-San is 54 and the maximum is 98, with a median sample size of 72 across all variables.

The majority of Khoe-San skeletons (n = 80) employed in this thesis are from the Iziko and National Museum collections, and most represent prehistoric specimens from the Late Stone Age. All but one of these skeletons has a radiocarbon date. The specimens range in age from 9,688 to 200 years before present (BP), with a median age of 2,490 years BP (Stynder, 2006). Only three dated specimens are younger than 500 years BP. The Khoe-San specimens from the McGregor Museum (n = 18) were recovered from historic burials along the Riet River, a tributary of the Orange River, in the general vicinity of Kimberley, South Africa. Radiocarbon dates are available for only four Riet River specimens (110 ±50, 380 ±50, 390 ±50, and 990 ±50 years BP), confirming that they are generally much younger than the LSA specimens described above (Morris, 1992b). The association of many burials with typical European contact-period pastoralist settlements, as well as evidence from grave goods, indicates that the remaining Riet River skeletons are also relatively young (Morris, 1992). When considered together with the older specimens, the complete Khoe-San sample employed in this study spans roughly 10,000 years.

The Khoe-San ethnic group encompasses two distinct peoples believed to share a common heritage, the pastoralist Khoe (also known as Khoi) and the hunter-gatherer San (also known as Bushmen), who were displaced and greatly reduced in numbers during the Bantu expansion and later European colonization of southern Africa (Nurse et al., 1985). Although their lifestyles had diverged by the arrival of European colonists (and possibly as early as 2,000 BP), the Khoe and the San share many similarities including the use of click consonants, as well as various biological adaptations (probably to hot environments) such as localized bodily fat deposits called steatopygia (a marked accumulation of fat in and around the buttocks, most developed in females) and hair distribution patterns (Tobias,

1957; Nurse et al., 1985). Both prehistoric and historic Khoe-San are also characterized by small body size and short stature (Tobias, 1957, 1975; Pfeiffer and Sealy, 2006).

Archaeological Africans: Sudanese

A total of 94 skeletons were measured from two collections: $n = 44$ from the site of Jebel Sahaba, housed in the Wendorf Skeletal Collection, Department of Ancient Egypt and Sudan, British Museum (London, UK), and $n = 50$ from the site of Kerma, housed in the Duckworth Laboratory, University of Cambridge (Cambridge, UK). The preservation of these archaeological skeletal remains is variable, especially among the Jebel Sahaba skeletons. Natural partial mummification helped to preserve the integrity of many of the Kerma remains. For the combined Sudanese sample (Jebel Sahaba + Kerma), sample size varies from 28 to 88 specimens per variable, with a median of 68.

The Jebel Sahaba skeletons, donated to the British Museum by Dr. F. Wendorf, were excavated from the cemetery at Site 117 during UNESCO salvage operations in the 1960s in advance of regional flooding by the Aswan High Dam Project (Wendorf, 1968a). This site, now submerged by Lake Nasser, was located along both sides of the Nile River in northern Sudan, near the Second Cataract and the Egyptian border. The cemetery contained 59 burials, including those of adults and children. Wendorf (1968) proposed an age of 14 to 12 kya BP for the Jebel Sahaba burials based on associated artifacts and geologic evidence. The Wendorf Skeletal Collection Catalogue, compiled by Dr. M. Judd in 2003, reports a radiocarbon date of 13,740 ±600 BP for burial 43 from Site 117 based on a sample sent by Dr. Wendorf to Dr. Vogel at the Pretoria Dating Laboratory in South Africa. Although this date remains unpublished, it does provide support for the Epipaleolithic age initially proposed by Wendorf. As noted by Judd, the

specimens exhibit varying degrees of postcranial preservation, and many long bones bear significant damage to the epiphyses. Several individuals have fragments of stone thrusting or throwing implements embedded in their skeleton, as well as numerous cases of healed fractures, which may suggest a high degree of violence in this population (Wendorf, 1968b).

The extensive cemetery associated with the ancient capital city of Kerma is located along the east bank of the Nile River in northern Sudan near the Third Cataract (Bonnet, 1992). The city of Kerma was a major urban center during the Middle Kingdom period of Egyptian history, and appears to have been continuously occupied from ca. 4,500 to 3,500 years BP; the cemetery, which contains over 30,000 graves, is believed to span this time (Bonnet, 1992). Several hundred graves were excavated in the early 20th century, and the skeletons transported to England for curation (Reisner, 1923). While many skeletons did not survive the rough overland and ocean journey, over 200 are presently housed in the Duckworth Laboratory, University of Cambridge (M. Okamura, pers. comm.).

Based on the geographic proximity of the Jebel Sahaba and Kerma sites in ancient Nubia, the skeletons from these sites are combined in a single prehistoric Sudanese sample. The time range encompassed by this sample is roughly 10,000 years. The combined Sudanese sample has near-equal distribution of specimens from both sites (Jebel Sahaba, $n = 44$; Kerma, $n = 50$), however, since the Jebel Sahaba specimens tend to be more poorly preserved, the sample distribution is less equal when whole elements are considered.

Archaeological Africans: Taforalt

A total of 30 skeletons from the cave site of Taforalt were measured from the collection housed at the Institut de paléontologie humaine (Paris, France).

Located in northeast Morroco near the Algerian border, the Taforalt Cave (also known as Grotte des Pigeons) is an Epipaleolithic burial site (Ferembach, 1962). While deposits in the cave may extend back to roughly 80 ka BP, the burials found in the cave are attributed to the Ibermaurusian culture that began around 18 ka BP and intensified between ca. 13 to 9 ka BP, according to radiocarbon analyses of charcoals found in the cave (Bouzouggar et al., 2008). The 28 multiple graves from the cave are likely associated with the later period of intensification, although this cannot be verified due to a lack of association between the skeletons, which were excavated in the mid-20th century, and the charcoals used more recently for ^{14}C dates (Ferembach, 1962; Bouzouggar et al, 2008). Therefore, current evidence suggests that the Taforalt individuals may have been interred between approximately 18 to 9 ka, and the sample employed here may represent anywhere from ca. 4,000 to 9,000 years of time, most likely towards the lower range estimate. Mariotti et al. (2009) recently reported a revised minimum number of individuals at Taforalt, identifying 40 adults and adolescents amongst the burials, significantly lower than the 86 individuals proposed by Ferembach (1962). One specimen (grave No. 20) is excluded from the sample due to possible dwarfism (Ferembach, 1962; Marotti et al., 2009). Preservation is somewhat variable across the specimens: sample size ranges from 13 to 31 specimens per variable, with a median sample size of 26.

Early *Homo sapiens* Fossils

Early *Homo sapiens* are defined here as those hominin fossils that are attributed to our species by general consensus, and predate the Last Glacial Maximum (LGM, ca. 22 – 18 kya BP), potentially extending as far back as the late Middle Pleistocene. Since early *H. sapiens* tend to exhibit a variable mosaic of modern and archaic anatomical features, these fossils may "sample a

population that is on the verge of anatomical modernity but not yet fully modern" (White et al., 2003: 745). Numerous studies have noted the sporadic appearance of modern anatomical features, especially in the cranium (e.g., Kidder et al., 1992; van Vark et al., 1992; van Vark and Schaafsma, 1992; Turbon et al., 1997; Harvati, 2003; Grine et al., 2007; Rougier et al., 2007), but also in postcranial elements (Pearson, 2000b) from the late Middle Pleistocene to the Late Pleistocene. Yet the conclusion consistently drawn from these diverse analyses is that fully modern morphology does not appear commonly and unequivocally until the LGM.

Research into the biological origin and evolution of our own species has traditionally emphasized aspects of cranial morphology, leading to a particularly cephalocentric view of human evolution. Clearly there is a need to expand beyond crania and teeth to better integrate the postcranial skeleton in our understanding of modern human evolution. By focusing explicitly on the major appendicular elements, this dissertation will increase our understanding of skeletal diversity during the biological transition to modernity, and compliment previous work on the skull. Trinkaus (2005) identified 14 sub-Saharan and Levantine localities that preserve fossils considered to represent the earliest members of *H. sapiens*. Among these, eight sites have yielded postcranial remains ranging from isolated elements to partial skeletons. In addition, at least a dozen European sites and a smaller number from Asia and North Africa also preserve early *H. sapiens* postcranial remains including numerous nearly complete skeletons, often in association with the local early Upper Paleolithic industries ranging in age from approximately 36 to 22 kya BP (Trinkaus, 2005). Thus, early *H. sapiens* are represented by a considerable sample of postcranial fossils. With few exceptions, the specimens recovered to-date fit into one of two geographically and temporally exclusive sets: the earliest *H. sapiens* specimens tend to come from sub-Saharan Africa, while the later specimens generally come from Europe.

Using this dichotomy in the fossil record of early *H. sapiens*, the specimens included in this study are grouped into two samples named after the predominant archaeological industry associated with them: the Middle Stone Age (MSA) sample groups together the older – mostly sub-Saharan African – fossils, while the early Upper Paleolithic (EUP) sample groups together later-occurring – mostly European – fossils. Although these technological stages do no have a perfect correspondence with geological periods and absolute dates, they are sufficiently deep temporally to accommodate fossils that lack reliable radiometric dates, and thus are convenient categories for the present study. The MSA and EUP samples and the fossils they include are listed in Table 2.7 and described in turn below.

Middle Stone Age Sample

Early *H. sapiens* fossils from seven localities ranging in age from approximately 195,000 to 65,000 years old are grouped in the Middle Stone Age (MSA) sample (Table 2.6). Five of the MSA sites are found in sub-Saharan Africa. For the purpose of this study, the fossils from the Levantine sites of Skhūl and Qafzeh are considered as part of the African MSA group. Their inclusion in this group is justified for two reasons. First, the antiquity of the Israeli fossils makes them more contemporaneous with the African MSA material than the later European Upper Paleolithic fossils (Schwarcz et al., 1988; Stringer et al., 1989; McDermott et al., 1993; Mercier et al., 1993; Millard, 2008) . Second, faunal evidence recovered from Qafzeh contains a high number of African taxa, suggesting that the Levant was effectively an extension of Africa during the early Late Pleistocene (Tchernov, 1992).

MSA: Kibish Formation (Omo I and AHS)

The Omo I partial skeleton from the site of KHS in southwestern Ethiopia represents the oldest currently known *H. sapiens* fossil (Day, 1969; Day and Stringer, 1982; Pearson et al., 2008b). Laser-fusion $^{40}Ar/^{39}Ar$ dating of feldspars from tuffs in Members I and III of the Kibish Formation bracket the age of this fossil between 196 ± 2 ka and 104 ± 1 ka BP, which is further narrowed to ca. 195 ± 5 kya BP by correlation to dated sapropel phases in the Mediterranean Sea, evidence of istopic ages of pumice clasts recovered from Member I, and geological evidence for the rapid deposition of Member I (McDougall et al., 2005). Using stricter chronometric hygiene standards, Millard (2008) recently proposed an age closer to 189.6 ± 1.4 ka BP for the Member I fossils.

In addition to securing the age of this important fossil, renewed exploration of Member I of the Kibish Formation yielded new postcranial specimens attributed to the Omo I individual (Pearson et al., 2008b), including a partial left os coxae included in this study. Previous attempts to determine the sex of Omo I based on this partial os coxae have been inconclusive: the shape and angle of the sciatic notch is ambiguous, the acetabulum is large, suggesting a male, but a shallow preauricular sulcus is present, suggesting a female (Royer et al., 2007; Pearson et al, 2008b). Pearson et al. (2008b) also proposed a tall, linear physique for Omo I by predicting stature (178 – 182 cm) from the preserved length of the left humerus, and predicting body mass (70.7 ± 5 kg) from the maximum acetabuluar diameter. As shown in Figure 2.2, all the major long bones are represented in Omo I, albeit some in a very fragmentary state (Table 2.8).

Workers also discovered a new site in Member I of the Kibish Formation (Awoke's Hominid Site, AHS) that yielded a nearly complete adult tibia (Pearson et al., 2008a). The AHS tibia is believed to be roughly contemporaneous with the Omo I fossil. Pearson et al. (2008a) reconstruct this individual's stature from the

estimated maximum length of the tibia at approximately 166 – 176 cm and 162 – 174 cm for a male and female respectively, suggesting that the AHS individual was somewhat shorter than Omo I. The original Omo I and AHS fossils were studied at the National Museum of Ethiopia (Addis Ababa, Ethiopia).

MSA: Skhūl

The Mugharet es-Skhūl cave is situated on the slopes of Mount Carmel in Israel. The Levalloiso-Mousterian levels of this site have yielded numerous human remains believed to represent intentional burials, as well as large lithic and faunal assemblages (McCown and Keith, 1939). Resolution on the antiquity of the Skhūl hominins required major advances in radiometric dating methods. Using electron spin resonance (ESR), bovine teeth from the burial level (Layer B) provided an average age of 81 ± 15 ka BP under an early uptake model and 101 ± 12 ka BP under a linear uptake model (Stringer et al., 1989). Applying thermoluminescence (TL) dating to six burnt flints excavated from the lower portions of Layer B, Mercier and colleagues (1993) proposed an average age of 119 ±18 ka BP for the site. Attempts were made to confirm this age through U-series dating of animal teeth recovered from the same layer. The results indicated an age closer to 80 ka BP for the human fossils, but possibly as young as 40 ka BP (McDermott et al., 1993). These conflicting dates highlight the complex stratigraphy at Skhūl, and raised the possibility that two ages were actually represented within the hominin burial layer. Indeed, such a scenario was originally proposed based on the relative depth, mineralization, color, and state of preservation of the fossils: several individuals (Skhūl 6, 7, 8, 9, 10, and possibly 3) were believed to represent an earlier, older occurence, while a few others (Skhūl 1, 4 and 5) were argued to represent a later, younger burial event (McCown, 1937). However, this stratigraphic scenario was quickly rejected in

favour of a single homogeneous assemblage based on the overall similar morphological character of the fossils (McCown and Keith, 1939).

More recently, Grün et al. (2005) applied ESR and U-series techniques directly to the bones and teeth of Skhūl 2 and 9, and fauna directly associated these individuals in addition to Skhūl 5. Assuming rapid deposition in the cave, Grün and colleagues proposed an age range of 130 – 100 ka BP for the entire fossil assemblage. Alternatively, they reported an age of ca. 140 ka BP for Skhūl 9 alone, and a significantly younger age of ca. 98 ka BP for the Skhūl 2 and 5 fossils. Employing a Bayesian computational model of the available dates for the Skhūl fossils, Millard (2008) recently proposed the following 95% probability age ranges for the site: Skhūl 9 = 106 – 173 ka BP, Skhūl 5 = 71 – 115 ka BP, all other Skhūl fossils (i.e., those lacking reliable directly associated dated remains) = 43 – 158 ka BP. Again, a disparity in age between at least some of the individuals seems likely. Interestingly, the age ranking for the two fossils with directly associated dates (i.e., Skhūl 9 and 5) is consistent with the relative ages originally proposed by McCown (1937) but later retracted (McCown and Keith, 1939), placing Skhūl 9 in older deposits relative to Skhūl 5.

Skeletons from seven adults were recovered in the cave, with skeletal preservation ranging from partial to complete skeletons; the list of elements and estimated sex of each individual is listed in Table 2.9. McCown and Keith (1939) concluded that the fossils displayed some Neandertal characters, but overall the assemblage was most similar to the Cro-Magnon fossils from western Europe, which were at the time regarded as the earliest modern *H. sapiens*. Today, many paleoanthropologists support the interpretation of the Skhūl fossils as early representatives of *H. sapiens*, albeit without the full expression of modern skeletal traits (e.g., Stringer et al., 1984; Vandermeersch, 1992; Trinkaus, 2005). A minority of workers view the craniodental morphology of the assemblage as

presenting significant overlap with the range of variation documented in Neandertals (e.g., Corruccini, 1992; Wolpoff and Lee, 2001).

Measurements were recorded on the original remains of Skhūl 2, 5, 6, and 7 housed in the Peabody Museum of Archaeology and Ethnology at Harvard University, Cambridge MA. The original Skhūl 9 fossil was studied at the Natural History Museum, London UK. The author viewed the original remains of complete Skhūl 4 skeleton at the Rockefeller Museum in Jerusalem, although no measurements were obtained due to the mostly immobile glass case surrounding the exhibit. Casts of the humeri, radi, ulnae and tibiae from Skhūl 4 were kindly provided for study by Dr. Y. Rak at Tel Aviv University, while casts of this individual's os coxae and femora were measured at the Institut de paléontologie humaine in Paris.

MSA: Qafzeh

Qafzeh cave is situated on a hill (Djebel Qafzeh) near the town of Nazareth in Israel. Investigations led by R. Neuville began in the early 1930s, but were interrupted by WWII and other political conflicts in the region until 1965, when B. Vandermeersch and a team of researchers from the CNRS returned to the site (Vandermeersch, 1981). In addition to the remains of 16 human fossils (five of whom are adults), some fauna, and an abundant Mousterian lithic assemblage dominated by scrapers were recovered from the site.

Detailed stratigraphic provenance for each fossil has been used to link Neuville's hominin level (Level L) with the hominin-bearing levels (XVII to XIX) of the later excavation, which suggests that all of the adult fossils recovered from Qafzeh are generally contemporaneous. TL dating of burnt flints excavated from the hominin-bearing layers indicated an weight mean age of 92 ± 5 ka BP (Valladas et al., 1988), a date which was later confirmed through isochron

analysis (Aitken and Valladas, 1992). The results of ESR on tooth enamel of fauna recovered from the homining layers suggested a mean age of 96 ± 13 ka BP under the early uptake model and 115 ± 15 ka BP under the linear uptake model, providing independent support for the antiquity of the site (Schwarcz et al., 1988). The ESR study also found no significant difference in age estimates between the various hominin-bearing layers identified by Vandermeersch (1981), indicating that the cave sediments were deposited quickly and that the fossils were most likely of similar age. A recent review of the dating at Qafzeh using a Bayesian stratigraphic model proposed an age range of 96.9 – 87.6 ka BP for the assemblage, and supports the view that the human specimens are contemporaneous (Millard, 2008). This differs from the situation at Skhūl described previously, where the human remains appear to span a considerable time. Importantly for this study, the Levantine assemblage may incorporate greater temporal variation than is typically assumed (e.g., Bar-Yosef, 2000).

Vandermeersch (1981, 1992) concluded that the Qafzeh fossils represent regional Levantine early *H. sapiens* characterized by an essentially modern morphology, including a well-defined chin on some individuals, combined with the retention of some archaic or Neandertal-like features throughout the skull and postcranial skeleton. This view is currently widely supported among paleoanthropologists (e.g., Trinkaus, 1984, 2005; Kidder et al., 1992; Schwartz and Tattersall, 2000). Vandermeersch (1981) and others (e.g., Kidder et al., 1992; van Vark and Schaafsma, 1992) have observed a relatively high degree of morphological variation within the Qafzeh assemblage, as well as strong similarities to the Skhūl fossils.

The elements of the Qafzeh assemblage represented in the present study are listed in Table 2.9. On the basis of overall morphological appearance, Vandermeersch (1981) suggested that Qafzeh 3 and 9 represent females, while Qafzeh 8 was diagnosed as male; no diagnosis was provided for Qafzeh 7 due to

the limited material preserved for this individual. The original remains of Qafzeh 3 and 7 were studied at the Institut de paléontologie humaine in Paris, France (a femoral diaphysis fragment from Qafzeh 6 was also studied at IPH, but no measurements were recorded on this poorly preserved specimen). The original fossils of the Qafzeh 8 and 9 individuals were studied at Tel Aviv University in Israel.

MSA: Klasies River

The Klasies River site complex is located along the Indian Ocean coast of the Eastern Cape Province of South Africa. Caves 1 and 2 and their associated rockshelters constitute the 'Main Site' which was first excavated in the 1960s (Singer and Wymer, 1982), followed by subsequent excavations in the 1980s (Rightmire and Deacon, 1991). In addition to human remains, the site has yielded a large number of lithics associated with various MSA and LSA industries, as well as a rich faunal assemblage. Using istopic analyses of shells found *in situ*, Shackleton (1982) attributed the MSA I levels to oxygen isotope stage (OIS) 5e (ca. 120 ka BP), while the MSA II levels were attributed to either OIS 5c (ca. 100 ka BP) or OIS 5a (ca. 80 ka BP). When excavations resumed in the 1980s, the Main Site was partitioned into finer stratigraphic units such levels with MSA I archaeology were included within the Lower Brown Sands (LBS) Member, while the overlying MSA II levels were encompassed in the Sand-Ash-Sand (SAS) Member (Deacon and Geleijnse, 1988). Finding additional evidence for a period of lowered sea levels, these workers proposed an age in excess of 100 ka BP for the LBS member, and an age greater than 80 ka BP for the overlying SAS deposits, generally concurrent with the dates proposed by oxygen isotope correlation. At present, there is general agreement that the LBS occupations are older than 100 ka BP, while the stratigraphically-higher SAS member is bracketed

between approximately 80 – 100 ka BP, although Millard (2008) cautions that the latter may be as young as 63 ka BP.

The human fossils at Klasies are represented primarily by craniodental remains. However, there are a few well-preserved postcranial elements known from the deposits, including the proximal right ulna (KRM1) and proximal left radius (KRM27889) studied here. Like most of the human remains from Klasies, the ulna and radius were recovered from the younger SAS member (Rightmire and Deacon, 1991). Although the Klasies fossils are generally attributed to *H. sapiens* (e.g., Singer and Wymer, 1982; Bräuer, 1984; Rightmire, 1984; Rightmire and Deacon, 1991; Grine et al., 1998; Rightmire et al., 2006), this assemblage is morphologically diverse and not uniformly modern in character (e.g, Smith, 1992; Trinkaus, 2005). For example, the mandibles have a variable expression of the chin, ranging from incipient to one indistinguishable from those of living humans (Frayer et al., 1993; Lam et al., 1996), and aspects of the proximal ulna and radius display a mixture of archaic and modern morphologies (Churchill et al., 1996; Pearson and Grine, 1997; Pearson et al., 1998). The archaic versus modern nature of an isolated zygomatic has been much debated (Smith, 1992; Frayer et al., 1993; Smith, 1994; Bräuer and Singer, 1996a, b; Wolpoff and Caspari, 1996), and a frontal fragment that bears a gracile supraorbital region and glabella is argued to represent an adolescent, raising the possibility that the adult morphology might be more robust and archaic in appearance (Smith, 1994). Concomitant with the presence of some archaic morphologies, the mandibles and molars from Klasies also exhibit a level of size variation – and probably sexual dimorphism – that is beyond that of recent humans (Royer et al., 2009). There is undoubtedly "substantial morphological variation among the Klasies humans" (Rightmire, 1989: 18). The original Klasies radius fragment was studied at the Iziko South African Museum (Cape Town, South Africa), while the proximal ulna was studied at Dr. Hilary Deacon's home in Stellenbosch, South Africa.

MSA: Border Cave

Situated in northern KwaZulu-Natal province in South Africa, near the border with Swaziland, Border Cave preserves deposits rich in cultural artifacts spanning the MSA to the Iron Age (Beaumont et al., 1978). Several human fossils, including two mandibles (BC2 and 5), part of a calvarium (BC1), and a complete infant skeleton (BC3) were found in the cave. According to Beaumont and colleagues (1978), BC1 and 2 were disturbed from their original depositional context due to disturbances in the cave by the land owners in the 1940s, but appear to come from one of the eight MSA horizons. In contrast, BC5 and 3 were excavated *in situ* from MSA levels, with dates in excess of the limits of radiocarbon (Beaumont et al., 1978).

The Border Cave remains have been consistently described as *H. sapiens* (Beaumont et al., 1978; Rightmire, 1979; Bräuer, 1984), but some workers have expressed doubt concerning their modernity or their association with MSA occupations at the site (e.g., Corruccini, 1992; Klein, 1999). Using ESR on animal teeth from known stratigraphic contexts, Grün et al. (1990) proposed an age of 70 – 80 ka BP for the BC3 infant burial, and an age of 50 – 65 ka BP for the BC5 mandible. Grün and Beaumont (2001) reported new ESR dates consistent with the previous ESR dates, and provided a tentative age of 82 ka BP or 170 ka BP for the unprovenanced BC1 and 2 fossils, depending on their supposed stratigraphic context. Millard's (2008) Bayesian model provides general support for these ESR dates. Recently, Bird et al. (2003) employed new AMS ^{14}C protocols to date charcoal samples excavated from the site. They obtained an age in excess of 58.2 ka BP for the level directly overlying the BC5 mandible, suggesting that most of the Border Cave fossils may be older than ca. 60 ka BP.

In addition, several unprovenanced postcranial elements were recovered from the sediments that had slumped back into the earlier excavation trench, presumably from the walls of the trench. These elements cannot be associated with any specific stratigraphic layer, but mineralization and preservation suggests that they are most like older than 38,000 and possibly contemporaneous with the oldest deposits in the site (Morris, 1992a). The Border Cave postcranial remains include a portion of the right humeral shaft (in two fragments), a proximal ulna, and two sub-adult metatarsals. In early 2008, all postcranial specimens except the proximal-most humeral shaft fragment were found to be missing from the McGregor Museum (Kimberley, South Africa).

MSA: Cave of Hearths

The Cave of Hearths is located near the famous Pliocene site of Makapansgat in the Limpopo Province (formerly the Northern Transvaal) of South Africa. The cave has a deep stratified sequence spaning the Early Stone Age (ESA) to the Iron Age (Tobias, 1971). A partial juvenile mandible was excavated from Bed 3 together with late Acheulean lithics, suggesting an ESA age for the fossil. A radius fragment, however, has an uncertain provenance because it was discovered along with other fauna in the fill of a swallow hole; it is believed to derive from either late ESA or MSA deposits (Tobias, 1971). No radiometric age assessments of this fossil are currently available (Millard, 2008).

Tobias (1971) characterized the mandible as representing a transitional stage between *H. erectus* and *H. sapiens*. Similarly, Pearson and Grine (1997) reported a mosaic of modern and archaic features for the radius. The radius consists of two fragments from the right side glued together, preserving the head, neck, radial tuberosity and a short portion of shaft distal to the tuberosity. The

original fossil was measured at the Tobias Fossil Hominid Collection, University of the Witwatersrand (Johannesburg, South Africa).

MSA: East Turkana (Ileret)

KNM-ER 999 is a partial left femur discovered in the early 1970s from Area 6A near the town of Ileret to the east of Lake Turkana in northern Kenya (Day and Leakey, 1974). The exact stratigraphic provenance of the fossil is debated. It may derive from either the upper deposits of the Chari Formation (ca. 500 – 100 ka BP), or from the Holocene sediments of the overlying Galana Boi Formation (Trinkaus, 1993b). Direct dating of the fossil by U-series gamma-spectrometry provides a minimum age of 180 ka BP (Bräuer et al., 1997), which strongly suggests that the femur predates the Holocene. In a recent review of African chronology, Millard (2008) concludes that although this method is unreliable, it may nonetheless provide a good indication of the fossil's minimum age.

According to Trinkaus (1993b), a small yet clear pilaster, a probable minimum diaphyseal breadth situated proximal to midshaft, and a high neck-shaft angle align KNM-ER 999 with recent modern humans. In particular, Trinkaus observed many similarities with the specimens from Skhūl and Qafzeh (1993b; 1993a). The specimen is represented by three major fragments. The head, neck and trochanters and sub-trochanteric shaft are preserved – although the head and greater trochanter exhibit substantial damage – and conjoin with the diaphyseal fragment to form roughly the proximal two thirds of the shaft. Part of the medial distal condyle was also recovered, but does not conjoin with the other pieces. Measurements were recorded from the original specimen housed at the National Museums of Kenya in Nairobi.

Early Upper Paleolithic Sample

Across Europe, Aurignacian archaeological industries appear between approximately 40 to 35 ka BP, marking the beginning of the Upper Paleolithic (Conard and Bolus, 2003). In contrast with Middle Paleolithic industries such as the Mousterian, the Aurignacian is marked by an increase in the production of lithic blades, worked bone, antler and ivory tools, an explosion of symbolic or ornamental artifacts, and secure evidence of intentional burials (Churchill and Smith, 2000). These trends intensify across the transition to the Gravettian, an industry that began approximately 29 ka BP, spanning until ca. 24 ka BP, although this cultural shift may occur a few thousand years later in more western parts of Europe (Conard and Bolus, 2003). The present study focuses on fossils attributed to the early Upper Paleolithic (EUP), defined here the period encompassing the Aurignacian and Gravettian industries.

While there is general agreement regarding the artifacts used to define these industries (e.g., de Sonneville-Bordes, 1960; Henry-Gambier, 2002; Conard and Bolus, 2003), the hominins associated with the early Upper Paleolithic are less well known due to the paucity of human remains. However, where taxonomically diagnostic fossils are securely associated with Aurignacian levels, these clearly represent *H. sapiens* (Churchill and Smith, 2000). The majority of EUP fossil sample is European, comprised of 22 skeletons plus unassociated elements from seven site complexes; a single north African fossil (Nazlet Khater 2) is grouped with the EUP sample on the basis of its age and similar cranial morphology (e.g., Crevecoeur, 2006). The EUP fossils included in this study are described in turn below from oldest to youngest. The fossil localities are summarized in Table 2.7, and a detailed list of the elements represented at each site is provided in Table 2.10.

EUP: Nazlet Khater

The Nazlet Khater 2 burial was discovered in 1980 in the Nile Valley of Egypt, near the site of Nazlet Khater 4, an Upper Paleolithic chert quarry exploited between roughly 35 to 40 ka BP (Vermeersch et al., 1984). Although not directly associated with the mine, skeletal lesions on the skeleton are consistent with stress incurred by habitual heavy load carrying and repeated movements (Crevecoeur and Villotte, 2007). Nazlet Khater 2 has been directly dated by ESR on dental enamel to 38 ± 6 ka BP (Crevecoeur, 2006), making it contemporaneous with the earliest Upper Paleolithic of Europe. The skeleton exhibits a mosaic of modern and archaic characters, but is accepted as *H. sapiens* by all workers (Thoma, 1984; Pinhasi and Semal, 2000; Crevecoeur, 2006). In particular, the fossil bears cranial similarities to European Upper Paleolithic specimens (Bräuer and Rimbach, 1990). The lower limbs appear disproportionately short relative to their shaft diameters and to the upper limbs, a condition which Crevecoeur (2006) observed to be reminiscent of the pathological Dolní Věstonice 15 individual (Formicola et al., 2001), although she found no other evidence for displaysia or a similar condition in Nazlet Khater. Crevecoeur (2006) diagnosed this specimen as male on the basis of pelvic morphology. The original fossil was studied at l'Université de Bordeaux 1 in Bordeaux, France.

EUP: Mladeč

Excavations in the Mladeč Cave I and II in the Czech Republic yielded over 100 human fossils over the course of the late 19th and early 20th centuries, but well over half of these were lost during the 1945 fire at Mikulov Castle (Svoboda, 2000). Artifacts such as bone points and awls found with the fossils suggest an Early to Middle Aurignacian age for these humans (Churchill and

Smith, 2000). Radiocarbon dates from sedimentary carbonates in levels bracketing the human remains provide an age of 34,160 to 34,930 (+520/–490) years BP (Svoboda et al., 2002). Geological evidence suggests a rapid deposition for the fossiliferous levels in both caves (Svoboda, 2000). Recently, AMS ^{14}C dating of the teeth from four individuals confirmed the contemporaneous age of the fossils, and provided an uncalibrated age of ca. 31 ka BP (Wild et al., 2005). An isolated ulna was found to be younger (ca. 26 ka BP), but there are concerns of modern contamination in the sample (Wild et al., 2005).

The assemblage has long been described as essentially modern, although some workers have identified certain aspects of morphology that are reminiscent of Neandertals including occipital bunning, large teeth, and relatively large postcranial articular surfaces in the presumed male specimens (Teschler-Nicola, 2007). However, mtDNA extracted from two inviduals does not exhibit the sequences found in the Neandertals sampled to date (Serre et al., 2004). All postcranial elements are unassociated finds, but on the basis of cranial size and morphology, both sexes are believed to be represented at the site (Teschler-Nicola, 2007). Eight of the best-preserved original postcranial specimens (2 humeri, 1 ulna, 1 radius, 2 os coxae, and 2 femora) were studies at the Naturhistorische Museum in Vienna, Austria.

EUP: Paviland

Found in 1823 by an Oxford geologist, the partial skeleton from Goat's Hole near Paviland in southern Wales was romantically dubbed "The Red Lady" because of extensive ochre-staining and feminine ornaments such as perforated shells and polished ivory rings (Aldhouse-Green, 2000). A rich lithic assemblage recovered from the cave is attributed to the late Aurignacian, but until recently the fossil was believed to represent a slightly younger burial (ca. 26 ka BP) intrusive

into the older Aurignacian levels (Pettitt, 2000). Jacobi and Higham (2008) recently provided revised AMS ^{14}C dates of ca. 28 to 29 ka BP for the specimen based on collagen extracted from rib and scapula fragments, placing it in the early Gravettian.

The specimen is interpreted as a young adult male based on the overall morphology of the preserved postcrania including the left os coxae (Trinkaus, 2000), and the specimen is accepted as *H. sapiens* by all workers (e.g., Aldhouse-Green, 2000). A high quality cast of the fossil was studied at the Oxford University Museum of Natural History, Oxford UK, because the original was undergoing preparation for exhibition in Wales.

EUP: Cro-Magnon

The Cro-Magnon rockshelter in Dordogne, France, was discovered in 1868 by railway workers, and immediately recognized as a Pleistocene locality based on the presence of extinct fauna such as the woolly mammoth (Lartet, 1868). Lithics, worked bone, and perforated shells and teeth associated with the human remains are attributed to an evolved Aurignacian industry, suggesting an age of ca. 30 ka BP based on comparisons with other French sites (de Sonneville-Bordes, 1960). Recently, Henry-Gambier (2002) reported an AMS ^{14}C date of 27,680 ± 200 BP for a perforated shell associated with the burials, an age which corresponds to the early Gravettian of western Europe. The site yielded three associated partial adult skeletons, including the edentulous "Old Man" (No. 1), a probable female (No. 2), and a probable male (No. 3), in addition to numerous isolated elements (Vallois and Billy, 1965). These fossils are universally accepted as *H. sapiens*, and the name Cro-Magnon has become synonymous with early modern Europeans (e.g., Broca, 1868; Verneau, 1908; Vallois and Billy,

1965; Vlcek, 1967). The original Cro-Magnon fossils were studied at the Musée de l'Homme in Paris, France.

EUP: Dolní Věstonice & Pavlov

The Dolní Věstonice site complex in the Czech Republic consists of three sites (Dolní Věstonice I and II, and Pavlov I) along the hillside between the villages of Dolní Věstonice and Pavlov (Svoboda et al., 2000). Dolní Věstonice I was extensively explored in the 1920s and 30s, but most of the human material found at this time was destroyed in the 1945 fire of Mikulov Castle (Sládek et al., 2000). Renewed excavation of the hillside resulted in the discovery of the other sites which yielded six associated skeletons, including a triple burial, in addition to several isolated remains (Jelínek, 1987; Sládek et al., 2000). The sites preserve a rich cultural deposit including evidence of structures, hearths, lithics, worked bone, antler and ivory pieces, as well as symbolic objects fashioned out of faunal remains and fired clay; these artifacts link the site complex to occupations from the Pavlovian period, a regional early Upper Paleolithic industry corresponding to the early Gravettian of western Europe (Svoboda et al., 2000). The site has been extensively dated by AMS ^{14}C applied to charcoal associated with the burials, as well as dates obtained directly from human bones recovered from the Dolní Věstonice II site; these dates confirm an age between 25 to 27 ka BP for the fossils (Trinkaus et al., 2000; Svoboda et al., 2002).

Specimen 3 from the Dolní Věstonice I site is the only female associated skeleton presently known for the area (Trinkaus and Jelínek, 1997). Specimen 16 from Dolní Věstonice II and the associated skeleton of Pavlov I are interpreted as adult males (Sládek et al., 2000). In the triple burial, the lateral two individuals (No. 13 and 14) are reportedly males between 17 – 20 years old and present no skeletal anomalies, but the central individual (No. 15) is believed to have been

younger (15 – 17 years old) and shows a suite of pathological deformations throughout its skeleton (Jelínek, 1987; Formicola et al., 2001). For this reason, specimen 15 is omitted from the present study. An isolated femur (No. 35) recovered amongst the faunal from the pre-WWII excavation of Dolní Věstonice I is included in the sample. All fossils recovered from these sites are recognized as *H. sapiens* (Sládek et al., 2000). Permission to study the original material was not granted (Svoboda, pers. comm.). Thus, data were culled from the literature (Trinkaus and Jelínek, 1997; Sládek et al., 2000), potentially introducing inter-observer error to analysis, and reducing the sample size for many variables due to non-overlapping measurements.

EUP: Predmostí

The site of Predmostí in the Czech Republic has yielded a large assemblage of lithics and worked bone and ivory tools, in addition to the remains of more than two dozen humans believed to have been intentionally buried (Matiegka, 1934). In terms of cranial morphology, the Predmostí humans are similar to other Upper Paleolithic European fossils such as Cro-Magnon and Mladeč, and exhibit clear differences from Neandertals (Matiegka, 1934; Kidder et al., 1992). The site corresponds to the Evolved Pavlovian, a central European regional variety of the early Gravettian; it is argued to date between 25 and 27 ka BP based on artifact comparisons to other dated sites such as Dolní Věstonice (Svoboda et al., 2000; Svoboda et al., 2002).

Specimens 1, 3, 9, and 14 are suggested to represent males, while specimens 4 and 10 are classified as females based on cranial and postcranial size and morphology (Matiegka, 1934). Unfortunately, all of the human remains were lost in the fire at Mikulov Castle during the mid-20th century. Therefore, data for the associated skeletons of six adult individuals were collected from Matiegka's

(1938) description of the postcranial remains, taking care to ensure that similar measurement protocols were employed. Nonetheless, this potentially adds inter-observer error to the study, and data for many variables used here were unavailable, reducing sample size in serveral instances.

EUP: Balzi Rossi (the Grimaldi Caves)

The Balzi Rossi cliffs – or red rocks – located along the Mediterranean coast in the Liguria region of western Italy comprise a complex of caves (also known as the Grimaldi Caves) used as internement sites by early Europeans (Villeneuve, 1906). The Balzi Rossi fossils have long been acknowledged as *H. sapiens*, although they were originally believed to represent two distinct ethnic groups: the "Grimaldi Race" (Grotte des Enfants 5 and 6), said to exhibit features reminiscent of modern sub-Saharan Africans, and the "Cro-Magnon Race" for the other individuals based on similarities with specimens from the eponymous French site (Verneau, 1908). Since their discovery in the 19th century, the Grimaldi burials have been attributed to the either the late Aurignacian or Gravettian period based on ornament types and burial style (Verneau, 1908; Mussi, 1986). However, direct ^{14}C dating of a rib from Barma Grande 2 suggested a surprisingly young age of ca. 15 ka BP, while radiocarbon dates obtained from faunal remains believed to be associated with the triple burial (re-discovered at McGill University, Canada, in bags labeled only with depth information) further supported a young age between 19 and 14 ka BP (Bisson et al., 1996) for the Grimaldi sites.

Recently, direct AMS ^{14}C obtained from the metatarsal of the Barma Grande 6 specimen provides an age of 24,800 ± 800 BP, confirming a Gravettian-age for the site (Formicola et al., 2004). These workers found insufficient collagen in the Barma Grande 2 and 5 specimens to permit radiocarbon dating,

which together with the dubious association of the dated faunal remains to the burial may explain the anomalously young age previously reported. On the basis of similarity between all the burials in Barma Grande, Formicola and colleagues proposed a contemporaneous age for the entire Grimaldi human assemblage.

Five individuals were recovered in Barma Grande (i.e., the large cave): two adult males were found in single burials (No. 5 and 6), while the others occupied a triple burial comprised of one adult male (No. 2) plus two adolescents (No. 3 and 4) (Verneau, 1908). Only the adult specimens are included in this study. The original remains of Barma Grande 2 were studied at the Museo Balzi Rossi in Ventimiglia, Italy. Churchill and Formicola (1997) have documented marked bilateral asymmetry in the upper limb of this individual. They suggest that the individual was affected by direct trauma to the left arm or shoulder, causing adult onset of modified loading patterns resulting in a significantly smaller upper limb skeleton on the left side. In light of this, measurement of the Barma Grande 2 upper limb is limited to the right side, even though these elements are less well preserved. Specimens 5 and 6 were unvailalbe for study, therefore measurements of these skeletons were taken from Pearson (1997). Care was taken to ensure consistency of measurement protocols, but these data may nonetheless introduce inter-observer error into the analysis.

Two adult specimens were excavated from the Grotte des Enfants. Verneau (1908) described a single burial (No. 4) containing the complete skeleton of an adult male, and listed a double burial that preserves the complete skeleton of an adult female (No. 5) and a adolescent (No. 6) ornamented with numerous shell beads. The original Grotte des Enfants 4 and 5 adults were studied at the Musée d'anthropologie préhistorique in Monaco.

A complete skeleton believed to represent a male was recovered from the Grotte du Cavillon (i.e., Barma del Caviglione); this specimen is sometimes called "l'Homme de Menton" in recognition of the neighboring French town (Rivière,

1872). The original specimen was measured at the Musée de l'Homme in Paris, France. Three additional skeletons discovered in Baousso da Torre, another cave in the Balzi Rossi complex, are not included in this study because their present repository could not be determined.

Figure 2.1 Size, shape and form changes. In this example, the sphere changes in size by undergoing an equal magnitude of change in all directions, while the original spherical shape is preserved. The sphere changes in shape as it undergoes a differential magnitude of change in several directions, while the original volume remains constant. A new form occurs when the sphere undergoes a simultaneous change in size and shape (adapted from Richtsmeier et al., 1992).

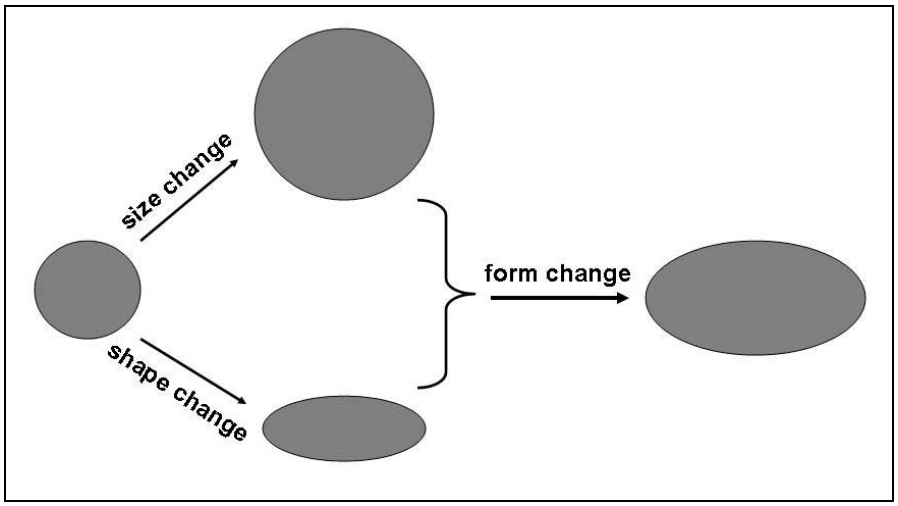

Figure 2.2 A schematic of the Omo I postcranial skeleton; the preserved portions, including newly recovered remains, are shown in black.

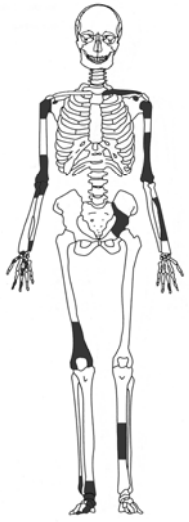

Table 2.1 Number of morphometric variables recorded per element.

Element	Number of Variables
Humerus	25
Ulna	21
Radius	16
Os Coxae*	11
Femur	18
Tibia	18
TOTAL	**109**

* Includes one angular measurement.

Table 2.2 Measurement error paired *t*-test results. Significant differences ($p < 0.05$) between the measurement assays are in bold. Table continues on the next page.

Variable	*p*	Variable	*p*	Variable	*p*
HUM1	0.266	***ULN1***	0.357	***RAD1***	0.616
HUM2	0.486	***ULN2***	0.374	***RAD2***	0.374
HUM3	0.621	***ULN3***	0.680	***RAD3***	0.286
HUM4	0.305	***ULN4***	0.101	***RAD4***	0.407
HUM5	0.398	***ULN5***	0.953	***RAD5***	0.330
HUM6	0.398	***ULN6***	0.566	***RAD6***	0.571
HUM7	0.515	***ULN7***	0.598	***RAD7***	0.454
HUM8	0.960	***ULN8***	0.241	***RAD8***	0.719
HUM9	0.620	***ULN9***	0.338	***RAD9***	0.380
HUM10	0.237	***ULN10***	**0.004**	***RAD10***	0.164
HUM11	0.749	***ULN11***	0.097	***RAD11***	**0.026**
HUM12	0.235	***ULN12***	0.750	***RAD12***	0.267
HUM13	0.066	***ULN13***	0.863	***RAD13***	0.068
HUM14	**0.013**	***ULN14***	0.670	***RAD14***	0.868
HUM15	0.459	***ULN15***	0.983	***RAD15***	0.266
HUM16	0.163	***ULN16***	0.386	***RAD16***	0.529
HUM17	0.099	***ULN17***	0.264		
HUM18	0.621	***ULN18***	0.857		
HUM19	0.653	***ULN19***	0.104		
HUM20	0.338	***ULN20***	0.938		
HUM21	0.541	***ULN21***	0.178		
HUM22	**0.033**				
HUM23	0.241				
HUM24	0.435				
HUM25	0.324				

Table 2.2 Continued.

Variable	*p*	Variable	*P*	Variable	*p*
PEL1	0.497	***FEM1***	0.374	***TIB1***	0.447
PEL2	0.319	***FEM2***	0.178	***TIB2***	0.757
PEL3	**0.022**	***FEM3***	0.315	***TIB3***	0.294
PEL4	0.253	***FEM4***	0.061	***TIB4***	0.225
PEL5	0.328	***FEM5***	0.491	***TIB5***	0.664
PEL6	0.396	***FEM6***	**0.034**	***TIB6***	0.940
PEL7	0.947	***FEM7***	0.326	***TIB7***	0.540
PEL8	0.482	***FEM8***	0.469	***TIB8***	0.395
PEL9	0.324	***FEM9***	0.504	***TIB9***	0.081
PEL10	0.767	***FEM10***	0.338	***TIB10***	0.357
PEL11	0.666	***FEM11***	0.148	***TIB11***	0.066
		FEM12	**0.015**	***TIB12***	0.191
		FEM13	0.692	***TIB13***	0.205
		FEM14	0.472	***TIB14***	0.589
		FEM15	0.094	***TIB15***	0.778
		FEM16	0.050	***TIB16***	0.495
		FEM17	0.178	***TIB17***	0.324
		FEM18	0.252	***TIB18***	0.529

Table 2.3 Average % Error for each variable employed in this study. Errors > 3% are in bold; these variables may be unreliable and should be treated with caution. Table continues on the next page.

Variable	% Error	Variable	% Error	Variable	% Error
HUM1	0.00	***ULN1***	0.53	***RAD1***	0.65
HUM2	0.14	***ULN2***	0.04	***RAD2***	0.15
HUM3	0.61	***ULN3***	0.62	***RAD3***	0.97
HUM4	0.20	***ULN4***	0.95	***RAD4***	1.22
HUM5	0.20	***ULN5***	1.79	***RAD5***	0.60
HUM6	0.48	***ULN6***	0.76	***RAD6***	1.45
HUM7	**5.05**	***ULN7***	2.22	***RAD7***	0.64
HUM8	**8.49**	***ULN8***	2.14	***RAD8***	**3.89**
HUM9	**3.23**	***ULN9***	0.91	***RAD9***	2.73
HUM10	**7.01**	***ULN10***	1.75	***RAD10***	1.13
HUM11	0.17	***ULN11***	1.05	***RAD11***	1.70
HUM12	0.31	***ULN12***	2.36	***RAD12***	2.62
HUM13	1.80	***ULN13***	1.31	***RAD13***	1.53
HUM14	1.23	***ULN14***	2.08	***RAD14***	0.67
HUM15	2.48	***ULN15***	1.92	***RAD15***	1.03
HUM16	1.27	***ULN16***	**6.19**	***RAD16***	1.68
HUM17	0.27	***ULN17***	**4.15**		
HUM18	0.35	***ULN18***	**3.24**		
HUM19	**3.08**	***ULN19***	1.62		
HUM20	1.16	***ULN20***	0.97		
HUM21	0.60	***ULN21***	0.57		
HUM22	1.56				
HUM23	1.87				
HUM24	2.09				
HUM25	1.52				

Table 2.3 Continued.

Variable	% Error	Variable	% Error	Variable	% Error
PEL1	1.54	***FEM1***	0.00	***TIB1***	0.37
PEL2	0.42	***FEM2***	0.04	***TIB2***	0.25
PEL3	0.56	***FEM3***	0.93	***TIB3***	1.65
PEL4	1.15	***FEM4***	0.46	***TIB4***	1.56
PEL5	1.48	***FEM5***	0.39	***TIB5***	1.28
PEL6	1.89	***FEM6***	0.21	***TIB6***	1.92
PEL7	0.54	***FEM7***	0.86	***TIB7***	1.87
PEL8	1.04	***FEM8***	2.91	***TIB8***	**3.89**
PEL9	2.63	***FEM9***	1.45	***TIB9***	1.04
PEL10	2.86	***FEM10***	2.79	***TIB10***	0.93
PEL11	2.02	***FEM11***	1.42	***TIB11***	0.37
		FEM12	1.90	***TIB12***	0.63
		FEM13	2.76	***TIB13***	1.74
		FEM14	**5.52**	***TIB14***	1.01
		FEM15	0.30	***TIB15***	0.35
		FEM16	0.76	***TIB16***	0.72
		FEM17	0.44	***TIB17***	1.29
		FEM18	1.94	***TIB18***	1.45

Table 2.4 Estimates of the intra-observer technical error of measurement (TEM) for the morphometric variables. TEM values have the same unit as the original measurement. Table continues on the next page.

Variable	TEM	Variable	TEM	Variable	TEM
HUM1	0.000	***ULN1***	2.214	***RAD1***	2.688
HUM2	0.791	***ULN2***	0.158	***RAD2***	0.632
HUM3	0.234	***ULN3***	0.180	***RAD3***	0.247
HUM4	0.063	***ULN4***	0.209	***RAD4***	0.250
HUM5	0.152	***ULN5***	1.072	***RAD5***	0.247
HUM6	0.342	***ULN6***	0.342	***RAD6***	0.541
HUM7	0.572	***ULN7***	0.870	***RAD7***	0.266
HUM8	0.917	***ULN8***	0.901	***RAD8***	2.062
HUM9	3.614	***ULN9***	0.338	***RAD9***	1.641
HUM10	1.015	***ULN10***	0.737	***RAD10***	0.297
HUM11	0.164	***ULN11***	0.370	***RAD11***	0.411
HUM12	0.231	***ULN12***	0.778	***RAD12***	0.683
HUM13	0.519	***ULN13***	0.376	***RAD13***	0.636
HUM14	0.424	***ULN14***	1.372	***RAD14***	0.345
HUM15	1.119	***ULN15***	0.693	***RAD15***	0.791
HUM16	0.664	***ULN16***	1.306	***RAD16***	1.581
HUM17	0.111	***ULN17***	1.831		
HUM18	0.104	***ULN18***	1.012		
HUM19	1.255	***ULN19***	0.443		
HUM20	0.240	***ULN20***	0.982		
HUM21	0.177	***ULN21***	0.316		
HUM22	0.354				
HUM23	4.902				
HUM24	5.692				
HUM25	1.739				

Table 2.4 Continued.

Variable	TEM	Variable	TEM	Variable	TEM
PEL1	1.404	***FEM1***	0.000	***TIB1***	2.372
PEL2	0.367	***FEM2***	0.316	***TIB2***	1.581
PEL3	0.993	***FEM3***	0.421	***TIB3***	0.610
PEL4	1.059	***FEM4***	0.212	***TIB4***	0.563
PEL5	0.715	***FEM5***	0.288	***TIB5***	1.116
PEL6	0.772	***FEM6***	0.152	***TIB6***	2.327
PEL7	0.329	***FEM7***	0.433	***TIB7***	1.290
PEL8	0.250	***FEM8***	1.331	***TIB8***	1.828
PEL9	1.704	***FEM9***	2.093	***TIB9***	0.718
PEL10	1.562	***FEM10***	2.071	***TIB10***	0.490
PEL11	2.579	***FEM11***	0.677	***TIB11***	0.164
		FEM12	0.942	***TIB12***	0.256
		FEM13	0.553	***TIB13***	1.126
		FEM14	3.763	***TIB14***	0.756
		FEM15	0.389	***TIB15***	1.581
		FEM16	0.866	***TIB16***	3.162
		FEM17	0.632	***TIB17***	1.739
		FEM18	3.162	***TIB18***	1.581

Table 2.5. Coefficient of reliability (*R*) for the morphometric variables selected for this study. Variables with *R* values < 0.95 are in bold; these variables should be used with caution. Variables marked with an asterisk have been removed from the study. Table continues on the next page.

Variable	*R*	Variable	*R*	Variable	*R*
HUM1	1.000	***ULN1***	1.000	***RAD1***	1.000
HUM2	1.000	***ULN2***	1.000	***RAD2***	1.000
HUM3	0.995	***ULN3***	0.996	***RAD3***	0.990
HUM4	0.998	***ULN4***	0.984	***RAD4****	**0.805**
HUM5	0.997	***ULN5***	0.955	***RAD5***	0.988
HUM6	0.999	***ULN6***	0.994	***RAD6***	0.983
HUM7*	**0.847**	***ULN7***	0.964	***RAD7***	0.988
HUM8*	**0.509**	***ULN8***	0.991	***RAD8***	**0.909**
HUM9	0.998	***ULN9***	0.973	***RAD9***	0.989
HUM10*	**0.498**	***ULN10***	0.970	***RAD10***	**0.936**
HUM11	1.000	***ULN11***	0.989	***RAD11****	**0.872**
HUM12	0.987	***ULN12***	0.952	***RAD12****	**0.404**
HUM13	**0.910**	***ULN13***	0.953	***RAD13***	0.982
HUM14	0.987	***ULN14***	0.992	***RAD14***	0.996
HUM15	0.995	***ULN15***	0.953	***RAD15***	0.998
HUM16*	**0.819**	***ULN16****	**0.612**	***RAD16***	0.995
HUM17	1.000	***ULN17***	0.992		
HUM18	0.999	***ULN18***	0.950		
HUM19	0.947	***ULN19***	0.996		
HUM20	0.973	***ULN20***	0.982		
HUM21	0.993	***ULN21***	1.000		
HUM22	**0.890**				
HUM23	0.994				
HUM24	0.993				
HUM25	0.996				

Table 2.5 Continued.

Variable	*R*	Variable	*R*	Variable	*R*
PEL1	0.976	***FEM1***	1.000	***TIB1***	1.000
PEL2	1.000	***FEM2***	1.000	***TIB2***	1.000
PEL3	1.000	***FEM3***	0.999	***TIB3***	1.000
PEL4*	**0.890**	***FEM4***	0.999	***TIB4***	0.986
PEL5	0.992	***FEM5***	0.988	***TIB5***	0.999
PEL6	0.993	***FEM6***	0.996	***TIB6***	0.994
PEL7	0.996	***FEM7***	0.998	***TIB7***	0.998
PEL8	1.000	***FEM8***	**0.921**	***TIB8***	0.992
PEL9	0.997	***FEM9***	0.998	***TIB9***	0.999
PEL10	0.958	***FEM10***	0.992	***TIB10***	0.999
PEL11	0.994	***FEM11***	0.992	***TIB11***	1.000
		FEM12	0.993	***TIB12***	0.999
		FEM13	0.963	***TIB13***	0.988
		FEM14	**0.948**	***TIB14***	0.996
		FEM15	1.000	***TIB15***	1.000
		FEM16	0.999	***TIB16***	1.000
		FEM17	1.000	***TIB17***	1.000
		FEM18	0.998	***TIB18***	1.000

Table 2.6 Composition of the skeletal reference samples.

	Sample Size*	Known Sex	Temporal Depth (years)
Recent African			
Zulu	42	Yes	negligible
Kikuyu	40	Yes	negligible
Nilotic Ugandan	33	Yes	negligible
Archaeological African			
Khoe-San	98	No	ca. 10,000
Sudanese	94	No	ca. 10,000
Taforalt	31	No	ca. 4,000 – 9,000

* Maximum number of individuals studied. Sample size may be less for select variables due to poor preservation (see Chapter 2 and Appendix 2 for details).

Table 2.7 Middle Stone Age and Early Upper Paleolithic early *H. sapiens* fossils included in this study.

Site	Skeletal Material	Approximate Age (years BP)
Middle Stone Age (MSA)		
Omo Kibish	1 skeleton plus an isolated tibia fragment	195,000
Skhūl	7 skeletons	43,000 – 173,000
Qafzeh	4 skeletons	88,000 – 97,000
Klasies River	Isolated postcranial elements	80,000 – 100,000
Border Cave	Isolated humerus fragment	60,000 – 170,000
Cave of Hearths	Isolated radius fragment	MSA or late ESA
East Turkana (Ileret)	Isolated femur fragment	≥ 180,000
Early Upper Paleolithic (EUP)		
Nazlet Khater	1 skeleton	38,000
Mladeč	Isolated postcranial fragments	31,000 – 34,000
Paviland	1 skeleton	28,000 – 29,000
Cro-Magnon	3 skeletons plus isolated postcranial fragments	28,000
Dolní Věstonice and Pavlov	5 skeletons plus isolated postcranial fragment	25,000 – 27,000
Predmostí	6 skeletons	25,000 – 27,000
Barma Grande	3 skeletons	25,000
Grotte des Enfants	2 skeletons	25,000
Grotte du Cavillon	1 skeleton	25,000

Table 2.8 Inventory of the Omo I elements included in this study.

Specimen Number*	Element	Side
KHS 1-32	Clavicle	Lt
KHS 1-33	Humerus, proximal	Rt
KHS 1-30	Humerus, diaphysis + distal	Rt
KHS 1-34	Humerus, proximal	Lt
KHS 1-31	Humerus, diaphysis + distal	Lt
KHS 1-39	Ulna, proximal	Rt
KHS 1-9	Ulna, distal	Rt
KHS 1-19	Radius, proximal + diaphysis	Rt
KHS 1-48	Radius, diaphysis	Lt
KHS 1-60A	Os coxae, central and posterior aspect	Lt
KHS 1-60B	Os coxae, iliac crest fragment	Lt
KHS 1-29A/B	Femur, diaphysis + distal	Rt
KHS 1-51A/B	Tibia, diaphysis + distal	Rt
KHS 1-47	Tibia, diaphysis	Lt

***** Following the revised sequence (Pearson et al., 2008b).

Table 2.9 Inventory of the Levantine early *H. sapiens* postcranial specimens included in this study.

Specimen	Elements	Sex*
Skhūl		
2	Humerus, ulna, radius	Female
3	Femur, tibia	Male
4 (cast)	Humerus, ulna, radius, os coxae, femur, tibia	Male
5	Humerus, ulna, radius, os coxae, femur, tibia	Male
6	Humerus, ulna, femur, tibia	Male
7	Humerus, ulna, radius, os coxae, femur	Female
9	Os coxae, femur	Male
Qafzeh		
3	Humerus, ulna, radius, femur, tibia	Female
7	Ulna	?
8	Humerus, ulna, tibia	Male
9	Humerus, ulna, radius, os coxae, femur, tibia	Female

***** Sex diagnosis for the fossils based on a qualitative assessment of all available skeletal remains in the original description of the material (Skhūl: McCown and Keith, 1939; Qafzeh: Vandermeersch, 1981).

Table 2.10 Inventory of the early Upper Paleolithic (EUP) *H. sapiens* fossils included in this study. Table continues on the next page.

Specimen	Elements	Sex*
Nazlet Khater		
2	Humerus, ulna, radius, os coxae, femur, tibia	Male
Mladeč		
21	Os coxae	Female
22	Os coxae	Male
23	Humerus	?
24	Humerus	?
25a	Radius	?
25c	Ulna	?
28	Femur	?
35	Femur	?
Paviland		
1 (cast)	Humerus, ulna, radius, os coxae, femur, tibia	Male
Cro-Magnon		
1	Humerus, ulna, os coxae, femur, tibia	Male
2	Humerus, ulna, radius, os coxae, femur, tibia	?Female
3	Humerus, ulna, femur, tibia	?Male
4305	Radius (left)	?
4307	Radius (left)	?
4315	Os coxae	?
Dolní Věstonice		
3	Humerus, ulna, radius, femur, tibia	Female
13	Humerus, ulna, radius, os coxae, femur, tibia	Male
14	Humerus, ulna, radius, os coxae, femur, tibia	Male
16	Humerus, ulna, radius, os coxae, femur, tibia	Male
35	Femur	?
Pavlov 1	Humerus, ulna, radius, femur	Male
Predmostí		
1	Femur, tibia	Male
3	Humerus, ulna, radius, femur, tibia	Male
4	Humerus, ulna, radius, femur, tibia	Female
9	Humerus, ulna, radius, femur, tibia	Male
10	Humerus, ulna, radius, femur, tibia	Female
14	Humerus, ulna, radius, femur, tibia	Male

Table 2.10 Continued.

Specimen	Elements	Sex*
Barma Grande		
2	Humerus, ulna, radius, os coxae, femur, tibia	Male
5	Humerus, tibia	Male
6	Femur, tibia	Male
Grotte des Enfants		
4	Humerus, ulna, radius, os coxae, femur, tibia	Male
5	Humerus, ulna, radius, os coxae, femur, tibia	Female
Grotte du Cavillon		
1	Humerus, ulna, radius, os coxae, femur, tibia	Male

***** Sex diagnosis for the fossils based on the assessment of all available elements preserved for the individual (Barma Grande: Verneau, 1908; Cro-Magnon: Vallois and Billy, 1965; Dolní Věstonice: Sládek et al., 2000; Grotte des Enfants: Verneau, 1908; Grotte du Cavillon: Verneau, 1908; Mladeč: Teschler-Nicola, 2007; Nazlet Khater: Crevecoeur, 2006; Paviland: Aldhouse-Green, 2000; Predmostí: Matiegka, 1934.

Chapter 3

A Test of Methods for Determining Sex Using Fragmentary Os Coxae

Introduction

Goals

The development of reliable sex classification methods for prehistoric humans is a necessary first step in evaluating the contribution of sexual dimorphism to both the magnitude and pattern of variation in past populations. The goal of this chapter is to compare the accuracy of two methods for sex determination from the central and posterior os coxae, in order to assess the appropriateness of these methods for samples where sex is undocumented and preservation is poor. One method, Bruzek's Visual Method (2002) is based on scoring non-metric traits, while the other, Discriminant Function Analysis, uses multivariate analyses of metric variation to classify sex (e.g., Pietrusewsky, 2000). As will be described below, each method offers possible advantages and drawbacks in the classification of sex from fragmentary os coxae. By testing the accuracy of the methods in modern African population samples, this study will specifically evaluate their applicability to reliably determine sex in human remains that may share biological adaptations to life in equatorial environments. Subsequently, the most successful method will be applied to the archaeological and fossil samples collected for this dissertation (Chapter 4), which will enable an assessment of possible differences in sexual dimorphism between these samples.

Determining Sex from Skeletal Remains

Due to the dual role of the female pelvis in parturition and locomotion, the pelves of adult humans exhibit a suite of anatomical differences that distinguish between the sexes. The os coxae is the most reliable skeletal indicator of sex (Buikstra and Ubelaker, 1994; Milner et al., 2000; White and Folkens, 2000). However, taphonomic processes acting on the archaeological and fossil record (and sometimes forensic contexts) play a critical role in limiting the suitability of sex classification methods (Abella Roth, 1992; White and Folkens, 2000; Scheuer, 2002). Not only is the skeleton frequently disarticulated in these situations, but individual elements may also suffer substantial postmortem damage. Thus, many of the features that are obstetrically related to sex differences in the pelvis such as the shape and width of the pelvic inlet and the angle of the sub-pubic arch (e.g., Phenice, 1969; MacLaughlin and Bruce, 1990) may be difficult or impossible to evaluate in incomplete specimens. Moreover, certain skeletal elements are particularly vulnerable to damage due to their shape, size or delicate composite (Reitz and Wing, 1999). The pubis is especially prone to poor preservation since it is narrow, covered by a thin layer of cortical bone, and maybe placed in a more vulnerable or exposed position in many burial postures due to its anterior placement in the skeleton (White and Folkens, 2000). Waldron (1987) estimates that the pubis is preserved in less than 30% of archaeological cases. Consequently, the many well-recognized sex differences observed on the pubis, such as those reported by Phenice (1969), and indices that capture the relative length of this element such as the ischiopubic or acetabulopubic index (e.g., Washburn, 1948; Thieme and Schull, 1957; Novotný, 1986; Bruzek, 2002), are of limited use in studies of archaeological remains.

In contrast to the pubis, the central and posterior aspects of the os coxae, especially the bony areas about the sacroiliac joint, the acetabulum and the ischial tuberosity, are more durable and less vulnerable to decay. Workers have observed that the region around the sacroiliac joint, including the proximally-situated sciatic notch, exhibits a suite of sex-specific morphologies (Lazorthes and Lhés, 1939; Singh and Potturi, 1978; Iscan and Derrick, 1984; MacLaughlin and Bruce, 1986b; Novotný, 1986; Hager, 1996; Walker, 2005; Takahashi, 2006). As with the dimorphic features of the pubis and pelvic inlet, many of these differences appear likely to allow efficient locomotion and successful parturition in females. However, unlike the sex-specific traits of the pubis which are secondary sex characteristics that develop at puberty or following childbirth (Coleman, 1969), the dimorphic nature of the sciatic notch can be observed even in fetal stages of development (Holcomb and Konigsberg, 1995). This suggests that the sex-specific features of the sciatic notch have a strong genetic component. In contrast, other traits such as the preauricular sulcus and dorsal pitting on the pubis develop in response to the stresses of partuition (Houghton, 1974; Ullrich, 1975; Suchey et al., 1979; Cox and Scott, 1992), and as such they may offer less reliability in determining sex. The presence of these traits may positively identify a parous female, but the absence of these traits does not distinguish between males and nulliparous females. This can lead to male bias in the classificaiton of sex (Weiss, 1972).

Recognizing the need for sexing methods that can be applied to incomplete pelvic remains, researchers have proposed various techniques that focus on the dimorphism expressed in the sciatic notch and other anatomically-proximate areas of the pelvis. The approaches all exploit dimorphism in either discrete (i.e., non-metric) traits or metric variation in order to successfully distinguish between the sexes. Bruzek (2002) developed a new non-metric method by combining five isolated features of the os coxae that had been

demonstrated by others (e.g., Ferembach et al., 1980; Iscan and Derrick, 1984; Rogers and Saunders, 1994) to distinguish between the sexes with 95% accuracy. Because Bruzek's method relies on scoring isolated features, it can readily be modified for use on fragmentary os coxae by focusing exclusively on dimorphic features of the central and posterior region. This more limited application of the method is slightly less reliable, but still provides a satisfactory success rate of 90.8% (Bruzek, 2002).

In contrast to a method like Bruzek's, multivariate statistical techniques such as Principal Component Analysis and Discriminant Function Analysis offer the opportunity to identify in terms of metric variation the features that best distinguish the sexes, while accounting for correlation and covariation among variables (Pietrusewsky, 2000). These morphometric methods have been applied with varying levels of success (ca. 78% to 100% accuracy) to classify sex using various skeletal elements – singly or in combination – including the cranium (e.g., van Vark et al., 1989; van Vark and Schaafsma, 1992), most of the long bones (e.g., Richman et al., 1979; Murail et al., 1999; Safont et al., 2000), as well as the pelvis (e.g., Schulter-Ellis et al., 1983; Taylor and DiBennardo, 1984; Hager, 1989; Arsuaga and Carretero, 1994; Weisheit, 1997; Murail et al., 2005). The present study compares the accuracy of Bruzek's Visual Method using discrete traits with the accuracy of a novel Discriminant Function Analysis devised from measurements of the central and posterior aspects of the os coxae. The particulars of these methods will be described in greater detail below.

Non-metric and morphometric approaches such as those described above each offer certain advantages and drawbacks for the classification of sex. Proponents of methods that rely on scoring discrete traits list the speed of diagnosis and the lack of special equipment requirements as benefits (e.g., Phenice, 1969; Buikstra and Ubelaker, 1994). In comparison, morphometric methods may require that researchers carefully record numerous metric variables

in order to adequately capture the size and shape of each specimen, a task that may take a significant amount of time and requires calipers or possibly more expensive instruments such as a digitizer or camera, in addition to statistical analyses. Despite these possible drawbacks, metric variables are believed to be more objective than discrete traits, mostly because more experience with the range of human skeletal variation seems to be necessary to train the observer's eye before discrete traits can be reliably scored (Milner et al., 2000; Bruzek, 2002; Walker, 2005). This observation may explain the highly inconsistent results available for tests of the accuracy of the Phenice method to sex the pubis, which has been found to range from barely above chance (59%) to nearly perfect (96%) (Phenice, 1969; Lovell, 1989; MacLaughlin and Bruce, 1990; Rogers and Saunders, 1994). On the other hand, metric variables can be recorded by anyone with sufficient osteological knowledge to recognize the anatomical landmarks described in the measurement definitions, providing of course that well-defined landmarks are chosen.

Compared to discrete traits, metric differences might appear at first glance to offer a more reliable way of separating sexes, in part because a clear directional difference in size exists between them (Tague, 1989). For example, across a global array of human groups, males tend towards greater stature (Gray and Wolfe, 1980; Wolfe and Gray, 1982), which translates into a size difference in skeletal elements including the os coxae. In particular, because the acetabulum articulates with the head of the femur, the diameter of which is documented to be an accurate indicator of body size in primates including humans (e.g., Van Gerven, 1972; Grine et al., 1995), it comes as no surprise that males tend to have greater acetabular diameters compared to females. Ischium length also correlates positively with body size in humans and non-human primates (Leutenegger, 1982), and it is consistently greater in males than females. The ischial tuberosity is also larger in males, providing increased area for the attachment of the

hamstring muscles. However, dimorphism in muscularity does not necessarily correspond with dimorphism in size, since muscles develop in response to physical activity. Therefore, a muscle attachment site may be a misleading indicator of sex unless additional information is known about the lifestyle and division of labor for the group under study (Hamilton, 1982).

While size is a useful criterion by which to distinguish the sexes, the relationship between body size and the size of pelvic features creates the potential for bias in the classification of sex of populations that differ in overall body size compared to a standard reference. Specifically, since many ancient peoples and living hunter-gatherers tend towards greater skeletal robusticity and size than modern sedentary urbanites, a greater number of specimens may be classified as males. One study (Weiss, 1972) estimated that male bias could occur in up to 12% of cases where size is used to separate the sexes.

A related issue is that the level of sex differences expressed in the skeleton appears to vary between populations of humans (Washburn, 1949; Eveleth, 1975; Tobias, 1975; Hall, 1982; Oxnard, 1987; van Vark et al., 1989; O'Higgins et al., 1990; Humphrey et al., 1999; Franklin et al., 2008). On average, human males tend to be bigger than females, but precisely how much differs from one population to the next. Given the strong relationship between body size and both acetabular and ischial size as noted above, population-specific sex differences can also be expected in these features. The magnitude of dimorphism may also change within a population through time, as Hamilton (1982) demonstrated among Amerindians during the transition from the Middle to Late Woodland period in Illinois, and Tobias (1975) found among various tribal groups in southern Africa.

The difficulties associated with sexing based on size criteria can be overcome by employing size-independent variables such as angles or ratios in the Mosimann family of shape variables (Mosimann, 1970; Jungers et al., 1995) as

described in Chapter 2, or through the use of non-metric traits. While these precautions may account for size differences, they may not fully account for the population-specific expression of dimorphism in discrete traits or the shape of the pelvis. Although these differences remain poorly studied, a limited body of work demonstrates that such differences exist (MacLaughlin and Bruce, 1986a; Patriquin et al., 2003; Steyn et al., 2004; Walker, 2005). By using the same African reference samples to test the accuracy of Bruzek's Visual Method and the new Discrimiant Function Analysis of the os coxae, this study will compare the suitability of each method to classify sex in different populations.

Skeletal Samples

Data were collected from two known-sex recent African samples (Zulu and Kikuyu; see Chapter 2 for detailed descriptions) with near equal sex distributions. The Zulu sample comprises 42 individuals (n = 20 females, n = 22 males) for which os coxae were measured and scored for the pelvis sexing criteria. Due to missing os coxae and discrepancies in the curatorial records (either no record of sex, or conflicting information concerning the sex of the individual such as unexplained corrections in the catalogue), the Kikuyu sample consists of 27 known-sex individuals (n = 12 females, n = 15 males), a smaller number than the total sample described in Chapter 2. The modern Nilotic Ugandan sample is excluded from the sex determination study because only three females with os coxae were available. The Zulu and Kikuyu samples are considered singly, and also pooled into a single African sample comprised of 69 individuals (n = 32 females, n = 37 males).

These three samples are used to test the accuracy of the visual method and discriminant function analysis in classifying sex using partial os coxae. The visual method will be described first, followed by the accuracy results and

discussion of the utility of the visual method. The discriminant function analysis of the pelvis will be described next, followed by the accuracy results and discussion of the utility of this statistical method.

Method: Testing the Accuracy of the Visual Method

Description of the Visual Method

The visual method for the determination of sex from the human bony pelvis was proposed by Bruzek (2002), building on a combination of earlier approaches that relied on scoring isolated characters of the pelvis (Phenice, 1969; Ferembach et al., 1980; Iscan and Derrick, 1984). In Bruzek's new method, five characters are selected to represent two separate regions of the modern pelvis known be dimorphic: the sacroiliac complex, including the preauricular surface, composite arch, and greater sciatic notch characters, and the ischiopubic complex, including the the inferior pubis and ischiopubic proportions characters. These five characters are individually scored as male, female or intermediate; final sex assignment is based on the majority score from the five characters, with equal male and female scores resulting in an indeterminate sex assignment. The score of three characters (preauricular surface, greater sciatic notch, and inferior pelvis) is based on the evaluation of three sub-characters each, with the majority score determining the final diagnosis for that particular character. The remaining two characters (composite arch and ischiopubic proportions) consist of a single aspect scored directly as male, female or intermediate. Bruzek (2002) demonstrated an accuracy of 95% for this method when he tested it against two known-sex European samples (n = 402).

This study employs a modified version of Bruzek's visual method to test its utility in studies of archaeological and fossil samples . Here, only the three

characters of the sacroiliac complex are considered in the determination of sex. The characters of the ischiopubic complex are omitted because the fragile and thin pubis is frequently damaged or missing in archaeological and fossil skeletons. Bruzek (2002) achieved an accuracy of 90.8% when testing this more limited visual method on two European samples, demonstrating the utility of the evaluating the sacroiliac complex alone in cases where the pubis is damaged or missing. The protocol for scoring the characters of the sacroiliac complex (preauricular surface, composite arch, and greater sciatic notch) will be described in turn. The following letter-based scoring system is employed for each character and sub-character: the female condition is scored as "F", the male condition is scored as "M", and an intermediate condition is scored as "I", while a blank represents the unavailability of material for evaluation. Efforts were made to minimize bias that could result from a priori knowledge of the sex of each individual when scoring the characters and sub-characters. For example, the sex was recorded in a separate spreadsheet from the sexing scores. The scoring of sexing features was performed at the end of data collection for an individual, to allow the greatest amount of time to have elapsed between recording the sex and scoring the characters for sex determination. However, knowledge of the sex of a specimen (and thus potential bias in scoring) could not be entirely avoided due to need to sample a roughly equal distribution of males and females from each population, and because the sex was occasionally marked directly on the os coxae.

Preauricular Surface Character: 3 sub-characters

The preauricular surface presents three sub-characters that may independently correlate with sex, and are therefore scored independently (Bruzek, 2002). The final diagnosis of sex determined from the preauricular surface (PS) character is based on the majority score from the three sub-characters. The

preauricular surface is located immediately inferior to the inferior demi-face of the auricular surface on the internal aspect of the os coxae (Figure 3.1). The first sub-character considers the presence of negative relief on the preauricular surface (PS1). Some degree of negative relief along the preauricular surface can result from the pull of ligaments across the sacroiliac joint (Weisl, 1954), and can be related to overall skeletal robusticity (Lazorthes and Lhés, 1939) or stress from partuition (Houghton, 1974; Ullrich, 1975; Cox and Scott, 1992). PS1 is scored using the following criteria: F = deep, well-delimited negative relief (deep depression or pits), M = no negative relief (smooth surface) to slight negative relief (slight depression or pits), or I = intermediate condition. A typical female and male example of PS1 is illustrated in Figure 3.2.

The second sub-character evaluates the development of negative relief on the preauricular surface (PS2) using the following criteria: F = depression or pits have a closed circumference (i.e., the arc presents as more than half a circle), M = there is no negative relief, or the depression has an open circumference (i.e., the arc presents as less than half a circle), or I = intermediate condition. Figure 3.3 depicts an typical female and male condition for PS2. Bruzek (2002) interprets negative relief (i.e., PS1 = F) scored as "F" in this sub-character as a true preauricular groove, which has been claimed to result from stress placed on the sacroiliac joint during parturition (e.g., Houghton, 1974). Thus, a score of F in sub-characters PS1 and PS2 characterizes the os coxae of a parous female. However, not all parous females exhibit a true preauricular groove (Ullrich, 1975). Therefore, although the presence of this trait positively identifies a parous female, the absence of this trait cannot distinguish between parous females, nulliparous females, and males. On the other hand, Bruzek (2002) interprets negative relief (i.e., PS1 = F) scored as "M" for PS2 as a paraglenoid groove, which is believed to form in robust individuals (usually males) due to stressors

unrelated to childbirth (Weisl, 1954; Lazorthes and Lhés, 1939). Note that a score of "M" in PS2 is used here also to indicate the absence of negative relief.

Finally, the preauricular surface is examined for the presence of positive relief (PS3) using the following scoring criteria: F = no positive relief, M = clear positive relief, or I = intermediate condition. The typical female and male condition for PS3 is shown in Figure 3.4. A PS3 score of "M" marks the presence of a piriform tubercle, the attachment for the piriformis muscle (Bruzek, 2002). This trait is associated with high levels of muscularity, especially in males; females rarely exhibit a clearly defined piriform tubercle (Genovés, 1959).

The preauricular surface sub-characters (PS1-3) are scored independently. The final diagnosis of sex based on the preauricular surface is determined from the majority score of the sub-characters. For example, the following score combinations each result in a female diagnosis based on the PS character: "F-F-F", "F-M-F", "F-I-F", "F-F-I". According to Bruzek (2002), the combination "F-F-F" represents the most reliable female diagnosis (Figure 3.5), while all other combinations have a greater potential for the misclassification of females.

Composite Arch Character

The composite arch character (CA) has no sub-characters. In females, the superior demi-face contour is usually not continuous with the anterior sciatic notch contour (Figure 3.6a), thereby creating a composite arch or double curve (Genovés, 1959). The presence of a composite arch is scored as "F" (Bruzek, 2002). In males, the contour of the superior demi-face of the auricular surface can usually be traced as a continuous arch or single curve with the anterior contour of the sciatic notch, as shown in Figure 3.6b (Genovés, 1959). This state, in which the composite arch is absent, is scored as "M" (Bruzek, 2002). As with PS, an intermediate form is scored as "I".

Greater Sciatic Notch Character: 3 sub-characters

Bruzek's (2002) method for scoring the sub-characters of the greater sciatic notch (SN) involves creating a 'shadow image' of the contour of greater sciatic notch using photosensitive paper. To simplify data collection, the present study established a rigorous photographic protocol in lieu of a 'shadow image'. Here, the SN sub-characters are scored from digital photographs in Sigma Scan 5.0©. The techniques are based on the same concept and should be equivalent, but the photographic protocol has the advantage of providing a digital record of each specimen against which the scoring of other characters can be checked, and from which the sciatic notch angle can be measured. To photograph the specimens, the os coxae is placed with the external aspect lying flat on a hard surface with the ischial tuberosity against the surface (as depicted in Figure 3.1). The os coxae is then positioned such that the ischial spine, posterior inferior iliac spine and apex (i.e., the deepest portion) of the sciatic notch lie on the same plane which is perpendicular to the observer. A scale is placed next to the notch on the flat surface, and a small bubble level is placed on the back of the digital camera (the LCD screen rotates outwards, providing a secure place for the level without obstructing the screen). The level ensures that the photographs are taken parallel to the flat surface and the area of interest on the os coxae. The lens is centered on the sciatic notch, and the macro setting is used to photograph the following landmarks on the internal os coxae: full extent of the auricular surface and sciatic notch, including the ischial spine (or base, if broken), the posterior inferior iliac spine (PIIS), and the apex of the sciatic notch (e.g., Figure 3.2).

Assessment of the greater sciatic notch (SN) character requires the independent scoring of three sub-characters (SN1-3) from photographs analyzed in SigmaScan Pro 5.0. SN1 evaluates the relative proportion of the posterior and anterior sciatic notch chords (Bruzek, 2002). As shown in Figure 3.7, the

posterior chord (AB) extends from point A (PIIS, or the top of the piriform tubercle if the latter is present) to point B, the terminus of a line placed through the apex of the sciatic notch, while the anterior chord (BC) extends from point B to the base of the ischial spine (point C). Together, the posterior and anterior chords span the full extent of the sciatic notch. Following Bruzek (2002), the relative proportion of the chords (SN1) is scored as follows: F = posterior chord is longer than or equal to the anterior chord (Figure 3.7a), M = posterior chord is shorter than the anterior chord (Figure 3.7b), or I = intermediate condition. Females tend to exhibit a posteriorly sweeping posterior sciatic notch contour, which acts to length the posterior chord relative to the anterior chord thereby creating more equal proportions between the chords, while males tend to bear a very short posterior chord relative to the anterior chord (e.g., Singh and Potturi, 1978; Novotný, 1986; Rogers and Saunders, 1994).

Next, the form of the sciatic notch contour (PS2) is evaluated using the guidelines described by Bruzek (2002): F = the notch contour is symmetrical about the apex (Figure 3.7a), M = the notch contour is asymmetrical about the apex (Figure 3.7b), or I = indeterminate condition. Finally, the relative location of the posterior aspect of the sciatic notch contour (SN3) is evaluated. Using Sigma Scan Pro 5.0, a line (AD) is drawn superiorly from point A (PIIS, or the piriformis tubercle, if present); as depicted in Figure 3.8, this line is parallel to the line transecting the apex of the notch and perpendicular to the posterior chord. With the placement of the AD line, the relative position of the posterior notch contour (SN3) can be scored as follows: F = the posterior sciatic notch contour is anterior to line AD (Figure 3.8a), M = the posterior sciatic notch contour is posterior to line AD (Figure 3.8b), or I = intermediate condition (Bruzek, 2002). The final SN character diagnosis is based on the majority score obtained from the three sub-characters evaluated on digital photographs. Figure 3.8 illustrates a typical female and male diagnosis based on sciatic notch morphology.

Sacroiliac Complex: Final Diagnosis and Determining Accuracy

Using the scores of three characters (PS, CA, and SN), the majority score determines the final sex diagnosis based on sacroiliac complex morphology. For example, a typical female is characterized by a score of "F-F-F", while a typical male is characterized by a score of "M-M-M" (Figure 3.9). Combinations offering no majority score (e.g., "F-I-I" or "F-M-I") are classified as Indeterminate. To assess the accuracy of the visual method, the count and frequency of correct, incorrect, and indeterminate sex classification is computed for two known-sex African samples (Zulu, Kikuyu) and the combined African sample (pooled Zulu and Kikuyu).

Results: Accuracy of the Visual Method

The visual method correctly determined sex in 82.6% of cases in the combined African sample (Zulu + Kikuyu), as reported in Table 3.1. The overall error rate (i.e., the rate at which a male is incorrectly classified as a female or vice versa) was 13.0%, while sex was deemed Indeterminate in 4.4% of individuals. Accuracy was slightly higher in the Kikuyu sample alone (88.0% correct), but lower in the Zulu samples (83.3%). However, a greater frequency of misclassifications (errors) occurred in the Kikuyu sample compared to the Zulu (14.% vs 11.9% respectively). Among the Zulu, there is a large discrepancy in the success rate of the method between the sexes: only 70.0% of Zulu females were correctly classified, with 25% of females misclassified as males. In contrast, 95.5% of Zulu males were correctly classified, with 0% of males misclassified as females. Rates of correct and erroneous classifications are roughly equal between Kikuyu males and females.

It may be informative to consider the performance of each sacroiliac character separately, in order to evaluate whether a single character contributes to the error rate more than others. The accuracy of sex determination using the preauricular surface, composite arch and greater sciatic notch characters is listed in Tables 3.2 to 3.4 respectively. Among the three characters, preauricular surface achieved the highest frequency of correct classification (84.1% in the combined African sample), while the composite arch and sciatic notch characters had much lower success rates (72.5% and 73.9% respectively). The rate of misclassification was highest when the sciatic notch character alone was evaluated (24.6% error).

Discussion: Utility of the Visual Method to Classify Sex

At 82.6%, the overall accuracy of the visual method for sexing the pelvis using characters of the sacroiliac complex demonstrates that this method performs adequately, although it is certainly less than ideal. Here, the overall accuracy of the method is 8.2% lower than the accuracy reported by Bruzek (2002) when he tested the method on French and Portuguese samples. Although a slightly higher success rate was obtained for the Kikuyu compared to the Zulu, this result still translates to nearly 3% lower accuracy than has been previously reported. The rate of "indeterminate" sex diagnoses was roughly similar in the Kikuyu and Zulu samples studied here (3.7% and 4.8% respectively). These rates are low and compare well with the frequency of indeterminate cases in Bruzek's (2002) test (4.3% of French classified as indeterminate and 4.5% of Portuguese classified as indeterminate). However, at 13.0%, the overall error rate (i.e., the rate of misclassified individuals) is substantially higher than the 4.7% error rate reported by Bruzek. The error rate is larger in the Kikuyu than the Zulu sample, but both are still much higher than is desirable for a reliable sex determination method.

Several factors may explain the discrepancy in accuracy of the visual method between Bruzek's tests and the present application. This is the first test of the visual method on samples of non-European origin. As discussed previously, human populations exhibit a certain degree of variation in the expression of both the magnitude and pattern of sexual dimorphism (e.g., Tobias, 1975; Hall, 1982; van Vark et al., 1989; Humphrey et al., 1999; Franklin et al., 2008). In addition, African people can have dramatically different physiques than Europeans (e.g., Hiernaux, 1968; Ruff, 1994). A difference body size and shape might necessitate changes in the expression of dimorphism throughout the sacroiliac complex in order to maintain locomotor and birthing functionality with a different build. In particular, because the sciatic notch influences the size and shape of the pelvic inlet (the more open wider notch typical of females helps to enlarge the inlet), it is possible that the notch shape and contour could be altered if a more linear physique is achieved. In such a scenario, the relationship between the curvature of the superior demi-face of the auricular surface and the anterior curvature of the notch could also deviate from the usual male and female condition observed by Bruzek in modern Europeans. The influence of body build on the skeletal determination of sex warrants further investigation.

Secondly, the effect of lifestyle may play a role in the applicability of this method to diverse human populations. The European samples employed by Bruzek (2002) span the 19th century through the first half of the 20th century, which means that they are comprised of industrial-age individuals who most likely lead sedentary, urban lifestyles. The African samples used here are also from the mid-20th century, but these individuals represent a more diverse range of lifestyles that were likely substantially less urban and less sedentary non-urban than their European contemporaries. In particular, muscularity and skeletal robusticity may be greater in the African samples used here compared to Bruzek's European samples due to these lifestyle differences. Specifically, a more active

way of life among the Zulu and Kikuyu may contribute to increased robusticity or muscularity of the pelvis, possibly resulting in the 'masculinization' of certain aspects of the sacroiliac complex. The higher frequency of errors in diagnosing the sex of females in both the Zulu and Kikuyu lends support to this idea (Table 3.1). Notably, Zulu males were never misclassified as females, but misclassification occurred with 25% of Zulu females. Thus, at least among the Zulu it seems likely that female robusticity may confound attempts to classify females according to standards developed from other populations such as modern Europeans. A propensity towards male-bias was reported by Weiss (1972) in a comparative study of 30 human groups. Alternatively, traits such as the preauricular sulcus may develop differently in response to the stresses of partuition in these two populations.

Method: Testing the Accuracy of Discriminant Function Analysis

Discriminant function analysis (DFA) is a multivariate statistical method that can be used to assign an unknown specimen to a predefined group (Pietrusewsky, 2000). In this dissertation, the goal is to determine the sex of an individual by assigning it to either the female or male group in a reference sample using a combination of metric variables of the partial os coxae. Since there are only two possible groups (female and male) in a classification of sex, the DFA extracts a single linear combination of the original variables, called the discriminant function (DF), which expresses the greatest difference between the groups by maximizing the ratio of between-group and within-group variances (Quinn and Keough, 2002). Each individual (i) is defined by a score for each discriminant function (k) based on the following equation:

$$\text{Score}_{ik} = \text{constant} + c_1 y_{i1} + \ldots c_z y_{iz}$$

where *c* is an unstandardized coefficient measuring the relative contribution of each variable to the linear combination (i.e., Function 1 in this case because there are only two groups), *y* is the original value of the individual for that variable, and the constant term adjusts the means so that for all the individuals the mean discriminant score is zero (Quinn and Keough, 2002). Using these scores, the predefined groups (i.e., the sexes) are represented in multivariate space by a centroid defined as the vector of means for the variables of each group (Neff and Marcus, 1980). Boxplots are employed to visualize the distribution of discriminant scores for the individuals in a group relative to its centroid (represented as the horizontal bar typically indicative of the mean).

The success of DFA depends on the presence of significant differences between the group centroids (essentially the multivariate mean of each group), otherwise the discriminant function will not be useful for separating the groups and classifying new observations. Using an F-distribution, Wilks' lambda (λ) is used to test the null hypothesis of no difference between group centroids; rejection of the null hypothesis ($p < 0.05$) indicates significant differences between the groups and opens the possibility for successful classification of sex (Quinn and Keough, 2002). Wilks' lambda ranges from 0 to 1, with smaller values indicating strong differences between group centroids. The amount of between-group variance explained by a DF is represented by its eigenvalue, which can be reported as a percentage of the total variance, and indicates the discriminating power of a function (Neff and Marcus, 1980). Larger eigenvalues are associated with functions that achieve strong separation of groups. Finally, the canonical correlation is another measure of a function's ability to maximize separation between groups (Neff and Marcus, 1980). Ranging from 0 to 1, higher canonical correlation values indicate a greater correlation between the discriminant scores and the groups.

Once the maximum differences between predefined groups have been defined by a DF, an unknown individual can be classified by determining its discriminant score. The new observation is assigned to the group with which it has the smallest Mahalanobis distance squared (D^2) to the centroid (Neff and Marcus, 1980). This allows for the classification of sex in cases where sex is unknown and provides a test of the accuracy of the method when known-sex individuals are employed. Posterior probabilities of membership represent the relative probabilities of obtaining the D^2 for each individual to the centroids of the predefined groups, with values approaching 1 indicating a high probability of membership in that group. Since there are only two possible groups here, the posterior probabilities for each individual sum to one (Neff and Marcus, 1980).

Assumptions of Discriminant Function Analysis

To estimate posterior probabilities of group membership, it is necessary to have a reliable estimate of prior probabilities for group membership (Neff and Marcus, 1980). With only two possibilities in a classification of sex, equal prior probabilities can be assumed. Like many other multivariate methods, DFA assumes multivariate normality and the homogeneity of variance-covariance structure between groups (Pietrusewsky, 2000). However, because DFA appears to be relatively robust to slight departures from multivariate normality, Quinn and Keough (2002) suggest that as long as samples are similar in size, it should be sufficient to ensure the approximate normality of the univariate dataset. Box's M test is available to test for variance-covariance equality, but it lacks robustness because it is highly sensitive to even slight departures from multivariate normality (Quinn and Keough, 2002), and will not be used here. As an alternative, Quinn and Keough recommend testing for univariate homogeneity of variances (homoscedasticity) using Levene's test; DFAs that are based on a univariate

dataset that shows substantial heteroscedasticity should be interpreted with caution.

Fortunately, applying a log-transformation (ln) to the raw data helps to ensure near-normal univariate distributions, while also reducing the heteroscedasticity of the data and lessening the influence of variables with high values (Sokal and Rohlf, 1995). Therefore, the raw measurements of the os coxae will be ln-transformed prior to analysis. The use of ln-transformed variables combined with a similar number of females and males within each of the two test samples (Zulu and Kikuyu) should be sufficient to satisfy the assumptions described above. For both Zulu and Kikuyu samples, Levene's test will be conducted along with *t*-tests to identify significant univariate differences in variances and means between the sexes.

Os Coxae Variables: Form *versus* Shape

Deciding which variables to include is a critical step in DFA (van Vark and van der Sman, 1982). As the purpose of this study is to develop a method to determine sex in archaeological remains, morphometric variables were limited to the ischium and ilium surrounding the auricular surface and acetabulum, arguably the most durable parts of the os coxae (White and Folkens, 2000). Variables in these regions were selected based on their utility in sex discrimination of the whole os coxae in previous work (Hager, 1989; Weisheit, 1997; Murail, 1999). Table 3.5 lists the ten morphometric variables recorded on the os coxae; measurement definitions are provided in Appendix 1. Nine of these variables are linear measurements that reflect aspects of the form of the pelvis because they capture both size and shape information. However, a single variable (PEL11, average sciatic notch angle) is dimensionless, thus reflecting only shape differences between individuals. The influence of this angle on discriminating

sex is evaluated by comparing the accuracy of functions that include it and those that exclude it. As noted above, the raw measurements are ln-transformed prior to analysis.

The linear variables are transformed into shape ratios from the Mosimann family of shape variables in order to limit the effect of scale and emphasize differences in shape. The general procedure for transforming data into Mosimann shape variables is outlined in Chapter 2. To assess the effect of different scaling variables, shape variables are created in two different ways. The basic shape variable is a ratio of each linear variable to the geometric mean of all nine linear pelvis variables. The new shape variables are identified by a lowercase 's' preceding the variable name. Because some of the variables are partially redundant with one another (e.g., ischial length and posterior acetabular ischial length), modified shape variables are computed as ratios of the linear pelvis variables to the geometric mean of two variables only (PEL1, acetabular width; PEL3, posterior acetabular ischial length). These measurements were selected based on prior work demonstrating the strong positive correlation between acetabular diameters and ischial length with measures of body size. The modified shape variables are identified by a lowercase 'ms' preceding the variable name. Average sciatic notch angle (PEL11) is already a shape variable, and as such it does not contribute to the geometric mean nor does it require scaling. Both types of shape variables are ln-transformed prior to analysis.

Stepwise Procedure

The inclusion of a greater number of variables does not necessarily lead to a greater discriminating ability of the function; in fact, the inclusion of variables that do not add to the separation between groups may actually decrease the overall discriminating ability of the function (e.g., van Vark and van der Sman, 1982; van

Vark and Schaafsma, 1992). Selecting the optimal variables prior to analysis is difficult because a variable may exhibit little to no differences between the sexes when considered alone (e.g., as demonstrated by *t*-test), but it may contribute significantly to the discriminating power in a multivariate setting due to the correlation between variables (van Vark and van der Sman, 1982; van Vark and Schaafsma, 1992). To evaluate the effect of variable choice on discrimination, the classification accuracy of a baseline DF computed from all pelvis variables is compared to the accuracy of a DF computed by means of the stepwise procedure. In a stepwise analysis, each variable is entered and removed separately in a forward and backwards routine that attempts to build a DF that maximizes group separation by minimizing Wilks' lambda overall (Pietrusewsky, 2000; Quinn and Keough, 2002). Standardized coefficients (obtained by multiplying the raw coefficient by the pooled within-group standard deviation for each variable) and structure coefficients (also called loadings) reflect the relative contribution of each variable to the DF (Neff and Marcus, 1980), although the standardized coefficients may offer a more informed view since they account for correlations between variables (Quinn and Keough, 2002).

Determining the Accuracy of DFA

The utility of DFA for the purpose of sex classification is evaluated separately for pelvis form and both sets of pelvis shape variables. For each, the combination of variables offering the most discrimination between the sexes is identified by comparing DFs using all variables and stepwise DFs. The Zulu and Kikuyu samples are first considered separately in order to determine whether the same combination of variables maximizes between sex differences in these groups. However, population-specific sexing methods are of limited value in archaeological and paleontological contexts where the population affiliation of a

specimen is unknown or irrelevant. Therefore, the Zulu and Kikuyu samples are also pooled to form a single African sample in order to assess the utility of DFA to classify sex in a mixed population sample. Again, the combination of variables offering the greatest discrimination between the sexes is sought by comparing DFs that combine all variables with stepwise DFs.

The accuracy of the DFs is evaluated using cross-validated classification results that report the frequency of correct and incorrect classifications using the leave-one-out jackknife procedure. Here, each individual is classified according to the function derived from all individuals except itself. Cross-validated results are more robust because they circumvent the circularity and bias associated with using an individual to help define a function, then using the same function to classify that individual (Quinn and Keough, 2002). All statistical analyses are performed in SPSS 11.0©.

Results: Accuracy of Discriminant Function Analysis

The untransformed univariate summary statistics of the pelvis for the sex-specific Zulu and Kikuyu samples are provided in Table A2-4 of Appendix 2. The results for pelvis form will be presented first, followed by the results of the pelvis shape analyses.

Accuracy of Form DFA

T-tests demonstrate that Zulu females and males differ significantly for all pelvis form variables, while the Kikuyu sexes exhibit significant differences in six of the ten variables (Table 3.6). Among the Kikuyu, females and males cannot be distinguished by ischial depth (PEL5), ischial tuberosity maximum width (PEL6), iliac tuberosity thickness (PEL8), and sciatic notch width (PEL9, although

significance is approached here). In both the Zulu and Kikuyu, Levene's test for homogeneity of variances identified no significant differences in variances between the sexes, demonstrating the homoscedasticity of the univariate form data.

Cross-validated discriminant function classification results based on pelvis form are summarized in Table 3.7. In the analysis of all form variables plus PEL11, the highest success rate was obtained among the Zulu where 90.5% of individuals were correctly classified according to sex. A slightly lower rate of correct classification was obtained in the pooled African sample (88.4%), while the lowest success rate was found in the Kikuyu (77.8%). When PEL11 was excluded from the analysis, the highest accuracy remained with the Zulu, although the proportion of classification error between the sexes changed (Table 3.7). The exclusion of PEL11 resulted in a slight increase in accuracy in the pooled African sample, and a small decrease in accuracy in the Kikuyu sample.

As shown in Table 3.7, stepwise analyses improved the frequency of correct classifications in all three cases, although a unique combination of variables was employed in each sample. Among the Zulu, a DF based on the combination of three variables (PEL7, PEL10, PEL11) resulted in 97.6% accuracy, an improvement of over 7% compared to the analysis using all available variables. Specifically, this improvement drastically reduced the occurrence of Zulu male misclassification from 18.2% to 4.5%. Figure 3.10 provides a visualization of the discriminating power of the Zulu stepwise DF. There is clearly little overlap between Zulu females and males using this combination of three variables. Wilks' lambda (0.218) confirms that the group centroids are significantly different at $p = 0.000$. This function, which explains 100% of the variance between the groups, has a high eigenvalue (3.581) and a high canonical correlation (0.884), confirming the ability of the function to successfully separate the sexes among the Zulu. Table 3.7 also shows the substantial improvement

achieved in the Kikuyu classification by using the stepwise procedure to select a different combination of variables (PEL2, PEL11). As depicted in Figure 3.11, the distribution of Kikuyu females and males relative to their respective group centroids allows for some overlap between the sexes, although an F-test on Wilks' lambda (0.407) shows significant differences between the centroids ($p = 0.000$). The Kikuyu stepwise function accounts for 100% of the between group variance, but it has a lower eigenvalue (1.457) and a canonical correlation (0.770) compared to the Zulu which corresponds to its lower accuracy. A more modest improvement was observed in the pooled African sample by using the stepwise procedure to identify a unique function of variables (PEL2, PEL7, PEL10, PEL11), as listed in Table 3.7. Figure 3.12 provides visual confirmation that the sex-specific centroids are significantly different, as indicated by Wilks' lambda ($p = 0.000$). The African stepwise DF has a moderately high eigenvalue (2.370) and high canonical correlation (0.839) consistent with a 91.3% correct classification rate. As with the Zulu, the improvement from stepwise analyses specifically reduced the occurrence of male misclassification in the pooled African sample.

Another way to assess the utility of functions is to use the DFs developed for a specific sample to classify the sex of individuals in the other samples, as summarized in Table 3.8. In each case, the application of a sample-specific DF to another sample results in an equal or lesser frequency of correct classifications. For example, the highest accuracy of sex classification in the Zulu occurs by employing the particular linear combination of variables selected by the stepwise procedure to maximize sex differences among the Zulu; the success rate drops when either the Kikuyu-specific stepwise DF or the pooled African DF is employed.

Accuracy of Shape DFA

The results using standard pelvis shape variables will be presented first, followed by the results using the modified pelvis shape variables. Table 3.9 summarizes the *t*-test results of the shape variables, which demonstrate that Zulu females and males are significantly different from each other for all pelvis shape variables, while the Kikuyu exhibit significant differences in only six of the ten variables. Among the Kikuyu, sexes cannot be distinguished by acetabuluar width (sPEL1), ischial depth (sPEL5), ischial tuberosity maximum width (sPEL6), and iliac tuberosity thickness (sPEL8). In the Zulu, Levene's test identified significant differences in variance between the sexes for ischial body thickness (sPEL7); none of the Kikuyu variables showed significant differences of variance, demonstrating the overall homoscedasticity of the univariate shape data.

Cross-validated discriminant function classification results based on pelvis shape are summarized in Table 3.10. As with the analysis of pelvis form, the shape variables were considered in combination with PEL11 and without PEL11, and using a stepwise procedure for each sample. Considering all shape variables together, the highest success rate was obtained in the Zulu sample, where 90.5% of individuals were correctly classified by sex. This high accuracy is corroborated by high eigenvalue, canonical correlation, and a low Wilks' lambda (Table 3.10). A moderately lower rate of correct classification was obtained in the pooled African sample (85.5%), while the lowest success rate was found in the Kikuyu (74.1%). When PEL11 was excluded from the shape analysis, the highest accuracy remained in the Zulu sample, although the frequency of misclassifications increased in all three samples (Table 3.10).

The stepwise procedure improved the occurrence of correct classification in all three samples, with the greatest accuracy remaining in the Zulu sample (Table 3.10). As with the analysis of form, a unique combination of pelvis shape

variables was employed in each sample. Among the Zulu, a DF based on the combination of three variables (sPEL9, sPEL10, PEL11) resulted in 92.9% accuracy, an improvement of over 2% compared to the analysis using all available variables. Specifically, this improvement drastically reduced the occurrence of Zulu male misclassification from 18.2% to 4.5%, but increased the rate of female misclassification from 0.0% to 10.0%. Figure 3.14 provides a visualization of the discriminating power of this stepwise DF for the Zulu. Clearly there is little overlap between Zulu females and males using this combination of three variables. Wilks' lambda (0.308) confirms that the group centroids are indeed significantly different ($p = 0.000$). This function, which explains 100% of the variance between the groups, has the highest eigenvalue (2.245) and canonical correlation (0.832) of all stepwise shape DFs, confirming the ability of the function to successfully separate the sexes.

Table 3.10 also shows the substantial improvement achieved in the Kikuyu classification success rate (from 74.1% to 85.2%) by application of the stepwise procedure to select a novel combination of variables (sPEL3, PEL11). As depicted in Figure 3.13, the distribution of Kikuyu females and males relative to their respective group centroids exhibits some overlap between the sexes, although an F-test on Wilks' lambda (0.477) shows significant differences between the centroids ($p = 0.000$). While the Kikuyu stepwise function does account for 100% of the between-group variance, it has the lowest eigenvalue (1.096) and canonical correlation (0.723) of the three samples, which corresponds to its lower accuracy. As shown in Table 3.10, a more modest improvement was observed in the pooled African sample by using the stepwise procedure to identify a unique linear combination of shape variables (sPEL2, sPEL7, PEL11). Figure 3.15 highlights the distribution of discriminant scores for the female and male individuals, and suggests some overlap between the sexes in the pooled African sample. The separation of the centroids is confirmed by Wilks' lambda, which is

significant at $p = 0.000$. The pooled African stepwise DF has a moderately high eigenvalue (2.085) and high canonical correlation (0.822), consistent with its moderately high rate of correct classification (88.4%). As with the Zulu, the improvement achieved though stepwise analysis specifically reduced the occurrence of male misclassification in the pooled African sample.

An alternative way to evaluate the utility of the functions is to employ the DFs developed for a specific sample to classify the sex of individuals in the other samples. The results of such comparisons are listed in Table 3.11. For the Kikuyu, the accuracy remained stable at 85.2% regardless of which sample-specific DF was used, and the proportion of female and male misclassifications also remained unchanged. Among the Zulu, accuracy remained stable at 92.9% by applying the pooled African DF, although the application of this function created a male bias in the occurrence of misclassifications (Table 3.11). Applying the Kikuyu-specific DF to the Zulu resulted in an impressive drop in accuracy of over 7%. The pooled African sample benefited from a slight increase in accuracy (from 88.4% to 91.3%) by applying the Zulu-specific DF.

Table 3.9 summarizes the *t*-test results of the modified shape variables created by scaling each linear pelvis variable by with geometric mean of acetabular width and posterior acetabular ischial length. Using the modified shape variables, both samples show strong reduction in the number of variables that are significantly different between the sexes. Among the Zulu, females and males differ in only three shape variables: sciatic notch width (msPEL9), sciatic notch depth (msPEL10), and sciatic notch angle (PEL11). The Kikuyu show sex difference in four shape variables: ischial tuberosity maximum width (msPEL6), sciatic notch width (msPEL9), sciatic notch depth (msPEL10), and sciatic notch angle (PEL11). Levene's test identified no significant differences in variance between the sexes in any variable, demonstrating the univariate homoscedasticity of the modified shape data.

The cross-validated discriminant function classification results based on modified pelvis shape variables are summarized in Table 3.13. As with the preceding set of analyses, the modified shape variables were considered in combination with PEL11 and excluding PEL11, and using a stepwise procedure for each of the three samples. When all shape variables are entered together, the highest success rate was again obtained in the Zulu with an accuracy of 90.5%. This degree of accuracy is corroborated by a high eigenvalue, a high canonical correlation, and a small Wilks' lambda (Table 3.13). A moderately lower rate of correct classification was obtained in the pooled African sample (85.5%), while the lowest success rate was again observed in the Kikuyu (74.1%). If PEL11 is excluded from the modified shape analysis, the highest accuracy remains in the Zulu sample, although the overall rate of correct classification dropped in all three samples (Table 3.13).

Use of the stepwise procedure improved the occurrence of correct classification in two out of the three samples, with the greatest accuracy remaining in the Zulu sample (Table 3.13). As with the previous analysis of shape, a unique combination of variables was employed in each sample. For the Zulu, a DF based on the combination of only two variables (msPEL9, msPEL10) resulted in 92.9% accuracy, an improvement of over 2% compared to the analysis using all variables. This improvement lowered the occurrence of Zulu male misclassification from 18.2% to 9.1%, but increased the rate of female misclassification from 0% to 5%. The distribution of Zulu females and males around their respective group centroids is depicted in Figure 3.16. There is little overlap between the sexes using this combination of two variables, and Wilks' lambda (0.335) confirms that the centroids are significantly different at $p = 0.000$. Although this function has the highest accuracy among the sample-specific stepwise DFs, it does not have the highest eigenvalue nor the highest canonical correlation. A more powerful function appears to be the DF developed for the

pooled African sample, even though the accuracy of this sample is slightly less than the Zulu accuracy (Table 3.13). This table also shows the dramatic improvement achieved in the accuracy of sex classification in the Kikuyu (from 74.1% to 88.9%) by application of the stepwise procedure to select a novel combination of variables (msPEL2, PEL11). As depicted in Figure 3.17, the distribution of Kikuyu females and males relative to their respective group centroids shows some overlap between the sexes, but still decent group separation. An F-test on Wilks' lambda (0.442) shows significant differences between the centroids ($p = 0.000$), confirm significant group separation. While the Kikuyu stepwise function accounts for 100% of the between-group variance, it has the lowest eigenvalue (1.262) and canonical correlation (0.747) of the three samples analyzed by stepwise procedure. To classify sex in the pooled African sample, the stepwise procedure identified a new combination of five shape variables (msPEL2, msPEL7, msPEL9, msPEL10, PEL11). Figure 3.18 highlights the distribution of discriminant scores for the female and male individuals, and suggests some overlap between the sexes in this sample. The separation of the centroids is confirmed by Wilks' lambda, which is significant at $p = 0.000$. As mentioned above, the stepwise DF created for the pooled African sample has the highest eigenvalue (2.182) and canonical correlation (0.828) across the functions devised through stepwise analysis, although the sexing accuracy of this function is slightly lower than the function developed specifically for the Zulu sample (88.4% versus 92.9%).

Another way to assess the utility of these functions is to employ the DFs developed for a specific sample to classify the sex of individuals in the other samples. The results of such comparisons are provided in Table 3.14. For the Kikuyu, greatest accuracy is obtained using the Kikuyu sample-specific DF. Among the Zulu, accuracy remains stable at 92.9% whether the Zulu-specific or pooled African DF is used, although the proportion of female and male errors

change. For the pooled African sample, the highest accuracy is obtained by applying the DF developed for the Zulu sample.

Discussion: Utility of Discrimnant Function Analysis to Classify Sex

Discriminant function analysis offers a powerful tool for classifying sex based on the os coxae. In particular, this study demonstrates that the central and posterior portions of the os coxae alone capture sufficient sex differences to allow highly accurate classification of sex in two different African populations. This thesis also demonstrates the presence of interesting differences between the Zulu and Kikuyu regarding the expression of sex differences in these regions, notably around the sciatic notch. These population-specific differences are reflected in the unique combinations of variables found to best discriminate sex. Considering the form of the pelvis, which separates the sexes based on both size and shape criteria, the highest classification accuracy (97.6%) was obtained in the Zulu by combining ischial body thickness, sciatic notch depth and average sciatic notch angle in a DF. For the Kikuyu, sexing accuracy never exceeded 85.2%, and achieving this accuracy required a different combination of variables (ischial length and average sciatic notch angle). The discrepancy between the best-discriminating variables and accuracy in these two populations clearly affects the classification of sex in the pooled African sample. Here, a satisfactory 91.3% accuracy is reached, again using a new combination of variables: ischial length, ischial body thickness, sciatic notch depth, and average sciatic notch angle. While this is lower than the accuracy observed for the Zulu alone, it is still much more reliable than the Kikuyu classification. Interestingly, when the pooled African DF is applied to the Kikuyu, accuracy remains stable at 85.2%, but the Zulu accuracy drops slightly to 95.2% (Table 3.8). Despite a slight loss of accuracy in the Zulu, this confirms the utility of the DF created for the pooled

African sample because high accuracy is still maintained across the Kikuyu and Zulu. As Table 3.8 shows, this function misclassified three females and three males, demonstrating that it is unbiased in its error rate. Thus, this function offers high classification accuracy (91.3%) without evidence for sexing bias in a mixed population sample.

It is clear from the results of the pelvis form analyses that females and males among both the Zulu and Kikuyu differ in size. This size dichotomy is stronger in the Zulu, who demonstrate significant differences between the sexes in all variables (Table 3.6). The lack of significant sex differences in four variables among the Kikuyu certainly accounts for the lower classification accuracy observed in this sample. However, the expression of dimorphism in these samples is not limited to size differences. The stepwise procedure consistently included the dimensionless sciatic notch angle variable to maximize sex differences in both groups, demonstrating that sex differences extend beyond simple size differences. The importance of sciatic notch angle in classifying sex seems particularly marked among the Kikuyu, who suffered a nearly 4% drop in accuracy when this variable was omitted from the analysis (Table 3.7). The Zulu accuracy remained stable at 90.5% when sciatic notch angle was excluded, although the proportion of female and male misclassifications was altered.

In addition to this single dimensionless variable, two different Mosimann shape ratios were employed to control for the effect of size differences among the individuals. As discussed previously, these shape variables differ only in the variables that were used to capture size in the geometric mean. The basic shape variables used all linear pelvis measurements, while the modified shape variables used a more limited set of variables (acetabular width and posterior acetabular ischial length) to reflect size. Overall, the classification results were strikingly similar across the two shape variables, with a very minor increase in accuracy using the modified shape variables. This is promising for fossil and

archaeological application of the method, since poor preservation often limits the availability of variables. The geometric mean of acetabular width and posterior acetabular ischial length (effectively ischial length plus acetabular height) appears to be effective at capturing the size of the pelvis. With this in mind, the discussion will focus on the classification of pelvis shape using the modified shape variables.

As with the classification of pelvis form, the highest classification accuracy of using all pelvis shape variables (90.5%) was observed in the Zulu, with a clear bias towards male classification errors (Table 3.13). The influence of sciatic notch angle is assessed by excluding this variable from the shape analyses. In all cases, removal of this angle reduces classification accuracy, thus highlighting the importance of sex differences expressed by this feature. Interestingly, this variable (PEL11) was not selected by the stepwise procedure to maximize the separation of the sexes in the Zulu sample, although it was included in the Kikuyu and pooled African stepwise DFs. Among the Zulu, it seems that two other variables from the sciatic notch area (PEL9, sciatic notch width; PEL10, sciatic notch depth) adequately reflect sex differences once they are rendered scale-free. These variables likely covary with sciatic notch angle. As the width of the notch increases, the posterior inferior iliac spine and the base of the ischial spine, two of the points used to define the sciatic notch angle, are spread further apart, thereby increasing the angle.

As discussed previously, the inclusion of correlated variables can negatively influence DFA. The relationship between these three shape variables may be expressed somewhat differently among the Kikuyu, where the highest accuracy is obtained by including the sciatic notch angle (Table 3.13). Nonetheless, the DF devised specifically for the Zulu (a linear combination of sciatic notch width and sciatic notch depth transformed into modified shape variables) offers the highest classification accuracy in the pooled African sample.

This function balances the occurrence of female and male misclassifications (three and two errors respectively) fairly evenly (Table 3.14). It also seems to balance the occurrence of misclassifications among the Zulu and Kikuyu fairly well, with the two male errors split evenly among the two samples, but two Kikuyu females were misclassified compared to a single Zulu female.

This function, combining the width and depth of the sciatic notch transformed into shape variables by scaling with the geometric mean of acetabular width and posterior acetabular ischial length, performs slightly better than the best-performing combination of pelvis form variables (92.8% versus 91.3% classification accuracy). This study demonstrates the usefulness of morphometrics of the posterior os coxae for classifying sex in two modern African groups, and can be reliably applied to a sample comprised of individuals of mixed population affinity.

Conclusions: Comparison of the Methods

While the visual method developed by Bruzek (2002) to classify sex based on partially preserved os coxae is relatively easy and quick to utilize, the results of this thesis found that a reliance on non-metric features alone comes at the expense of a substantial loss in accuracy compared to the morphometric analysis of the same region of the pelvis. The most effective discriminant function developed for use on a mixed African sample achieves an accuracy of 92.8%, compared to only 82.6% using the visual method to classify sex in the same sample. A nearly 10% or greater drop in accuracy is also found when the Zulu and Kikuyu samples are considered separately using the visual method compared to the morphometric method.

The best-performing discriminant function method by which to classify sex in the combined African sample uses two pelvic variables (sciatic notch width

and sciatic notch depth), and renders them dimensionless by scaling them using the geometric mean of another pair of pelvic variables (acetabular width and posterior acetabular ischial length). Because this sexing method emphasizes shape rather than size differences to identify females and males, it may be reliably applied to classify sex in groups of different body size and levels of robusticity. Furthermore, since it relies on only four measurements of the pelvis, this approach can be productively applied in forensic, archaeological and paleontological contexts where skeletal preservation tends to be poor. To record the necessary measurements, a pair of sliding calipers, a few minutes of time, and basic knowledge of osteology are the only requirements. Therefore, in terms of accuracy, ease of use and general applicability, the discriminant function method developed here is preferable to the visual method based on scores of non-metric traits of the pelvis.

Figure 3.1. Internal view of a left os coxae showing the location of the preauricular surface (boxed area) immediately inferior to the auricular surface (dashed area). Three sub-characters of the preauricular surface (PS) are scored independently to determine the final diagnosis of sex based on PS morphology.

Figure 3.2. Scoring the PS1 sub-character. Left: Kikuyu female exhibiting deep negative relief of the preauricular surface (boxed area, oblique view shown to reflect depth of the structure). This specimen is scored "F" for PS1. Right: Zulu male exhibiting no negative relief along the preauricular surface (boxed area). This specimen is scored "M" for PS1.

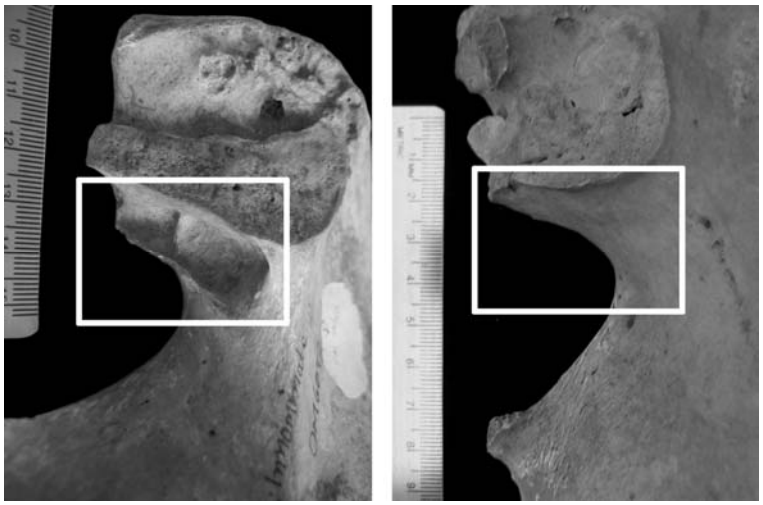

Figure 3.3. Scoring the PS2 sub-character. Left: Zulu female showing a preauricular surface bearing deep pits with closed arcs, indicating a true preauricular sulcus (boxed area). This specimen is scored "F" for PS2. Right: Zulu male exhibiting a depression with an open arc on the preauricular surface, indicating a paraglenoid groove (boxed area). This specimen is scored "M" for PS2.

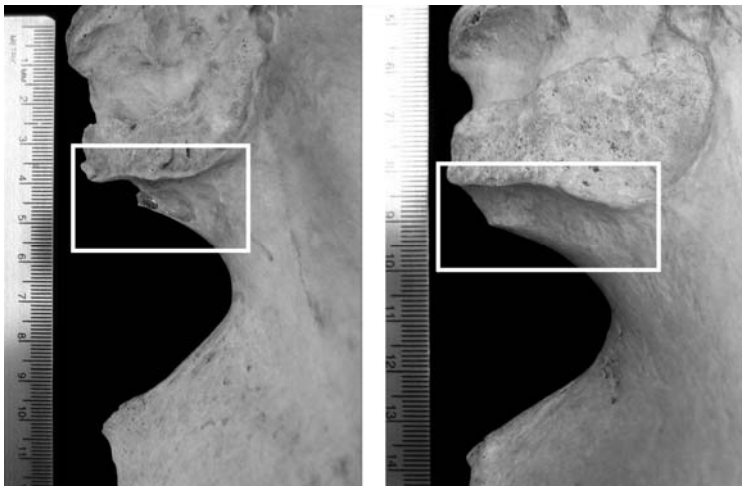

Figure 3.4. Scoring the PS3 sub-character. Left: Zulu male showing an absence of positive relief on the preauricular surface. This specimen is scored "F" for PS3. Right: Zulu male exhibiting clear positive relief (arrow) on the preauricular surface, indicating a piriform tubercle. This specimen is scored "M" for PS3.

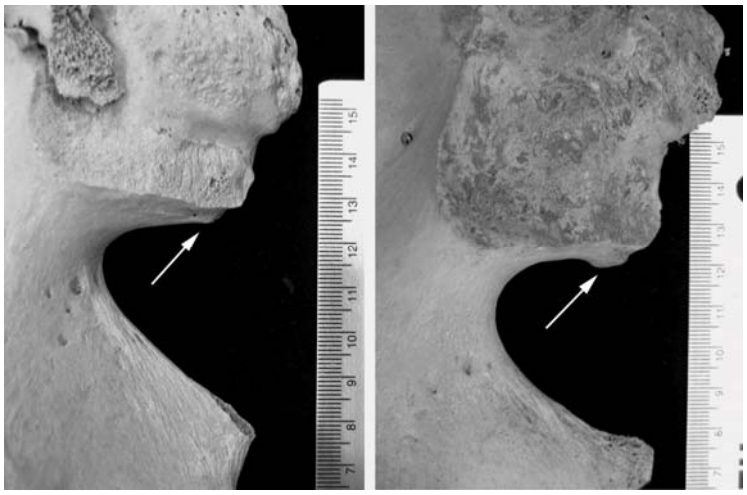

Figure 3.5. Majority score of the PS character. Left: Zulu specimen presenting a typical female score (F-F-F) for the three PS sub-characters. This individual is scored "F" for the PS character. Right: Zulu specimen presenting a typical male score (M-M-M) for the three PS sub-characters. This individual is scored "M" for the PS character.

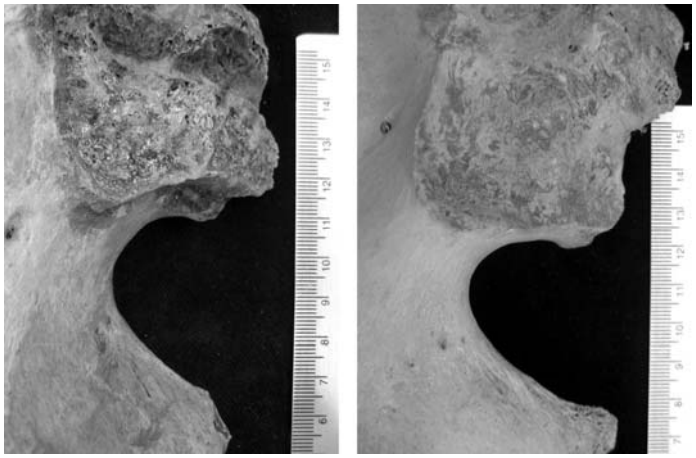

Figure 3.6. Scoring the composite arch (CA) character. Left: Zulu female exhibiting a composite arch (white lines mark the discontinuity between the superior curvature of the auricular surface and the anterior curvature of the sciatic notch). This specimen is score "F" for the CA character. Right: Zulu male lacking a composite arch (white line traces the superior curvature of the auricular surface continuously with the anterior curvature of the sciatic notch). This specimen is scored as "M" for the CA character.

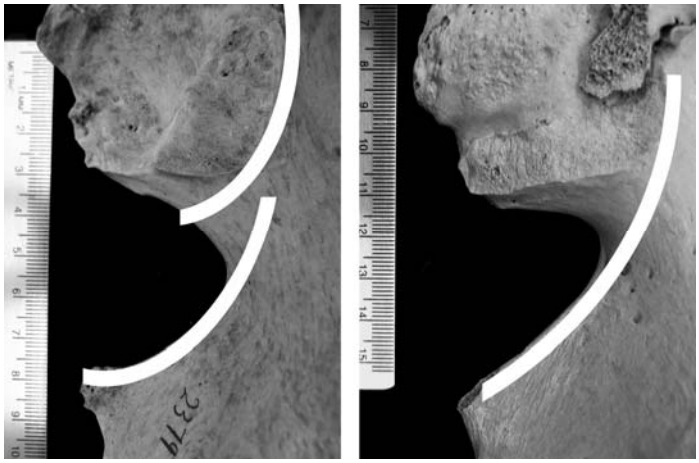

Figure 3.7. Scoring the sciatic notch (SN) sub-characters SN1 and SN2. A line is drawn connecting A (posterior inferior iliac spine, or top of the piriform tubercle, if present) and C (base of the ischial spine), spanning the maximum width of the sciatic notch. The line is divided by a perpendicular line that bisects the apex of the sciatic notch (B), creating a posterior chord (AB) and an anterior chord (BC). For SN1, the relative proportions of the chords are evaluated. For SN2, the symmetry of the notch about line B is evaluated. Left: Zulu female displays a longer posterior chord (AB) relative to the anterior chord (BC), and is symmetrical about line B. This specimen is scored "F" for SN1 and SN2. Right: Zulu male displays a substantially shorter posterior chord (AB) relative to the anterior chord (BC), and strong asymmetry about line B. This specimen is scored "M" for SN1 and SN2.

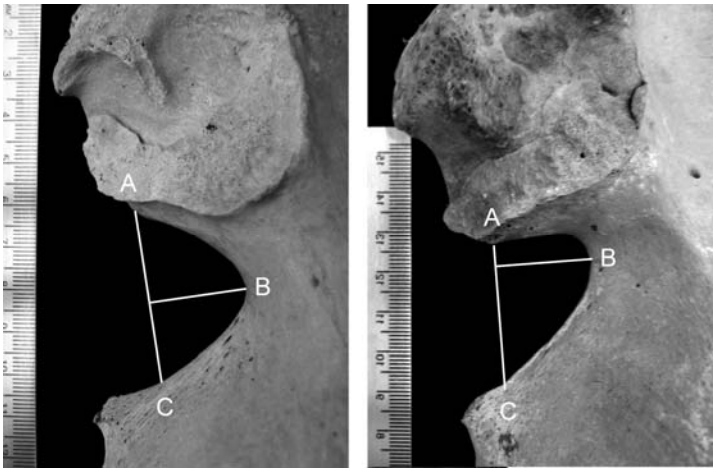

Figure 3.8. Scoring the SN3 sub-character and final SN diagnosis. Line AD is drawn parallel to line B, allowing the relative position of the posterior sciatic notch contour (i.e., the rim of the sciatic notch between PIIS and the apex of the notch) to be evaluated. Left: Zulu female exhibits a posterior notch contour clearly positioned anterior to line AD. This specimen is scored "F" for SN3, and thus presents a typical female score (F-F-F) for the three SN sub-characters. Right: Zulu male exhibits a posterior notch contour positioned posterior to line AD. This specimen is scored "M" for SN3, and thus presents a typical male score (M-M-M) for the three SN sub-characters.

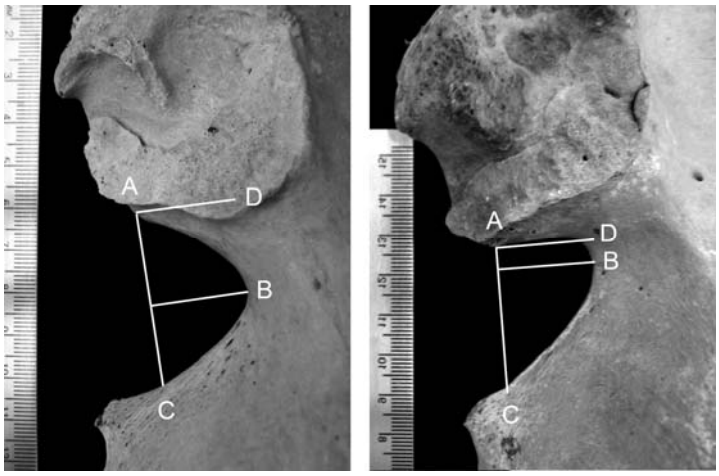

Figure 3.9. Final sex diagnosis of the sacroiliac complex based on the majority score of three independent characters (PS, CA, and SN). Left: Zulu specimen exhibits a typical female score (F-F-F) for the PS, CA and SN characters. This individual is classified as a female. Right: Zulu specimen exhibits a typical male score (M-M-M) for the PS, CA and SN characters. This individual is classified as a male.

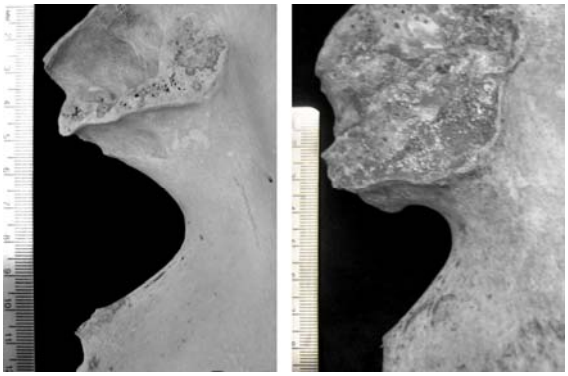

Figure 3.10 Distribution of discriminant function scores of Zulu individuals around the female and male group centroids (represented by horizontal line). The discriminant function represents a combination of three pelvis form variables (ischial body thickness, sciatic notch depth, average sciatic notch angle) selected by stepwise analysis. The group centroids are significantly different ($p < 0.05$) according to Wilks' lambda.

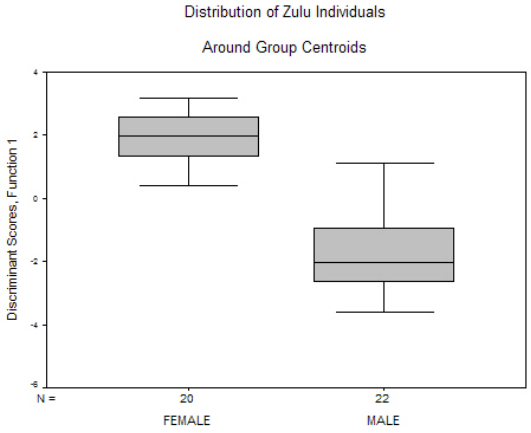

Figure 3.11 Distribution of discriminant function scores of Kikuyu individuals around the female and male group centroids (represented by the horizontal line). The discriminant function represents a combination of two pelvis form variables (ischial body thickness, average sciatic notch angle) selected by stepwise analysis. The group centroids are significantly different ($p < 0.05$) according to Wilks' lambda.

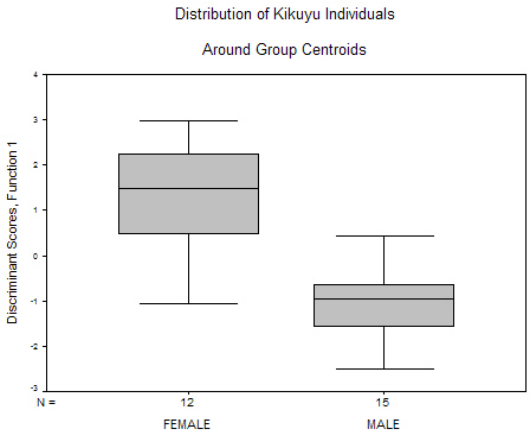

Figure 3.12 Distribution of discriminant function scores for the African individuals (pooled Zulu and Kikuyu) around the female and male group centroids (represented by the horizontal line). The discriminant function represents a combination of four variables (ischial length, ischial body thickness, sciatic notch depth, average sciatic notch angle) selected by stepwise analysis. The group centroids are significantly different ($p < 0.05$) according to Wilks' lambda.

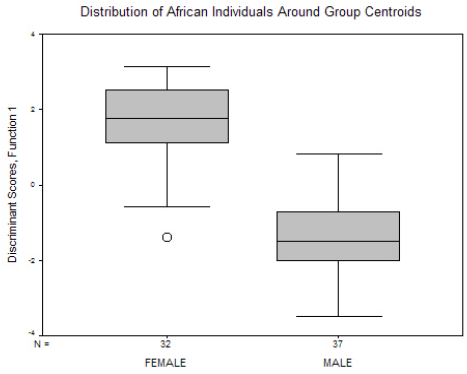

Figure 3.13 Distribution of discriminant function scores for the Zulu individuals around the female and male group centroids (represented by the horizontal line). The discriminant function represents a combination of a combination of three pelvis shape variables (sciatic notch width, sciatic notch depth, average sciatic notch angle) selected by stepwise analysis. The group centroids are significantly different ($p < 0.05$) according to Wilks' lambda.

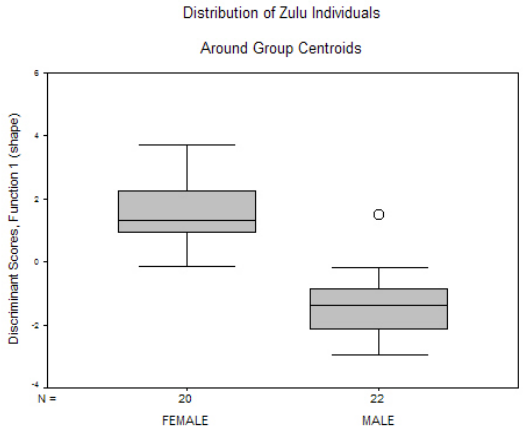

Figure 3.14 Distribution of discriminant function scores for the Kikuyu individuals around the female and male group centroids (represented by the horizontal line). The discriminant function represents a combination of a combination of two pelvis shape variables (posterior acetabular ischial length, average sciatic notch angle) selected by stepwise analysis. The group centroids are significantly different ($p < 0.05$) according to Wilks' lambda.

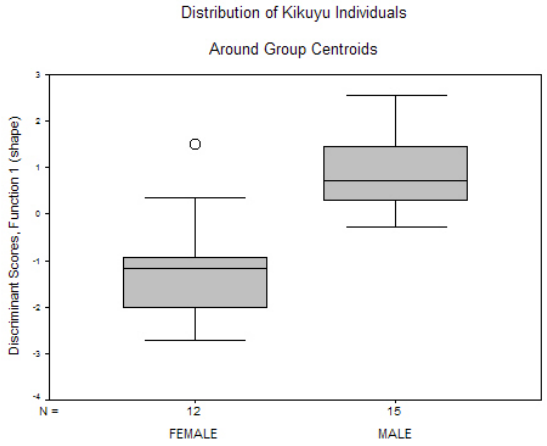

Figure 3.15 Distribution of discriminant function scores for the African individuals (pooled Zulu and Kikuyu samples) around the female and male group centroids (represented by the horizontal line). The discriminant function represents a combination of three pelvis shape variables (ischial length, ischial body thickness, average sciatic notch angle) selected by stepwise analysis. The group centroids are significantly different ($p < 0.05$) according to Wilks' lambda.

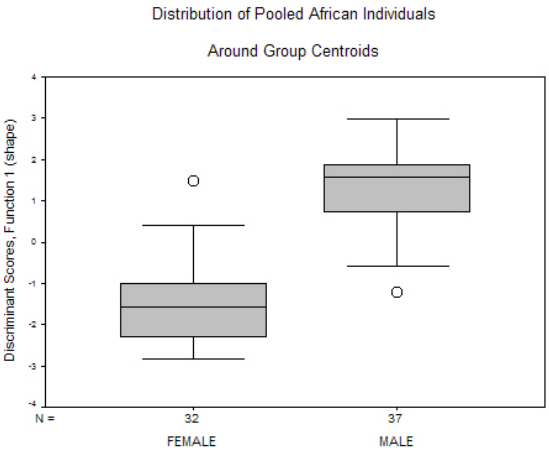

3.16 Distribution of discriminant function scores for the Zulu individuals around the female and male group centroids (represented by the horizontal line). The discriminant function represents a combination of two pelvis shape variables (sciatic notch width, sciatic notch depth) selected by stepwise analysis. The group centroids are significantly different ($p < 0.05$) according to Wilks' lambda.

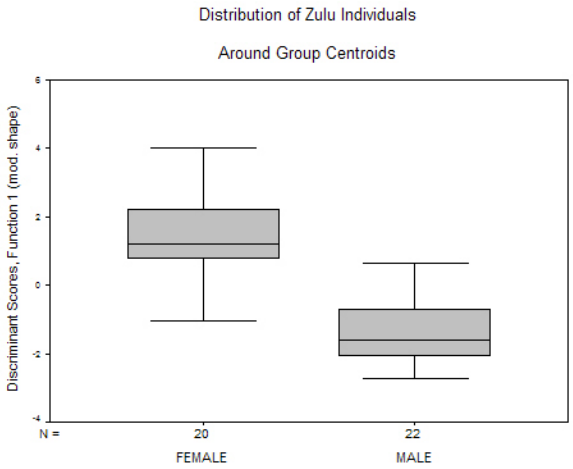

3.17 Distribution of discriminant function scores for the Kikuyu individuals around the female and male group centroids (represented by the horizontal line). The discriminant function represents a combination of two pelvis shape variables (ischial length, average sciatic notch angle) selected by stepwise analysis. The group centroids are significantly different ($p < 0.05$) according to Wilks' lambda.

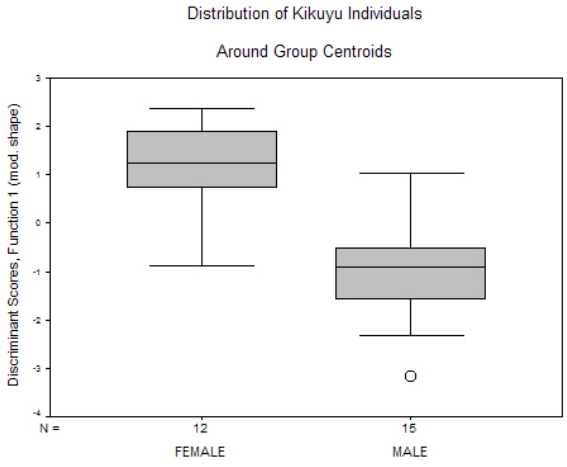

3.18 Distribution of discriminant function scores for the African individuals (pooled Zulu and Kikuyu samples) around the female and male group centroids (represented by the horizontal line). The discriminant function represents a combination of five pelvis shape variables (ischial length, ischial body thickness, sciatic notch width, sciatic notch depth, average sciatic notch angle) selected by stepwise analysis. The group centroids are significantly different ($p < 0.05$) according to Wilks' lambda.

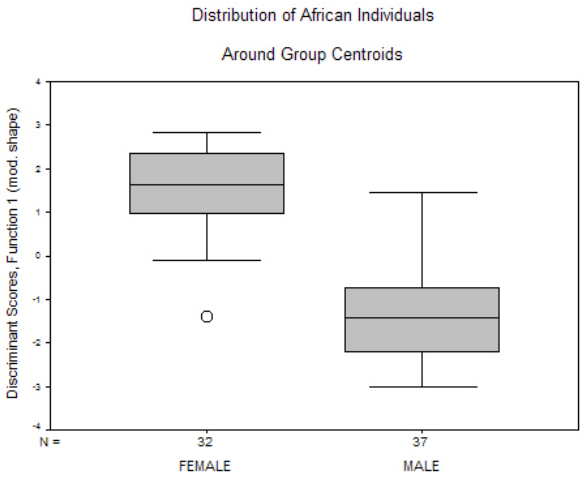

Table 3.1 Accuracy of the visual method for sex determination of the sacroiliac complex* in recent African samples.

Sample	*n*	Correct		Indeterminate		Error	
		n	%	*n*	%	*n*	%
Zulu							
female	20	14	70.00	1	5.00	5	25.00
male	22	21	95.45	1	4.55	0	0
TOTAL	42	35	**83.33**	2	4.76	5	11.90
Kikuyu							
female	12	10	83.33	0	0	2	16.67
male	15	12	80.00	1	6.67	2	13.33
TOTAL	27	22	**88.00**	1	3.70	4	14.81
African (combined)							
female	32	24	75.00	1	3.13	7	21.88
male	37	33	89.19	2	5.41	2	5.41
TOTAL	69	57	**82.61**	3	4.35	9	13.04

*Preauricular surface (PS), composite arch (CA), and greater sciatic notch (SN) characters considered together.

Table 3.2 Accuracy of the preauricular surface (PS) character for sex determination in recent African samples.

Sample	*n*	Correct		Indeterminate		Error	
		n	%	*n*	%	*n*	%
Zulu							
female	20	16	80.00	0	0	4	20.00
male	22	19	86.36	1	4.55	2	9.09
TOTAL	42	35	**83.33**	1	2.38	6	14.29
Kikuyu							
female	12	12	100.00	0	0	1	8.33
male	15	11	73.33	2	13.33	1	6.67
TOTAL	27	23	**85.19**	2	7.40	2	7.41
African (combined)							
female	32	28	87.50	0	0	6	18.75
male	37	30	81.08	3	8.11	3	8.11
TOTAL	69	58	**84.06**	3	4.35	9	13.04

Table 3.3 Accuracy of the composite arch (CA) character for sex determination in recent African samples.

Sample	*n*	Correct		Indeterminate		Error	
		n	%	*n*	%	*n*	%
Zulu							
female	20	11	55.00	2	10.00	7	35.00
male	22	19	86.36	3	13.64	0	0
TOTAL	42	30	**71.43**	5	11.90	7	16.67
Kikuyu							
female	12	10	83.33	0	0	2	16.67
male	15	10	66.67	0	0	5	33.33
TOTAL	27	20	**74.07**	0	0	7	25.93
African (combined)							
female	32	21	65.63	2	6.25	9	28.13
male	37	29	78.38	3	8.11	5	13.51
TOTAL	69	50	**72.46**	5	7.25	14	20.29

Table 3.4 Accuracy of the greater sciatic notch (SN) character for sex determination in recent African samples.

Sample	*n*	Correct		Indeterminate		Error	
		n	%	*n*	%	*n*	%
Zulu							
female	20	13	65.00	0	0	7	35.00
male	22	17	77.27	1	4.55	4	18.18
TOTAL	42	30	**71.43**	1	2.38	11	26.19
Kikuyu							
female	12	7	58.33	0	0	5	41.67
male	15	14	93.33	0	0	1	6.67
TOTAL	27	21	**77.78**	0	0	6	22.22
African (combined)							
female	32	20	62.50	0	0	12	37.50
male	37	31	83.78	1	2.70	5	13.51
TOTAL	69	51	**73.91**	1	1.45	17	24.64

Table 3.5 Pelvis variables employed in the discriminant function classification of sex. All measurements are in millimeters except for PEL11 (degrees). Measurement definitions are outlined in Appendix 1.

Variable	Name
PEL1	Acetabular width
PEL2	Ischial length
PEL3	Posterior acetabular length
PEL5	Ischial depth
PEL6	Ischial tuberosity max width
PEL7	Ischial body thickness
PEL8	Iliac tuberosity thickness
PEL9	Sciatic notch width
PEL10	Sciatic notch depth
PEL11	Average sciatic notch angle

Table 3.6 Results of the *t*-test for differences between the female and male means of the pelvis form variables. Significant differences ($p < 0.05$) between the sexes in each sample are in bold. No significant difference of variances (heteoscedasticity) between the sexes was found based on Levene's test.

Variable	Zulu	Kikuyu
PEL1	**0.000**	**0.028**
PEL2	**0.001**	**0.002**
PEL3	**0.000**	**0.001**
PEL5	**0.003**	0.089
PEL6	**0.001**	0.774
PEL7	**0.000**	**0.004**
PEL8	**0.006**	0.416
PEL9	**0.000**	0.055
PEL10	**0.000**	**0.023**
PEL11	**0.000**	**0.000**

Table 3.7 Cross-validated discriminant function classification results for recent African samples using the pelvis form variables, with and without PEL11 (average sciatic notch angle).

	♀ *n*	♂ *n*	Eigenvalue	Canonical Correlation	Wilks' λ	% Correct (*n*)	% ♀ Error (*n*)	% ♂ Error (*n*)
Form with PEL11								
Zulu	**20**	**22**	4.663	0.907	0.177	90.5 (38)	0.0 (0)	18.2 (4)
Kikuyu	**12**	**15**	2.057	0.820	0.327	77.8 (21)	25.0 (3)	20.0 (3)
African*	**32**	**37**	2.663	0.853	0.273	88.4 (61)	9.4 (3)	13.5 (5)
Form without PEL11								
Zulu	**20**	**22**	3.328	0.877	0.231	90.5 (38)	5.0 (1)	13.6 (3)
Kikuyu	**12**	**15**	1.799	0.362	0.362	74.1 (20)	25.0 (3)	26.7 (4)
African*	**32**	**37**	2.161	0.827	0.316	89.9 (62)	12.5 (4)	8.1 (3)
Form, Stepwise (variables)								
Zulu (PEL7+10+11)	**20**	**22**	3.581	0.884	0.218	97.6 (41)	0.0 (0)	4.5 (1)
Kikuyu (PEL2+11)	**12**	**15**	1.457	0.770	0.407	85.2 (23)	25.0 (3)	6.7 (1)
African (PEL2+7+10+11)	**32**	**37**	2.370	0.839	0.297	91.3 (63)	9.4 (3)	8.1 (3)

Table 3.8 Applying sample-specific stepwise discriminant functions (as per Table 3.7) to other samples. Values in bold on the diagonal represent the classification results obtained using the combination of variables selected by stepwise analysis for that particular sample, while the non-bold values represent the classification results obtained when the discriminant functions are applied to the other samples.

Discriminant Function	Zulu			Kikuyu			African*		
	% Correct (*n*)	% ♀ Error (*n*)	% ♂ Error (*n*)	% Correct (*n*)	% ♀ Error (*n*)	% ♂ Error (*n*)	% Correct (*n*)	% ♀ Error (*n*)	% ♂ Error (*n*)
[1]**PEL7,10,11**	**97.6 (41)**	**0.0 (0)**	**4.5 (1)**	81.5 (22)	25.0 (3)	13.3 (2)	91.3 (63)	9.4 (3)	8.1 (3)
[2]**PEL2,11**	92.9 (39)	0.0 (0)	13.6 (3)	**85.2 (23)**	**25.0 (3)**	**6.7 (1)**	91.3 (63)	6.3 (2)	10.8 (4)
[3]**PEL2,7,10,11**	95.2 (40)	0.0 (0)	9.1 (2)	85.2 (23)	25.0 (3)	6.7 (1)	**91.3 (63)**	**9.4 (3)**	**8.1 (3)**

* Zulu and Kikuyu samples combined.
[1]Linear combination of variables selected by stepwise procedure for the Zulu sample.
[2]Linear combination of variables selected by stepwise procedure for the Kikuyu sample.
[3]Linear combination of variables selected by stepwise procedure for the pooled African sample.

Table 3.9 Results of the *t*-test for differences between the female and male means of the pelvis shape variables (see text for details). Significant differences ($p < 0.05$) between the sexes are in bold. Asterisks indicate significant difference of variances (heteoscedasticity) between the sexes based on Levene's test; associated *t*-test probabilities are determined based on the assumption of unequal variances.

Variable	Zulu	Kikuyu
***s*PEL1**	**0.000**	0.172
***s*PEL2**	**0.002**	**0.001**
***s*PEL3**	**0.000**	**0.000**
***s*PEL5**	**0.045**	0.474
***s*PEL6**	**0.010**	0.125
***s*PEL7**	**0.000***	**0.004**
***s*PEL8**	**0.022**	0.733
***s*PEL9**	**0.000**	**0.008**
***s*PEL10**	**0.000**	**0.006**
PEL11	**0.000**	**0.000**

Table 3.10 Cross-validated discriminant function classification results for recent African samples using all pelvis shape variables and PEL11 (average sciatic notch angle).

	♀ *n*	♂ *n*	Eigenvalue	Canonical Correlation	Wilks' λ	% Correct (*n*)	% ♀ Error (*n*)	% ♂ Error (*n*)
Shape with PEL11								
Zulu	**20**	**22**	3.552	0.883	0.220	90.5 (38)	0.0 (0)	18.2 (4)
Kikuyu	**12**	**15**	1.773	0.800	0.361	74.1 (20)	25.0 (3)	26.7 (4)
African	**32**	**37**	2.313	0.836	0.302	85.5 (59)	6.3 (2)	21.6 (8)
Shape without PEL11								
Zulu	**20**	**22**	2.646	0.852	0.274	85.7 (36)	5.0 (1)	22.7 (5)
Kikuyu	**12**	**15**	1.377	0.761	0.421	63.0 (17)	33.3 (4)	40.0 (6)
African	**32**	**37**	1.843	0.805	0.352	84.1 (59)	12.5 (4)	18.9 (7)
Shape, Stepwise (variables)								
Zulu (*s*PEL9+10+PEL11)	**20**	**22**	2.245	0.832	0.308	92.9 (39)	10.0 (2)	4.5 (1)
Kikuyu (*s*PEL3+PEL11)	**12**	**15**	1.096	0.723	0.477	85.2 (23)	16.7 (2)	13.3 (2)
African (*s*PEL2+7+PEL11)	**32**	**37**	2.085	0.822	0.324	88.4 (61)	6.3 (2)	16.2 (6)

Table 3.11 Applying sample-specific stepwise discriminant functions of shape variables (as per Table 3.10) to other samples. Values in bold on the diagonal represent the classification results obtained using the combination of variables selected by stepwise analysis for that particular sample, while the non-bold values represent the classification results obtained when the discriminant functions are applied to the other samples.

Discriminant Function	Zulu			Kikuyu			African*		
	% Correct (*n*)	% ♀ Error (*n*)	% ♂ Error (*n*)	% Correct (*n*)	% ♀ Error (*n*)	% ♂ Error (*n*)	% Correct (*n*)	% ♀ Error (*n*)	% ♂ Error (*n*)
[1]**sPEL9+10+PEL11**	**92.9 (39)**	**10.0 (2)**	**4.5 (1)**	85.2 (23)	16.7 (2)	13.3 (2)	91.3 (63)	12.5 (4)	5.4 (2)
[2]**sPEL3+PEL11**	85.7 (36)	15.0 (3)	13.6 (3)	**85.2 (23)**	**16.7 (2)**	**13.3 (2)**	85.5 (59)	15.6 (5)	13.5 (5)
[3]**sPEL2+7+PEL11**	92.9 (39)	0.0 (0)	13.6 (3)	85.2 (23)	16.7 (2)	13.3 (2)	**88.4 (61)**	**6.3 (2)**	**16.2 (6)**

* Zulu and Kikuyu samples combined.
[1]Variables selected by stepwise procedure for the Zulu sample.
[2]Variables selected by stepwise procedure for the Kikuyu sample.
[3]Variables selected by stepwise procedure for the pooled African sample.

Table 3.12 Results of the *t*-test for differences between the female and male means of the pelvis modified shape variables (see text for details). Significant differences ($p < 0.05$) between the sexes are in bold. No significant difference of variances (heteoscedasticity) between the sexes was found based on Levene's test.

Variable	Zulu	Kikuyu
***ms*PEL1**	0.298	0.233
***ms*PEL2**	0.270	0.318
***ms*PEL3**	0.298	0.233
***ms*PEL5**	0.204	0.487
***ms*PEL6**	0.519	**0.008**
***ms*PEL7**	0.673	0.329
***ms*PEL8**	0.644	0.374
***ms*PEL9**	**0.000**	**0.003**
***ms*PEL10**	**0.000**	**0.002**
PEL11	**0.000**	**0.000**

Table 3.13 Cross-validated discriminant function classification results for recent African samples using the pelvis modified shape variables and PEL11 (average sciatic notch angle).

	♀ *n*	♂ *n*	Eigenvalue	Canonical Correlation	Wilks' λ	% Correct (*n*)	% ♀ Error (*n*)	% ♂ Error (*n*)
Modified Shape with PEL11								
Zulu	**20**	**22**	3.549	0.883	0.220	90.5 (38)	0.0 (0)	18.2 (4)
Kikuyu	**12**	**15**	1.783	0.800	0.359	74.1 (20)	25.0 (3)	26.7 (4)
African	**32**	**37**	2.317	0.836	0.301	85.5 (59)	6.3 (2)	21.6 (8)
Modified Shape without PEL11								
Zulu	**20**	**22**	2.647	0.852	0.274	85.7 (36)	5.0 (1)	22.7 (5)
Kikuyu	**12**	**15**	1.377	0.761	0.421	63.0 (17)	33.3 (4)	40.0 (6)
African	**32**	**37**	1.842	0.805	0.352	84.1 (58)	12.5 (4)	18.9 (7)
Modified Shape, Stepwise (variables)								
Zulu (*ms*PEL9+10)	**20**	**22**	1.988	0.816	0.335	92.9 (39)	5.0 (1)	9.1 (2)
Kikuyu (*ms*PEL2+PEL11)	**12**	**15**	1.262	0.747	0.442	88.9 (24)	8.3 (1)	13.3 (2)
African (*ms*PEL2+7+9+10+PEL11)	**32**	**37**	2.182	0.828	0.314	88.4 (61)	9.4 (3)	13.5 (5)

Table 3.14 Applying sample-specific stepwise discriminant functions of shape variables (as per Table 3.13) to other samples. Values in bold on the diagonal represent the classification results obtained using the combination of variables selected by stepwise analysis for that particular sample, while the non-bold values represent the classification results obtained when the discriminant functions are applied to the other samples.

Discriminant Function	Zulu			Kikuyu			African*		
	% Correct (*n*)	% ♀ Error (*n*)	% ♂ Error (*n*)	% Correct (*n*)	% ♀ Error (*n*)	% ♂ Error (*n*)	% Correct (*n*)	% ♀ Error (*n*)	% ♂ Error (*n*)
[1]***ms*PEL9+10**	**92.9 (39)**	**5.0 (1)**	**9.1 (2)**	81.5 (22)	16.7 (2)	20.0 (3)	92.8 (64)	9.4 (3)	5.4 (2)
[2]***ms*PEL2+PEL11**	85.7 (36)	10.0 (2)	18.2 (4)	**88.9 (24)**	**8.3 (1)**	**13.3 (2)**	84.1 (58)	9.4 (3)	5.4 (2)
[3]***ms*PEL2+7+9+10 +PEL11**	92.9 (39)	0.0 (0)	13.6 (3)	81.5 (22)	25.0 (3)	13.3 (2)	**88.4 (61)**	**9.4 (3)**	**13.5 (5)**

* Zulu and Kikuyu samples combined.
[1]Variables selected by stepwise procedure for the Zulu sample.
[2]Variables selected by stepwise procedure for the Kikuyu sample.
[3]Variables selected by stepwise procedure for the pooled African sample.

Chapter 4

Classifying Sex in Prehistoric Humans Using Fragmentary Os Coxae

Introduction

The development of reliable sex classification methods for prehistoric humans is a necessary first step in evaluating the contribution of sexual dimorphism to both the magnitude and pattern of variation in past populations. The goal of this chapter is to accurately predict the sex of the individuals in the prehistoric human samples collected for this study using the statistical and qualitative methods tested on known-sex African reference samples (see also Chapter 3).

Skeletal Samples

The pooled African sample comprising 32 females and 37 males of Zulu and Kikuyu origin is employed as a reference sample. Data were collected for three prehistoric African groups represented by archaeological remains of unknown sex: Khoe-San from various sites in South Africa, Sudanese from the sites of Jebel Sahaba and Kerma along the Nile River, and Moroccans from the site of Taforalt. The groups are described in detail in Chapter 2. From these samples, 51 Khoe-San, 31 Sudanese and 7 individuals from Taforalt preserve sufficient portions of the os coxae to record the variables necessary to classify sex using the best-performing discriminant function developed in Chapter 3: PEL1

(acetabular width), PEL3 (posterior acetabular ischial length), PEL9 (sciatic notch width), and PEL10 (sciatic notch depth). These variables were also measured for seven early *H. sapiens* fossils: three from the Middle Stone Age (MSA) group (Omo I, Qafzeh 9, and Skhūl 4), and four from the Early Upper Paleolithic (EUP) group (Grotte des Enfants 4 and 5, Nazlet Khater 2, and Paviland). The MSA and EUP os coxae are illustrated in Figures 4.1 and 4.2 respectively, and the measurements recorded on these fossils are reported in Table 4.1.

The remaining early *H. sapiens* specimens described in Chapter 2 preserve insufficient portions of the os coxae to classify sex using the best-performing discriminant function. However, in fossils for which the os coxae is preserved at least in part (Table 4.2), sex may be classified using other discriminant functions developed in Chapter 3 because these utilize unique combinations of variables. In addition, Bruzek's (2002) visual method based on the majority score of three non-metric characters (preauricular surface morphology, presence of a composite arch, and relative proportions of the sciatic notch – see Chapter 3) is applied to assign sex to all MSA and EUP fossils. Although this method may not be highly accurate for determining sex among modern Africans, it may prove useful in cases where insufficient portions of the os coxae are preserved to permit the classification of sex by discriminant function analysis. To assess the ultility of the visual method for classifying sex in the more fragmentary fossils, the method is applied to all MSA and EUP specimens, and the results of sex diagnosis are compared.

Methods

Discriminant function analysis (DFA) is a multivariate technique in which a new observation can be assigned to a predefined group (Neff and Marcus, 1980; Quinn and Keough, 2002). In this chapter, the goal is to determine the sex of an

individual by assigning it to either the female or male group from a reference sample of modern Africans using a specific combination of metric variables of the os coxae that have been shown to successfully distinguish the sexes. Specifically, sex is diagnosed in past humans using a discriminant function combining PEL9 (sciatic notch width) and PEL10 (sciatic notch depth) variables, each rendered dimensionless and scale-free by dividing by the geometric mean of PEL1 (acetabular width) and PEL3 (posterior acetabular ischial length). The resultant shape ratios are Ln-transformed in order to help satisfy the assumptions of multivariate normality and homoscedasticity required for DFA. As described in detail in Chapter 3, this discriminant function achieved an accuracy of 92.8% in a pooled African sample comprised of modern Zulu and Kikuyu. Other discriminant functions are applied in order to compare the predicted sex for each fossil, and to allow sex to be classified in some of the other fossils that do not preserve the four variables necessary for the function described above.

The archaeological and fossil human specimens are assigned to the sex to which each has the greatest likelihood of membership based on the basis of its discriminant score. With only two groups, *a priori* probabilities are equal (Neff and Marcus, 1980); that is, without any additional information, each specimen begins with a 50% chance of being female or male. Posterior probabilities represent the relative probabilities of obtaining the Mahalanobis distance squared (D^2) for each individual to the centroid of the female and male groups. Small D^2s tend to result in higher posterior probabilities, and the specimen will be assigned to the sex with which is has the highest posterior probability. Since there are only two sexes, the posterior probabilities for each specimen sum to one because it is assumed *a priori* that each specimen has been randomly drawn from one of the sexes (Quinn and Keough, 2002).

Moreover, for each specimen the typicality probability (also known as the conditional probability) indicates the probability of the observed score given

membership in the predicted group (van Vark and Schaafsma, 1992). That is, what is the probability that an individual randomly selected from this sex has a larger D^2 to the group centroid than the new observation? An observation located at the centroid of the sex to which it is assigned will have a typicality probability equal to one, while a low typicality probability suggests an observation that is atypical for that sex. An individual is deemed significantly different from the group if its typicality probability is less than 0.05 (van Vark and Schaafsma, 1992). The typicality probability effectively gauges how representative each specimen is relative to the other members in its assigned group. Recalling that posterior probabilities sum to one in the case of sex classification, it is possible to have a low typicality probability together with a high posterior probability because the analysis is essentially forcing the assignment of each new observation into one of the two sexes. In the interpretation of the results, it is important to remember that a prehistoric human may be unlikely to have been randomly drawn from either sex as defined by modern standards.

In order to evaluate the appropriateness of the classification predicted in each sample, the results from this analysis are compared with published claims concerning the sex of individual specimens. In many instances, however, no published information concerning sex attribution is available, making it difficult to evaluate the sex classification provided by this analysis. In a large skeletal sample such as the Khoe-San (and possible the Sudanese), it may be reasonble to expect an equal distribution of sexes similar to what occurs in a living population. Here, the predicted sex ratio is compared to an expected sex ratio of 50:50 using a chi-square test. This test is not conducted for the Taforalt and early *H. sapiens* samples because it is unreasonable to expect that the sexes be equally represented in such small samples.

Another way to assess the reliability of the results is to employ a *t*-test to compare mean differences between the sexes in other postcranial dimensions

known to be dimorphic in modern humans, with the expectation that a successful classification of sex will provide two groups that can be distinguished by these features. Importantly, the selected variables are not used in the classification of sex: length of the humerus, femur and ischium, angle of the sciatic notch, and shaft circumference at the level of the radial tuberosity and tibial nutrient foramen. On average, stature is greater in males than females across a global distribution of modern populations (e.g., Wolfe and Gray, 1982), and the length measurements selected here are expected to correlate with differences in stature. Tobias (1975) documented stature dimorphism in modern San and Khoi peoples, even though they are more diminutive on average than other sub-Saharan Africans (Hiernaux, 1968). Radial and tibial shaft circumferences were found by Safont et al. (2000) to be reliable predictors of sex among Europeans.

In contrast, significant differences in these dimensions are not expected when the archaeological samples are divided according to other criteria. As discussed in Chapter 2, the majority of the Khoe-San specimens are dated, either by radiocarbon or cultural association. Following this, the Khoe-San are grouped into an old (≥ 1,000 years BP) and young (≤ 1,000 years BP) sample, and these are compared by means of a *t*-test for the postcranial variables previously noted. The Sudanese and Taforalt specimens do not have dates associated with individual specimens and cannot be divided temporally like the Khoe-San. Instead, each group is randomly partitioned into two samples, each comprised of approximately 50% of the specimens; again, no significant differences are expected between the random groups. Discriminant function analyses, *t*-tests and 'random selection of cases' are performed in SPSS 11.0© and chi-square tests are performed in PAST.

Results: Classification of Sex

Archaeological Samples

The classification results for the three archaeological human samples are presented in Table 4.3. Of the 51 Khoe-San preserving the necessary os coxae dimensions, 29 are classified as female and 22 as male. This distribution does not deviate significantly from the expected 50:50 sex ratio according to a chi-square test. Three Khoe-San individuals have typicality probabilities for membership in the predicted sex ≤ 0.1, but only one is ≤ 0.05. Among the Sudanese, 22 are classified as female and 9 are classified as male. All but one of the Sudanese specimens for which sex could be diagnosed is from the cemetery at Kerma. This sex ratio is significantly different ($p = 0.0024$) from an expected 50:50 sex distribution (Table 4.3). Three of the Kerma Sudanese individuals have typicality probabilities for membership in the predicted sex of ≤ 0.1, but only one is ≤ 0.05. In the Taforalt sample, a single individual is classified as female, while the remaining six with preserved os coxae are classified as male (Table 4.3). All Taforalt individuals have typicality probabilities ≥ 0.1 for their predicted sex.

To assess the impact of imposing this sex classification on these archaeological samples, *t*-tests for the equality of means are performed using a selection of postcranial dimensions likely to be characterized by sex differences in adults from each sample. As shown in Table 4.4, all six variables exhibit significant differences when the Khoe-San are grouped by predicted sex. For comparison, *t*-tests between Khoe-San specimens classified into broad temporal periods (young specimens < 1,000 years BP *versus* old specimens > 1,000 BP) identified no significant differences in these postcranial dimensions. These six postcranial variables exhibit significant differences when the Sudanese sample is partitioned according to predicted sex (Table 4.5). In contrast, when the Sudanese

sample is split into two randomly-generated samples, significant differences are present in only one variable (FEM2). Dividing the Taforalt sample based on predicted sex results in significant differences in shaft circumference of the tibia at the nutrient foramen ($p = 0.038$), but the hypothesis of no difference cannot be rejected for the other postcranial variables (Table 4.6). When the Taforalt specimens are split into two randomly-generated samples, significant differences between the groups are present in a single variable (PEL2).

Early *H. sapiens* Fossils

The predicted sex of the seven early *H. sapiens* fossils in which the best-performing discriminant function (shape of PEL9 and PEL10) could be utilized is reported in Table 4.7, along with typicality probabilities, posterior probabilities and D^2 values quantifying the distance of each specimen to the centroid of male and female groups. Using this pelvis shape function, three fossils (Omo I, Grotte des Enfants 5, and Nazlet Khater 2) are classified as female (Figure 4.3), and four (Qafzeh 9, Skhūl 4, Grotte des Enfants 4, and Paviland) are classified as male (Figure 4.4). None of these fossils have typicality probabilities ≤ 0.1, although a range of probability values is observed: Omo I, Skhūl 4, Grotte des Enfants 5 and Paviland each have typicality probabilities ≥ 0.7, while Qafzeh 9, Nazlet Khater 2 and Grotte des Enfants 4 have typicality probabilities around 0.5 or lower (Table 4.7). In all cases, the posterior probability for membership in the predicted sex exceeds 0.7, while the probability of membership in the opposite (i.e., non-predicted) sex was always ≤ 0.3 (substantially less in some cases).

Table 4.8 reports the classification results for the same group of fossils using a discriminant function combining PEL2 and PEL11 shape variables and the Kikuyu reference sample. Using this function, only Omo I is classified as a female. The typicality probability for membership in the predicted sex is less than

0.1 in two instances: Qafzeh 9 and Grotte des Enfants 4. The classification results for these fossils using a discriminant function combining PEL2, PEL7, PEL9, PEL10 and PEL11 shape variables with a pooled African reference sample are listed in Table 4.9. Again, only Omo I is identified as a female. Using this function, only Grotte des Enfants 4 has a typicality probability less than 0.1.

The sex of the fossils is also classified using various combinations of form (i.e., raw) variables. Table 4.10 reports the classification results using a discriminant function of PEL2, PEL7, and PEL10 form variables together with PEL11 (a scale-free variable), and employing the pooled African reference sample. This function results in two female identifications (Omo I and Grotte des Enfants 5), while the others are classified as male. Only Grotte des Enfants 4 has a typicality probability less than 0.1. Using a discriminant function combining PEL7 and PEL10 form variables plus PEL11 and the Zulu reference sample, sex was classified for twelve early *H. sapiens* specimens. Again, only Omo I and Grotte des Enfants 5 are predicted as female, while the others are predicted as male (Table 4.11). This function results in low typicality probabilities (i.e., ≤ 0.1) for the following specimens: Grotte des Enfants 4 and 5, as well as Cro-Magnon 1 and 4315. Using only the PEL2 form variable in combination with PEL11 and the Kikuyu reference sample to classify sex in seven fossils, only one specimen (Grotte des Enfants 5) is assigned to the female group (Table 4.12). Here, Grotte des Enfants 4 is the only specimen with a typicality probability lower than 0.1.

In thirteen early *H. sapiens* specimens, sex is evaluated using the visual method devised by Bruzek (2002). Table 4.13 lists the classification results based on the majority score obtained from independent scoring of three non-metrical characters: preauricular surface morphology, presence or absence of composite arch, and relative proportions of the sciatic notch. Four individuals are classified as female (Omo I, Grotte des Enfants 5, Grotte du Cavillon 1, and Mladeč 21), and eight are classified as male (Qafzeh 9, Skhūl 4, Grotte des Enfants 4, Nazlet

Khater 2, Paviland 1, Barma Grande 2, Cro-Magnon 1 and 4315). Sex is deemed indeterminate for Skhūl 5 because the preauricular surface character cannot be evaluated, and the other two characters provide a different diagnosis of sex (Table 4.13). Table 4.14 summarizes the predicted sex results obtained for the early *H. sapiens* fossils preserving a sufficient portion of the os coxae to be included in at least one of the discriminant functions described above, or for which sex could be diagnosed using Bruzek's visual method.

Discussion: Utility of the Methods to Classify Sex in Prehistoric Humans

The most reliable method of determining the sex of an individual represented only by skeletal remains is from a DNA sample (Stone, 2000). Unfortunately, despite numerous advances, molecular genetics DNA remains difficult – sometimes impossible – and expensive to extract from prehistoric samples, and even if it is successfully extracted, ancient DNA may be so heavily degraded that it still cannot resolve the issue of sex (Milner et al., 2000; Stone, 2000). Nonetheless, the reliability of skeletal sex classification results can be evaluated in other ways.

Archaeological Samples

In the large sample of Khoe-San skeletons, discriminant function analysis identified a near-equal number of females and males, as would be expected if the individuals were randomly drawn from a population with an approximately 50:50 sex ratio. In contrast, significantly more females were identified in the Sudanese sample. However, the Sudanese sample (n = 31) may not be large enough to warrant an expectation of equal sex representation. Many factors such as burial practices and taphonomical processes can influence the distribution of sex in

archaeological samples (Milner et al., 2000), such that the observed sex ratio in the Sudanese sample is difficult to interpret without a clear understanding of these and other factors. Thus, while the Chi-square test supports the validity of the Khoe-San sex classificaiton results, it is equivocal for the Sudanese classification.

A more informative view of the Khoe-San sex classification is obtained by univariate comparison of sex-specific means in postcranial dimensions known to be dimorphic in modern humans. As shown in Table 4.4, the Khoe-San exhibit significant differences when the sample is partitioned according to predicted sex. Furthermore, in all cases the difference follows the expected direction. Males have significantly longer humeri, femora, and ischia, along with significantly greater radial and tibial shaft circumferences compared to females, but females have significantly more obtuse sciatic notch angles relative to males. In contrast, if the Khoe-San sample is partitioned according by temporal period instead of sex, there are no significant differences in these dimensions between the older (i.e., $\geq$ 1,000 years BP) and younger (i.e., $\leq$ 1,000 years BP) individuals (Table 4.4). This suggests that the sex classification used here adequately captures the distribution of sexes in the Khoe-San sample.

Recalling that this method achieved 92.8% accuracy when tested against modern known-sex samples (see Chapter 3), certain Khoe-San individuals may nonetheless be misclassified. However, by relying on shape differences of the pelvis, this classification avoids diagnosing sex on the basis of size alone. This is important given the overall small size of the Khoe-San compared to the modern Zulu and Kikuyu comprising the reference sample (e.g., Hiernaux, 1968). A classification based solely on size would be expected to result in a strongly female-biased distribution. Although the present Khoe-San classification does result in a slightly greater number of females relative to males (29 and 22 respectively), a chi-square test finds that the percent of females and males does not deviate significantly ($p = 0.3295$) from an expected 50:50 distribution. Still, it

would be prudent to exclude the three specimens characterized by typicality probabilities ≤ 0.1, since these individuals appear to be atypical compared to the African reference sample, exhibiting high distances (D^2) from the centroid of both the female and male groups. These 'atypical' observations may stem from various causes including pathology (although none were documented on the skeletons), errors in data collection, or they may represent Khoe-San individuals who exhibit marked morphological differences compared to the chosen reference samples. For the purpose of the present study, the 'known-sex' Khoe-San sample is thus comprised of 48 individuals (n = 27 presumed females and n = 21 presumed males). Using these sex-specific samples, differences in the magnitude of sexual dimorphism across the appendicular skeleton and differences in the level of postcranial variation compared to modern Africans will be assessed in Chapter 6.

In the Sudanese sample partitioned according to predicted sex, all six postcranial dimensions exhibit a significant difference, which follows expectations if the classification reliably separates specimens by sex (Table 4.5). Again, the direction of mean differences in all variables follows the prediction from human dimorphism: the specimens classified as male exhibit increased bone lengths and shaft circumferences relative to those classified as female, while the latter exhibit a greater sciatic notch angle. In contrast, differences between two randomly-generated Sudanese samples are not significant, with a single exception (femoral bicondylar length, FEM2). Overall, these results suggest that the sex classification of the Sudanese sample performs adequately, despite the fact that a chi-square test identified a significant deviation from an expected 50:50 sex distribution. As with the Khoe-San, three Sudanese individuals express very low typicality probabilities, suggesting that these individuals are morphologically distinct compared to the modern African males and females in the reference sample. Based on this result, these three specimens (one female, two males) are

removed from the 'known-sex' Sudanese sample. Thus, the final 'known-sex' Sudanese sample is comprised of 28 individuals (n = 21 presumed females and n = 7 presumed males); these sex-specific samples will be assessed for differences in magnitude of sexual dimorphism and postcranial variation compared to modern Africans (see Chapter 6).

Is it more difficult to evaluate the appropriateness of the Taforalt sex classification because of the limited number of Taforalt individuals that preserve the os coxae. Only one female was identified out of seven Taforal specimens. The t-test results indicate a single significant difference out of five postcranial dimensions whether the Taforalt specimens are grouped according to predicted sex or partitioned into two randomly-generated samples (Table 4.6). While this runs counter to expectations, it is nonetheless possible that the single identified female is not representative or typical of females from the Taforalt population. Alternatively, this population may exhibit very low dimorphism in these postcranial dimensions, although this seems unlikely based on other work (Ferembach, 1962). Encouragingly, the single significant difference between the lone female and the males (TIB18, tibia shaft circumference at the nutrient foramen) follows the expected direction, with the female exhibiting a significantly smaller circumference than the males. The observed male bias thus likely reflects a true bias in the sex ratio of these seven specimens, although this is difficult to verify.

In her osteological report on the Taforalt burials, Ferembach (1962) provided a qualitative assessment of sex based on all available elements for each individual. Ferembach reported an approximately equal distribution of sex in the 80 adult skeletons: n = 39 males, n = 31 females, and n = 10 indeterminate. Unfortunately, most of the individuals from the site were excavated from multiple burials, and Ferembach reported only the total number of adult males versus females in each grave, without reference to specific individuals. The seven

Taforalt individuals sexed here were recovered from four burials (No. 12, 15, 17 and 22); the number of females and males identified by this analysis does not exceed Ferembach's count of females and males in these burials. Nor does it exceed the revised count of males and females reported by Mariotti and colleagues (2009), who proposed a substantially lower minimum number of individuals amongst these burials (MNI = 40) compared to Ferembach's initial estimate of 80 adults. While this is correspondence is admittedly weak evidence, it does suggest that the Taforalt sex classification employed here performs satisfactorily, and that there is a real surplus of males in the seven individuals for which sex could be assessed. No Taforalt specimens are excluded on the basis of low typicality probabilities. Thus, the final 'known-sex' Taforalt sample comprises seven individuals (n = 1 female, n = 6 males). These sex-specific samples are very small and cannot be used to assess differences in sexual dimorphism compared to modern Africans. The Taforalt sample will therefore be assessed in its entirety, with the assumption that it represents a mixed-sex assemblage as suggested by earlier work (Ferembach, 1962; Mariotti et al., 2009).

Early *H. sapiens* Fossils

Developing methods to classify sex in hominin fossils is problematic due to the poor preservation typical of ancient specimens and because of evolutionary changes in the expression of pelvic sexual dimorphism. However, since the methods employed here were developed specifically for partial os coxae, they are particularly well suited for use on fossils. Yet both methods rely on the modern sexing criteria exhibited by two African populations, and it is unclear whether such criteria were characteristic of early *H. sapiens*, particularly more ancient specimens like Omo I which is nearly 200,000 years old.

In a study on the evolution of sex differences in the hominin pelvis, Hager (1989) found that Late Pleistocene fossils attributed to *H. sapiens*, including specimens from the ca. 120 – 100 ka BP Levantine sites as well as the European Upper Palaeolithic, generally exhibit modern male and female morphologies of the pelvis. However, she found that these fossils tend to retain the large acetabulae typical of archaic *Homo*. Acetabular size thus appears to reflect a trend for increased robusticity in both sexes among early *H. sapiens* (Ruff et al., 1993, 1997), rather than differences between the sexes.

The sciatic notch is a key region for assessing sex in both of the methods employed here. Hager (1989) documented the earliest occurrence of the modern male sciatic notch pattern in KNM-ER 3228, an *H. erectus* fossil dated to approximately 1.8 – 1.9 million years ago (Rose, 1984). Based on this evidence, as well as the notch morphologies reminiscent of modern pelves exhibited by other archaic *Homo* fossils such as OH 28, Arago 44 and Kabwe E719, Hager suggested that the modern pattern of dimorphism expressed in the sciatic notch may have been established as a response to selective pressure on females to accommodate the birth of a neonate with increased cranial capacity while maintaining effective bipedal locomotion. These findings support the application of the modern dimorphic characters of the pelvis employed here to determine sex in the earlier representatives of our species, but suggest caution in the use of size as a criterion, particularly in the acetabulum.

The classification results for each fossil are discussed in turn below. The reliability of the classification is assessed by comparing the results obtained through the use of various discriminant functions of pelvis size and shape, as well as those obtained by the visual method (Table 4.14). Furthermore, the typicality probability is evaluated as a means of identifying fossil morphologies that may not conform to the modern pattern of dimorphism. As the summary of results reported in Table 4.14 shows, there is a good agreement between the statistical

and qualitative sexing methods. The prediction of female sex for Omo I and Grotte des Enfants 5 remains relatively stable across all methods, while the remaining early *H. sapiens* fossils are predicted as male in most instances.

Omo I

Omo I is identified as female in all cases except the discriminant function of os coxae form using ischium length (PEL2) and average sciatic notch angle with a known-sex Kikuyu reference sample (Table 4.14). Omo I exhibits a much longer ischium (57.26 mm, Table 4.1) compared to the Kikuyu average (male = 50.94 mm, female = 46.17 mm; Appendix Table A2-4). Thus, a male diagnosis for Omo I is not surprising given the importance of the size of the ischium in this function. None of the analyses conducted here found Omo I to be atypical relative to the modern females included in the African sample based on moderate to high typicality probabilities for membership in the predicted group.

This fossil represents a newly discovered element attributed to the Omo I skeleton (Pearson et al., 2008b). In the description of the postcranial skeleton, Pearson et al. (2008b) refrained from proposing a formal diagnosis of sex, reporting only a mosaic of male and female traits in Omo I. The male features are mostly linked to the large size and robusticity of this specimen, as seen in the os coxae and other elements, while the female characters include a wide sciatic notch and a shallow but distinct preauricular sulcus (Figure 4.3). As discussed above, Omo I tends to be classified as female regardless of whether size, shape, or non-metric aspects of the os coxae are considered.

Qafzeh 9

This fossil is attributed to the male group in all analyses (Table 4.14). Qafzeh 9 has a low typicality probability ($p = 0.092$) in one analysis, suggesting that this specimen may be atypical compared to both sexes, although it receives substantially higher typicality probabilities in the other analyses. Several measurements for this specimen had to be estimated due to the state of preservation (Figure 4.4). The pelvic basin is nearly complete but it is fully articulated, posing some difficulty in obtaining the correct orientation for recording some measurements. Moreover, the fossil has suffered antero-posterior compression, creating some distortion in the elements. However, the distortion appears less severe on the left side, where it seems mostly limited to the iliac blade; measurements for this study were limited to this side.

Vandermeersch (1981) identified this specimen as female based on an *estimated* ischiopubic index of 100, together with the overall gracility and size of the skull and limb elements. Judging by postcranial epiphyseal fusion, cranial sutures, dental eruption and wear, and the morphology of the pubic symphysis, this individual is argued to have died around the time of the adolescent-to-adult transition (ca. 16 – 20 years old) (Vandermeersch, 1981). As such, young age may account for its more gracile skeleton compared to other specimens such as Qafzeh 8, since male secondary sex traits such as increased muscularity and concomitant skeletal robusiticty may not be fully developed (Coleman, 1969). Furthermore, Walker (2005) found a strong relationship between age-at-death and sciatic notch morphology in known-age and sex samples of modern Europeans and Americans of European and African descent: younger adults tend to have wider, and thus more feminine-looking sciatic notches. A female diagnosis is not supported in the present study, although it is possible that the current male diagnosis is influenced by the poor preservation of the specimen.

Skhūl 4

The cast of this specimen used in this study is illustrated in Figure 4.5. All of the discriminant function analyses unambiguously classify this fossil as male (Table 4.14). This diagnosis receives support from the non-metrical visual classification, which also assesses Skhūl 4 as male based on the absence of a composite arch and the relative proportions of the sciatic notch (Table 4.13). Preauricular surface morphology could not be scored for this fossil due to poor preservation, but even with a female score for this character, the majority score and hence the final diagnosis of sex would remain male. This diagnosis supports the male classification originally reported by McCown and Keith (1939). This specimen consistently receives moderate to high typicality probability for membership in the male group, which lends further support to the male diagnosis.

Grotte des Enfants 4

Similarly, Grotte des Enfants 4 is consistently classified as male by discriminant function analysis (Table 4.14). The visual method also supports a male diagnosis, as does the more constricted shape of the pelvic inlet, short pubic bones, and narrow sub-pubic angle documented on the articulated basin (Figure 4.6). However, this specimen has a very low typicality probability for membership in the male group in most analyses, indicating that it is unusual relative to the reference sample. This is mostly like due to the strikingly large size of this specimen. As Table 4.1 demonstrates, this is a large, robust pelvis, with a notably large acetabulum and elongated ischium, easily surpassing all other early *H. sapiens* fossils included in this study. It is therefore unsurprising that it appears somewhat atypical compared to the smaller Zulu and Kikuyu specimens. The male diagnosis proposed here supports the interpretation of sex by Verneau

(1908) based on the overall appearance of the skeleton and the tall stature (189 to 194 cm) predicted for this individual.

Grotte des Enfants 5

Grotte des Enfants 5 is classified as a male in only two instances of discriminant function analysis based on shape variables, while all other analyses including the majority score of non-metric characters, identify this specimen as female (Table 4.14). As shown in Figure 4.7, the overall diminutive size of the specimen, combined with a relatively wide sciatic notch (81^{o}, Table 4.1) accounts for the female diagnosis based on pelvis form. Unlike Grotte des Enfants 4, this fossil tends to exhibit moderate to high typicality probabilities for membership in the predicted group. Yet in one analysis (form combining PEL7, PEL10, PEL11), the typicality probability was very low, suggesting some departure from the typical pelvic morphology characterizing modern Zulu. Comparing the values of this fossil for these variables (Table 4.1) to the mean female Zulu values (Appendix 2), it is clear that ischial body thickness (PEL7) is driving this difference. In Grotte des Enfant 5, this dimension (36 mm) is nearly three standard deviations removed from the Zulu female mean (31.7 mm), potentially creating an odd morphology when combined with a broad, deep and wide sciatic notch. Overall, the morphometric and non-metric evidence supports a female diagnosis for this fossil. Verneau (1908) also reported a female diagnosis for Grotte des Enfants 5 based on the overall appearance of the skeleton and its short estimated stature (159 to 165 cm).

Nazlet Khater 2

The fossil is depicted in Figure 4.8. Nazlet Khater 2 is classified as male in five out of six discriminant function analyses, as well as by the visual method scoring non-metric characters associated with sex (Table 4.14). This specimen is characterized by moderate to high typicality probabilities for membership in the predicted group in all cases. This indicates that the fossil exhibits the usual suite of male pelvis morphology relative to modern Zulu and Kikuyu. The one instance of female diagnosis for this fossil may be due to the combination of a short ischium and small acetabular width combined with typically female sciatic notch dimensions. Recalling that the former variables are used to scale the sciatic notch dimensions in this analysis, this combination may account for the greater female similarity. However, small ischium size alone does not preclude a male diagnosis, as shown by the consistent male diagnosis for this fossil in the form analyses. A male diagnosis for Nazlet Khater 2 concurs with the diagnosis reported by Crevecoeur (2006), who also observed the disproportionately short ischium of this individual.

Paviland 1

This study finds strong support for a male diagnosis of Paviland 1 (Figure 4.9), as shown by a consistent male classification across all the statistical and morphological analyses (4.14). Furthermore, this specimen consistently had among the highest typicality probabilities for membership in the male group, demonstrating classic male pelvis morphology compared to modern Zulu and Kikuyu.

Dubbed the "Red Lady" following the late 19th century discovery of the skeleton apparently buried with fine ivory ornaments suitable as a lady's

adornment (Aldhouse-Green, 2000), the present male diagnosis supports the conclusion of Trinkaus (2000) based on characters of the pubis. Trinkaus also documented femoral bicondylar length that is comfortably within the male range for contemporaneous Upper Paleolithic Europeans, but lies nearly two standard deviations removed from the female mean. Interestingly, while Hager (1989) also concluded that Paviland 1 represented a male based quantitative analyses of the pubis, acetabulum, ischium and obturator foramen, she found support for a female diagnosis based on the sciatic notch, although this effect weakened when a size correction was applied. Trinkaus (2000) also commented on the sciatic notch, describing it as intermediate in form between that of a typical male and female. This result is not supported here, where all morphometric analyses take into account the sciatic notch. Furthermore, as noted above, this specimen has among the highest typicality probabilities for classification among Zulu and Kikuyu males. As noted by others (e.g., Walker, 2005), the shape of the notch varies across modern populations such that the classic female or male form may change from one group to the next. Hager and Trinkaus' observations on the female shape of the notch may stem from their use of reference samples of European descent. By all accounts, the "Red Lady" of Paviland is unambiguously male.

Skhūl 5

The os coxae attributed to Skhūl 5 is shown in Figure 4.10. Due to its fragmentary preservation, the sex of this specimen could only be classified by the discriminant analysis of pelvis form using three variables (PEL7, PEL10 and PEL11) compared to the known-sex Zulu reference sample (Table 4.14). The results of this analysis provide a male diagnosis for Skhūl 5, with a moderately high posterior probability ($p = 0.854$) but a low typicality probability ($p = 0.157$) for membership in the male group. This suggests that the specimen may exhibit

an unusual combination of features, at least compared to modern Zulu. As listed in Table 4.2, this specimen presents a very thick ischial body (PEL7 = 38.8 mm), together with a shallow sciatic notch (PEL10 = 26.3 mm) and an obtuse sciatic notch angle (PEL11 = 100^{o}). Compared to the Zulu (Appendix 2), the latter feature is hyper-female (female mean = 85.8^{o} *versus* male mean = 69.6^{o}), while the others dimensions are hyper-male (PEL7: female mean = 31.7 mm *versus* male mean = 35.6 mm; PEL10: female mean = 37.8 mm *versus* male mean = 30.7 mm). As indicated by the low typicality probability, such a combination is atypical among modern Zulu. Since the only discriminant analysis permitted by the state of preservation of the fossil emphasized its size, a male diagnosis is unsurprising. However, the two non-metric features that could be evaluated also exhibit typical male character states (Table 4.13), lending additional support to the male diagnosis. McCown and Keith (1939) also reported a male diagnosis for this individual, based on a qualitative assessment of all available elements.

Barma Grande 2

The Barma Grande 2 fossil (Figure 4.11) is diagnosed as male based on a single discriminant analysis of pelvis form; this diagnosis is supported by a visual assessment of non-metric characters (Table 4.14). As reported in Table 4.11, this specimen is very distantly removed (D^2 = 26.142) from the modern Zulu female centroid when PEL7, PEL10 and PEL11 are considered together. While it is much nearer to the male centroid (D^2 = 2.003), and as a result is unambiguously attributed to the male group (posterior p = 1.0), the typicality probability for membership in it is low (p = 0.157). The somewhat unusual male morphology relative to modern Zulu seems to be driven by its very deep sciatic notch (PEL10 = 38.9 mm, Table 4.2), which resembles Zulu females more than males (female mean = 37.8 mm *versus* male mean = 30.7 mm, Appendix 2). However, ischial

body thickness and sciatic notch angle of Barma Grande 2 are more typically male. The visual assessment identified no typical female characters (Table 4.13), in support of a male diagnosis for this individual. This is concordant with the male diagnosis reported by Verneau (1908) based on the overall morphology of this skeleton and its tall – presumably male – estimated stature of 188 to 193 cm.

Cro-Magnon 1

The Cro-Magnon 1 os coxae, shown in Figure 4.12, is classified as male based on both a visual assessment of dimorphic characters and by discriminant analysis of pelvis form (Table 4.14). While this individual is unambiguously male, it does not appear to conform to the usual Zulu male condition, as indicated by an extremely low typicality probability ($p = 0.000$) for membership in the group (Table 4.11). The unusual combination of pelvic features is further indicated by the fact that this specimen is the furthest removed from the modern male centroid ($D^2 = 19.962$) among all fossils included in the analysis. As listed in Table 4.2, Cro-Magnon 1 appears to be a hyper-male compared to the reference sample, presenting a strongly acute sciatic notch angle (PEL11 = 51.3^{o}) combined with a very thick ischial body (PEL7 = 42.9 mm). While this morphology is certainly not female, it appears to be an extreme form of the typical modern male condition.

Hager (1989) also diagnosed this individual as male based on discriminant analyses of the pubis, acetabulum and sciatic notch. However, her analyses of estimated pelvic basin dimensions (inlet, midpelvis, and outlet) for this fossil provided weak support for a female classification. It is possible that the pinched and somewhat posteriorly oriented sciatic notch (Figure 4.12), combined with an antero-posteriorly broad ischial body contribute to a broad pelvic basin reminiscent of the female condition. The "Old Man" from Cro-Magnon is

commonly interpreted as male (e.g., Verneau, 1908; Vallois and Billy, 1965), and this diagnosis is supported here.

Cro-Magnon 4315

This damaged isolated left os coxae (Figure 4.13) is diagnosed as male based on discriminant analysis of pelvic form as well as by majority score of three non-metric characters (Table 4.14). Like Cro-Magnon 1, this fossil presents a hyper-male combination of features, including a strongly acute sciatic notch angle, very shallow sciatic notch, and extremely thick ischial body (Table 4.2). This combination is certainly more similar to modern males than females, as indicated by the Mahalanobis squared distances, yet the low typicality probability ($p = 0.000$) for membership in the male group confirms the unusual morphology by modern standards (Table 4.11). Cro-Magnon 4315 is unambiguously diagnosed as male.

This specimen is a good size and morphological match for the Cro-Magnon 4318 isolated right os coxae; these elements may be attributed to the same individual. The two Cro-Magnon males analyzed in this study appear to share a unique pelvic morphology. A third os coxae from the site (Cro-Magnon 2) preserved insufficient portions of the os coxae for analysis here, although it has a substantially thinner ischial body (PEL7 = 34.3 mm, Table 4.2) compared to the other specimens, which suggests that it represents a female, as has been proposed based on its gracile cranial morphology (e.g., Vallois and Billy, 1965).

Grotte du Cavillon 1

Also known as l'Homme de Menton (Figure 4.14), this specimen proved difficult to classify. A discriminant analysis of pelvis form results in a male

diagnosis, while the majority score of non-metric characters supports a female diagnosis (Table 4.14). The moderate (p = 0.342) typicality probability associated with a male diagnosis strengths the morphometric interpretation, although recalling that this is an analysis of form, the classification is most likely driven by the greater thickness of the ischial body (PEL7 = 37.8 mm, Table 4.2) compared to modern Zulu (female mean = 31.7 mm *versus* male mean = 35.6 mm, Appendix 2). At 77^{o}, the angle of the sciatic notch is not great for this individual, further supporting a male diagnosis, even though the sciatic notch is broad and deep, reminiscent of modern females. The feminine qualitites of this individual are also evident by the female majority score obtained by visual diagnosis of three dimorphic characters of the os coxae (Table 4.13). However, without the ability to scale the os coxae for size using the geometric mean of PEL1 and PEL3, the diagnosis of sex for this individual cannot be ascertained through additional shape-based discriminant analyses. Verneau (1908) proposed a male diagnosis for this individual based on an estimated stature of 175 to 180 cm predicted from the length of major long bones. While this is moderately tall, it may still be up to 19 cm shorter than the other males from the Balzi Rossi caves (Grotte des Enfants 4 and Barma Grande 2) (Verneau, 1908). The classification of sex for Grotte du Cavillon 1 remains ambiguous; this individual is considered 'indeterminate' for sex for the purposes of the present study.

Mladeč 21

The sex of this specimen (Figure 4.15) can only be assessed on the basis of a visual diagnosis of non-metric characters of the os coxae (Table 4.14). Mladeč 21 is classified as a female, in support of Hager (1989) and Teschler-Nicola's (2007) interpretation based primarily on sciatic notch morphology. These workers proposed a male diagnosis for a second unassociated partial os

coxae from this site (No. 22, Figure 4.15) based on the large size of the preserved ischium and acetabulum, although this was not evaluated here due to the limited preservation of this specimen.

Conclusions

The final classification of sex for the early *H. sapiens* fossils included in this study is summarized in Table 4.15. This summary brings together the concensus of sex diagnosis obtained in the present study, and supplements this with the sex classification results proposed by other workers for those specimens that could not be analyzed here due to poor preservation of the os coxae. Among the MSA early *H. sapiens*, four are interpreted as female and seven as male, while isolated postcranial elements from six localities cannot be sexed. In the EUP early *H. sapiens* group, six females and seveenteen males (including two represented solely by unassociated os coxae) are identified, and one skeleton (Grotte du Cavillon 1) is classified as indeterminate, as are unassociated postcranial remains.

This study has applied numerous discriminant analyses of pelvis form and shape to achieve a rigorous diagnosis of sex in diverse archaeological African samples and early *H. sapiens* fossils, including the Omo I specimen which had yet to receive a formal sex classification. The morphometric analyses were complimented by a visual assessment of sex based on the majority score of non-metric characters. In most instances, a clear statistical diagnosis of sex was obtained by comparing the results of different discriminant analyses. The majority morphometric diagnosis was commonly in agreement with the visual determination of sex undertaken here. This congruence suggests that a visual, non-metric diagnosis of sex may be reliably employed in early *H. sapiens* when

insufficient portions of the os coxae are preserved to allow a more rigorous morphometric sex assignment.

Through the application of discriminant analysis, this study also demonstrated that several early *H. sapiens* tend to be characterized by moderate to high typicality probabilities for their predicted sex, which suggests that this group of fossil humans generally conforms to the pattern of pelvic dimorphism exhibited by modern males and females. Indeed, some fossils were characterized by hyper-male or hyper-female morphologies. Thus, despite some changes in the expression of pelvic dimorphism during hominin evolution, the application of modern sexing criteria to the earliest representatives of *H. sapiens* appears to be justified. Future work should focus on refining the discriminant analyses developed here using a more global sample of human populations to confirm their utility to classifying sex among *H. sapiens* from diverse regions.

Figure 4.1 Internal view of Middle Stone Age (MSA) early *H. sapiens* os coxae: A) Omo I, left os coxae, B) Skhūl 4, cast of right os coxae, C) Qafzeh 9, close up of left os coxae in articulation with sacrum.

A)

B)

C)

Figure 4.2 Internal view of Early Upper Paleolithic (EUP) early *H. sapiens* os coxae: A) Grotte des Enfants 4, left os coxae in articulation with sacrum, B) Grotte des Enfants 5, left os coxae, C) Nazlet Khater 2, left os coxae, D) Paviland, cast of left os coxae.

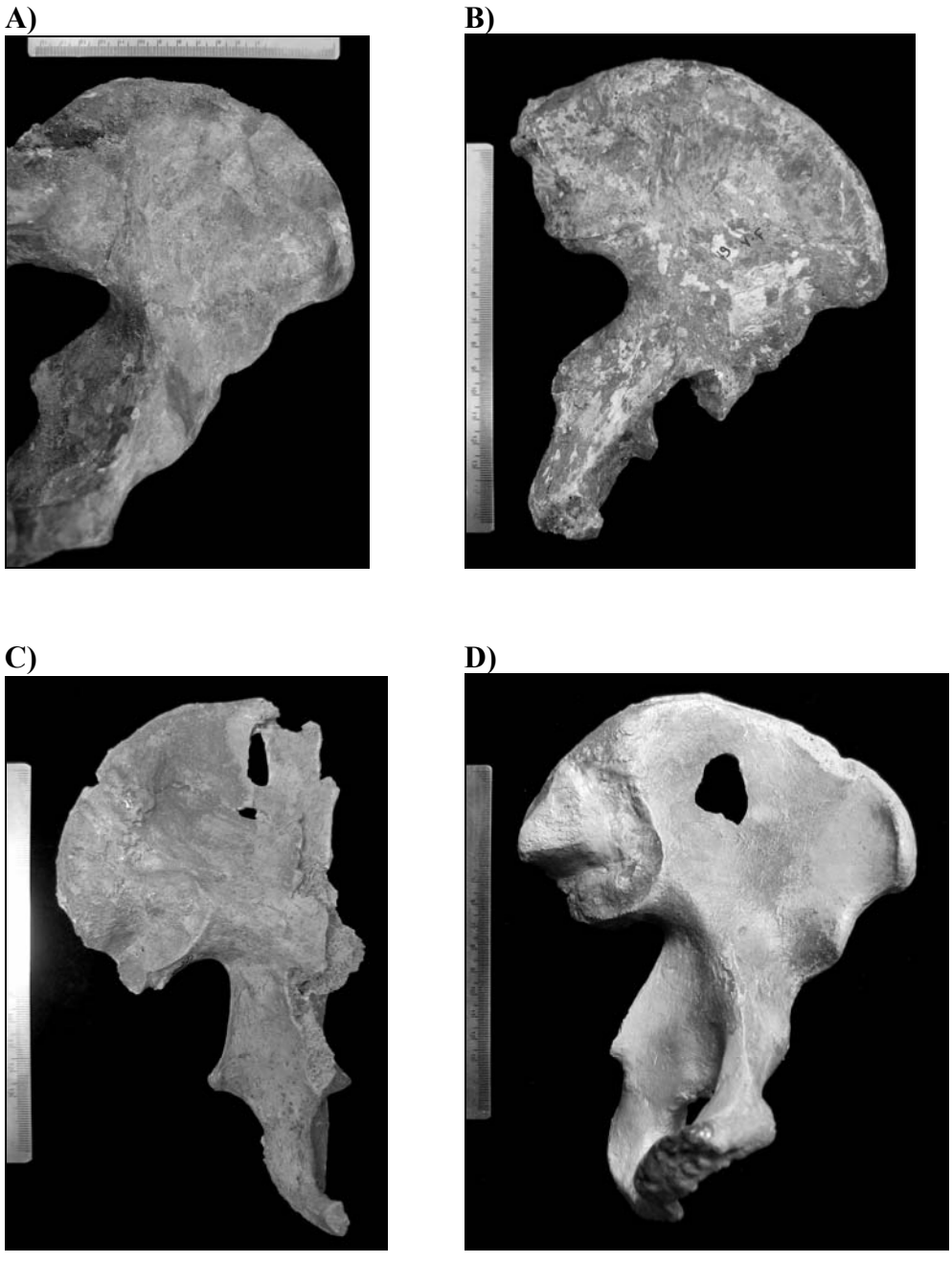

Figure 4.3 Omo I is consistently classified as female by discriminant function analysis and the visual method, despite its large size and robusticity. A) internal view, left os coxae, B) view of the preauricular surface exhibiting a preauricular sulcus, C) external view including a fragment of the iliac tuberosity; note the large acetabulum.

A)

B)

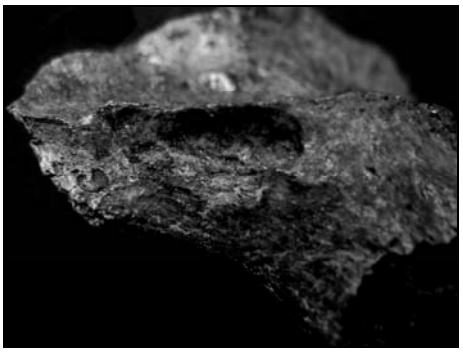

C)

Figure 4.4 Qafzeh 9 is consistently classified as male in the discriminant function analysis and by visual diagnosis. This is contra Vandermeersch's (1981) female diagnosis for this individual based on a qualitative assessment of all preserved elements. A) internal view, left os coxae in articulation with the sacrum, B) articulated pelvis, note the distortion and antero-posterior compression.

A)

B)

Figure 4.5 Skhūl 4 is unambiguously classified as male in all discriminant function analyses (internal view, cast of right os coxae).

Figure 4.6 Grotte des Enfants 4 is consistently classified as male in discriminant function analysis and by majority score of non-metric characters. A) internal view, left os coxae, B) superior and anterior views of the articulated pelvis. Note the constricted pelvic inlet, the short pubis, and the narrow sub-pubic angle; these additional features support a male diagnosis.

A)

B)

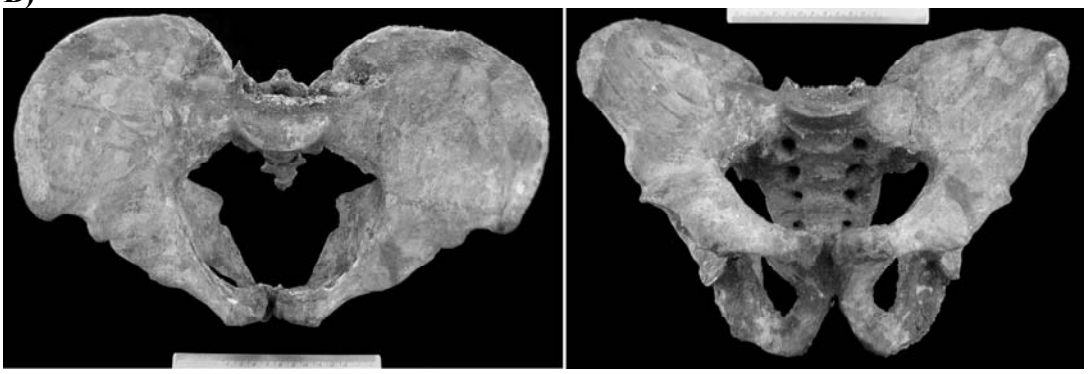

Figure 4.7 Grotte des Enfants 5 tends to be classified as female according to discriminant function analysis. The visual method also supports a female diagnosis (internal view, left os coxae).

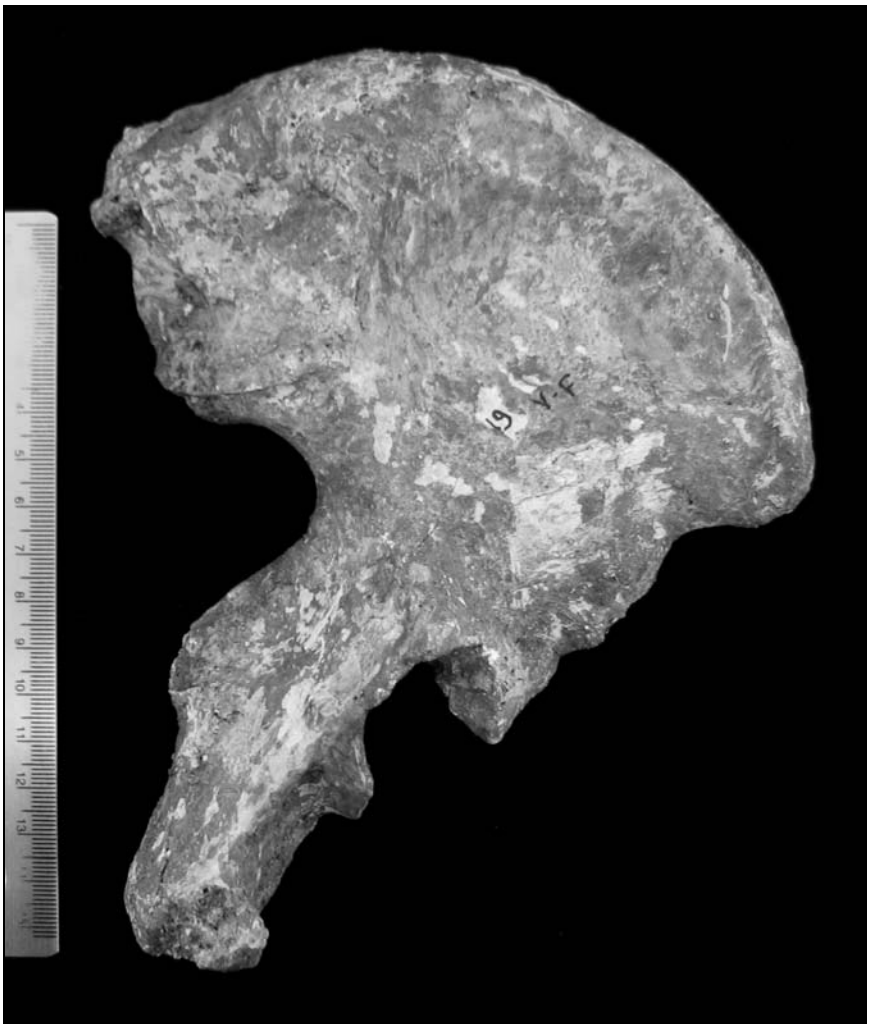

Figure 4.8 Nazlet Khater 2 tends to be classified as male in most discriminant analyses and by non-metric features (internal view, left os coxae). A male diagnosis supports Crevecoeur's (2006) interpretation.

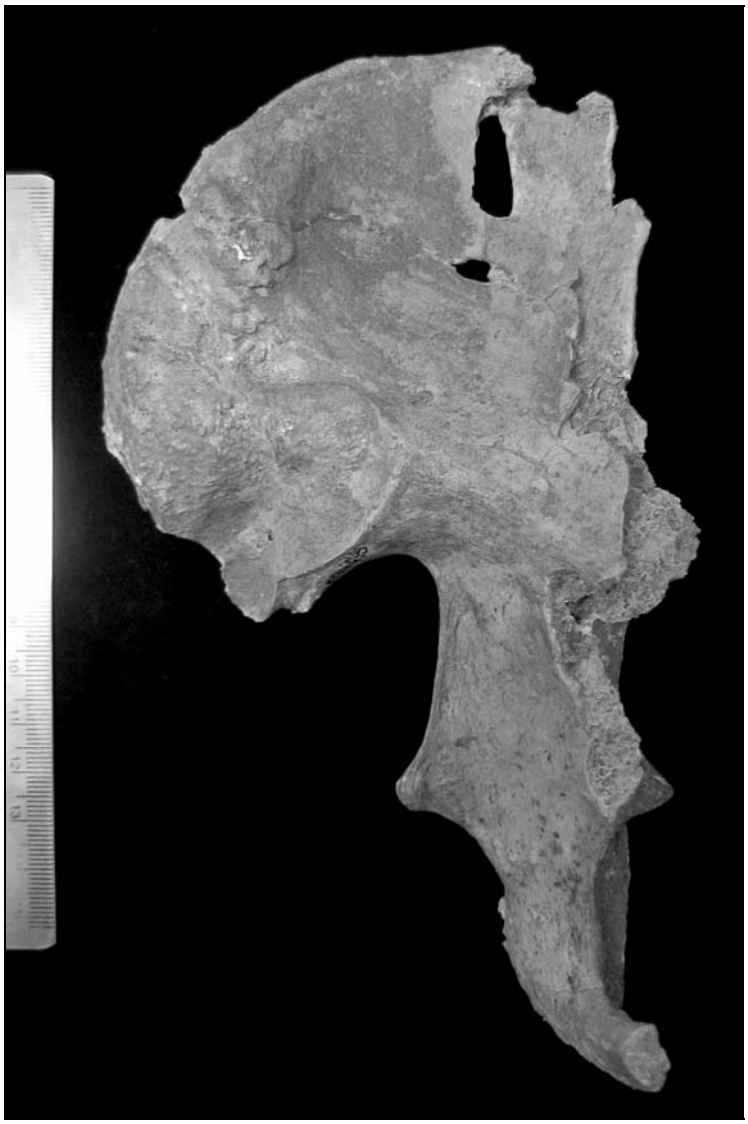

Figure 4.9 Paviland 1 is unambiguously classified as male by discriminant function analyses and by majority score of non-metric characters (internal view, cast of left os coxae).

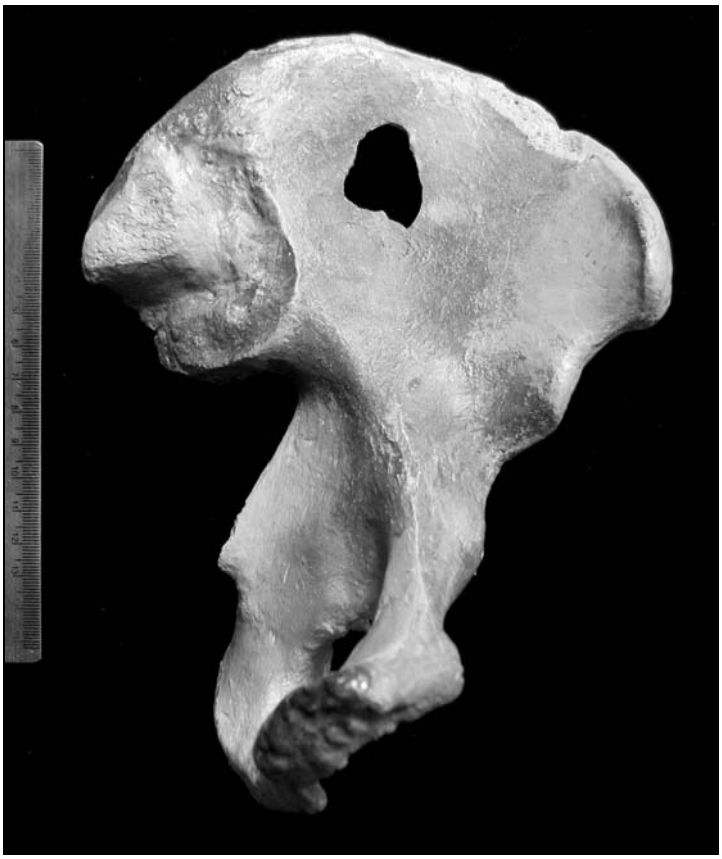

Figure 4.10 The sex of Skhūl 5 could only be diagnosed in one discriminant analysis of pelvis form due to the poor preservation; it is classified as male despite a broad sciatic notch. This diagnosis supports the sex reported by McCown and Keith (1939) based a visual assessment of all elements attributed to this specimen (internal view, right os coxae).

Figure 4.11 Barma Grande 2 is classified as male according to a discriminant analysis of pelvis form and by visual diagnosis (internal view, left os coxae).

Figure 4.12 Cro-Magnon 1 is classified as male based on the discriminant analysis of pelvis form and by majority score of non-metric characters (internal view, right os coxae).

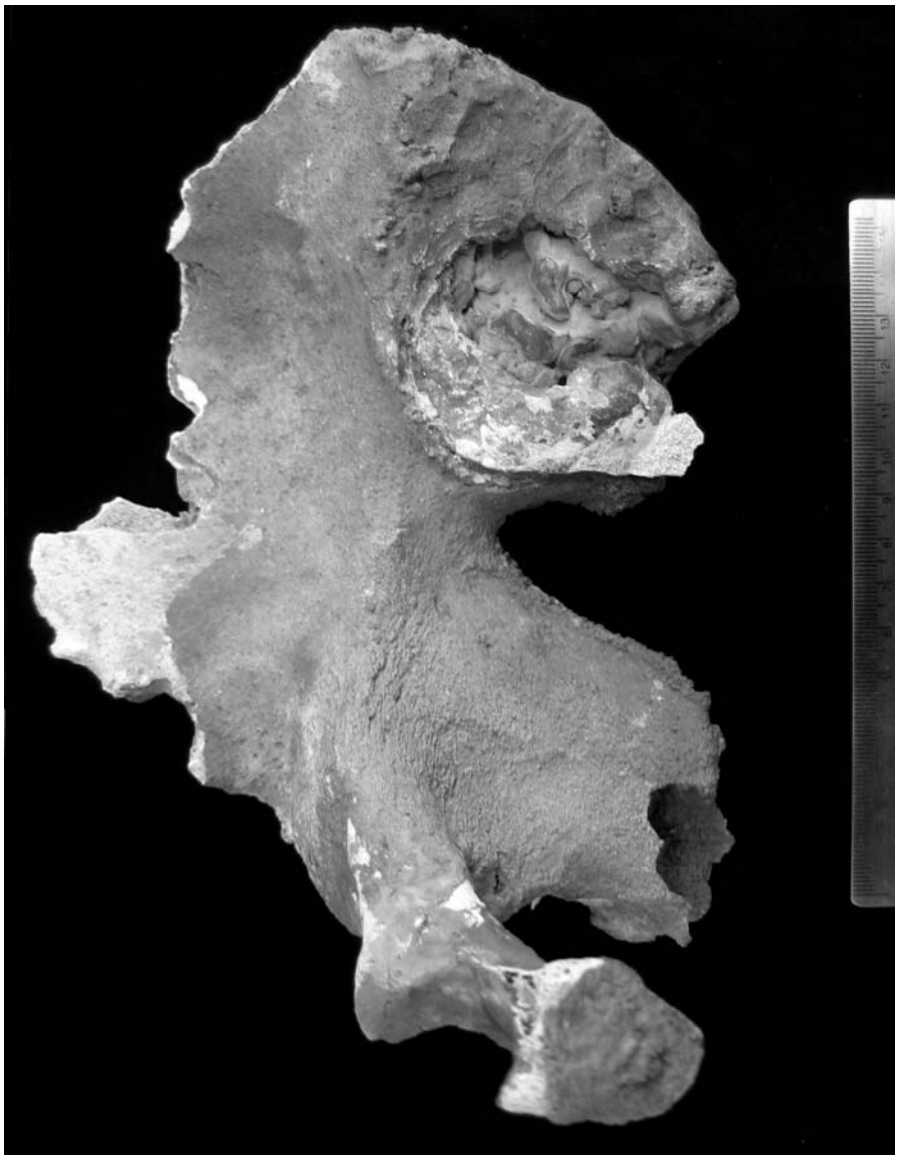

Figure 4.13 The isolated os coxae Cro-Magnon 4315 is classified as male by discriminant function analysis of form and according to a visual diagnosis of the os coxae (internal view, left os coxae).

Figure 4.14 The diagnosis for Grotte du Cavillon 1 oscillates between male, based on discriminant analysis of pelvis form, and female, based on the majority score of non-metric characters (internal view, left os coxae).

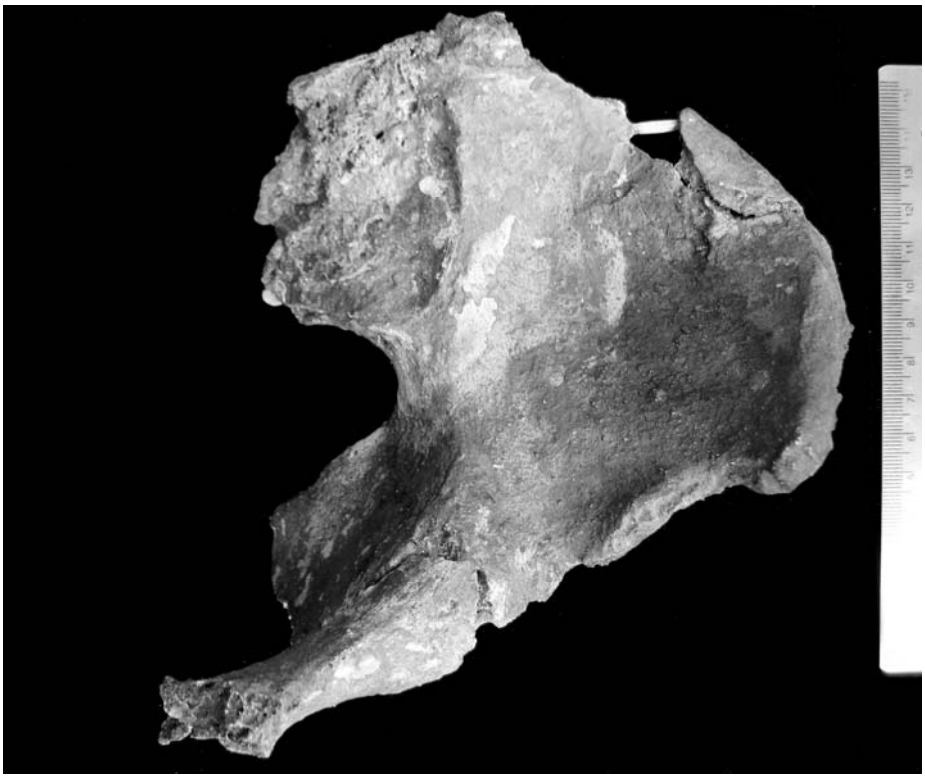

Figure 4.15 Os coxae remains from Mladeč. A) Mladeč 21 is too poorly preserved for discriminant analysis using the variables employed in this study (internal view, left os coxae). A visual assessment of three non-metric characters classifies this individual as female. B) Mladeč 22 does not preserve sufficient morphology to evaluate sex using the methods in this study, although the large acetabulum and ischium compared to Mladeč 21 are suggestive of a male (lateral view, right os coxae).

A)

B)

Table 4.1 Raw os coxae measurements for the early *H. sapiens* fossils for which sex is classified in Chapter 4. All measurements are in millimeters (except PEL11). Measurement definitions are provided in Appendix 1.

Fossil	Side	PEL1	PEL2	PEL3	PEL5	PEL6	PEL7	PEL8	PEL9	PEL10	PEL11 (degree)
Omo I	Lt	53.95	57.26	108.65	30.73	28.90	36.33	20.91	40.03	44.38	87.59
Qafzeh 9	Lt	48.49	49.67	100.01	26.05	(25.60)	33.81	--	(30.50)	(26.50)	(64.40)
Skhūl 4 (cast)	Lt	54.54	54.62	113.32	31.68[a]	26.87	37.00	21.53	40.89[a]	29.76[a]	82.74[a]
Grotte des Enfants 4	Lt	60.93	64.69	124.72	40.14	38.80	42.73	23.79	(32.00)	(37.00)	66.54
Grotte des Enfants 5	Lt	45.75	49.44	97.02	34.90	29.66	(36.00)	19.29	35.52	38.78	81.21
Nazlet Khater 2	Rt	45.82	51.48	100.62	29.71	28.74	39.55	15.02	35.71	36.31	70.49
Paviland 1 (cast)	Lt	57.60	57.59	112.61	31.33	31.86	36.89	(15.40)	37.46	32.00	72.71

Key: PEL1: acetabuluar width, PEL2: ischium length, PEL3: posterior acetabular ischial length, PEL5: ischial depth, PEL6: ischial tuberosity maximum width, PEL7: ischial body thickness, PEL8: iliac tuberosity thickness, PEL9: sciatic notch width, PEL10: sciatic notch depth, PEL11: average sciatic notch angle.

[a] Denotes a measurement recorded on the opposite side. Measurements in parenthesis are estimates, double parentheses indicate a minimum estimate.

Table 4.2 Raw os coxae measurements for the early *H. sapiens* fossils with insufficient data to classify sex using DFA. All measurements are in millimeters (except PEL11). Measurement definitions are provided in Appendix 1.

Fossil	Side	PEL1	PEL2	PEL3	PEL5	PEL6	PEL7	PEL8	PEL9	PEL10	PEL11 (degree)
Skhūl 5	Rt	--	--	--	31.57	31.88	38.08	(21.10)	(44.65)	26.31	100.06
Skhūl 7	Rt	--	--	--	--	--	--	(13.45)	--	--	--
Skhūl 9	Lt	49.76	50.22	(104.30)	--	--	36.68	--	--	--	--
Barma Grande 2	Lt	--	--	--	37.37	39.25	45.39	22.47[a]	40.41	38.88	77.15
Cro-Magnon 1	Rt	(54.20)	--	--	--	32.68	42.88	--	(36.90)[a]	(31.20)	51.27
Cro-Magnon 2	Rt	48.77	57.89	111.54	33.38	26.90	34.25	--	--	--	--
Cro-Magnon 4315	Lt	54.45	--	--	36.96[a]	29.03	41.93	--	40.31	28.89	55.33
Grotte du Cavillon 1	Lt	49.12	--	--	--	--	37.75[a]	20.74	40.53	40.07	76.96
Mladeč 21	Lt	--	--	--	32.20	--	34.59	--	((40.00))	--	91.24
Mladeč 22	Rt	--	50.55	110.33	21.93	29.24	36.64	--	--	--	--
Dolní Věstonice[b] 13	Lt	52.00	--	--	--	30.20	--	18.60	--	--	--
Dolní Věstonice[b] 14	Lt	55.00	--	--	--	25.70	--	16.00	--	--	--
Dolní Věstonice[b] 16	Lt	--	--	--	--	29.20	--	21.10	--	--	--

[a] Denotes a measurement recorded on the opposite side. [b] Data from Sládek et al. (2000). Measurements in parenthesis are estimates, double parentheses indicate a minimum estimate.

Table 4.3 Predicted sex classification results for the archaeological human samples. The chi-square test results report significant differences (in bold) between the observed and expected (50:50) sex ratio in each sample.

Sample	*N* os coxae	Predicted ♀		Predicted ♂		Chi-square	
		N	%	*N*	%	$X^2_{(df=1)}$	*p*
Khoe-San	51	29	56.86	22	43.14	0.9507	0.3295
Sudanese	31	22	70.97	9	29.03	9.2046	**0.0024**
Taforalt	7	1	14.29	6	85.71	--	--

Table 4.4 *T*-test results for select postcranial dimensions in the Khoe-San sample divided into sex and temporal classes. The probabilities reported in the left column are from *t*-tests of equality of means between males and females following the sex classification in Chapter 4; the probabilities reported in the right column are from *t*-tests of equality of means between older (> 1,000 years BP) and younger (< 1,000 years BP) specimens. Significant differences ($p \leq 0.05$) are in bold.

Variable	*N* ♀	*N* ♂	Differences by Sex	*N* 'young'	*N* 'old'	Differences by Time
Humerus, total length **(HUM2)**	25	20	**0.040**	22	51	0.087
Radius, shaft circumference at radial tuberosity **(RAD16)**	29	22	**0.000**	23	43	0.916
Ischium length **(PEL2)**	26	20	**0.049**	25	46	0.157
Sciatic notch angle **(PEL11)**	29	22	**0.000**	19	35	0.569
Femur, bicondylar length **(FEM2)**	29	21	**0.003**	24	54	0.877
Tibia, nutrient foramen shaft circumference **(TIB18)**	25	22	**0.000**	25	48	0.526

Table 4.5 *T*-test results for select postcranial dimensions in the Sudanese sample. The probabilities reported in the left column indicate differences when the sample is divided into sex classes following the sex classification in Chapter 4. The probabilities reported in the right column indicate differences between two randomly-generated samples. Significant differences ($p \leq 0.05$) are in bold.

Variable	*N* ♀	*N* ♂	Differences by Sex	N_A	N_B	Differences, Random Sampling
Humerus, total length **(HUM2)**	20	9	**0.000**	25	27	0.187
Radius, shaft circumference at radial tuberosity **(RAD16)**	20	9	**0.003**	26	21	0.223
Ischium length **(PEL2)**	22	9	**0.029**	24	22	**0.038**
Sciatic notch angle **(PEL11)**	22	9	**0.000**	21	17	0.377
Femur, bicondylar length **(FEM2)**	20	9	**0.000**	51	36	0.125
Tibia, nutrient foramen shaft circumference **(TIB18)**	21	9	**0.000**	44	34	0.062

Table 4.6 *T*-test results for select postcranial dimensions in the Taforalt sample. The probabilities reported in the left column indicate differences when the sample is divided into sex classes following the sex classification in Chapter 4. The probabilities reported in the right column indicate differences between two randomly-generated samples. Significant differences ($p \leq 0.05$) are in bold.

Variable	*N* ♀	*N* ♂	Differences by Sex	N_A	N_B	Differences, Random Sampling
Humerus, total length **(HUM2)**	0	4	--	12	12	0.122
Radius, shaft circumference at radial tuberosity **(RAD16)**	1	3	0.962	9	11	0.597
Ischium length **(PEL2)**	1	6	0.725	10	9	0.278
Sciatic notch angle **(PEL11)**	1	6	0.481	10	10	**0.020**
Femur, bicondylar length **(FEM2)**	1	4	0.360	15	11	0.580
Tibia, nutrient foramen shaft circumference **(TIB18)**	1	3	**0.038**	13	12	0.142

Table 4.7 Classification results for the fossil *H. sapiens* using the discriminant function combining PEL9 and PEL10 shape variables, with the pooled African reference sample. For the predicted sex, the typicality probability indicates the probability of the observed discriminant score given membership in that group. Sex is assigned based on the highest posterior probability (shown in bold) and smallest D^2 to the group centroid.

Fossil	Predicted Sex	Typicality Prob.	♀ Post. Prob.	D^2 to ♀ centroid	♂ Post. Prob.	D^2 to ♂ centroid
Omo I	Female	0.703	**0.829**	0.145	0.171	3.308
Qafzeh 9	Male	0.520	0.021	8.085	**0.979**	0.414
Skhūl 4	Male	0.883	0.110	4.211	**0.890**	0.022
Grotte des Enfants 4	Male	0.289	0.009	10.630	**0.991**	1.125
Grotte des Enfants 5	Female	0.783	**0.860**	0.076	0.140	3.702
Nazlet Khater 2	Female	0.503	**0.720**	0.449	0.280	2.341
Paviland 1	Male	0.847	0.055	5.725	**0.945**	0.037

Table 4.8 Classification results for the fossil *H. sapiens* using the discriminant function combining PEL2 and PEL11 shape variables, with a Kikuyu reference sample. For the predicted sex, the typicality probability indicates the probability of the observed discriminant score given membership in that group; probabilities ≤ 1.0 (shown in italics) indicate an atypical morphology for that group. Sex is assigned based on the highest posterior probability (shown in bold) and smallest D^2 to the group centroid.

Fossil	Predicted Sex	Typicality Prob.	♀ Post. Prob.	D^2 to ♀ centroid	♂ Post. Prob.	D^2 to ♂ centroid
Omo I	Female	0.453	**0.675**	0.564	0.325	2.029
Qafzeh 9	Male	*0.092*	0.002	14.920	**0.998**	2.847
Skhūl 4	Male	0.704	0.177	3.224	**0.823**	0.144
Grotte des Enfants 4	Male	*0.063*	0.002	16.291	**0.998**	3.463
Grotte des Enfants 5	Male	0.548	0.257	2.479	**0.743**	0.361
Nazlet Khater 2	Male	0.144	0.004	13.224	**0.996**	2.135
Paviland 1	Male	0.815	0.053	5.806	**0.947**	0.055

Table 4.9 Classification results for the fossil *H. sapiens* using the discriminant function combining PEL2, PEL7, PEL9, PEL10, and PEL11 shape variables, with a pooled African reference sample. For the predicted sex, the typicality probability indicates the probability of the observed discriminant score given membership in that group; probabilities ≤ 1.0 (shown in italics) indicate an atypical morphology for that group. Sex is assigned based on the highest posterior probability (shown in bold) and smallest D^2 to the group centroid.

Fossil	Predicted Sex	Typicality Prob.	♀ Post. Prob.	D^2 to ♀ centroid	♂ Post. Prob.	D^2 to ♂ centroid
Omo I	Female	0.572	**0.931**	0.320	0.069	5.539
Qafzeh 9	Male	0.158	0.000	18.769	**1.000**	1.998
Skhūl 4	Male	0.309	0.216	3.615	**0.784**	1.035
Grotte des Enfants 4	Male	*0.098*	0.000	20.916	**1.000**	2.737
Grotte des Enfants 5	Male	0.230	0.320	2.953	**0.680**	1.441
Nazlet Khater 2	Male	0.488	0.002	13.055	**0.998**	0.482
Paviland 1	Male	0.986	0.015	8.415	**0.985**	0.000

Table 4.10 Classification results for the fossil *H. sapiens* using the discriminant function combining PEL2, PEL7, PEL10, and PEL11 form variables, with a pooled African reference sample. For the predicted sex, the typicality probability indicates the probability of the observed discriminant score given membership in that group; probabilities ≤ 1.0 (shown in italics) indicate an atypical morphology for that group. Sex is assigned based on the highest posterior probability (shown in bold) and smallest D^2 to the group centroid.

Fossil	Predicted Sex	Typicality Prob.	♀ Post. Prob.	D^2 to ♀ centroid	♂ Post. Prob.	D^2 to ♂ centroid
Omo I	Female	0.194	**0.663**	1.685	0.337	3.041
Qafzeh 9	Male	0.478	0.001	14.077	**0.999**	0.504
Skhūl 4	Male	0.790	0.022	7.703	**0.978**	0.071
Grotte des Enfants 4	Male	*0.014*	0.000	30.359	**1.000**	6.092
Grotte des Enfants 5	Female	0.160	**0.587**	1.975	0.413	2.678
Nazlet Khater 2	Male	0.665	0.003	12.071	**0.997**	0.187
Paviland 1	Male	0.505	0.001	13.750	**0.999**	0.448

Table 4.11 Classification results for the fossil *H. sapiens* using discriminant function of PEL7, PEL10, and PEL11 form variables, with a Zulu reference sample. For the predicted sex, the typicality probability indicates the probability of the observed discriminant score given membership in that group; probabilities ≤ 1.0 (shown in italics) indicate an atypical morphology for that group. Sex is assigned based on the highest posterior probability (shown in bold) and smallest D^2 to the group centroid.

Fossil	Predicted Sex	Typicality Prob.	♀ Post. Prob.	D^2 to ♀ centroid	♂ Post. Prob.	D^2 to ♂ centroid
Omo I	Female	0.331	**0.962**	0.946	0.038	7.427
Qafzeh 9	Male	0.704	0.000	16.628	**1.000**	0.144
Skhūl 4	Male	0.459	0.016	8.749	**0.984**	0.547
Grotte des Enfants 4	Male	*0.054*	0.000	31.653	**1.000**	3.719
Grotte des Enfants 5	Female	*0.066*	**0.510**	3.377	0.490	3.460
Nazlet Khater 2	Male	0.539	0.000	18.599	**1.000**	0.378
Paviland 1	Male	0.951	0.001	13.226	**0.999**	0.004
Skhūl 5	Male	0.170	0.146	5.410	**0.854**	1.882
Barma Grande 2	Male	0.157	0.000	26.142	**1.000**	2.003
Cro-Magnon 1	Male	*0.000*	0.000	66.676	**1.000**	19.962
Cro-Magnon 4315	Male	*0.000*	0.000	57.590	**1.000**	15.141
Grotte du Cavillon	Male	0.342	0.035	7.545	**0.965**	0.904

Table 4.12 Classification results for the fossil *H. sapiens* using discriminant function of PEL2 and PEL11 form variables, with a Kikuyu reference sample. For the predicted sex, the typicality probability indicates the probability of the observed discriminant score given membership in that group; probabilities ≤ 1.0 (shown in italics) indicate an atypical morphology for that group. Sex is assigned based on the highest posterior probability (shown in bold) and smallest D^2 to the group centroid.

Fossil	Predicted Sex	Typicality Prob.	♀ Post. Prob.	D^2 to ♀ centroid	♂ Post. Prob.	D^2 to ♂ centroid
Omo I	Male	0.678	0.147	3.695	**0.853**	0.172
Qafzeh 9	Male	0.440	0.011	9.673	**0.989**	0.597
Skhūl 4	Male	0.674	0.148	3.674	**0.852**	0.177
Grotte des Enfants 4	Male	*0.001*	0.000	31.326	**1.000**	10.624
Grotte des Enfants 5	Female	0.296	**0.571**	1.094	0.429	1.669
Nazlet Khater 2	Male	0.715	0.027	7.304	0.997	1.606
Paviland 1	Male	0.205	0.003	12.995	**0.977**	1.606

Table 4.13 Classification results for the MSA and EUP fossils using the visual method to determine sex. The final sex diagnosis is based on the majority score obtained from three independent characters (see Chapter 3). F = typical female character state, M = typical male character state, I = indeterminate character state, dash = character not preserved.

Fossil	Side	Preauricular Surface				Composit Arch	Sciatic Notch				Sex
		PS1	PS2	PS3	PS majority	CA	SN1	SN2	SN3	SN majority	
Omo I	Lt	F	M	F	F	F	F	F	F	F	♀
Qafzeh 9	Lt	M	M	F	M	M	M	M	F	M	♂
Skhūl 4 (cast)	Rt	--	--	--	--	M	M	M	F	M	♂
Skhūl 5	Rt	--	--	--	--	M	F	F	F	F	**?**
Nazlet Khater 2	Lt	F	M	F	F	M	M	M	M	M	♂
Grotte du Cavillon 1	Lt	F	F	M	F	F	F	F	I	F	♀
Barma Grande 2	Lt	M	M	F	M	M	F	M	F	F	♂
Grotte des Enfants 4	Lt	M	M	I	M	M	M	M	M	M	♂
Grotte des Enfants 5	Lt	F	F	F	F	F	F	F	I	F	♀
Cro-Magnon 1	Rt	M	M	--	M	M	M	M	M	M	♂
Cro-Magnon 4315	Lt	M	M	F	M	M	M	M	M	M	♂
Paviland 1 (cast)	Lt	M	M	M	M	M	M	M	M	M	♂
Mladeč 21	Lt	F	I	F	F	F	F	F	F	F	♀

Table 4.14 Comparison of sex assignments using discriminant functions of os coxae shape and form, and the visual method. Shape variables are ratios of the raw measurement and the geometric mean of PEL1 and PEL3.

Fossil	Shape (Ln)			Form (Ln)			Visual Method
	PEL9+10 (African)	PEL2+11 (Kikuyu)	PEL2+7+9+10+11 (African)	PEL2+7+10+11 (African)	PEL7+10+11 (Zulu)	PEL2+11 (Kikuyu)	
Omo I	Female	Female	Female	Female	Female	Male	Female
Qafzeh 9	Male	Male	Male	Male	Male	Male	Male
Skhūl 4	Male	Male	Male	Male	Male	Male	Male
Grotte des Enfants 4	Male	Male	Male	Male	Male	Male	Male
Grotte des Enfants 5	Female	Male	Male	Female	Female	Female	Female
Nazlet Khater 2	Female	Male	Male	Male	Male	Male	Male
Paviland 1	Male	Male	Male	Male	Male	Male	Male
Skhūl 5	--	--	--	--	Male	--	--
Barma Grande 2	--	--	--	--	Male	--	Male
Cro-Magnon 1	--	--	--	--	Male	--	Male
Cro-Magnon 4315	--	--	--	--	Male	--	Male
Grotte du Cavillon 1	--	--	--	--	Male	--	Female
Mladeč 21	--	--	--	--	--	--	Female

Table 4.15 Summary of sex classification for the early *H. sapiens* fossils. Table continues on the next page.

Middle Stone Age (MSA)		Early Upper Paleolithic (EUP)	
		Grotte des Enfants 5	Female
Omo I	Female	**Mladeč 21**	Female
Skhūl 2[a]	Female	**Dolni Vestonice 3**[d]	Female
Skhūl 7[a]	Female	**Predmosti 4**[e]	Female
Qafzeh 3[b]	Female	**Predmosti 10**[e]	Female
		Cro-Magnon 2[f]	Female
		Barma Grande 2	Male
		Barma Grande 5[g]	Male
		Barma Grande 6[g]	Male
		Grotte des Enfants 4	Male
		Nazlet Khater 2	Male
Skhūl 3[a]	Male	**Paviland 1**	Male
Skhūl 4	Male	**Cro-Magnon 1**	Male
Skhūl 5	Male	**Cro-Magnon 4315**	Male
Skhūl 6[a]	Male	**Dolni Vestonice 13**[d]	Male
Skhūl 9 [a,c]	Male	**Dolni Vestonice 14**[d]	Male
Qafzeh 8[b]	Male	**Dolni Vestonice 16**[d]	Male
Qafzeh 9	Male	**Pavlov 1**[d]	Male
		Mladeč 22[c]	Male
		Predmosti 1[e]	Male
		Predmosti 3[e]	Male
		Predmosti 9[e]	Male
		Predmosti 14[e]	Male

Table 4.15 Continued.

Middle Stone Age (MSA)		Early Upper Paleolithic (EUP)	
AHS (tibia)	Uncertain		
Border Cave (humerus, ulna)	Uncertain	**Grotte du Cavillon 1**	Uncertain
Cave of Hearths (radius)	Uncertain	**Cro-Magnon**[f] (isolated postcrania)	Uncertain
KNM-ER 999 (femur)	Uncertain	**Dolni Vestonice 35**[d]	Uncertain
Qafzeh 7 (ulna)	Uncertain	**Mladeč**[h] (isolated postcrania)	Uncertain
Klasies River (ulna, radius)	Uncertain		

Unless otherwise stated, the diagnosis of sex is evaluated in this study. Source: [a] McCown and Keith (1939), [b] Vandermeersch (1981), [c] Hager (1989), [d] Trinkaus and Jelínek (1997) and Sládek et al. (2000), [e] Matiegka (1934), [f] Vallois and Billy (1965), [g] Verneau (1908), [h] Teschler-Nicola (2007).

Chapter 5

Morphometric Variation in the Appendicular Skeleton: Testing the Assumption of Equality Among Recent Sub-Saharan Africans

Introduction

Goals

Paleontologists regularly rely on living humans and apes as reference samples against which to interpret diversity in the hominin fossil record. Implicit in the use of modern analogs is the assumption that closely-related taxa are characterized by similar magnitudes and patterns of morphological variation. As will be addressed below, morphological variation in the human skeleton stems from numerous potential sources. Genetic studies have shown that more variation is represented among modern groups than between them, and that populations from sub-Saharan Africa are more diverse than non-Africans. However, the equality of variation in the appendicular skeleton between African populations has yet to be tested. Furthermore, it is often assumed that males and females also exhibit a similar magnitude of variation, though the sexes may be dimorphic. The goals of this chapter are to test for equality of variation between Africans in a large selection of appendicular measurements from the major long bones. Specifically, differences in postcranial variability will be evaluated 1) among the sexes between populations, 2) between the sexes among populations, and 3) between pooled-sex samples drawn from recent African populations.

The Assumption of Equality of Variation in Modern Humans

That humans differ genetically, and thus phenotypically, is certainly no surprise. Based on highly visible traits such as skin color, hair color and texture, and the shape of soft tissue structures of the face, variation in our species was historically understood in racial terms that corresponded to broad geographic regions (e.g., Coon, 1962). A closer look at the range of both genetic and morphological differences has consistently demonstrated that the majority of the variation within our polytypic species can be accounted for by differences between individuals within populations, rather than between populations (e.g., Hiernaux, 1968; Lewontin, 1972; Relethford, 1994, 2009). For example, Lewontin (1972) concluded that approximately 85% of the total *Homo sapiens* diversity in nine different blood groups is encompassed within populations, whereas only 15% of the variation can be accounted for by 'racial' differences, that is, differences between populations. Relethford obtained similar results based on analyses of a large craniometric and molecular dataset from a worldwide distribution of modern populations (Relethford, 1994).

Furthermore, the unequal patterning of genetic diversity among modern populations is not random, but instead appears to follow an isolation by distance model in which diversity decreases as distance from Africa increases (see review in Weaver and Roseman, 2008). This is confirmed by the high diversity of nuclear DNA, mtDNA and cranial morphology in African populations compared to non-Africans (Cann et al., 1987; Relethford, 1994; Cann and Wilson, 2003; Zhivotovsky et al., 2003). The greater diversity of sub-Saharan African populations stems from the fact that they reside within the geographic epicenter of the *H. sapiens* lineage, a fact supported by the fossil record which clearly shows the temporal primacy of this species in Africa (e.g., White et al., 2003;

McDougall et al., 2005). Thus, this pattern likely reflects either the greater depth of our lineage in Africa (Cann et al., 1987; Cann and Wilson, 2003), or simply the larger size of African versus non-African populations for most of the time since the species originated (Relethford and Jorde, 1999). Recent molecular evidence suggests that it is length of time since the founding and not population size that plays a more dominant role in the patterning of modern diversity (Weaver and Roseman, 2008).

Variation is the raw material on which evolution acts, regardless of whether the taxa in question are bacteria, fossil hominins, or modern *H. sapiens*. While genetic data are commonly analyzed to assess the level and pattern of variation within populations, skeletal morphology, whether metric or non-metric, is less commonly considered in light of within-population variability (Schmitt, 1995). The primary focus of much of the anthropological literature has been define and compare populations based on their means (e.g., Howells, 1973), with little biological interpretation of the magnitude and pattern of variability present within a population, and potential differences in variability between groups. Characterizing the morphological differences that exist between populations is obviously critical for ethnic identification in forensic applications (Scheuer, 2002), and to understand patterns of taxonomic relationships and phenetic similarities between fossils (e.g., Kidder et al., 1992; Pearson, 2000), but the study of intrapopulation variability can also contribute to the resolution of these and other issues.

Paleoanthropologists regularly employ modern human populations to resolve the taxonomic or phenetic relationships between fossils. Implicit in the use of modern humans as a standard or reference group is the assumption that living and past people share a similar magnitude and pattern of morphological variation. This assumption may not be satisfied, given some evidence which suggests that even living populations differ with regard to magnitude and pattern

of variation. For example, Ackermann (1998) found a similar level of cranial variation between a sub-specific human sample comprised of individuals from select closely-related South African tribes, and a world-wide human sample. Importantly, Ackermann's rationale for employing a South African tribal sample as a reference was that it would represent less variation than a global human sample, an assumption which was not satisfied. This example illustrates the need to gain a better appreciation of human intrapopulation variation. Clearly, our assumptions regarding modern morphometric variation, whether implicit or not, would benefit from explicit testing.

The genetic contribution to phenotypic variance in most traits is believed to be mostly constant between populations (e.g., Hiernaux, 1968; Schmitt, 1995). But the evolutionary forces that act on the variation within a population, whether these forces are random such as genetic drift, or non-random such as directional selection, will differ between populations (Ackermann, 2002; Ackermann and Cheverud, 2002, 2004), as will the influence of other factors that affect the demographic structure of the population such as migration and gene flow (e.g., Harding and McVean, 2004; Castri et al., 2009), local contraction or expansion of the breeding population (e.g., Excoffier, 2002). Therefore, an understanding of population-level variation not only provides a framework for interpreting the results of fossil studies, but it can also provide insights onto the evolutionary and demographic forces that have shaped our species.

Sources of Variation in Modern Humans

At the intraspecific level, morphological variation can arise from diverse biological causes. Some of these sources of variation, such as development, pathology or trauma, are readily recognizable in their influence on the skeletal variation within a population. To a great extent, the influence of these sources on

variation can be easily controlled by employing sampling strategies that restrict comparisons to a specific age class (e.g, adults), and recording measurements on bones that appear healthy. The human species is polytypic, with populations exhibiting geographically patterned morphology which tends to reflect physical adaptations to local environment and climate. Significant relationships between body size and shape and environmental variables such as mean annual temperature are well documented (e.g., Ruff, 1994). However, the influence of geographic variation can be controlled largely by focusing on well-defined populations in which the individuals likely express similar skeletal responses to environmental pressures.

Morphological differences between adult males and females occur in all human populations, although sexual differences tend to be expressed to a lesser degree than in closely-related hominoids (Leutenegger, 1982; Oxnard, 1987; Wood et al., 1991). Sexual dimorphism, whether expressed as size or shape differences, likely contributes to the magnitude of variation observed in any given population. As dimorphism increases, the sex-specific means will diverge, which could result in a higher magnitude of variation when the sexes are pooled. Among *H. sapiens*, the level of sexual dimorphism varies between populations. This has been documented not only in overall bodily dimorphism as represented by stature (e.g., Wolfe and Gray, 1982), but also in the finer details of anatomy as represented in the cranium (e.g., van Vark et al., 1989; O'Higgins et al., 1990), mandible (e.g., Humphrey et al., 1999; Franklin et al., 2008), and postcranium (Hamilton, 1982; Patriquin et al., 2003; Steyn et al., 2004 – see also Chapter 4 of this dissertation) across diverse modern populations. Because the magnitude and pattern of dimorphism itself varies across populations, the contribution of dimorphism to the overall level of morphological variation within any given population may also differ. However, employing same-sex samples helps to

control for the potentially different influence of dimorphism on sample variation among populations.

Temporal variation also needs to be considered as a potential source of variation because over time, fluctuations in the mean of a trait, whether directional or not, may inflate the overall level of variation. Although this is more of a concern for fossil studies where specimens are typically sampled over a large time span (see Chapter 6), temporal variation may still impact the variation documented in skeletal samples drawn from modern populations. For example, better access to healthcare and improvements in nutrition are believed to contribute to secular trends towards increasing stature and body size, and faster skeletal and physiological maturation over the course of only a few generations (Mielke et al., 2006). Samples drawn from a burial site that was used over the course of several centuries may thus provide inflated measures of variation.

On a more practical level, measurement error may inflate relative variation, especially in very small specimens or in the measurement of small features; this effect is not necessarily remedied by applying a log transformation (Polly, 1998). However, Polly found that the influence of measurement error is limited if the error represents < 10% of the size of the feature. In the human appendicular skeleton, most measurements are comparatively large, but measurement error may still adversely influence sample variation. In this dissertation, an error study found that measurement error never exceeded 10%; in fact, as reported in Chapter 2, error is substantially less than 3% for the majority of variables employed here. Therefore, measurement error likely has a negligible influence on variation in the present study.

Genetic and morphometric studies show that more variation is represented within modern human populations than between them, and despite the possible evolutionary and historical insights afforded by studies of intrapopulation morphometric variation in humans, paleoanthropologists regularly assume that

populations exhibit equal magnitude and pattern of variation. The assumption of constant variation through time may be a necessary starting point for a historical science such paleontology which is fraught by small sample sizes that cover large spans of time, but, as some workers have acknowledged (Plavcan and Cope, 2001; Ackermann, 2003), it is nonetheless important to consider the effect of these assumptions on our interpretations of the fossil record. As Plavcan and Cope remarked: "the study of variation in living species as it relates to the variation in the fossil record is surprisingly open" (2001: 220).

In this chapter, the assumption of an equal magnitude of variation in the appendicular skeleton of three recent African populations will be directly tested. To provide a detailed understanding of the patterning of variation within these populations, variability will be compared among sexes between populations (i.e., female *versus* female, male *versus* male), between the sexes within populations (i.e., female *versus* male), and between pooled-sex samples from these populations. By examining differences in the level of variability across joints, diaphyses and muscle attachment sites of five major long bones, this chapter will elucidate potential dissimilarities in the patterning of postcranial variation between these groups.

Skeletal Samples

A suite of 98 morphometric variables was recorded on the major long bones (humerus, ulna, radius, femur, and tibia) of humans selected from three African populations: the Zulu, the Kikuyu, and Nilotic Ugandans. All measurements are defined in Appendix 1. Nine variables that exhibit high measurement error were identified in Chapter 2, and these were excluded from the present analysis. As described in Chapter 2, each skeletal sample is comprised of known-tribe, known-sex individuals selected from restricted geographic and

temporal ranges. Thus, within each population sample the influence of cultural factors, geographic distance and time on skeletal variation is limited. The Zulu and Kikuyu samples each consist of female and male sub-samples (Table 5.1). The Nilotic Ugandan sample is strongly male-biased (Table 5.1). As a result, this sample is only partitioned into a male sub-sample.

Methods: Equality of Relative Variation

In order to compare the magnitude of variation between individuals, the effect of scale must be considered because absolute variation tends to increase proportionally with the mean (Van Valen, 1978). A classic example provided by Simpson and colleagues (1960) illustrates this point: elephants and shrews may exhibit a standard deviation of 50 mm and 0.5 mm respective for a linear variable such as tail length, but that does not mean that elephants are relatively more variable than shrews in the length of their tails. The most common measure of relative variation is the coefficient of variation (CV):

$$CV = \frac{\text{s.d } x \text{ } 100}{\text{mean}}$$

where the standard deviation (s.d, multiplied by 100 for convenience) of each variable is divided by its mean (Sokal and Rohlf, 1995). Alternatively, the effect of scale on absolute variation can be eliminated by applying a log transformation to the raw data (Lewontin, 1966; Van Valen, 1978). As Plavcan and Cope (2001) have pointed out, the CV should not be computed from log-transformed data since both treatments act to mitigate the effect of size, and using both simultaneously effectively re-introduces size.

In the paleontological literature, the main interest in comparing relative variation between samples has been to test the hypothesis that a fossil sample is

comprised of multiple species (e.g., Pilbeam and Zwell, 1972; Cope and Lacy, 1992, 1995). Alternatively, excess variation in a fossil sample may suggest a high level of sexual dimorphism for the extinct taxon, as Kelley and Xu (1991) have proposed for the Miocene ape *Lufengpithecus*, and others have proposed for *Australopithecus afarensis* (e.g., Richmond and Jungers, 1995; Lockwood et al., 1996). Comparing the relative variation of a fossil sample to that of a reference sample (usually a closely-related extant taxon) can help to resolve the issue of "two sexes or two species" (Plavcan and Cope, 2001: 205). However, as Donnelly and Kramer (1999) and others (e.g., Plavcan and Cope, 2001) have cautioned, the only hypothesis that is directly tested in such studies is whether a fossil sample exhibits greater relative variation compared to a reference sample. Interpretations such as the presence of multiple species or high levels of sexual dimorphism remain second-order hypotheses that are not directly tested simply by comparisons of relative variation. Tests of relative variation allow researchers to reject the null hypothesis of equal relative variation, but the cause(s) of excess variation in a fossil sample must be evaluated in a broader framework that considers biological, chronological, and taphonomic factors, as well as sampling issues.

The CV provides a simple way to quantify the level of relative variation in univariate data. Unlike range-based statistics such as the maximum:minimum ratio, the CV is less sensitive to outliers (Donnelly and Kramer, 1999; Plavcan and Cope, 2001). But how does one interpret differences in CVs between samples? Based on a large number of linear dimensions from various skeletal elements, Simpson et al. (1960) observed that CVs between 4 and 10 are typical of a range of morphological measurements across mammals when homogenous samples (i.e., those comprised of individuals from a single sex and age class) are compared. Their observation has since been used by paleontologists as a yardstick by which to gauge variation: fossil samples with a CV > 10 are often

interpreted as comprising more than one species (Plavcan and Cope, 2001). However, simply documenting CVs that are greater than this value does not represent an robust test.

There is considerable debate concerning which statistical methods are most appropriate to test for significant differences in the magnitude of relative variation. Since homoscedasticity (i.e., homogeneity of variances) is a fundamental assumption of numerous univariate and multivariate statistical tests (e.g., Neff and Marcus, 1980; Sokal and Rohlf, 1995; Quinn and Keough, 2002), statisticians have developed a number of methods by which to test for equality of variances. However, as Donnelly and Kramer (1999) have pointed out, many of these tests are not applicable to paleontological studies because they require large samples, or have subsequently been demonstrated through simulations to lack either robustness (i.e., the ability to minimize the occurrence of type I errors – the rejection of a true null hypothesis – under varying test conditions), or power (i.e., the ability to reject the null hypothesis when it is false, thus not commit a type II error), or both. Using a series of Monte Carlo simulations to mimic the types of samples typical of paleontological studies, Donnelly and Kramer (1999) tested the robustness and power of eleven tests for equality of relative variation in univariate data. They determined that the Fligner-Killeen (FK) test is the most optimal method under a range of conditions such as sample sizes as small as $n = 7$, samples that deviate from normality, and distributional differences between the samples under comparison.

The basic principles of the FK test are as follows: In order to remove differences of scale, thus converting a test for equality of absolute variation into one of relative variation, the data are transformed using natural logarithms (ln). Each sample is centered on its median value, and the median value (or one of the values bracketing the median, in the case of an even number of individuals) is excluded. The absolute deviation of each individual from the median is

computed; the deviates are first ranked, then each rank (r_i) is replaced with a weighted score for that individual (s_i) based on the following formula:

$$s_i = \left\{ \Phi^{-1} \left(\frac{N + 1 + r_i}{2(N + 1)} \right) \right\}^2$$

where Φ is a function for the standard normal distribution, and N is the combined size of the two samples being compared (Donnelly and Kramer, 1999). The test statistic (T) represents the sum of the weighted scores for the smaller sample. The observed T is then compared to $E(T)$, the expected value for T, which is calculated as the product of the number of individuals and the average weighted score of the smaller sample. To assess significant differences between T and $E(T)$, critical values are approximated as follows:

$$z = \frac{T - E(T)}{\sqrt{\text{variance } T}}$$

The analyses described above serve to explore differences in relative variation in postcranial variables when each is tested separately, but they do not account for correlations between the variables recorded for each element, and nor do they account for redundancies in the data. Therefore, multivariate methods are employed to investigate differences in variation in the long bones in a more comprehensive manner. Principal components analysis (PCA) is conducted on the ln-transformed variables for each element separately. As noted above, the ln-transformation eliminates the effect of scale, and allows relative variation to be studied. PCA transforms the original variables into new, uncorrelated variables called principal components (Quinn and Keough, 2002). Each principal component represents an axis in the direction of the greatest variance among

individuals in multivariate space, and is orthogonal (i.e., independent) to all other components (Neff and Marcus, 1980). Components are extracted sequentially, such that each reflects a decreasing amount of the total variance present between individuals (Neff and Marcus, 1980). Typically, most of the variance is concentrated in the first few components.

In PCA, individuals are characterized by scores on each of the principal components extracted in the analysis (Neff and Marcus, 1980). This allows the scatter of individuals to be visualized through plots of their scores on different components. Since components are extracted sequentially starting with the one that captures most of the variance between individuals, the first and second principal components, PC1 and PC2 respectively, tend to represent a substantial portion of the variation. Hence, bivariate scatterplots of PC1 and PC2 are used to help visualize the distribution of individuals in multivariate space. The variables that contribute most heavily to each component are identified by high loadings on a particular component. Since this study employs correlation matrices, the loadings represent the correlation between each variable and the components (Neff and Marcus, 1980).

As with the univariate analyses described above, PCA is used to investigate relative variation within each sex between populations (e.g., Zulu *versus* Kikuyu *versus* Ugandan males), and within populations between sexes (e.g., Zulu females *versus* males). The latter analyses capture the extent of sexual dimorphism expressed in each element in the Zulu and Kikuyu. As discussed by Neff and Marcus (1980), the principal component scores themselves constitute new data that can be analyzed in various ways; this will be addressed below as it pertains specifically to each hypothesis.

The choice of which association matrix (i.e., correlation *versus* covariance matrix) to employ to best capture the interconnectedness of variables is important. Since all variables employed in this study are measured in the same unit

(millimeters), and the raw data have been log-transformed such that their variance is independent of the mean, both the correlation and covariance matrices could be appropriate (Neff and Marcus, 1980; Quinn and Keough, 2002). However, using a covariance matrix may attach importance to differences in variance between variables, such that those variables with higher variances contribute more to the analysis. Since this study combines samples from up to three different populations, the samples may differ in the amount of variation exhibited by each variable, in which case PCA performed using a correlation matrix may be preferrable. However, since the correlation matrix standardizes the data so that each sample has a mean of zero and a standard deviation of one (Quinn and Keough, 2002), the use of such a matrix may undermine attempts to assess differences in sample variability. As there is no clear answer regarding the choice of association matrix for this novel application of PCA, both methods were used in a test case. Encouragingly, the results were very similar under both models. PCA using a correlation matrix was used to test the hypotheses in the present chapter.

The main goal of this chapter is to test the assumption of equality of relative variation in the appendicular skeleton of three modern human groups. To provide a detailed understanding of the patterning of variation within these populations, variability will be compared among sexes between populations (i.e., female *versus* female, male *versus* male), between the sexes within the populations (i.e., female *versus* male), and between pooled-sex samples from the populations; these methods employed to test each hypothesis will be described below. Throughout this chapter, line graphs of the CV – computed from the raw data – are used to help visualize levels of relative variation across the samples. The FK test and the modified Levene's test using the PCA scores are performed using PAST, following the procedure outlined above as recommended by

Donnelly and Kramer (1999), while PCA and other tests are conducted using SPSS 11.0. Specifically, four hypotheses are tested here:

Hypothesis 1 (H_1): Female samples drawn from different populations exhibit an equal magnitude of morphometric variation across the appendicular skeleton.

The FK test is employed to test the null hypothesis of equal relative variation between females from different populations. Two-tailed tests are employed because there is no *a priori* expectation that females from either of the modern samples represents a more appropriate standard against which to evaluate variation. This differs from a paleontological design in which the goal is to test specifically for excess variation in fossil samples relative to a reference. As noted above, too few Ugandan females are available to compare variation in this group; therefore tests of H_1 are limited to a comparison between Zulu and Kikuyu females. With a single planned comparison, no adjustment to the testwise alpha is needed to maintain a familywise probability set at 0.05.

To test for differences in the magnitude of variation in a multivariate context, the scores of individuals obtained from PCA are analyzed for differences in relative variation using a modified version of Levene's test for homogeneity of variances. In its original form, Levene's test is a test for absolute variation, whereby the absolute difference of each individual from the sample mean is computed, and the mean deviates are tested using a *t*-test or ANOVA (van Valen, 1978). More precisely, this is a test of mean deviation or dispersion from the mean (van Valen, 1978), but it functions as a test of variation because as variance in a sample increases, the mean of the deviates will also increase. As noted by van Valen (1978) and Donnelly and Kramer (1999), Levene's test can be used as a test for the equality relative variation if log-transformed data are employed because the effect of scale has been eliminated.

To apply this version of Levene's test, the data are first transformed using the natural log, then converted into deviates (X') about their means such that $X' = \ln X - \text{mean}(\ln X)$. Then, a *t*-test is used to determine whether there are significant differences between the samples based on the mean of the deviates. Again, this is actually a test for the equality of dispersion between samples since the greater the variance in a sample, the greater the mean of deviates will be. Simulation trials have shown this test to be quite robust and powerful for sample sizes ≥ 7; robustness and power also increase when the deviates are centered about the median rather than the mean (van Valen, 1978; Donnelly and Kramer, 1999). These recommendations are followed here.

Hypothesis 2 (H_2): Male samples drawn from different populations exhibit an equal magnitude of morphometric variation across the appendicular skeleton.

A two-tailed FK test is employed to test the null hypothesis of equal relative variation of linear measurements of the major long bones between Zulu, Kikuyu, and Ugandan males (H_2). In addition, differences in the dispersion of PCA scores between the males are tested using a modified Levene's test in order to compare the magnitude of variation in multivariate space, as outlined in H_1. Here, three comparisons are planned: Zulu versus Kikuyu, Kikuyu versus Ugandan, and Ugandan versus Zulu. Therefore, the Bonferonni Approximation is used to adjust the probability level for multiple comparisons using the same data in order to maintain a familywise probability at 0.05, thus preventing an inflated Type I error rate (Abdi, 2007). The following equation is used to determine the adjusted testwise probability level:

$$\alpha_T = \frac{\alpha_F}{C}$$

where α_T is the probability level per test, α_F is the desired familywise probability level to be maintained across all tests, and C is the number of planned comparisons that are needed to test the hypothesis (Abdi, 2007). For the three planned comparisons needed to test H_2, 0.5/3 = 0.0167; thus $p < 0.0167$ is the adjusted testwise probability level that preserves a familywise probability of 0.05.

Hypothesis 3 (H_3): Within the same population, the sexes exhibit an equal magnitude of morphometric variation across the appendicular skeleton.

In the groups for which both sexes are available (i.e., the Zulu and Kikuyu), the equality of relative variation between females and males will be tested using a two-tailed FK test for the univariate data. In addition to the FK test, *t*-tests are performed to assess significant differences of means between the sexes, thereby identifying postcranial variables that are sexually dimorphic among the Zulu and Kikuyu. It is expected that many of the variables will exhibit differences between the sexes, since the log-transformed data capture aspects of both size and shape, but these tests will explore the relationship between the presence of dimorphism and differences in relative variation for each variable. With a single planned comparison performed on the data from each population, there is no need to correct testwise probability level ($p < 0.05$).

Differences in the dispersion of PCA scores between the sexes are tested using a modified Levene's test in order to compare the magnitude of variation in multivariate space, as outlined in H_1. PC1 tends primarily to capture differences in size between individuals. Thus, this component can be used to assess the influence of sexual dimorphism on multivariate variation in the Zulu and Kikuyu

samples, where both sexes are represented in sufficient numbers. To test whether PC1 reflects variation in size in these samples, the Pearson product-moment correlation is used to test for a significant relationship between individual scores along PC1 and the size of the individual, as represented by the geometric mean (GM) of all variables for that element. A significant positive correlation is expected if PC1 captures size-related variation between the sexes. On the other hand, PC2 (and PC3, if a third component is extracted) is not expected to exhibit a significant correlation with the GM. Additionally, a *t*-test is expected to identify significant differences between female and male mean PC1 scores.

Hypothesis 4 (H_4): With sexes pooled, the populations exhibit an equal magnitude of morphometric variation across the appendicular skeleton.

A two-tailed FK test is employed to test the null hypothesis of equal relative variation between the Zulu and Kikuyu pooled-sex samples. In addition, differences in the dispersion of PCA scores between the samples are tested using a modified Levene's test in order to compare the magnitude of variation in multivariate space, as outlined in H_1. Furthermore, differences in sexual dimorphism may influence intra-population variability because as dimorphism increases, the sex-specific means diverge, which may increase the variability within the population. To investigate this relationship, the index of sexual dimorphism (ISD) is computed for each measurement:

$$\text{ISD} = \frac{\text{male mean}}{\text{female mean}} \times 100$$

A population with a higher degree of dimorphism is expected to have a higher magnitude of variation relative to a less dimorphic sample.

Results

The results for each hypothesis are presented sequentially. For each hypothesis, univariate results are presented first by element starting with the upper limb (humerus, ulna, radius), then the lower limb (femur, tibia), followed by the multivariate test results. As noted above, the Ugandan sample comprises an insufficient number of females for sexual dimorphism to be evaluated in this sample, and nor are the Ugandan females compared to females from the other samples. Summary statistics for the sex-specific samples are provided in Appendix 2 in separate tables for each element.

Equality of Variation Between Females (H_1)

The magnitude of relative variation in the humerus exhibited by females from the Zulu and Kikuyu samples, illustrated in the CV line plot in Figure 5.1, shows a clear divergence between the samples. For most measurements, the Kikuyu females appear to have distinctly higher variability. This trend is supported by the FK test (Table 5.2), which found significant differences in variation between these samples in seven out of twenty humeral measurements: humeral length (HUM1-2), DV head diameter (HUM6), epicondylar width (HUM11), capitulum + trochlea width (HUM12), capitulum height (HUM14), and AP diameter of the capitulum (HUM15). In each case, Kikuyu females have a greater level of variation than Zulu females. The Zulu show a trend for elevated variation in the minimum midshaft diameter of the humerus (HUM4) and the breadth of the medial dorsal pillar (HUM20) compared to the Kikuyu, but these differences are statistically nonsignificant (Table 5.2). Females from both populations exhibit high variability (CV = 14) in deltoid tuberosity length (HUM9), as expected for a muscle attachment site, and both show relatively low

variability in the breadth of the lateral dorsal pillar (HUM19, CV = 9) and minimum shaft circumference of the humerus (HUM25, CV = 7).

Across the twenty ulnar measurements, Kikuyu females show a trend for increased variability compared to Zulu females (Figure 5.2). The FK test results reject the null hypothesis of equal relative variation for nine of the ulnar measurements (Table 5.3): ulnar lengths (ULN1-2), ML coronoid breadth (ULN6), olecranon height (ULN7), mid-trochlear notch thickness (ULN12), AP notch thickness (ULN13), length of the radial notch (ULN15), transverse breadth of the distal epiphysis (ULN20), and minimum ulnar shaft circumference (ULN21). In each case, it is females from the Kikuyu population that have a greater magnitude of variation than the Zulu. Females from both samples have high variability (i.e, CV > 10) for ULN17, position of the brachialis insertion on the proximal ulna, as expected for a rather poorly-defined muscle attachment site, although the Kikuyu females seem to be substantially more variable in this measurement than the Zulu (Figure 5.2). The Zulu only exhibit more variability (but not significantly more) than Kikuyu females in shaft diameters: maximum ulnar midshaft diameter (ULN3) and AP diameter of the proximal ulnar shaft (ULN18).

CVs of the thirteen radius measurements also show a trend for greater variability among Kikuyu females compared to Zulu females (Figure 5.3). This trend is supported by the FK test results (Table 5.4), whereby the null hypothesis for equal variation is rejected in seven out of thirteen measurements: length of the radius (RAD1-2), radial head diameters (RAD5-7), AP diameter of the radial neck (RAD10), and DV breadth of the distal epiphysis (RAD11). Zulu females have a nonsignificant trend for increased variation in maximum midshaft diameter (RAD3) and radial tuberosity length (RAD8) compared to the Kikuyu (Figure 5.3). Surprisingly among the Kikuyu females, variability in radial tuberosity

length, a muscle insertion site expected to exhibit high variability, is approximately the same as variability in head dimensions within this group.

The pattern of excess variability among Kikuyu females relative to Zulu females extends into the lower limb, as illustrated by the CV plot of variation across eighteen femoral measurements (Figure 5.4). Based on the FK test results, the null hypothesis of equal relative variation between Zulu and Kikuyu females is rejected for six out of eighteen measurements (Table 5.5): femoral lengths (FEM1-2), minimum neck breadth (FEM8), biomechanical neck length (FEM9), ML subtrochanteric femoral shaft diameter (FEM12), and biepicondylar breadth of the distal femur (FEM15). In each instance, the female sample from the Kikuyu population exhibits greater variation than the Zulu females. As expected, females from both populations are characterized by a high level of variation (CV = 21) for gluteal tuberosity breadth. Variability among Zulu females only exceeds that of Kikuyu females in two measurements: AP midshaft diameter (FEM3; at $p = 0.0627$, this difference approaches significance) and neck length (FEM10).

Similarly, Kikuyu females tend to exhibit higher variability across the tibia compared to Zulu females (Figure 5.5). The FK test results demonstrate that variability among Kikuyu females is significantly greater than that of Zulu females in eight out of eighteen tibial measurements (Table 5.6): tibia lengths (TIB1-2, and TIB15-16), maximum breadth of the tibial plateau (TIB6), AP diameter of the medial and lateral condyles (TIB7 and TIB9 respectively), and AP length of the talar articular surface (TIB13). Furthermore, Kikuyu females show a trend for relatively greater variation than Zulu females in tibial condyle length (TIB5) and ML breadth of the distal epiphysis (TIB14); these differences approach significance (Table 5.6). In contrast, the only tibial measurements where variation among Zulu females exceeds that of Kikuyu females are shaft diameters: midshaft AP and ML diameter (TIB3-4) and AP diameter at the level

of the nutrient foramen (TIB11). Differences in AP midshaft diameter approach significance, with greater variation exhibited by Zulu females relative to Kikuyu females (Table 5.6).

Levene's (median) test is used to assess differences in dispersion between the scores of females from the Kikuyu and Zulu samples along PC1. This test found significant differences between the females in all long bones (Table 5.7). In contrast, the null hypothesis of equal dispersion along PC2 is supported for all elements (Table 5.7), although differences in PC2 scores approach significance for the humerus ($p = 0.0795$).

Equality of Variation Between Males (H_2)

CVs for the humeral measurements across Zulu, Kikuyu and Ugandan males are plotted in Figure 5.6. As this figure illustrates, the males from these African populations tend to exhibit similar magnitude of variation across most dimensions, showing consistent peaks in variability in measurements such as deltoid tuberosity length (HUM9) and breadth of the medial dorsal pillar (HUM20), and consistently low variability in measurements such as humeral length (HUM1-2). Using an adjusted probability level ($p < 0.0167$) for multiple comparisons, the FK test results do not reject the null hypothesis of equal relative variation for any of the humeral measurements (Table 5.8). The same pattern of equal relative variation between the males is observed for the ulna and radius, as illustrated by CV plots in Figures 5.7 and 5.8 respectively. The equality of variation is also supported by the FK test for all measurements of both these elements (Tables 5.9 and 5.10).

For most lower limb measurements, the CVs show a close correspondence across the males sampled from the Zulu, Kikuyu, and Ugandan populations, as illustrated in Figure 5.9 and 5.10 for the femur and tibia respectively. Lengths of

the femur (FEM1-2) and tibia (TIB1-2) consistently exhibit a low magnitude of variation across the samples, while muscle attachement sites such as the breadth of the gluteal tuberosity (FEM13) are highly variable (CV > 10) in all groups. Out of eighteen femoral measurements, the FK test identifies a single occurrence where it is possible to reject the null hypothesis of equal variability (Table 5.11): the biomechanical neck length (HUM9) of the Zulu males is significantly more variable than that of Kikuyu males. No significant differences are found in any of the tibial measurements (Table 5.12). The multivariate results, reported in Table 5.13, accord with the univariate results, showing no significant differences in dispersion along PC1 or PC2 between males from these three populations.

Equality of Variation Between the Sexes (H_3)

T-tests and FK tests are employed to test for the equality of means and magnitude of relative variation respectively between the sexes in both the Zulu and Kikuyu samples, in order to assess whether dimorphic features tend to also show dimorphism of variance (i.e, inequality of relative variation between the sexes). For most of the measurements of the humerus, males and females appear to exhibit similar levels of variability in each population (Figure 5.11). This is supported among the Kikuyu by the FK test results which show no significant differences in magnitude of relative variation between the sexes for any humeral measurements, despite the fact that the Kikuyu are sexually dimorphic for most of these measurements, as demonstrated by the *t*-test results (Table 5.14). In contrast, among the Zulu the sexes differ significantly in humeral length (HUM1-2), with males exhibiting greater levels of variation (Table 5.14). While most other measurements of the humerus are significantly dimorphic among the Zulu, none of them exhibit significant variance dimorphism (Table 5.14).

In the ulna, variability between the sexes seems to be mostly of equal magnitude among the Zulu and Kikuyu (Figure 5.12), despite significant dimorphism across the ulna (Table 5.15). However, as reported by Table 5.15, both samples are characterized by limited evidence for dimorphism of variance. Among the Zulu, males exhibit significantly more variation than females in two measures of trochlear notch thickness (ULN12 and ULN13), while Kikuyu females exhibit significantly more variation in the breadth of the distal epiphysis.

The Kikuyu are characterized by significant dimorphism in the radius, as attested by the *t*-test results, but shows no evidence of significant differences in the magnitude of variation between the sexes based on the FK test results (Table 5.16). The similar variability in features of the radius comprised by the Kikuyu sexes is visually represented in Figure 5.13. A similar pattern of sexual dimorphism and equal relative variation between the sexes is also documented among the Zulu across most features of the radius (Figure 5.13), although Zulu males do exhibit significantly more variation than females in the DV breadth of the distal epiphysis (RAD13, see Table 5.16).

As depicted in Figures 5.14 and 5.15 for CVs of femoral and tibial measurements respectively, the overall pattern in both the Zulu and Kikuyu is one of equal relative variation, despite significant dimorphism in most of the measurements of the femur (Table 5.17) and tibia (Table 5.18). However, significant inequalities of variation between the sexes are apparent in the lower limbs from both populations. Among the Zulu, males exhibit greater variability than females in biomechanical neck length (FEM9) and biepicondylar breadth (FEM15), while among the Kikuyu, it is the females who exhibit greater variability than the males in horizontal head diameter (FEM6), biomechanical neck length (FEM9), and AP subtrochanteric shaft diameter (Table 5.17). A trend in the same directional is evident in the tibia (Table 5.18): there is more variation in the length of the tibia (TIB1-2) and the AP length of the talar articular surface

among Zulu males than females, while among the Kikuyu, females exhibit more variation in breadth of the tibial plateau (TIB6), AP and ML dimensions of the lateral condyle (TIB9-10), and the AP length of the talar articular surface (TIB13).

PCA conducted for each element show the extent of morphometic variation in multivariate space among the Zulu and Kikuyu samples, while the *t*-test and Levene's (median) test are used to assess significant differences between the mean and dispersion of male and female scores along the first two principal components. Figures 5.16 to 5.20 depict the spread of Zulu and Kikuyu individuals along PC1 and PC2 for the five long bones (humerus, ulna, radius, femur, and tibia). In all these plots, the sexes appear to diverge primarily along PC1, but it is difficult to assess differences in the extent of dispersion between the sexes in many cases. However, in some instances such as the plot of PC1 and PC2 scores for the humerus (Figure 5.16), the Zulu females appear more tightly clustered in multivariate space than the males, while no such difference is apparent among the Kikuyu. Levene's test supports significant differences in dispersion between the sexes along PC1 for the upper limb elements within the Zulu sample, but not the Kikuyu, while no differences were identified in the lower limbs in either population (Table 5.19). As this table also shows, both the Zulu and Kikuyu exhibit significant dimorphism between the means of the sexes along PC1. To assess the extent to which PC1 is correlated with differences in size between the sexes, the correlation between PC1 scores and a size proxy for each element (the geometric mean of all measurements for that element) is evaluated among both samples. The results, presented in Table 5.20 and 5.21 for the Zulu and Kikuyu respectively, indicate a strong correlation between PC1 scores and the size of each element, while the relationship between element size and the remaining components (i.e., PC2 and PC3) is non-significant in all elements in both samples.

Equality of Variation Between Populations (H_4)

The sexes were pooled in order to assess differences in magnitude of postcranial variation between the Zulu and Kikuyu. By comparing these samples with the sexes pooled, the influence of sexual dimorphism on intra-population variability can be better understood. The ISD is a ratio of the male mean to the female mean; thus, values greater than 100 indicate that males are larger than females. As shown in Figure 5.21, sexual dimorphism in the humerus tends to range between 10 to 15% among both the Zulu and Kikuyu. That is, males of each population are on average 10-15% bigger than the females, as suggested by the *t*-tests reported above. There are some differences in the level of dimorphism between these African populations: the Kikuyu exhibit more dimorphism in olecranon fossa width and breadth of the lateral dorsal pillar compared to the Zulu, but the Zulu are more strongly dimorphic in the breadth of the medial dorsal pillar (Figure 5.21). Despite some differences in the level of sexual dimorphism, the FK cannot reject the null hypothesis of equal relative variation in the humerus between the Zulu and Kikuyu (Table 5.22). The high dimorphism in medial dorsal pillar breadth (ISD = 126%) documented in the Zulu is matched by a high magnitude of variation in this dimensions (CV = 24%). Both samples have negligible dimorphism in deltoid tuberosity length, despite elevated variation in this muscle attachment site (CV = 14%).

Both populations seem to be characterized by similar levels of sexual dimorphism and morphometric variability across ulnar dimensions, as illustrated in Figure 5.22. The FK test supports the null hypothesis of equal variation between the Zulu and Kikuyu in all but one measurement: the Kikuyu exhibit significantly more variation in radial notch length compared to the Zulu (Table 5.23). Interestingly, the level of dimorphism in this feature also appears to differ

between these groups, with the Kikuyu being roughly 5% more dimorphic than the Zulu in radial notch length (Figure 5.22).

For all measurements of the radius, the FK test results cannot reject the null hypothesis of equal relative variation between the Zulu and Kikuyu samples (Table 5.24). However, as shown in Figure 5.23, these populations show a somewhat divergent pattern of sexual dimorphism in the radius. The Kikuyu are more dimorphic in radial neck length (RAD9), AP diameter of the neck (RAD10), as well as minimum shaft circumference (RAD15), while the Zulu are more dimorphic in radial head diameters (RAD6-7).

In the femur, the predominant pattern reflects the equality of relative variation between the Zulu and Kikuyu samples (Table 5.25). However, variability is not equal in all femoral dimensions. The FK test results demonstrate that the Kikuyu are more variable than the Zulu in ML subtrochanteric shaft diameter (FEM12), while a significant difference in the opposite direction is found for variability in gluteal tuberosity breadth (FEM13). Variability in this feature is elevated in both populations (CV = 15 and 22 for the Kikuyu and Zulu respectively), as expected for a muscle insertion site, but as Figure 5.24 illustrates, these populations differ in the level of dimorphism in the gluteal tuberosity. In fact, the Zulu are more than 10% more dimorphic than the Kikuyu in this feature.

In the tibia, all measurements show equal relative variation between the Zulu and Kikuyu, as indicated by the FK test results in Table 5.26. Sexual dimorphism in this element also seems rather constant at about 10% in both populations (Figure 5.25), although the Zulu do appear to have somewhat elevated dimorphism in some measurements, including the AP and ML dimensions of the lateral tibial condyle (TIB9-10).

Results of Levene's (median) test for equality of dispersion of PC1 scores between the Zulu and Kikuyu demonstrate that the null hypothesis of equal relative variation cannot be rejected for any long bones (Table 5.27). Similarly,

these populations have equal dispersion along PC2 in the five appendicular elements studied here (Table 5.27).

Discussion: The Assumption of Equality

The results of this study demonstrate the presence of similarities and significant differences in the magnitude of appendicular morphometric variation in samples drawn from three recent African populations. Not surprisingly, measurements with high CVs (i.e., > 10) represent features that are expected to be highly variable such as those related to muscle attachment sites that develop in response the level of physical activity. For example, deltoid tuberosity length (HUM9), the position of the brachialis muscle insertion site on the proximal ulna (ULN17), radial tuberosity length (RAD8), and gluteal tuberosity breadth (FEM13) are consistently the most variable measurements in all samples, whether sexes are considered separately or together. In contrast, articular surfaces, element lengths, and shaft dimensions exhibit much lower variability. In fact, CVs of these features tend to be lower than 10, in line with the threshold suggested by Simpson et al. (1960) for typical intra-population morphometric variability.

Furthermore, the results of this chapter demonstrate that the intra-population magnitude of variation in various measurements of joints, bone lengths and diaphyseal dimensions is mostly equal, at least among the two modern African populations tested here. Among living people worldwide, diversity of mtDNA (e.g., Cann et al., 1987), nuclear genetic markers (e.g., Zhivotovsky et al., 2003), and skeletal morphology (e.g., Hiernaux, 1968; Relethford, 1994) appears to be highest among sub-Saharan Africans. This pattern has been argued to reflect either the greater depth of our lineage in Africa (Cann et al., 1987), or the fact that African human populations were of a larger size than non-African

populations for a longer time (Relethford and Jorde, 1999). Recent molecular evidence suggests that time since the founding of *H. sapiens* and not population size has played a more dominant role in the patterning of modern diversity, as attested by the fact that intra-population genetic variation decreases sequentially with increasing distance from Africa (see review in Weaver and Roseman, 2008). Preliminary evidence from cranial morphology suggests that modern human craniometric diversity also appears to fit an isolation by distance model or a sequence of iterative founder events (Manica et al., 2007; Betti et al., 2009).

Since the present study is limited to African populations, the results cannot address the issue of equality between African and non-African postcranial variability, nor can they be used to test an isolation by distance or other model argued to account for the patterning of modern diversity. Skeletons sampled from a global distribution of populations are needed to test the hypothesis of decreasing appendicular variability with distance from Africa. However, the equal magnitude of variation across the appendicular skeleton between the Zulu and Kikuyu documented here does provide evidence for similar levels of skeletal diversity within at least two sub-Saharan African populations. Further tests are required to confirm whether the pattern of greater variability among Africans compared to non-African populations extends throughout the appendicular skeleton, and whether the equality of variation found here between two African populations can be extended to all Africans. The preliminary implications for paleoanthropological studies in which modern populations are used as reference samples suggested by these results is that African populations may be interchangeable in that they contribute a similar baseline pattern and magnitude of skeletal variation.

Yet the results of this chapter also provide evidence for significant differences in appendicular morphometric variability when the sexes are evaluated separately. This inequality of variation is most apparent between

females, where the Kikuyu consistently exhibit a greater level of postcranial variability than Zulu females. This pattern of higher variation among the Kikuyu females is supported by both univariate and multivariate analyses of measurements across the five major long bones. The majority of measurements characterized by different levels of variation between the females from these populations include mostly measurements of articular surfaces. Joints are likely to be less sensitive to mechanical loading and activity level compared to diaphyseal dimensions (e.g., Ruff and Runestand, 1992; Ruff et al., 2006), although articular surfaces may still respond to external factors through modifications of internal morphology such as trabecular orientation or Haversian remodeling (Lieberman et al., 2001). Thus, increased variability in the joints of the Kikuyu females may reflect their increased genetic diversity compared to females in the Zulu population.

Furthermore, it is telling that the inequality of variation follows a consistent directional trend, with greater variation always found among the Kikuyu relative to the Zulu. If the pattern documented here was the result of sampling bias or an artifact of the smaller number of females sampled among the Kikuyu (n = 12) compared to the Zulu (n = 20), which could cause unreliable estimates of variation, then random differences in variability would be expected. Instead, Kikuyu females show a consistent directional pattern of surplus variability in articular dimensions compared to Zulu females.

However, the principal component scatterplots (Figures 5.16 – 5.20) of Kikuyu females and males show that two female specimens (OM1943 and OM5986) have PC1 scores that consistenly positioned them within the male cluster for each long bone. If these specimens had been incorrectly categorized as females, this could artificially inflate the variability of the Kikuyu female sample. Alternatively, these females may simply exhibit more masculine features. To investigate this, the original data collection record was checked to rule out the

possibility of data entry error. Encouragingly, all records list these individuals as female, although it is not possible to confirm the original curatorial catalogue at the National Museums of Kenya at this time. The sex classification results of Chapter 3 are used to investigate the possibility that these specimens represent masculine females. Three discriminant functions of os coxae form and six discriminant functions of os coxae shape were developed to classify sex in the Kikuyu sample. In each of the form-based analyses, the specimens in question are classified as male. However, specimen OM5986 is classified as female in all six of the shape-based analyses, while specimen OM1943 is classified as female in three of the shape analyses. The visual method provides a female diagnosis. Thus, although these individuals do seem to be masculine in terms of pelvis size, a male diagnosis tends not to be supported on the basis the shape and non-metric features of their pelves. While the possibility of that these bones were mislabelled as females cannot be completely ruled out, the sex classification results provide compeling evidence suggesting that they represent masculine females. Indeed, that five other Kikuyu females have scores that place them within or very near the male clusters along PC1, an axis dominated by the effect of size, across different elements attests to the fact some Kikuyu females may be characterized by rather large body size. Therefore, it seems likely that there is a real difference in appendicular variation among females from the Kikuyu and Zulu populations, with Kikuyu females exhibiting elevated morphometric variability.

Interestingly, the only measurements for which Zulu females demonstrate a trend for more variation than Kikuyu females are shaft dimensions: minimum midshaft diameter of the humerus, maximum midshaft diameter and AP proximal shaft diameter of the ulna, maximum midshaft diameter of the radius, and AP midshaft diameters of the femur and tibia. Because diaphyses can be heavily influenced by activity level and mechanical loading (e.g., Ruff and Runestad, 1992; Ruff et al., 2006), the pattern of elevated variability in shaft dimensions

among Zulu females may reflect the fact that these individuals engaged in a greater diversity of behaviors compared to Kikuyu females. The excess variability among Zulu females compared to Kikuyu females does not reach statistical significance, but these differences nonetheless represent a consistent trend in which morphometric variability among Kikuyu females may reflect underlying their genetic diversity (possible due to migrations and/or mating patterns), while the pattern of variation among Zulu females points to their genetic similarity but also suggests that they engaged in a diversity of physical activities that could have differentially shaped their long bone diaphyses.

To put these differences in a broader context, it is informative to compare the variation in a selection of postcranial dimensions across a more global sample. Figure 5.26 illustrates the CVs of the Zulu and Kikuyu females sampled in this study for a selection of measurements across the upper limb elements (humerus, ulna, and radius), as well as those of females sampled from three additional human populations: the Sami or Lapps from northern Europe, Americans of European ancestry (i.e., US Whites), and the Inuit from Alaska. The CVs for these comparative samples are computed from the summary statistics (sample means and standard deviations) from Pearson (1997). As Figure 5.26a illustrates, the level of morphometric variation in the upper limb tends to vary by roughly 5% among females between the populations. For numerous measurements, the two northern samples (Sami and Inuit) appear to have quite similar magnitudes of variation, while the other samples have more divergent levels of variation. Contrary to expectations based on higher African diversity, the Zulu females consistently exhibit the lowest magnitude of variation. On the other hand, variation in Kikuyu females tends to be among the highest of the populations sampled here. At least among these five modern populations, the Zulu and Kikuyu females appear to sample the two extremes of morphometric variation in

the upper limb. The same general pattern is observed in a selection of measurements from the femur and tibia (Figure 5.26b).

Again, this suggests that there is a real difference in variation among females in the sub-Saharan populations studied here. One possible explanation might be that Zulu females (at least those sampled here) tend to be more closely related than Kikuyu females. This could reflect differences in migration or mating patterns between the populations. Both the Zulu and Kikuyu are Bantu-speaking tribes (Oschinsky, 1954; Nurse et al., 1985). Archaeological (Chami, 2001) and linguistic (Ehret, 2001) data point to strong interactions across Bantu groups, and between Bantu-speakers and local populations as the former expanded across sub-Saharan Africa. Mitochondrial DNA analyses also provide evidence for population admixture among the Bantu (Castri et al., 2009), although there are indications that gene flow between Bantu and non-Bantu groups may have been asymmetric or predominantly uni-directional in some instances (Quintana-Murci et al., 2008). In contrast, Y-chromosome studies demonstrate a different pattern, with lower diversity in the paternal line of descent (i.e., Y-chromosome) among the Bantu than in the maternally inherited mtDNA (Pereira et al., 2002).

Such differences in genetic diversity between the sexes likely reflect the influence of sociocultural factors gene flow. Specifically, this pattern could stem from a bias in demographic factors such as a trend for females, and not males, from other tribes (whether other Bantu groups or native hunter-gatherers) to be assimilated into the population (Destro-Bisol et al., 2004; Wood et al., 2005). Such a scenario may be envisaged among the Kikuyu, where females exhibit greater postcranial variability than Zulu females. Thus, differences in the magnitude of skeletal diversity may reflect differing demographic processes among the same sex from different populations. The relationship between same-

sex intra-population skeletal diversity and demographic factors such as patterns of unidirectional marriage and migration warrants further study.

In contrast, the results of comparisons of variability between males from three African populations demonstrate an unambiguous pattern for similarity in the magnitude of postcranial variation among males. But does this pattern extend to males from a more global distribution? That is, does morphometric variability among males tend to be similar across a range of human populations, in contrast to female variability? To investigate this, CVs for a selection of upper and lower limb measurements were computed using summary statistics from Pearson (1997) for males from four additional populations: Sami, White Americans, Inuit, and Australian Aborigines. As Figure 5.27 illustrates, the range of variation exhibited by males from seven different populations seems to more restricted than was observed among females for the same measurements. Furthermore, neither the Zulu nor Kikuyu males tend towards either extreme of variation, unlike the striking differences observed between the females sampled from these populations, although variability among African males does tend to be slightly higher than that of the non-African groups, as expected based on a trend for higher genetic diversity in Africa. To summarize, while relative morphometric variation is equal among the males of three African populations, the assumption of equal variation is not supported for the Zulu and Kikuyu females. Whether this pattern between the sexes holds across human populations requires further study, although preliminary comparisons suggest that males may be more constrained in the magnitude of variation than females. The reasons for this remain unclear, but as discussed earlier, it may reflect the influence of sociocultural factors on demographic processes including but not limited to a tendency for unidirectional marriages between native males and non-native females (e.g., Destro-Bisol et al., 2004; Wood et al., 2005).

Turning to differences in the magnitude of variation between the sexes within a population, this chapter demonstrated that within the Zulu and Kikuyu, many but not all appendicular measurements exhibit equal variation. That is, there is no evidence for significant dimorphism of variances in most postcranial measurements, despite the fact that the majority of measurements exhibit significant dimorphism of means. In both groups, appendicular measurements that are not sexual dimorphic never show significant differences in variability between the sexes; however, not all sexual dimorphic measurements show complimentary sex differences in the magnitude of variation. Thus, differences in variation between the sexes appear to be the exception rather the rule in these African populations. Interestingly, the direction of this difference, when present, differs between the Zulu and Kikuyu: when unequal variation in documented within the Zulu, it is the males that always show the excess of variation, while the opposite is true among the Kikuyu. This pattern suggests that the factor(s) influencing variation in males and females likely differs in these populations. Based on the results discussed above, which showed strong differences in variability between Zulu and Kikuyu females, the pattern of sexual dimorphism of variances in these populations appears to be driven primarily by the level of female variation. Based on the broader global comparative context described above, Zulu females appear to have somewhat low levels of variation while Kikuyu females tend to be more variable than is typical for articular surfaces. Again, this may reflect differences in the underlying genetic diversity of females from these two populations, since other factors such as environmental influences would be expected to influence the males from the same populations as well as the females.

Not surprisingly, multivariate analyses of the five long bones demonstrate that differences between the sexes reflect primarily size differences, which supports univariate results that highlight significant sexual dimorphism in the

majority of variables in both populations. However, the presence of sexual dimorphism in a population does not necessarily mean that the sexes will exhibit significant differences in magnitude of variation. For some measurements, peaks in variability occur in measurements that also exhibit elevated sexual dimorphism. That is, among the Zulu males are more than 25% larger for than females in breadth of the medial dorsal pillar on the distal humerus, while among the Kikuyu, males are only 10% bigger. Thus, there is a more than 12% difference in the level of sexual dimorphism in this feature among the Zulu and Kikuyu. Variability among the Zulu is also much higher than the Kikuyu (CV = 24% versus 15%), which supports the claim intra-population variability increases as dimorphism increases. However, other measurements show no increase in variability as dimorphism increases. Still, the differences in dimorphism between the Zulu and Kikuyu tend to be small, and it is possible that a population with substantially high levels of dimorphism would exhibit a concomitant increase in morphometric variability.

Conclusions

This chapter provides a detailed study of morphometric variation in the appendicular skeleton of three modern human populations from sub-Saharan Africa. The populations studied here generally exhibit a similar magnitude of variation when the sexes are pooled. Therefore, they likely provide the same baseline pattern and level of variability when they are employed as reference samples for paleoanthropological studies. This chapter also identified important differences suggesting that equality of variation among the sexes cannot be assumed. The most dramatic difference in variation was documented between females of the Zulu and Kikuyu tribes, where females sampled from the Kikuyu population exhibited a greater magnitude of variation in numerous measurements

of the joints and diaphyses of the five major long bones. In contrast, equal variability was found between Zulu, Kikuyu and Ugandan males. The pattern of equal variation in males but not females requires further study across a wider range of populations, although preliminary comparisons suggest that males tend to have more constrained variability than females. Similar differences in diversity between the sexes have been identified in studies of maternally inherited mtDNA and the paternally inherited Y-chromosome, and may reflect sex-biased demographic processes stemming from sociocultural factors such as a tendency for unidirection gene flow between populations. While the groups sampled here are characterized by sexual dimorphism across most postcranial dimensions, only a few cases of dimorphism in variation were documented. This suggests that while sexual dimorphism does contribute to the overall level of intra-population variability, it is not the only factor involved. Interestingly however, although dimorphism in variation is not common among either the Zulu or the Kikuyu, the direction of differences presented a clear pattern: in the Zulu, males always exhibit an excess of variation compared to the females, while in the Kikuyu, females always exhibit more variation than the males. This pattern suggests that different factors, likely related to differences in demographic history stemming for the influence of sociocultural factors, have influenced levels of skeletal variation (and presumably genetic variation) in males and females.

Although the issue of equality in appendicular variability between African and non-African populations was not addressed here, there is clearly a need for such studies. The isolation by distance model, supported by the global patterning of genetic as well as craniometric diversity among modern humans, predicts that African populations should exhibit greater variability than non-Africans. If this hold across the skeleton, then paleoanthropological analyses should be cautious in the choice of samples to represent baseline measures of modern human diversity, as non-African populations may exhibit reduced morphological variability.

Worldwide skeletal samples are needed to test the hypothesis of decreasing appendicular variability with distance from Africa, and to place to results obtained here in a broader global context.

Figure 5.1 Coefficient of variation (CV) illustrating variation in humerus measurements between females from two recent African samples.

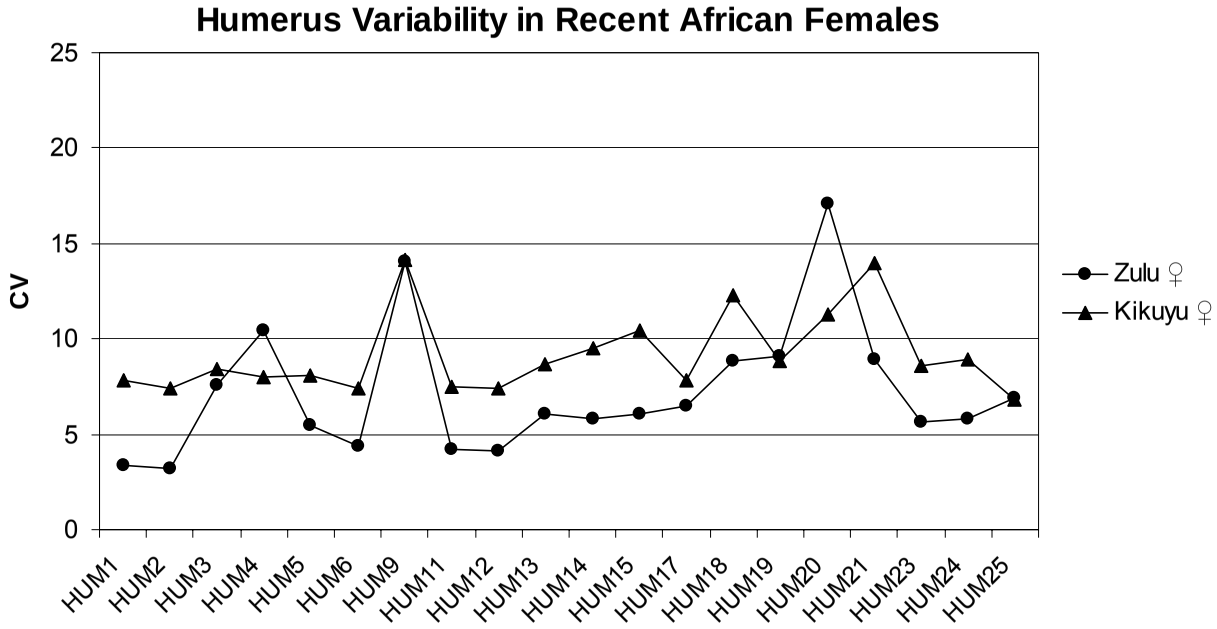

*HUM1: max length, HUM2: total length, HUM3: max midshaft diameter, HUM4: min midshaft diameter, HUM5: head proximo-distal diameter, HUM6: head DV diameter, HUM9: deltoid tuberosity max length, HUM11: epicondylar width, HUM12: capitulum + trochlear width, HUM13: capitulum width, HUM14: capitulum height, HUM15: capitulum AP thickness, HUM17: medial trochlear lip AP diameter, HUM18: min trochlear AP diameter, HUM19: olecranon fossa width, HUM20: medial dorsal pillar breadth, HUM21: lateral dorsal pillar breadth, HUM23: deltoid to capitulum distance, HUM24: deltoid to trochlea distance, HUM25: min shaft circumference.

Figure 5.2 Coefficient of variation (CV) illustrating variation in ulna measurements between females from two recent African samples.

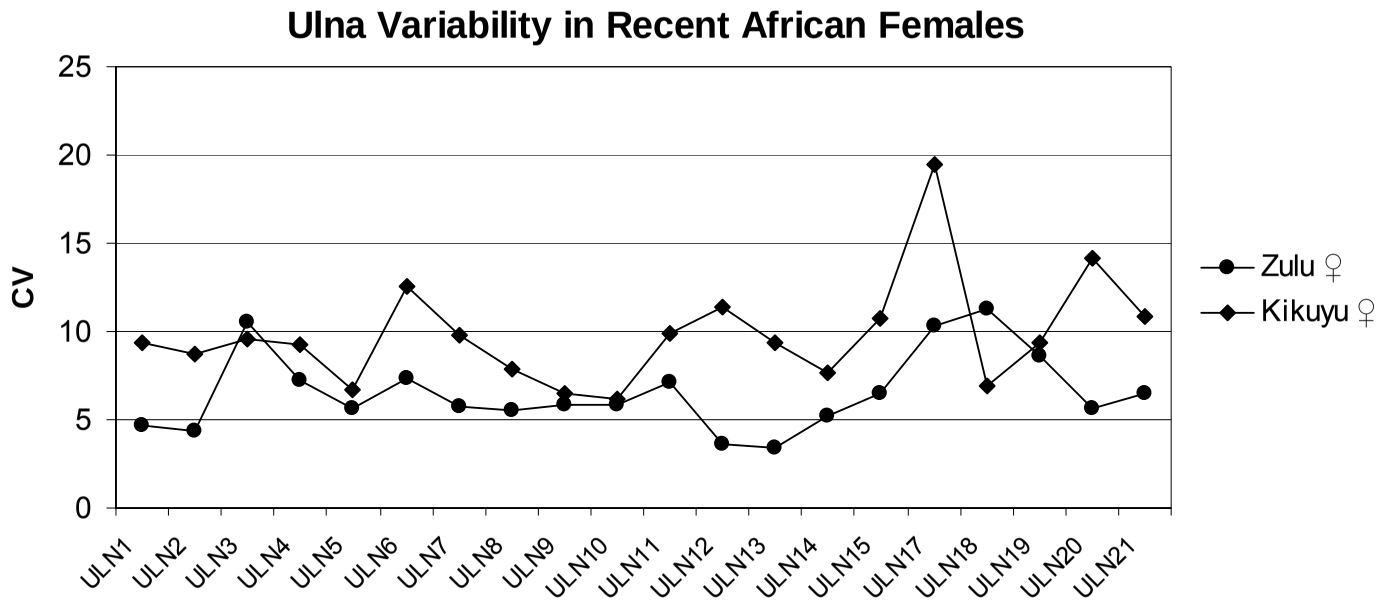

*ULN1: articular length, ULN2: total length, ULN3: max midshaft diameter, ULN4: min midshaft diameter, ULN5: coronoid height, ULN6: max coronoid ML breadth, ULN7: olecranon height, ULN8: olecranon ML breadth, ULN9: olecranon length, ULN10: trochlear notch length, ULN11: trochlear notch transverse breadth, ULN12: mid-trochlear notch thickness, ULN13: trochlear notch AP thickness, ULN14: radial notch position, ULN15: radial notch length, ULN17: brachialis insertion position, ULN18: proximal shaft AP diameter, ULN19: proximal shaft ML diameter, ULN20: distal epiphysis transverse breadth, ULN21: min shaft circumference.

Figure 5.3 Coefficient of variation (CV) illustrating variation in radius measurements between females from two recent African samples.

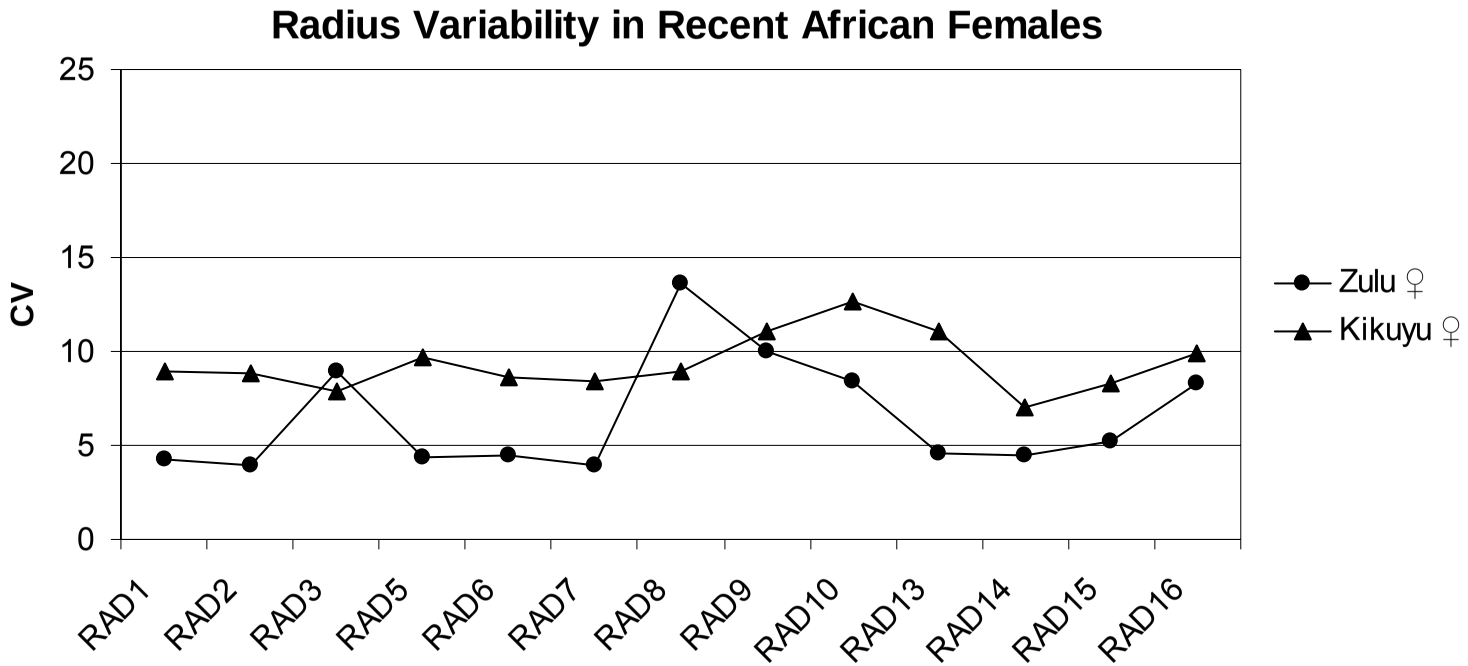

*RAD1: articular length, RAD2: max length, RAD3: max midshaft diameter, RAD5: max head AP diameter, RAD6: max head ML diameter, RAD7: max head diameter, RAD8: radial tuberosity length, RAD9: neck length, RAD10: neck AP diameter, RAD13: distal epiphysis DV breadth, RAD14: distal epiphysis ML breadth, RAD15: min shaft circumference, RAD16: radial tuberosity circumference.

Figure 5.4 Coefficient of variation (CV) illustrating variation in femur measurements between females from two recent African samples.

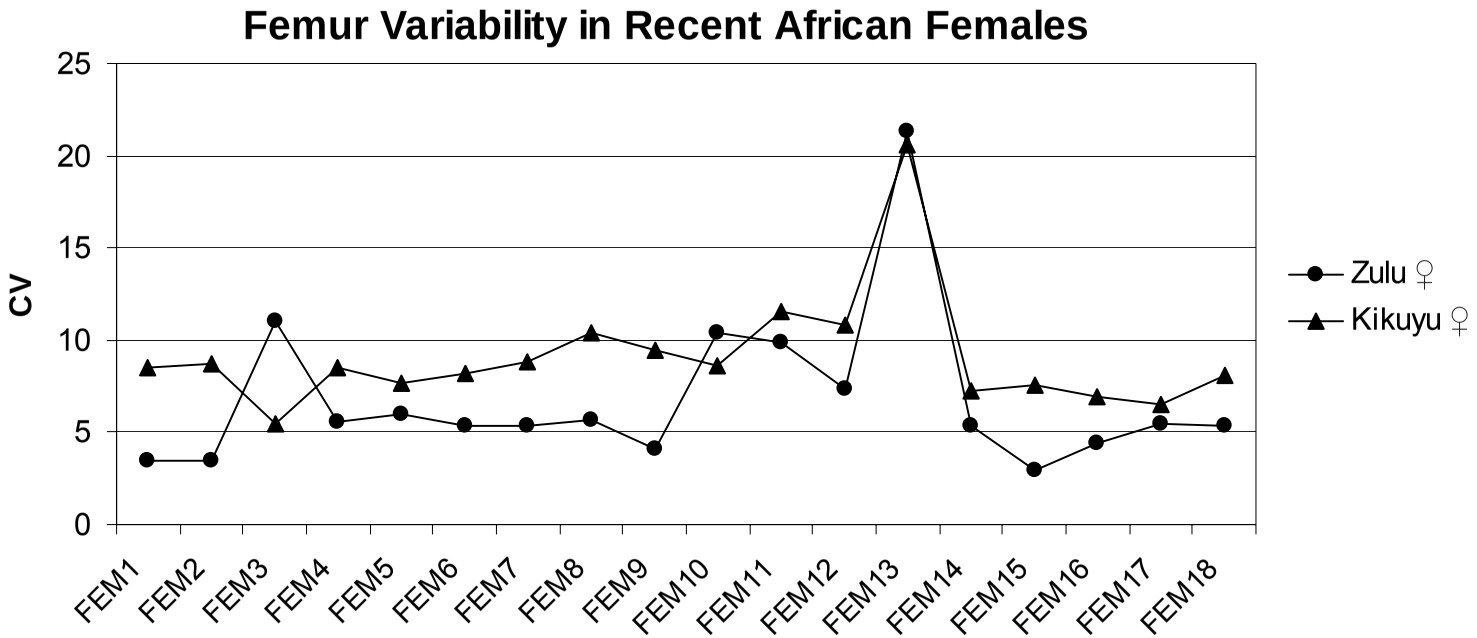

*FEM1: max length, FEM2: bicondylar length, FEM3: midshaft AP diameter, FEM4: midshaft ML diameter, FEM5: vertical head diameter, FEM6: horizontal head diameter, FEM7: min neck height, FEM8: min neck breadth, FEM9: biomechanical neck length, FEM10: neck length, FEM11: subtrochanteric AP shaft diameter, FEM12: subtrochanteric ML shaft diameter, FEM13: gluteal tuberosity breadth, FEM14: patellar notch width, FEM15: biepicondylar breadth, FEM16: max distal articular breadth, FEM17: min shaft circumference, FEM18: subtrochanteric shaft circumference.

Figure 5.5 Coefficient of variation (CV) illustrating variation in tibia measurements between females from two recent African samples.

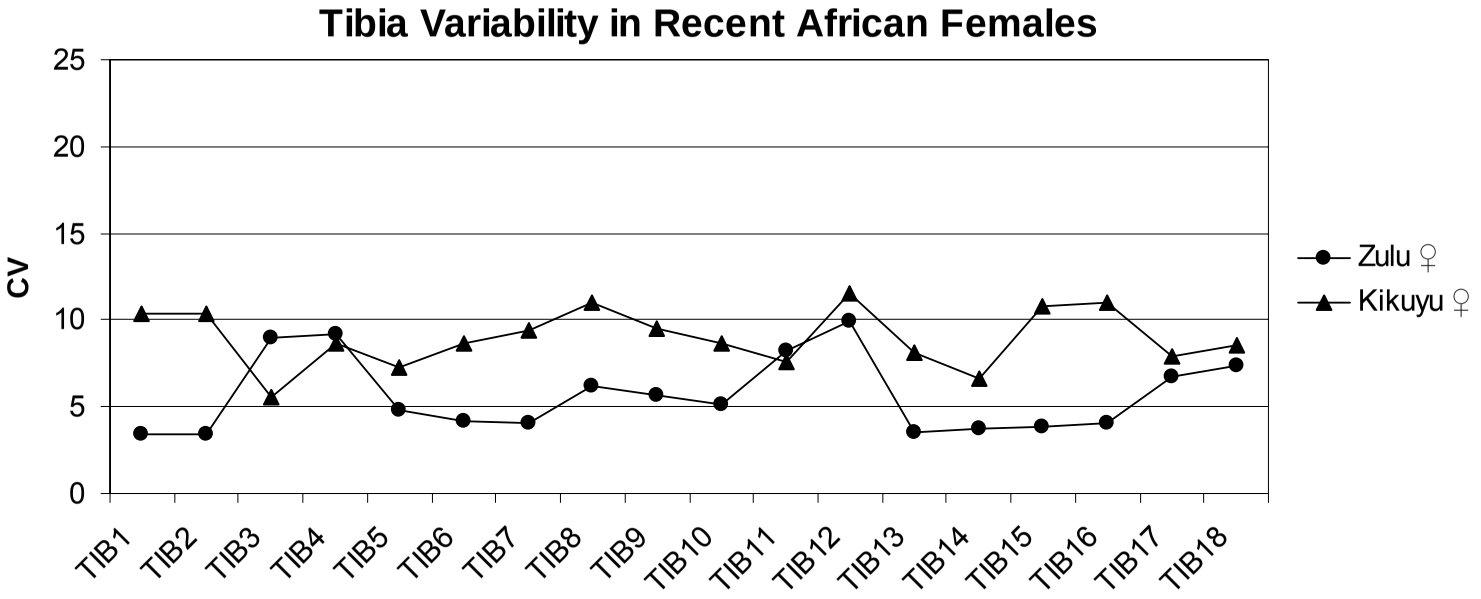

*TIB1: articular length, TIB2: total length, TIB3: midshaft AP diameter, TIB4: midshaft ML diameter, TIB5: proximal epiphysis max length, TIB6: proximal epiphysis max breadth, TIB7: medial condyle AP length, TIB8: medial condyle ML breadth, TIB9: lateral condyle AP length, TIB10: lateral condyle ML breadth, TIB11: shaft AP diameter at nutrient foramen, TIB12: shaft ML diameter at nutrient foramen, TIB13: talar AP length, TIB14: distal epiphysis ML breadth, TIB15: nutrient foramen to medial malleolus distance, TIB16: nutrient foramen to talar articular surface distance, TIB17: min shaft circumference, TIB18: shaft circumference at nutrient foramen.

Figure 5.6 Coefficient of variation (CV) illustrating variation in humerus measurements between males from two recent African samples.

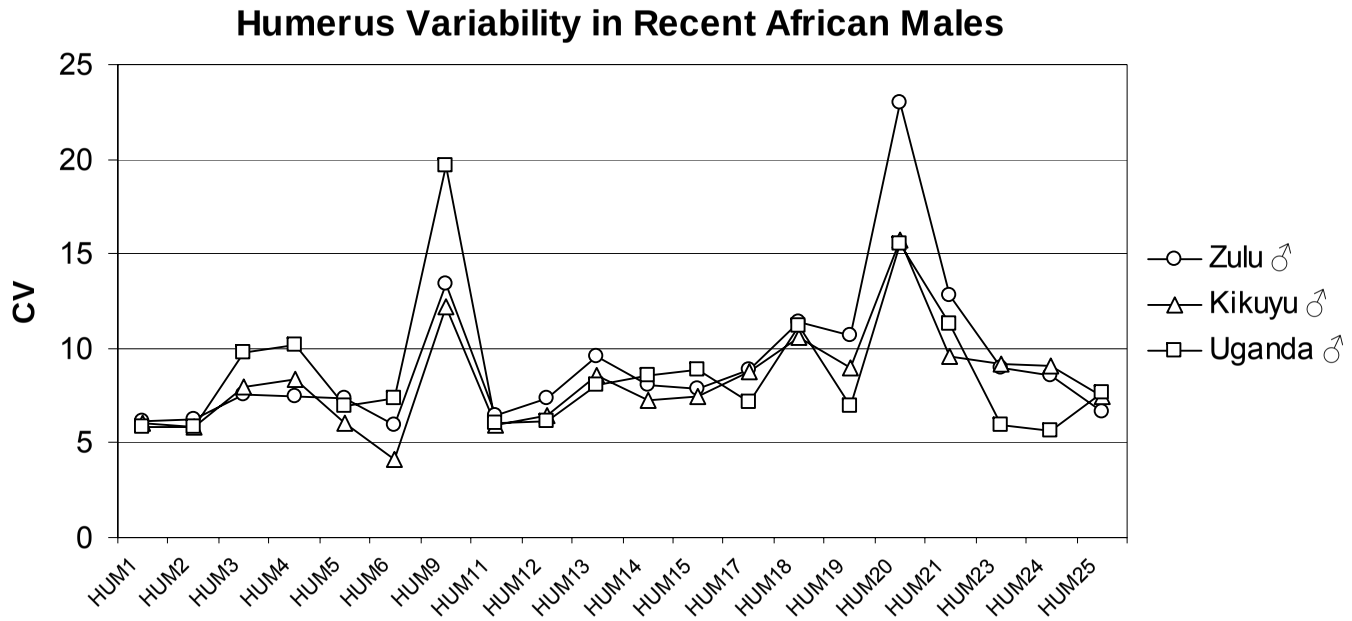

*HUM1: max length, HUM2: total length, HUM3: max midshaft diameter, HUM4: min midshaft diameter, HUM5: head proximo-distal diameter, HUM6: head DV diameter, HUM9: deltoid tuberosity max length, HUM11: epicondylar width, HUM12: capitulum + trochlear width, HUM13: capitulum width, HUM14: capitulum height, HUM15: capitulum AP thickness, HUM17: medial trochlear lip AP diameter, HUM18: min trochlear AP diameter, HUM19: olecranon fossa width, HUM20: medial dorsal pillar breadth, HUM21: lateral dorsal pillar breadth, HUM23: deltoid to capitulum distance, HUM24: deltoid to trochlea distance, HUM25: min shaft circumference.

Figure 5.7 Coefficient of variation (CV) illustrating variation in ulna measurements between males from two recent African samples.

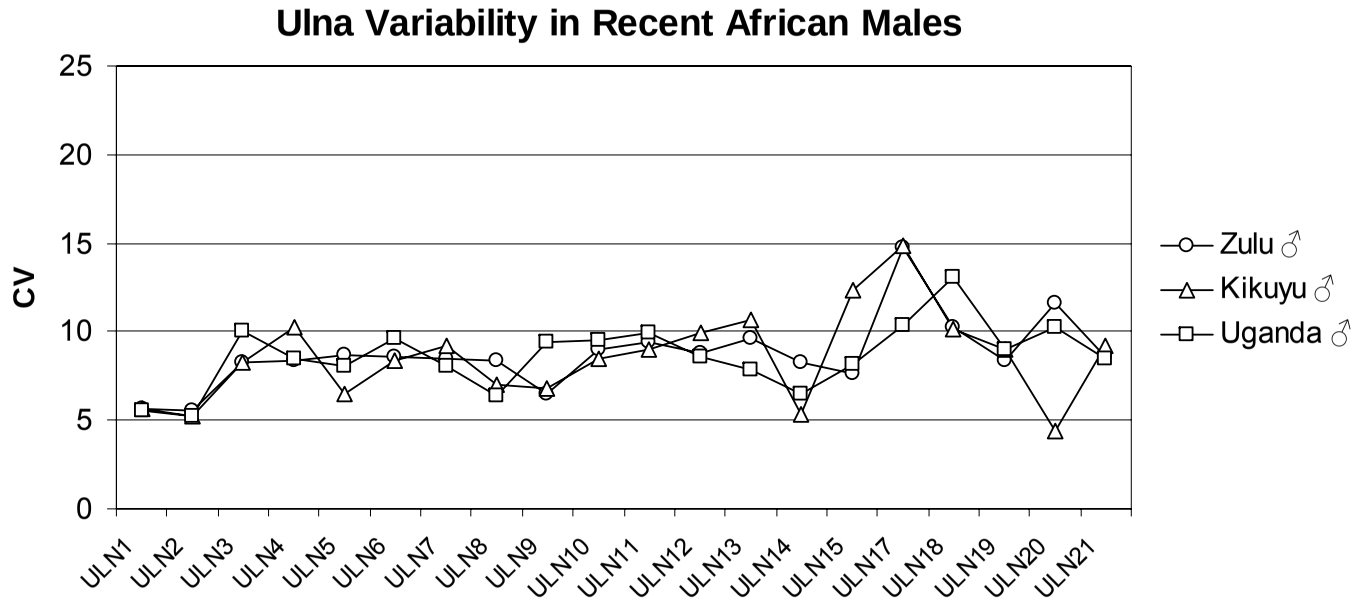

*ULN1: articular length, ULN2: total length, ULN3: max midshaft diameter, ULN4: min midshaft diameter, ULN5: coronoid height, ULN6: max coronoid ML breadth, ULN7: olecranon height, ULN8: olecranon ML breadth, ULN9: olecranon length, ULN10: trochlear notch length, ULN11: trochlear notch transverse breadth, ULN12: mid-trochlear notch thickness, ULN13: trochlear notch AP thickness, ULN14: radial notch position, ULN15: radial notch length, ULN17: brachialis insertion position, ULN18: proximal shaft AP diameter, ULN19: proximal shaft ML diameter, ULN20: distal epiphysis transverse breadth, ULN21: min shaft circumference.

Figure 5.8 Coefficient of variation (CV) illustrating variation in radius measurements between males from two recent African samples.

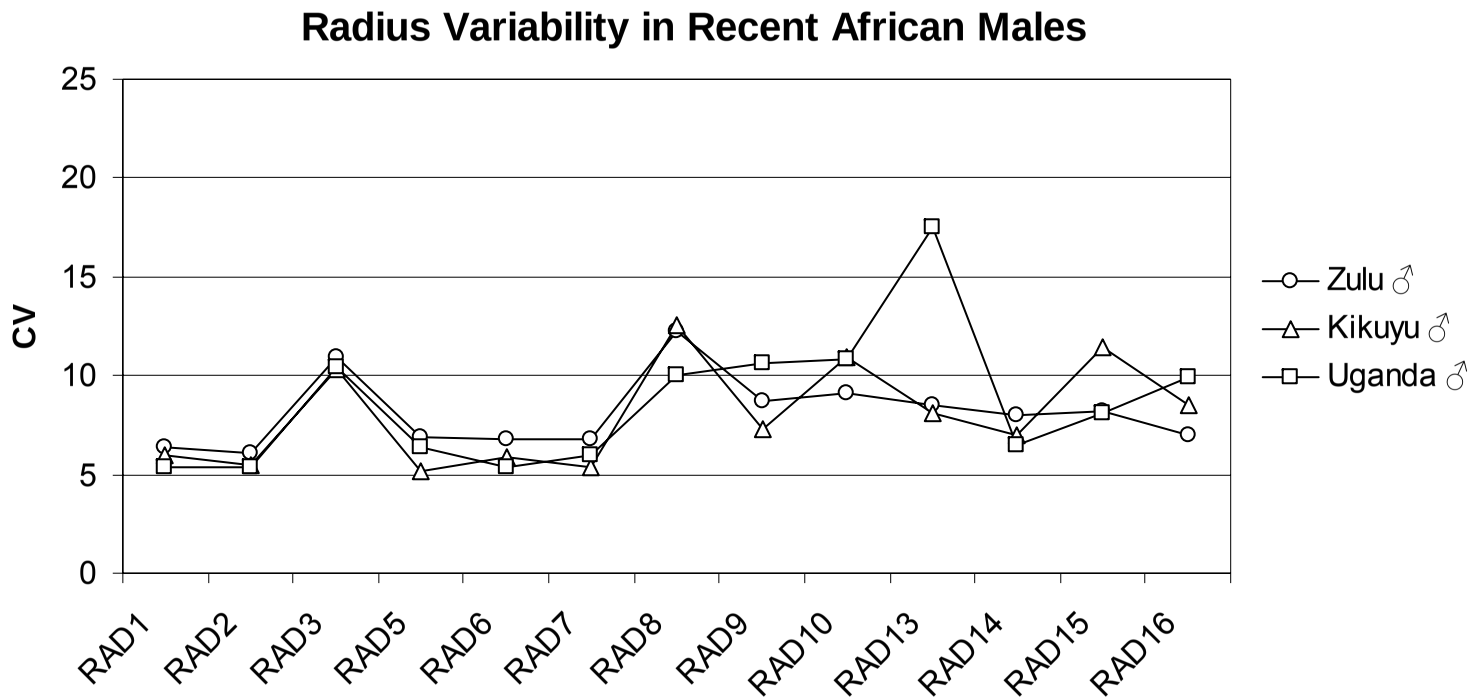

*RAD1: articular length, RAD2: max length, RAD3: max midshaft diameter, RAD5: max head AP diameter, RAD6: max head ML diameter, RAD7: max head diameter, RAD8: radial tuberosity length, RAD9: neck length, RAD10: neck AP diameter, RAD13: distal epiphysis DV breadth, RAD14: distal epiphysis ML breadth, RAD15: min shaft circumference, RAD16: radial tuberosity circumference.

Figure 5.9 Coefficient of variation (CV) illustrating variation in femur measurements between males from two recent African samples.

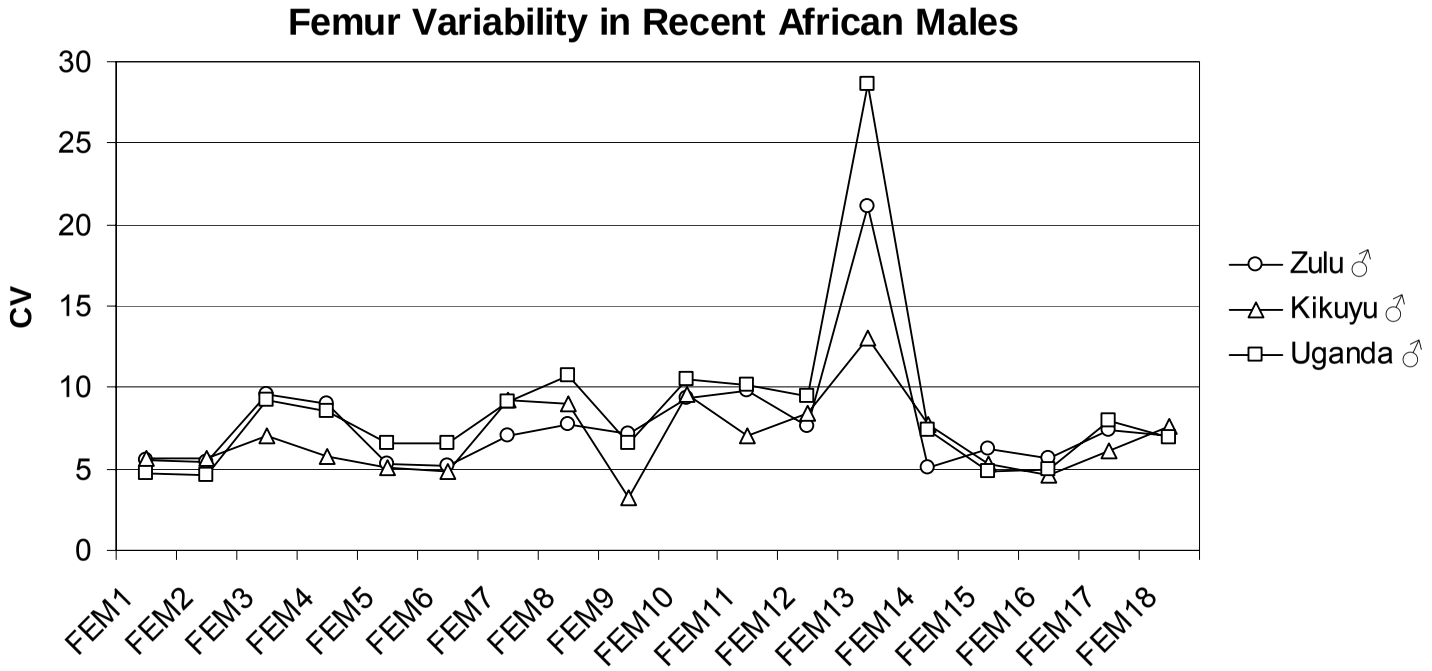

*FEM1: max length, FEM2: bicondylar length, FEM3: midshaft AP diameter, FEM4: midshaft ML diameter, FEM5: vertical head diameter, FEM6: horizontal head diameter, FEM7: min neck height, FEM8: min neck breadth, FEM9: biomechanical neck length, FEM10: neck length, FEM11: subtrochanteric AP shaft diameter, FEM12: subtrochanteric ML shaft diameter, FEM13: gluteal tuberosity breadth, FEM14: patellar notch width, FEM15: biepicondylar breadth, FEM16: max distal articular breadth, FEM17: min shaft circumference, FEM18: subtrochanteric shaft circumference.

Figure 5.10 Coefficient of variation (CV) illustrating variation in tibia measurements between males from two recent African samples.

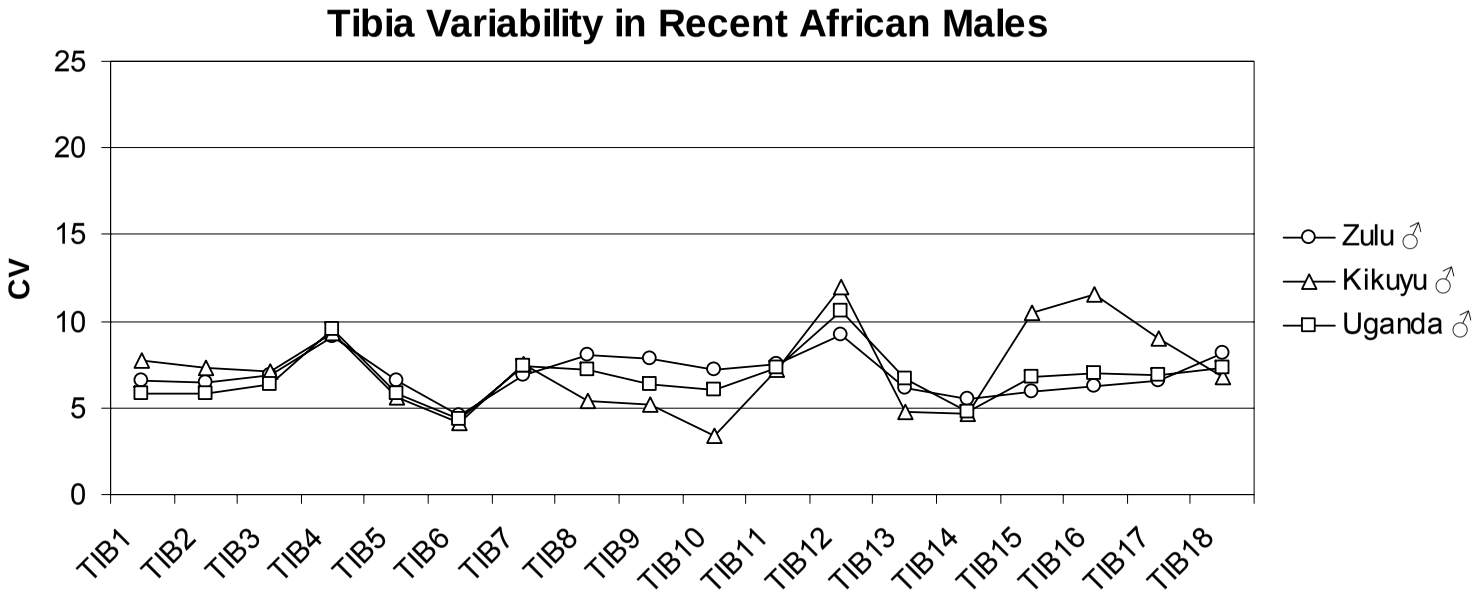

*TIB1: articular length, TIB2: total length, TIB3: midshaft AP diameter, TIB4: midshaft ML diameter, TIB5: proximal epiphysis max length, TIB6: proximal epiphysis max breadth, TIB7: medial condyle AP length, TIB8: medial condyle ML breadth, TIB9: lateral condyle AP length, TIB10: lateral condyle ML breadth, TIB11: shaft AP diameter at nutrient foramen, TIB12: shaft ML diameter at nutrient foramen, TIB13: talar AP length, TIB14: distal epiphysis ML breadth, TIB15: nutrient foramen to medial malleolus distance, TIB16: nutrient foramen to talar articular surface distance, TIB17: min shaft circumference, TIB18: shaft circumference at nutrient foramen.

Figure 5.11 Coefficient of variation (CV) illustrating variation in humerus measurements between the sexes in two recent African samples.

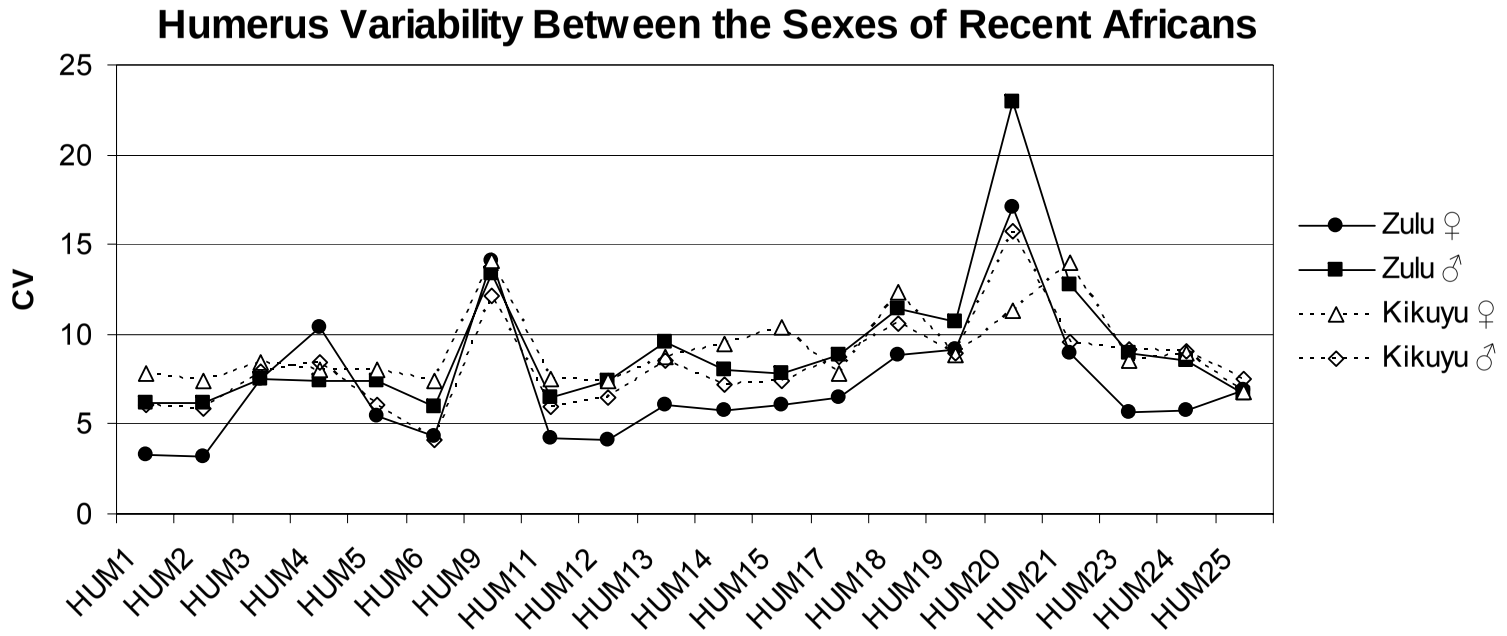

*HUM1: max length, HUM2: total length, HUM3: max midshaft diameter, HUM4: min midshaft diameter, HUM5: head proximo-distal diameter, HUM6: head DV diameter, HUM9: deltoid tuberosity max length, HUM11: epicondylar width, HUM12: capitulum + trochlear width, HUM13: capitulum width, HUM14: capitulum height, HUM15: capitulum AP thickness, HUM17: medial trochlear lip AP diameter, HUM18: min trochlear AP diameter, HUM19: olecranon fossa width, HUM20: medial dorsal pillar breadth, HUM21: lateral dorsal pillar breadth, HUM23: deltoid to capitulum distance, HUM24: deltoid to trochlea distance, HUM25: min shaft circumference.

Figure 5.12 Coefficient of variation (CV) illustrating variation in ulna measurements between the sexes in two recent African samples.

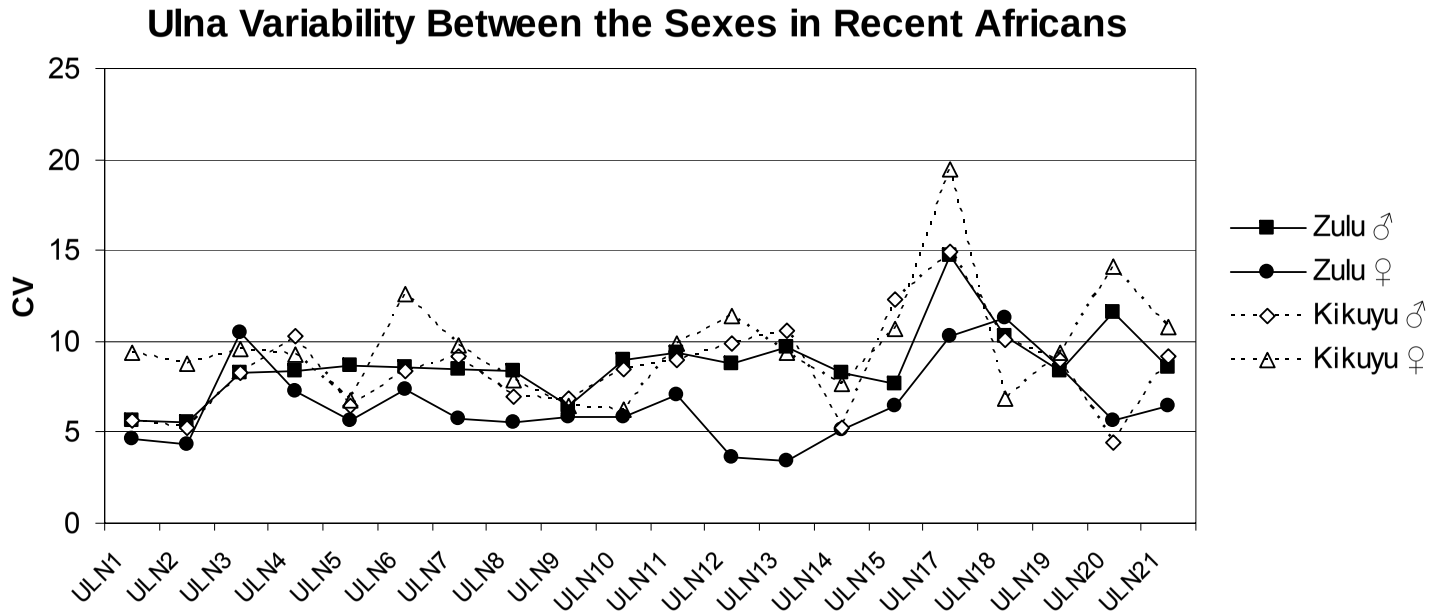

*ULN1: articular length, ULN2: total length, ULN3: max midshaft diameter, ULN4: min midshaft diameter, ULN5: coronoid height, ULN6: max coronoid ML breadth, ULN7: olecranon height, ULN8: olecranon ML breadth, ULN9: olecranon length, ULN10: trochlear notch length, ULN11: trochlear notch transverse breadth, ULN12: mid-trochlear notch thickness, ULN13: trochlear notch AP thickness, ULN14: radial notch position, ULN15: radial notch length, ULN17: brachialis insertion position, ULN18: proximal shaft AP diameter, ULN19: proximal shaft ML diameter, ULN20: distal epiphysis transverse breadth, ULN21: min shaft circumference.

Figure 5.13 Coefficient of variation (CV) illustrating variation in radius measurements between the sexes in two recent African samples.

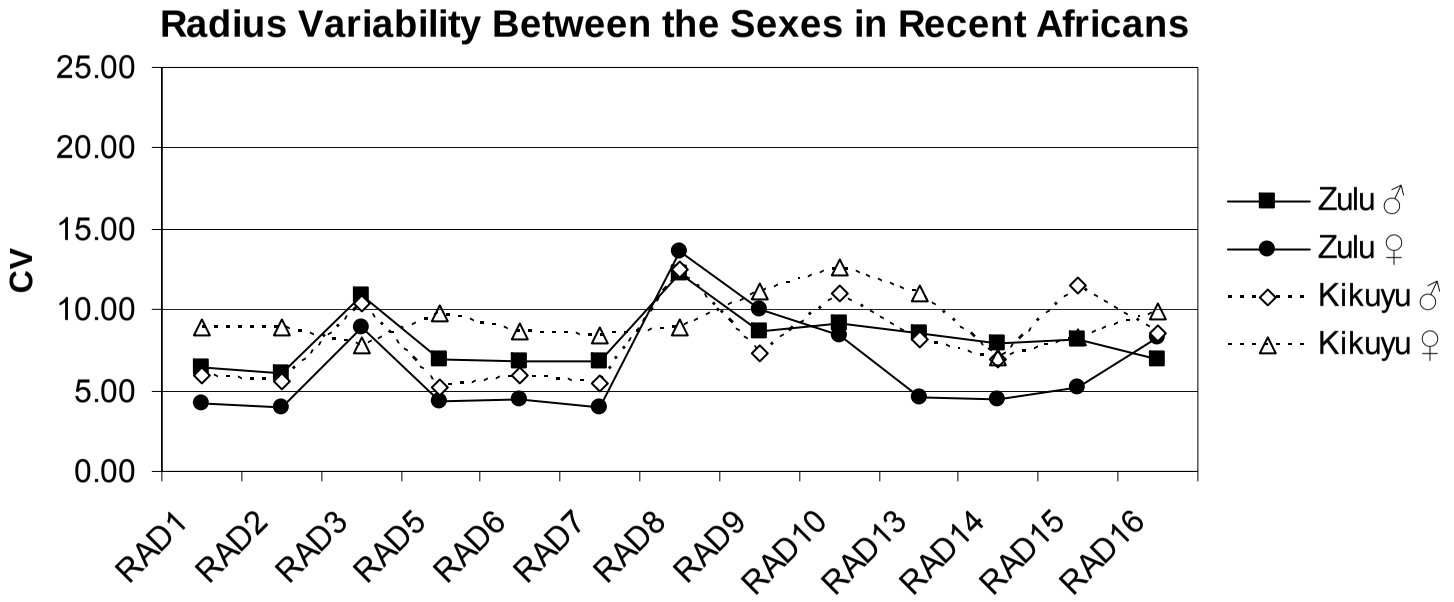

*RAD1: articular length, RAD2: max length, RAD3: max midshaft diameter, RAD5: max head AP diameter, RAD6: max head ML diameter, RAD7: max head diameter, RAD8: radial tuberosity length, RAD9: neck length, RAD10: neck AP diameter, RAD13: distal epiphysis DV breadth, RAD14: distal epiphysis ML breadth, RAD15: min shaft circumference, RAD16: radial tuberosity circumference.

Figure 5.14 Coefficient of variation (CV) illustrating variation in femur measurements between the sexes in two recent African samples.

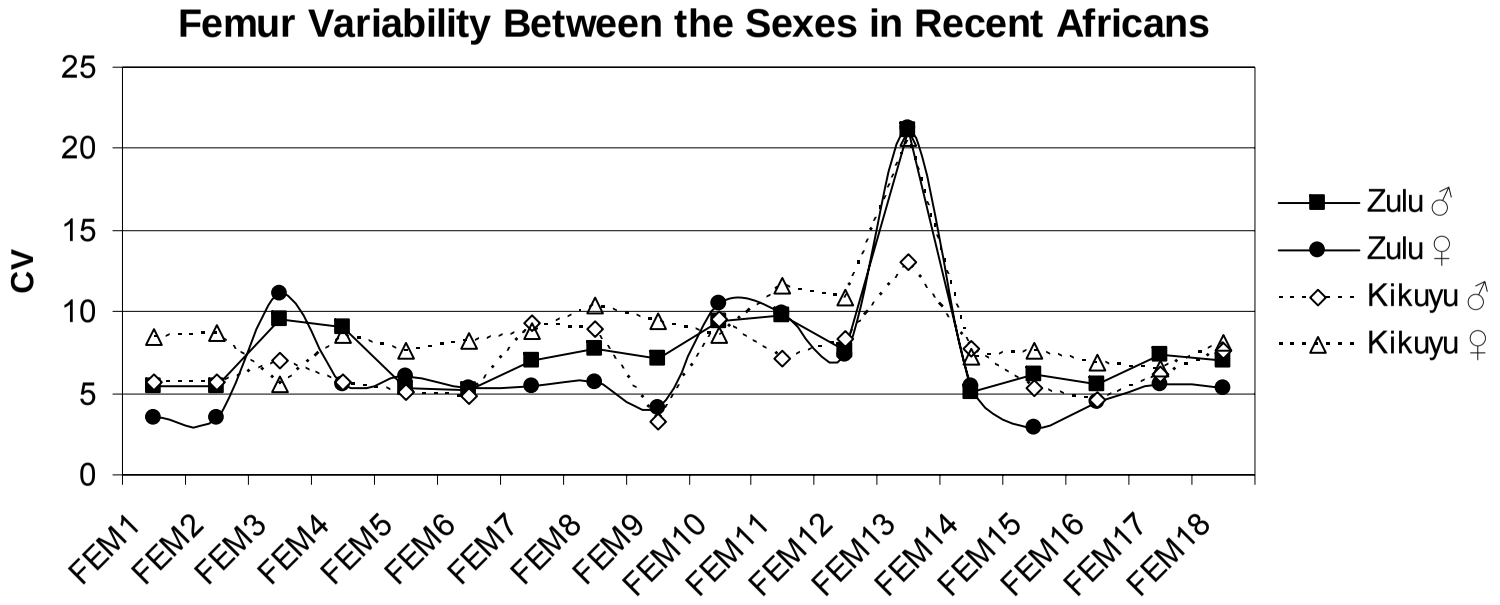

*FEM1: max length, FEM2: bicondylar length, FEM3: midshaft AP diameter, FEM4: midshaft ML diameter, FEM5: vertical head diameter, FEM6: horizontal head diameter, FEM7: min neck height, FEM8: min neck breadth, FEM9: biomechanical neck length, FEM10: neck length, FEM11: subtrochanteric AP shaft diameter, FEM12: subtrochanteric ML shaft diameter, FEM13: gluteal tuberosity breadth, FEM14: patellar notch width, FEM15: biepicondylar breadth, FEM16: max distal articular breadth, FEM17: min shaft circumference, FEM18: subtrochanteric shaft circumference.

Figure 5.15 Coefficient of variation (CV) illustrating variation in tibia measurements between the sexes in two recent African samples.

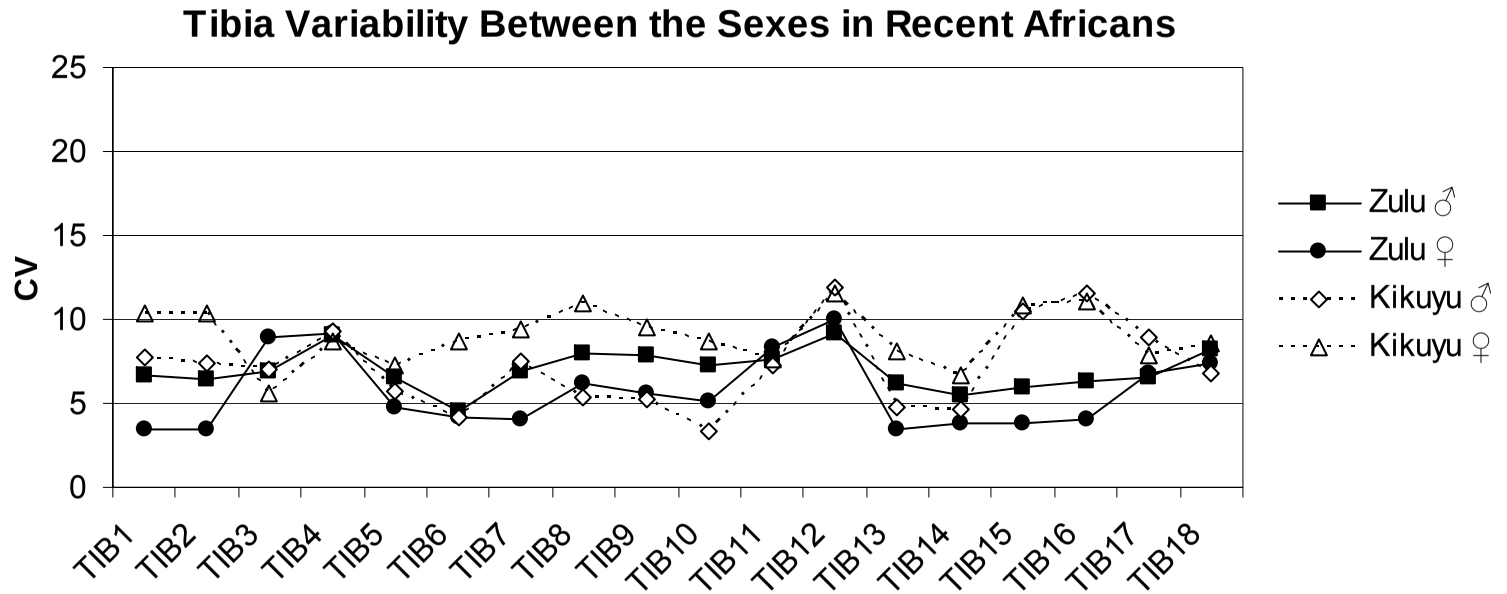

*TIB1: articular length, TIB2: total length, TIB3: midshaft AP diameter, TIB4: midshaft ML diameter, TIB5: proximal epiphysis max length, TIB6: proximal epiphysis max breadth, TIB7: medial condyle AP length, TIB8: medial condyle ML breadth, TIB9: lateral condyle AP length, TIB10: lateral condyle ML breadth, TIB11: shaft AP diameter at nutrient foramen, TIB12: shaft ML diameter at nutrient foramen, TIB13: talar AP length, TIB14: distal epiphysis ML breadth, TIB15: nutrient foramen to medial malleolus distance, TIB16: nutrient foramen to talar articular surface distance, TIB17: min shaft circumference, TIB18: shaft circumference at nutrient foramen.

Figure 5.16 Plots of PC1 *versus* PC2 for the principal components analyses of the humerus: A) Zulu, PC1 and PC2 explain 59.44% and 9.71% of the variance respectively, B) Kikuyu, PC1 and PC2 explain 66.85% and 9.82% of the variance respectively.

A)

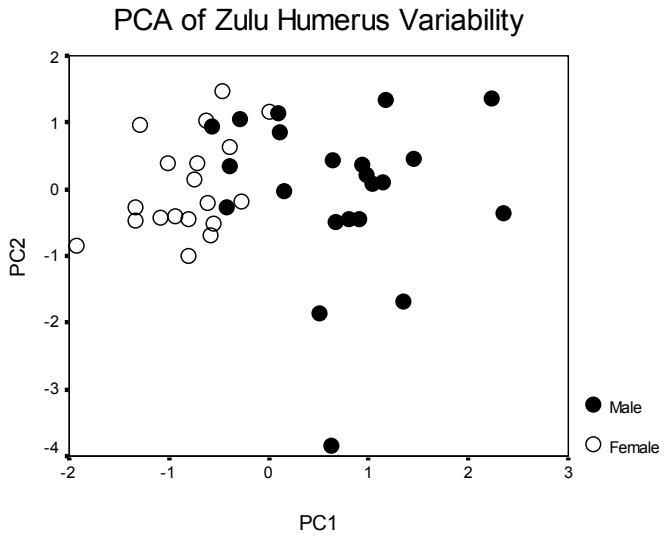

B)

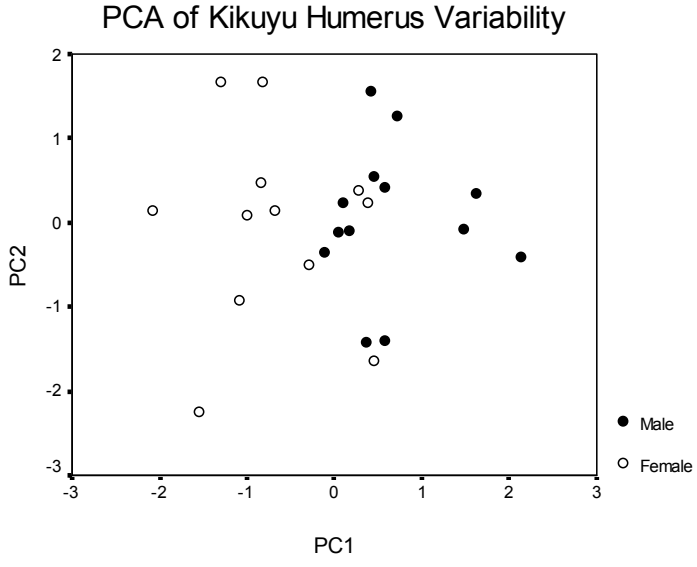

Figure 5.17 Plots of PC1 *versus* PC2 for the principal components analyses of the ulna: A) Zulu, PC1 and PC2 explain 57.48% and 7.07% of the variance respectively, and B) Kikuyu, PC1 and PC2 explain 63.57% and 8.61% of the variance respectively.

A)

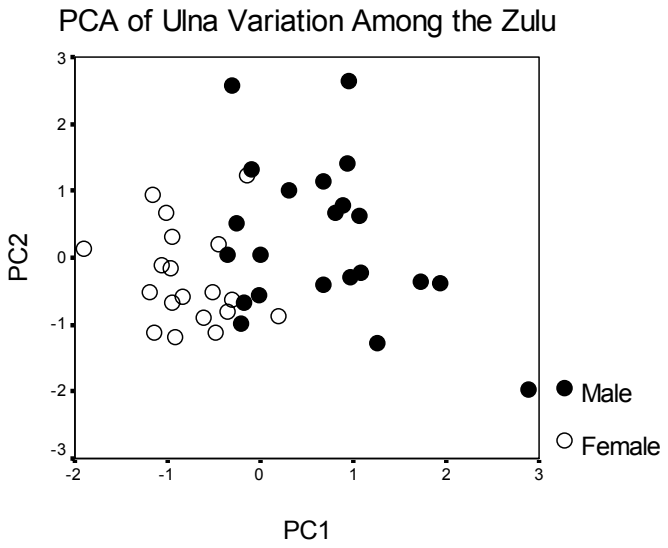

B)

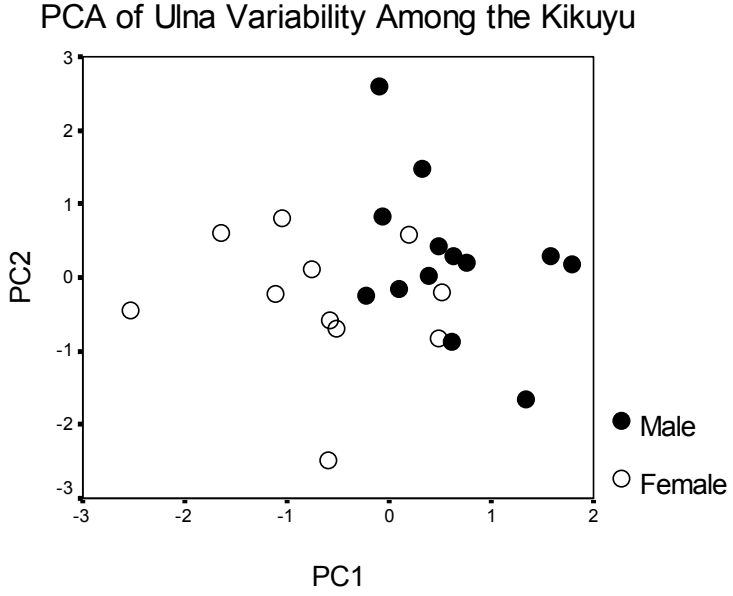

Figure 5.18 Plots of PC1 *versus* PC2 for the principal components analyses of the radius: A) Zulu, PC1 and PC2 explain 63.30% and 12.33% of the variance respectively, and B) Kikuyu, PC1 and PC2 explain 69.60% and 12.84% of the variance respectively.

A)

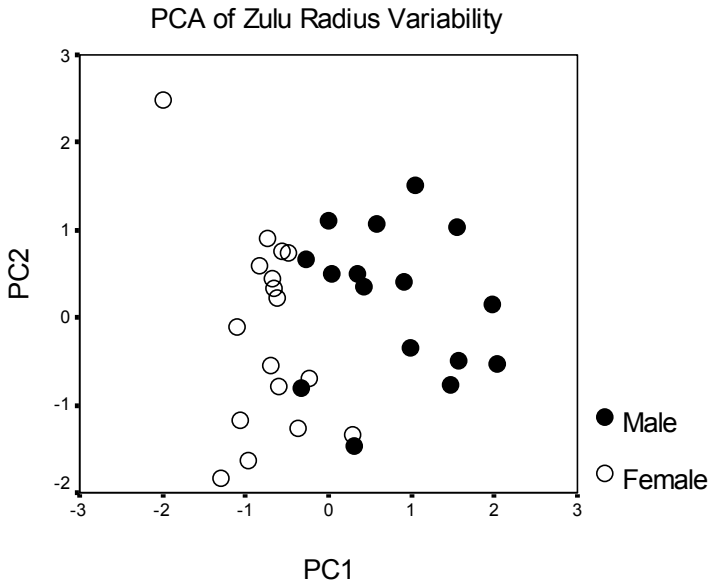

B)

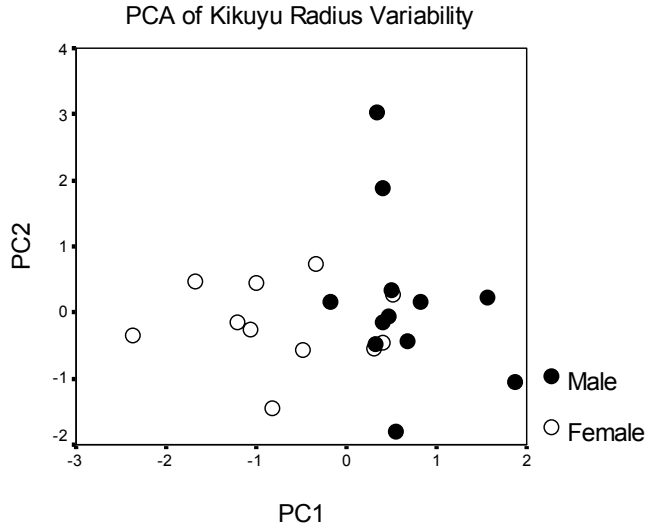

Figure 5.19 Plots of PC1 *versus* PC2 for the principal components analyses of the femur: A) Zulu, PC1 and PC2 explain 67.03% and 7.82% of the variance respectively, and B) Kikuyu, PC1 and PC2 explain 67.87% and 8.89% of the variance respectively.

A)

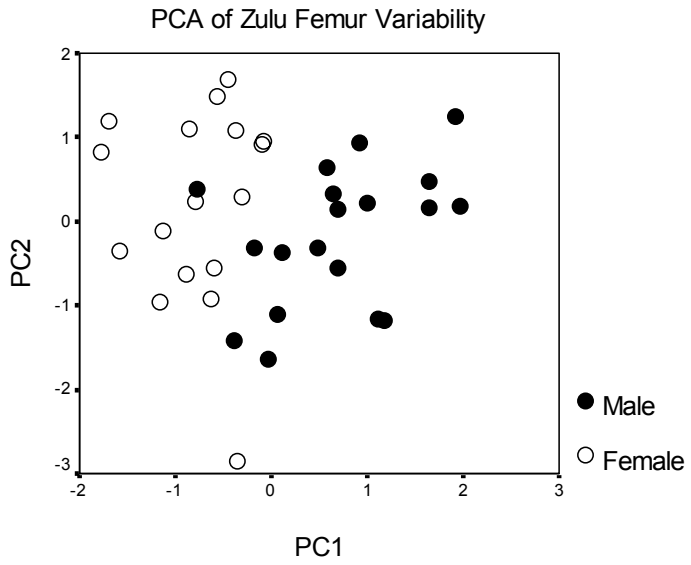

B)

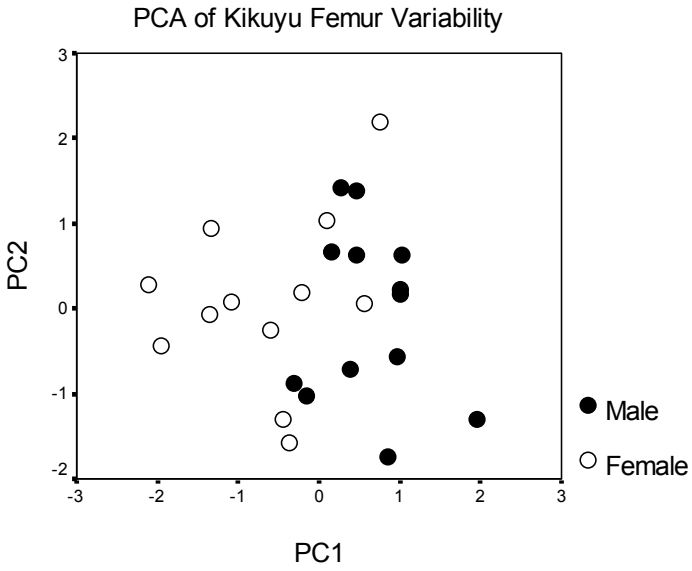

Figure 5.20 Plots of PC1 *versus* PC2 for the principal components analyses of the tibia: A) Zulu, PC1 and PC2 explain 77.14% and 6.76% of the variance respectively, and B) Kikuyu, PC1 and PC2 explain 76.24% and 7.66% of the variance respectively.

A)

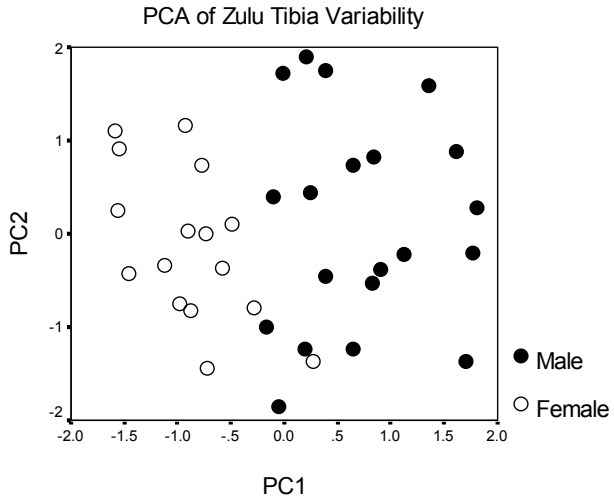

B)

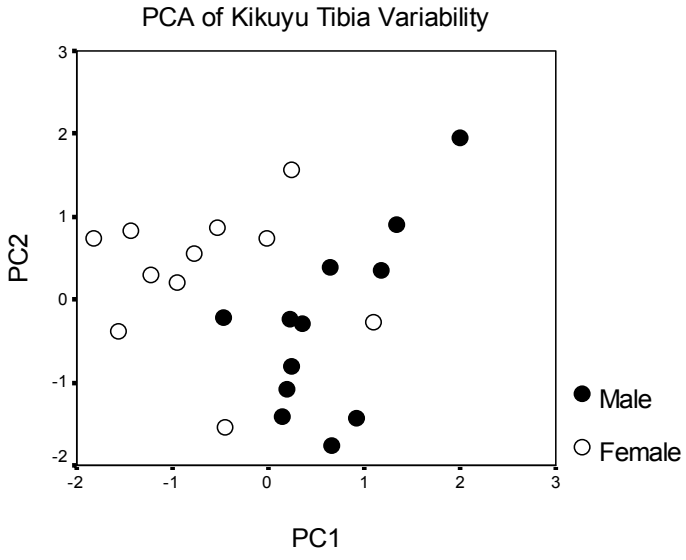

Figure 5.21 Comparison of the magnitude of sexual dimorphism and variability of the humerus between the Zulu and Kikuyu. Solid lines represents the index of sexual dimorphism (ISD %) from the left vertical axis; dashed lines represent the coefficient of variation (CV) from the right vertical axis.

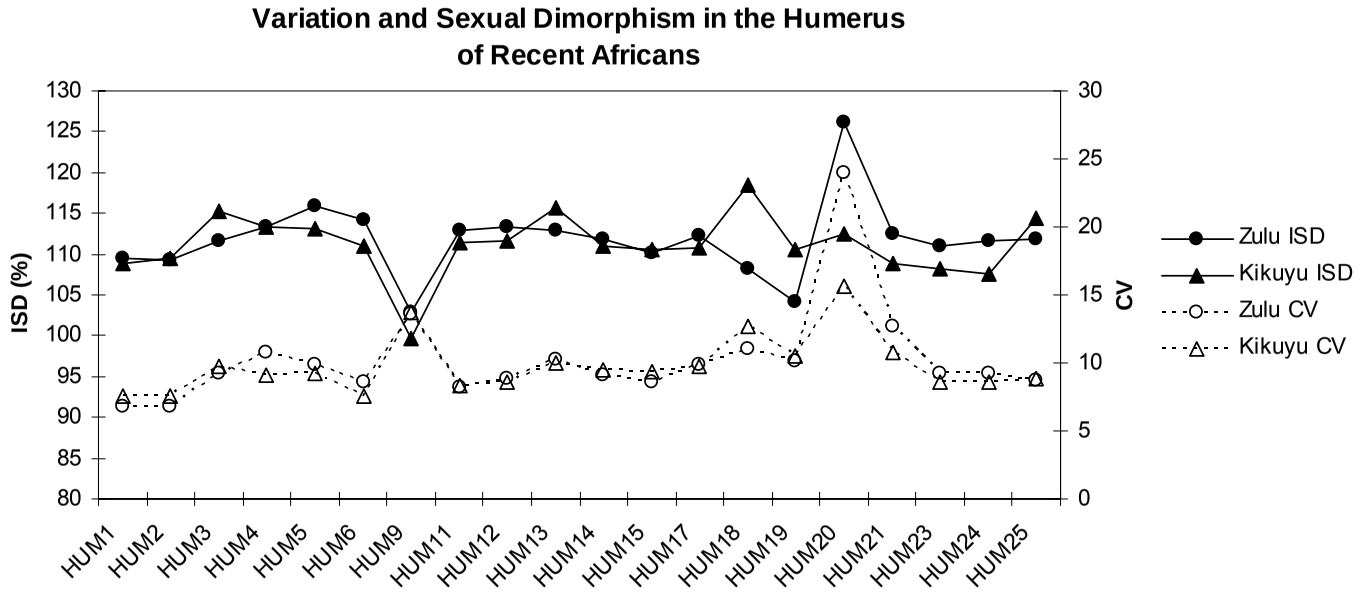

*HUM1: max length, HUM2: total length, HUM3: max midshaft diameter, HUM4: min midshaft diameter, HUM5: head proximo-distal diameter, HUM6: head DV diameter, HUM9: deltoid tuberosity max length, HUM11: epicondylar width, HUM12: capitulum + trochlear width, HUM13: capitulum width, HUM14: capitulum height, HUM15: capitulum AP thickness, HUM17: medial trochlear lip AP diameter, HUM18: min trochlear AP diameter, HUM19: olecranon fossa width, HUM20: medial dorsal pillar breadth, HUM21: lateral dorsal pillar breadth, HUM23: deltoid to capitulum distance, HUM24: deltoid to trochlea distance, HUM25: min shaft circumference.

Figure 5.22 Comparison of the magnitude of sexual dimorphism and variability of the ulna between the Zulu and Kikuyu. Solid lines represents the index of sexual dimorphism (ISD %) from the left vertical axis; dashed lines represent the coefficient of variation (CV) from the right vertical axis.

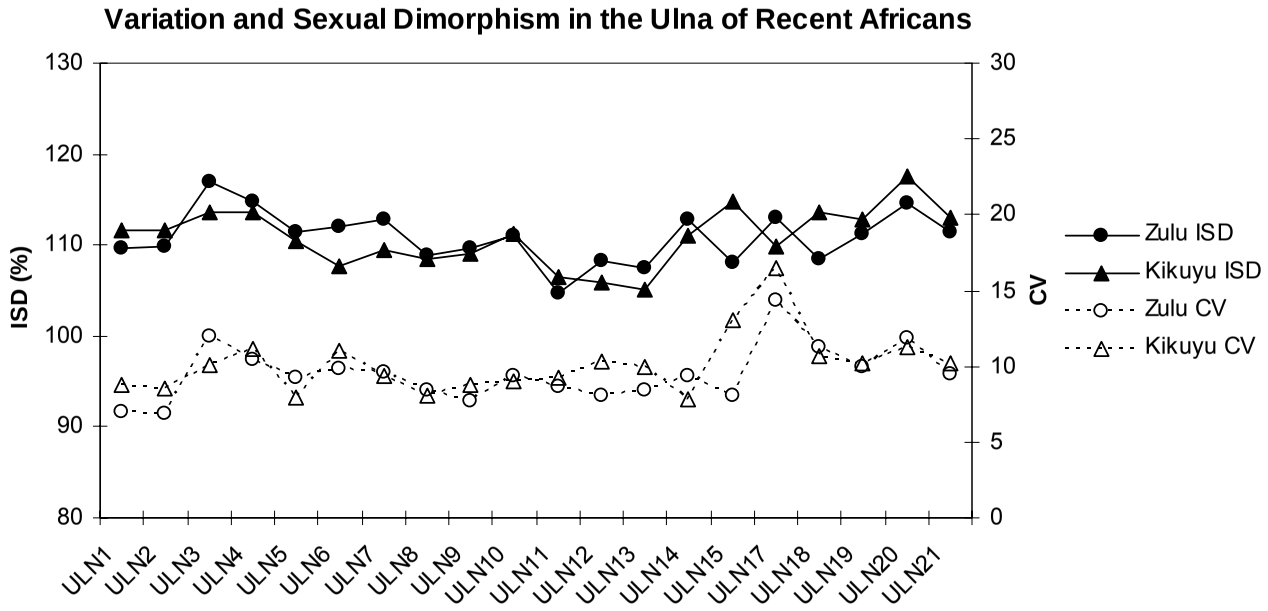

*ULN1: articular length, ULN2: total length, ULN3: max midshaft diameter, ULN4: min midshaft diameter, ULN5: coronoid height, ULN6: max coronoid ML breadth, ULN7: olecranon height, ULN8: olecranon ML breadth, ULN9: olecranon length, ULN10: trochlear notch length, ULN11: trochlear notch transverse breadth, ULN12: mid-trochlear notch thickness, ULN13: trochlear notch AP thickness, ULN14: radial notch position, ULN15: radial notch length, ULN17: brachialis insertion position, ULN18: proximal shaft AP diameter, ULN19: proximal shaft ML diameter, ULN20: distal epiphysis transverse breadth, ULN21: min shaft circumference.

Figure 5.23 Comparison of the magnitude of sexual dimorphism and variability of the radius between the Zulu and Kikuyu. Solid lines represents the index of sexual dimorphism (ISD %) from the left vertical axis; dashed lines represent the coefficient of variation (CV) from the right vertical axis.

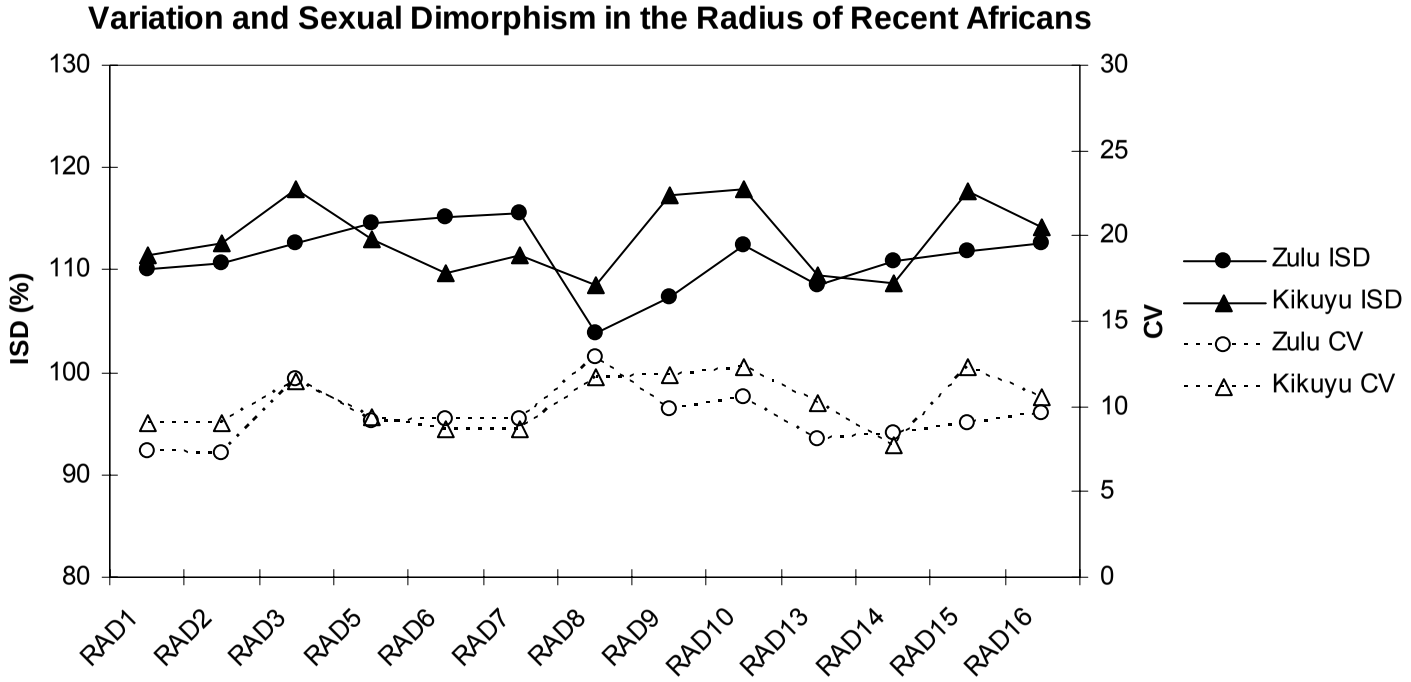

*RAD1: articular length, RAD2: max length, RAD3: max midshaft diameter, RAD5: max head AP diameter, RAD6: max head ML diameter, RAD7: max head diameter, RAD8: radial tuberosity length, RAD9: neck length, RAD10: neck AP diameter, RAD13: distal epiphysis DV breadth, RAD14: distal epiphysis ML breadth, RAD15: min shaft circumference, RAD16: radial tuberosity circumference.

Figure 5.24 Comparison of the magnitude of sexual dimorphism and variability of the femur between the Zulu and Kikuyu. Solid lines represents the index of sexual dimorphism (ISD %) from the left vertical axis; dashed lines represent the coefficient of variation (CV) from the right vertical axis.

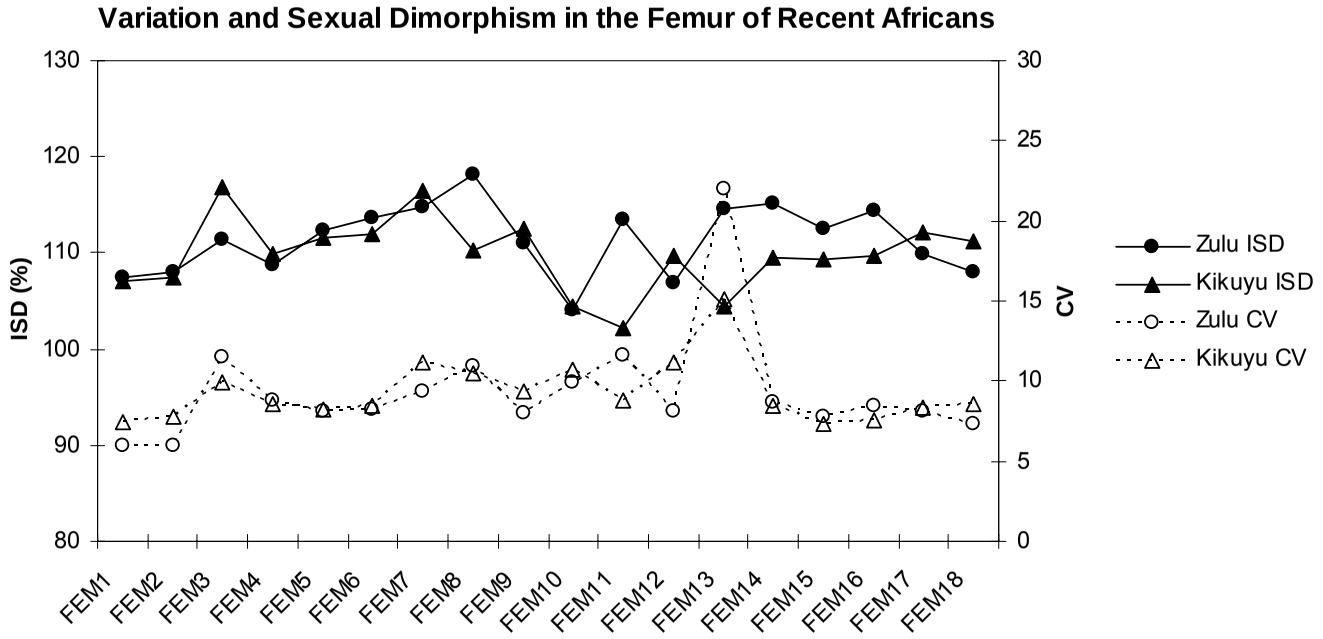

*FEM1: max length, FEM2: bicondylar length, FEM3: midshaft AP diameter, FEM4: midshaft ML diameter, FEM5: vertical head diameter, FEM6: horizontal head diameter, FEM7: min neck height, FEM8: min neck breadth, FEM9: biomechanical neck length, FEM10: neck length, FEM11: subtrochanteric AP shaft diameter, FEM12: subtrochanteric ML shaft diameter, FEM13: gluteal tuberosity breadth, FEM14: patellar notch width, FEM15: biepicondylar breadth, FEM16: max distal articular breadth, FEM17: min shaft circumference, FEM18: subtrochanteric shaft circumference.

Figure 5.25 Comparison of the magnitude of sexual dimorphism and variability of the tibia between the Zulu and Kikuyu. Solid lines represents the index of sexual dimorphism (ISD %) from the left vertical axis; dashed lines represent the coefficient of variation (CV) from the right vertical axis.

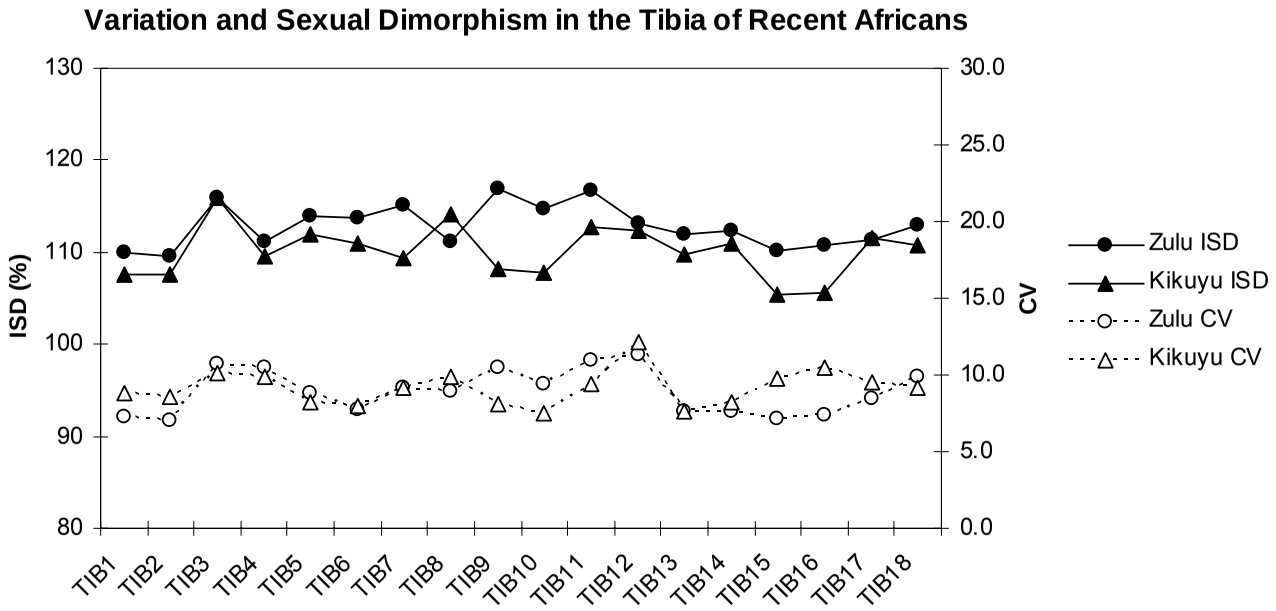

*TIB1: articular length, TIB2: total length, TIB3: midshaft AP diameter, TIB4: midshaft ML diameter, TIB5: proximal epiphysis max length, TIB6: proximal epiphysis max breadth, TIB7: medial condyle AP length, TIB8: medial condyle ML breadth, TIB9: lateral condyle AP length, TIB10: lateral condyle ML breadth, TIB11: shaft AP diameter at nutrient foramen, TIB12: shaft ML diameter at nutrient foramen, TIB13: talar AP length, TIB14: distal epiphysis ML breadth, TIB15: nutrient foramen to medial malleolus distance, TIB16: nutrient foramen to talar articular surface distance, TIB17: min shaft circumference, TIB18: shaft circumference at nutrient foramen.

Figure 5.26 Comparison of variability in a selection of appendicular measurements among females from a global human sample: A) Upper limb elements, and B) Lower limb elements. Data for the Sami, US White, and Inuit samples are from Pearson (1997). Figure continues on the next page.

A)

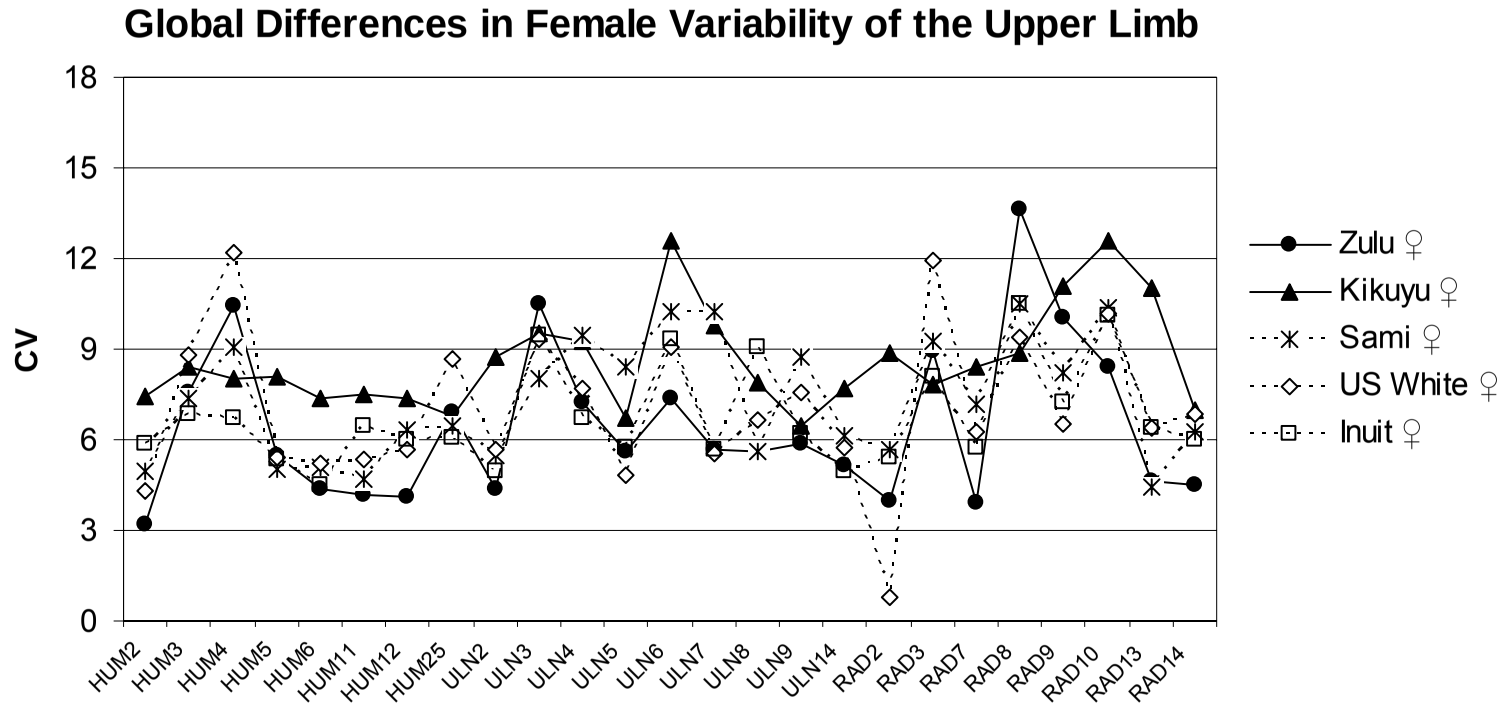

Figure 5.26 Continued.

B)

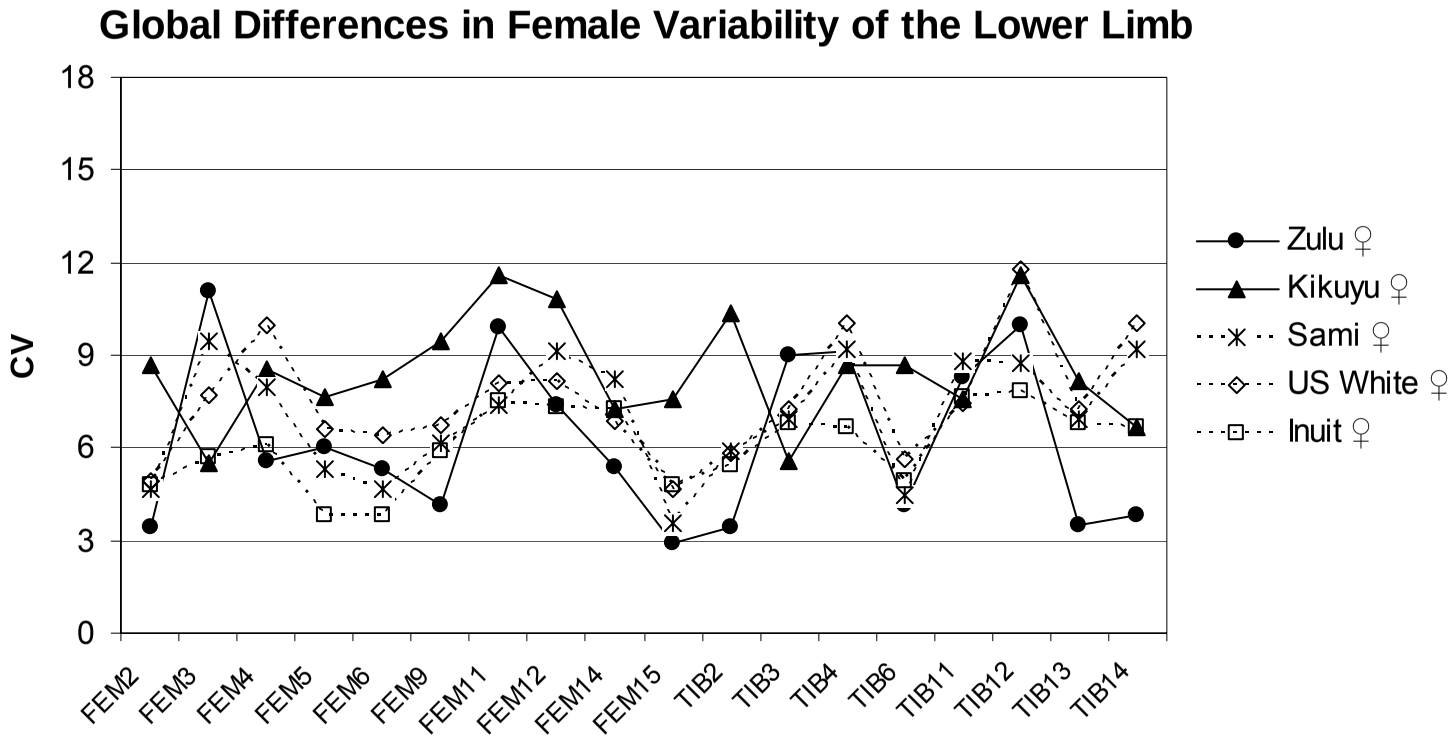

Figure 5.27 Comparison of variability in a selection of appendicular measurements among males from a global human sample: A) Upper limb elements, and B) Lower limb elements. Data for the Sami, US White, Inuit, and Australian Aborigines samples are from Pearson (1997). Figure continues on the next page.

A)

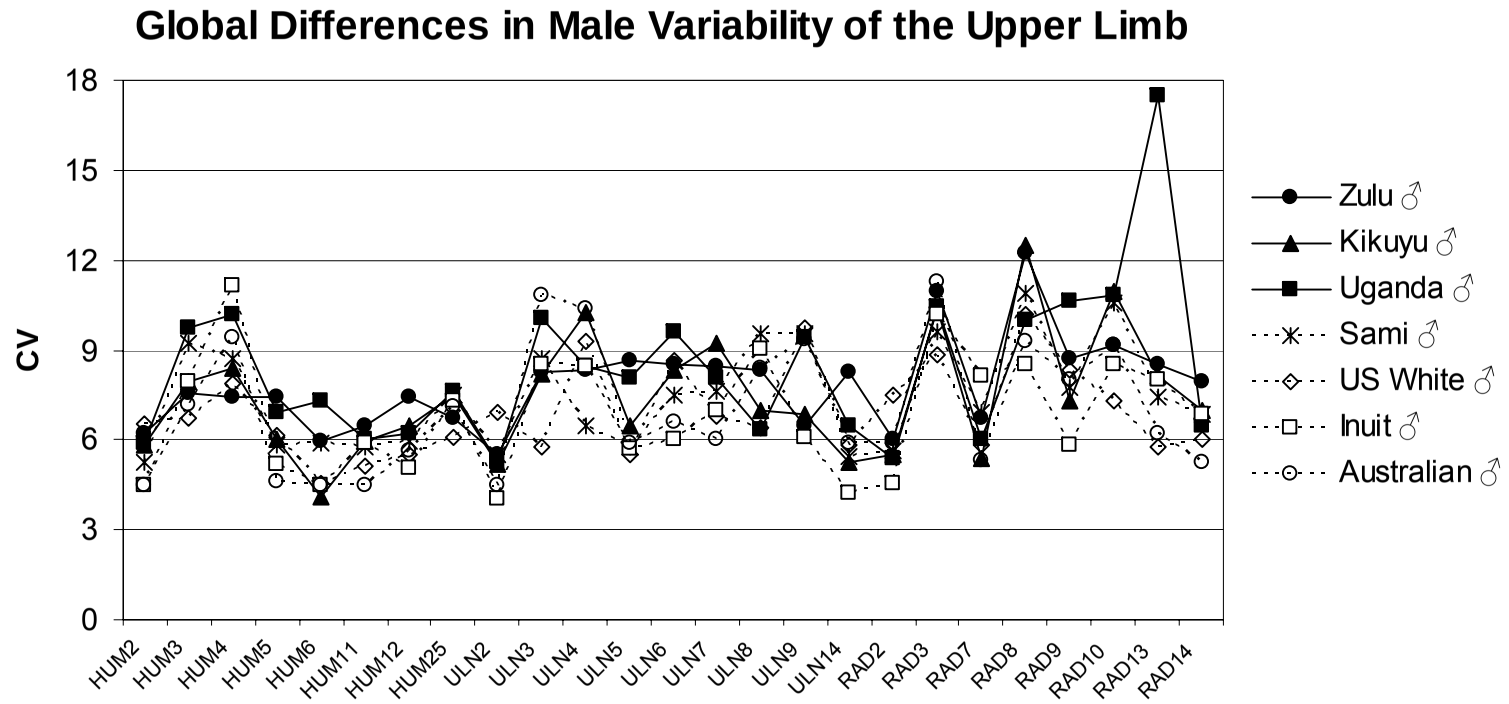

Figure 5.27 Continued.

B)

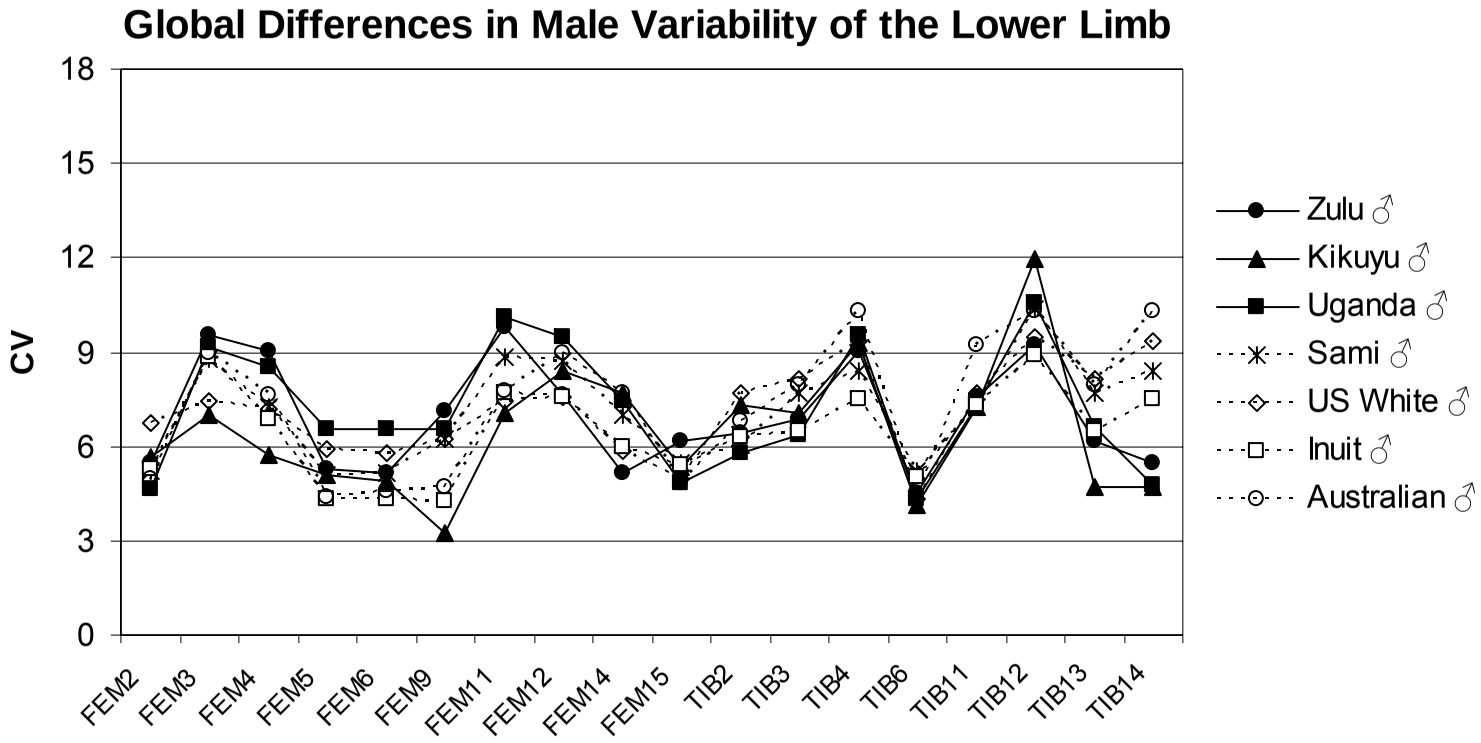

Table 5.1 Composition of the recent human skeletal samples.

Sample	Total	Female	Male	Indeterminate Sex
	N	*N*	*N*	*N*
Zulu	42	20	22	0
Kikuyu	40	12	16	12
Nilotic Ugandan	--	--	26	--

Table 5.2 Results of the Fligner-Killeen (FK) test for equality of relative variation in the humerus between Zulu and Kikuyu females. Significant differences ($p < 0.05$) are in bold.

Variable	Zulu ♀		Kikuyu ♀		Zulu *vs* Kikuyu FK	
	N	CV	*N*	CV	*T*	*p*
HUM1	19	3.34	12	7.82	17.814	**0.0067**
HUM2	19	3.19	12	7.43	18.18	**0.0047**
HUM3	19	7.55	12	8.39	10.964	0.7173
HUM4	19	10.42	12	8.01	8.3053	0.5850
HUM5	19	5.48	12	8.05	13.13	0.2704
HUM6	19	4.37	12	7.39	15.781	**0.0446**
HUM9	19	14.07	12	14.12	13.159	0.2969
HUM11	19	4.18	12	7.53	17.576	**0.0088**
HUM12	19	4.13	12	7.37	15.738	**0.0462**
HUM13	19	6.02	12	8.70	14.685	0.1024
HUM14	19	5.78	12	9.50	16.995	**0.0154**
HUM15	19	6.04	12	10.40	16.621	**0.0217**
HUM17	19	6.47	12	7.80	12.218	0.4291
HUM18	19	8.81	12	12.31	13.328	0.2421
HUM19	19	9.12	12	8.84	8.9403	0.7420
HUM20	19	17.07	12	11.28	7.4771	0.4071
HUM21	19	8.95	12	13.95	12.985	0.2925
HUM23	19	5.68	12	8.54	13.558	0.2119
HUM24	19	5.79	12	8.92	13.697	0.1950
HUM25	19	6.89	12	6.80	9.8365	0.9816

Table 5.3 Results of the Fligner-Killeen (FK) test for equality of relative variation in the ulna between Zulu and Kikuyu females. Significant differences ($p < 0.05$) are in bold.

Variable	Zulu ♀		Kikuyu ♀		Zulu *vs* Kikuyu FK	
	N	CV	*N*	CV	*T*	*p*
ULN1	19	4.63	11	9.34	14.998	**0.0332**
ULN2	19	4.35	11	8.75	14.682	**0.0435**
ULN3	19	10.51	11	9.54	8.3384	0.8207
ULN4	19	7.24	11	9.25	12.022	0.8979
ULN5	19	5.62	11	6.73	12.718	0.1858
ULN6	19	7.40	11	12.57	15.121	**0.0297**
ULN7	19	5.70	11	9.77	14.949	**0.0346**
ULN8	19	5.58	11	7.89	13.026	0.1521
ULN9	19	5.85	11	6.46	9.7907	0.7738
ULN10	19	5.81	11	6.22	8.6663	0.9119
ULN11	19	7.11	11	9.87	12.918	0.1633
ULN12	19	3.59	11	11.37	19.419	**0.0002**
ULN13	19	3.38	11	9.38	18.306	**0.0010**
ULN14	19	5.18	11	7.70	10.675	0.5484
ULN15	19	6.49	11	10.73	15.33	**0.0246**
ULN17	19	10.33	11	19.45	13.443	0.1142
ULN18	19	11.24	11	6.90	5.6036	0.2324
ULN19	19	8.60	11	9.35	11.456	0.3808
ULN20	19	5.64	11	14.12	17.679	**0.0021**
ULN21	19	6.46	11	10.83	14.981	**0.0333**

Table 5.4 Results of the Fligner-Killeen (FK) test for equality of relative variation in the radius between Zulu and Kikuyu females. Significant differences ($p < 0.05$) are in bold.

Variable	Zulu ♀		Kikuyu ♀		Zulu *vs* Kikuyu FK	
	N	CV	*N*	CV	*T*	*p*
RAD1	19	4.21	12	8.96	16.179	**0.0320**
RAD2	19	3.98	12	8.87	16.277	**0.0295**
RAD3	19	8.95	12	7.85	11.233	0.6497
RAD5	17	4.39	11	9.73	14.646	**0.0365**
RAD6	17	4.51	11	8.63	16.065	**0.0090**
RAD7	17	3.93	11	8.40	15.264	**0.0205**
RAD8	19	13.60	12	8.89	5.4867	0.1313
RAD9	19	10.05	12	11.10	11.353	0.6205
RAD10	19	8.44	12	12.61	15.792	**0.0442**
RAD13	19	4.61	12	11.03	18.82	**0.0023**
RAD14	19	4.50	12	7.01	15.151	0.0730
RAD15	19	5.23	12	8.27	15.246	0.0676
RAD16	19	8.34	12	9.89	12.279	0.4164

Table 5.5 Results of the Fligner-Killeen (FK) test for equality of relative variation in the femur between Zulu and Kikuyu females. Significant differences ($p < 0.05$) are in bold.

Variable	Zulu ♀		Kikuyu ♀		Zulu *vs* Kikuyu FK	
	N	CV	*N*	CV	*T*	*p*
FEM1	18	3.51	12	8.49	16.656	**0.0186**
FEM2	18	3.45	12	8.67	17.017	**0.0132**
FEM3	18	11.08	12	5.51	4.5149	0.0627
FEM4	18	5.59	12	8.55	14.55	0.1047
FEM5	18	6.03	12	7.62	11.884	0.4859
FEM6	18	5.34	12	8.25	15.039	0.0731
FEM7	18	5.41	12	8.77	15.23	0.0631
FEM8	18	5.70	12	10.44	16.908	**0.0137**
FEM9	18	4.13	12	9.47	16.655	**0.0186**
FEM10	18	10.45	12	8.62	7.7635	0.4632
FEM11	18	9.88	12	11.58	13.483	0.2106
FEM12	18	7.39	12	10.83	15.537	**0.0494**
FEM13	18	21.29	12	20.59	10.181	0.9159
FEM14	17	5.40	12	7.23	13.447	0.2036
FEM15	18	2.94	12	7.59	16.918	**0.0145**
FEM16	18	4.44	12	6.90	14.12	0.1313
FEM17	18	5.51	12	6.49	11.739	0.5172
FEM18	18	5.32	12	8.05	14.044	0.1474

Table 5.6 Results of the Fligner-Killeen (FK) test for equality of relative variation in the tibia between Zulu and Kikuyu females. Significant differences ($p < 0.05$) are in bold.

Variable	Zulu ♀		Kikuyu ♀		Zulu *vs* Kikuyu FK	
	N	CV	*N*	CV	*T*	*p*
TIB1	18	3.46	12	10.37	15.701	**0.0438**
TIB2	18	3.41	12	10.39	15.624	**0.0460**
TIB3	18	8.98	11	5.57	4.076	0.0796
TIB4	18	9.16	11	8.68	8.887	0.9812
TIB5	17	4.78	12	7.23	14.916	0.0734
TIB6	17	4.15	12	8.69	16.303	**0.0226**
TIB7	16	4.02	12	9.39	16.884	**0.0110**
TIB8	17	6.21	12	11.00	14.248	0.1201
TIB9	17	5.62	12	9.50	15.789	**0.0358**
TIB10	17	5.16	12	8.66	14.341	0.1124
TIB11	18	8.28	11	7.59	8.2221	0.7925
TIB12	18	9.97	11	11.59	11.21	0.4172
TIB13	18	3.47	12	8.14	18.66	**0.0023**
TIB14	18	3.79	12	6.65	15.123	0.0685
TIB15	18	3.81	12	10.81	19.344	**0.0010**
TIB16	18	4.04	12	11.03	19.056	**0.0014**
TIB17	18	6.77	11	7.89	10.417	0.5985
TIB18	18	7.32	11	8.58	11.996	0.2740

Table 5.7 Results of Levene's (median) test for equality of relative variation of PC scores among females between the samples. Significant differences ($p < 0.05$) are in bold. Separate PCA were conducted for each element. % Variance represents the percentage of the total variance explained by the first two principal components (additional components were extracted for most elements, but account for < 7% of the total variance).

Element	N_Z	N_K	% Variance	Zulu *vs* Kikuyu Levene's *p*
PC1				
Humerus	19	12	40.60	**0.0279**
Ulna	20	12	47.43	**0.0139**
Radius	17	11	54.01	**0.0132**
Femur	17	12	53.30	**0.0296**
Tibia	16	11	61.09	**0.0476**
PC2				
Humerus	19	12	16.59	0.0795
Ulna	20	12	11.0	0.5401
Radius	17	11	13.82	0.2696
Femur	17	12	13.31	0.6186
Tibia	16	11	9.93	0.8055

Table 5.8 Results of the Fligner-Killeen (FK) test for equality of relative variation in the humerus between Zulu, Kikuyu and Ugandan males. Significant differences ($p < 0.0167$) are in bold.

Variable	Zulu ♂		Kikuyu ♂		Ugandan ♂		Zulu *vs* Kikuyu FK		Kikuyu *vs* Ugandan FK		Ugandan *vs* Zulu FK	
	N	CV	*N*	CV	*N*	CV	*T*	*p*	*T*	*p*	*T*	*p*
HUM1	22	6.13	15	6.04	25	5.83	13.014	0.9435	15.202	0.4946	22.043	0.5160
HUM2	22	6.20	15	5.84	25	5.87	12.963	0.9557	14.069	0.7234	20.647	0.7665
HUM3	22	7.54	15	7.95	25	9.76	14.407	0.6246	10.37	0.4727	14.089	0.1741
HUM4	22	7.46	15	8.41	25	10.21	15.147	0.4767	9.695	0.3609	14.121	0.1768
HUM5	22	7.41	13	6.03	25	6.93	7.9988	0.3558	9.2669	0.6007	20.346	0.8250
HUM6	22	5.95	13	4.12	25	7.32	6.5243	0.1641	6.117	0.1363	16.639	0.4747
HUM9	22	13.36	14	12.15	25	19.65	9.4039	0.4522	5.2064	0.0460	11.774	0.0520
HUM11	22	6.50	14	5.96	25	6.04	10.754	0.7374	12.796	0.7919	20.431	0.8085
HUM12	22	7.40	14	6.44	25	6.20	10.647	0.7125	12.191	0.9333	22.108	0.5053
HUM13	22	9.54	14	8.53	25	8.04	12.079	0.9416	13.901	0.5533	22.041	0.5163
HUM14	22	8.04	15	7.21	25	8.52	11.461	0.6924	11.002	0.5925	17.352	0.5925
HUM15	22	7.83	15	7.41	25	8.88	12.601	0.9575	10.683	0.5302	17.121	0.5529
HUM17	22	8.88	15	8.77	25	7.16	11.606	0.7248	13.262	0.9044	22.826	0.3969
HUM18	22	11.43	15	10.61	25	11.22	10.93	0.5787	10.066	0.2100	19.396	0.4925
HUM19	22	10.72	15	8.96	25	6.97	12.31	0.8881	16.042	0.1767	23.898	0.1316
HUM20	22	22.98	15	15.77	25	15.48	11.642	0.3664	14.692	0.2965	21.541	0.3001
HUM21	22	12.77	15	9.56	25	11.31	9.4491	0.1587	8.7624	0.1181	19.01	0.4537
HUM23	22	8.93	15	9.15	25	5.95	13.707	0.3901	19.472	0.0546	26.845	0.0626
HUM24	22	8.54	15	9.08	25	5.67	14.456	0.6141	19.929	0.0402	26.728	0.0667
HUM25	22	6.69	15	7.49	25	7.64	14.586	0.5869	11.647	0.7278	15.19	0.2795

Table 5.9 Results of the Fligner-Killeen (FK) test for equality of relative variation in the ulna between Zulu, Kikuyu and Ugandan males. Significant differences ($p < 0.0167$) are in bold.

Variable	Zulu ♂		Kikuyu ♂		Ugandan ♂		Zulu *vs* Kikuyu FK		Kikuyu *vs* Ugandan FK		Ugandan *vs* Zulu FK	
	N	CV	*N*	CV	*N*	CV	*T*	*p*	*T*	*p*	*T*	*p*
ULN1	22	5.65	14	5.64	24	5.57	12.742	0.7812	12.298	0.9017	18.493	0.8076
ULN2	22	5.54	14	5.20	24	5.23	10.062	0.5832	10.956	0.7790	21.391	0.6188
ULN3	22	8.28	14	8.23	24	10.08	13.275	0.6584	9.1754	0.4142	15.077	0.2640
ULN4	22	8.34	14	10.23	24	8.46	13.983	0.5091	14.439	0.4426	18.657	0.8403
ULN5	22	8.63	15	6.50	24	8.09	11.147	0.6242	10.686	0.5306	18.87	0.8830
ULN6	22	8.53	15	8.34	24	9.61	11.588	0.7207	10.084	0.4218	16.97	0.5269
ULN7	22	8.45	15	9.21	24	8.07	12.915	0.9671	13.74	0.7870	19.143	0.9384
ULN8	22	8.34	15	6.97	24	6.37	10.497	0.6784	13.717	0.5820	24.208	0.2234
ULN9	22	6.47	15	6.84	24	9.44	12.952	0.9584	8.1404	0.1697	12.175	0.0630
ULN10	22	9.01	15	8.46	24	9.52	12.943	0.9604	10.889	0.5704	17.131	0.5540
ULN11	22	9.38	15	9.01	24	9.90	11.634	0.7311	10.258	0.4518	15.774	0.3479
ULN12	22	8.74	15	9.91	24	8.63	14.383	0.6298	13.836	0.7673	18.044	0.7201
ULN13	22	9.66	15	10.62	24	7.86	11.873	0.7858	14.121	0.7042	22.623	0.4165
ULN14	22	8.29	15	5.28	24	6.49	8.3114	0.1797	10.165	0.4355	21.901	0.5301
ULN15	22	7.66	15	12.33	24	8.18	17.808	0.1308	17.898	0.1371	16.77	0.4940
ULN17	22	14.76	15	14.87	24	10.33	12.966	0.9551	16.358	0.3006	24.405	0.2048
ULN18	22	10.25	15	10.11	24	13.10	11.893	0.7904	14.114	0.7059	17.126	0.5532
ULN19	22	8.36	15	9.01	24	8.98	12.234	0.8702	12.702	0.9711	17.805	0.6749
ULN20	22	11.63	13	4.44	24	10.29	4.9836	0.0560	4.1757	0.0356	18.81	0.8710
ULN21	22	8.60	15	9.18	23	8.50	13.519	0.8236	13.482	0.8380	21.958	0.5083

Table 5.10 Results of the Fligner-Killeen (FK) test for equality of relative variation in the radius between Zulu, Kikuyu and Ugandan males. Significant differences ($p < 0.0167$) are in bold.

Variable	Zulu ♂		Kikuyu ♂		Ugandan ♂		Zulu *vs* Kikuyu FK		Kikuyu *vs* Ugandan FK		Ugandan *vs* Zulu FK	
	N	CV	*N*	CV	*N*	CV	*T*	*p*	*T*	*p*	*T*	*p*
RAD1	20	6.40	15	5.97	23	5.33	11.515	0.7082	14.891	0.5357	21.434	0.2951
RAD2	20	6.04	14	5.51	23	5.35	9.7909	0.5260	12.275	0.9007	21.199	0.3252
RAD3	20	10.93	15	10.36	23	10.47	12.172	0.8642	13.24	0.8968	17.165	0.9244
RAD5	17	6.92	12	5.16	21	6.33	5.6295	0.1362	8.8967	0.7256	17.551	0.3957
RAD6	17	6.79	12	5.91	22	5.36	7.8657	0.4838	10.503	0.8630	19.585	0.1575
RAD7	16	6.75	12	5.40	21	6.01	7.9555	0.5026	9.3379	0.8379	16.059	0.4814
RAD8	20	12.23	15	12.52	23	10.02	11.286	0.6564	14.216	0.6751	21.404	0.2989
RAD9	20	8.70	15	7.28	23	10.62	11.568	0.7204	10.135	0.4289	15.374	0.5661
RAD10	20	9.15	15	10.97	23	10.80	14.753	0.5312	12.837	0.9919	15.763	0.6384
RAD13	20	8.50	14	8.12	23	17.47	12.362	0.8563	8.4008	0.2914	12.684	0.1959
RAD14	20	7.97	14	6.96	23	6.49	10.301	0.6367	14.027	0.5104	22.216	0.2091
RAD15	20	8.18	15	11.47	23	8.09	15.251	0.4349	15.549	0.4150	17.27	0.9467
RAD16	20	6.96	15	8.54	23	9.89	13.582	0.7911	10.99	0.5907	13.4	0.2701

Table 5.11 Results of the Fligner-Killeen (FK) test for equality of relative variation in the femur between Zulu, Kikuyu and Ugandan males. Significant differences ($p < 0.0167$) are in bold.

Variable	Zulu ♂		Kikuyu ♂		Ugandan ♂		Zulu *vs* Kikuyu FK		Kikuyu *vs* Ugandan FK		Ugandan *vs* Zulu FK	
	N	CV	*N*	CV	*N*	CV	*T*	*p*	*T*	*p*	*T*	*p*
FEM1	20	5.49	15	5.66	26	4.70	13.672	0.7701	17.279	0.2060	19.268	0.6659
FEM2	20	5.46	15	5.65	26	4.63	13.745	0.7527	17.745	0.1612	20.211	0.4998
FEM3	20	9.53	15	7.00	26	9.19	8.9535	0.2438	7.8762	0.1522	17.145	0.9079
FEM4	20	9.04	15	5.72	26	8.51	7.4433	0.1027	8.5617	0.2158	17.755	0.9667
FEM5	20	5.28	14	5.09	26	6.56	11.021	0.8072	8.0895	0.2578	15.558	0.5997
FEM6	20	5.17	15	4.87	26	6.54	12.739	0.9968	8.8394	0.2479	15.021	0.5071
FEM7	20	7.06	15	9.27	26	9.15	14.551	0.5729	11.937	0.7893	11.384	0.1094
FEM8	20	7.79	15	8.95	26	10.70	15.119	0.4597	12.425	0.8987	13.071	0.2436
FEM9	20	7.14	15	3.23	26	6.54	3.7026	**0.0053**	6.3349	0.0610	20.465	0.4591
FEM10	20	9.40	15	9.53	26	10.49	12.439	0.9293	11.708	0.7392	16.156	0.7108
FEM11	20	9.77	15	7.07	26	10.11	9.351	0.2971	8.4856	0.2088	16.014	0.6838
FEM12	20	7.66	15	8.38	26	9.48	12.069	0.8392	11.479	0.6903	13.851	0.3345
FEM13	20	21.08	15	13.09	26	28.65	6.8898	0.0713	4.9812	0.0237	14.146	0.3741
FEM14	20	5.13	14	7.69	25	7.43	17.856	0.0545	13.103	0.7225	10.492	0.0649
FEM15	20	6.17	14	5.35	26	4.80	10.354	0.6500	14.924	0.3777	21.103	0.2418
FEM16	20	5.61	14	4.61	25	4.92	10.278	0.6314	9.5495	0.4823	17.934	0.9243
FEM17	20	7.39	15	6.17	26	7.98	10.57	0.5046	7.9879	0.1615	15.333	0.5598
FEM18	20	7.02	15	7.59	26	6.97	12.739	0.9967	13.637	0.8253	16.773	0.8314

Table 5.12 Results of the Fligner-Killeen (FK) test for equality of relative variation in the tibia between Zulu, Kikuyu and Ugandan males. Significant differences ($p < 0.0167$) are in bold.

Variable	Zulu ♂		Kikuyu ♂		Ugandan ♂		Zulu *vs* Kikuyu FK		Kikuyu *vs* Ugandan FK		Ugandan *vs* Zulu FK	
	N	CV	*N*	CV	*N*	CV	*T*	*p*	*T*	*p*	*T*	*p*
TIB1	21	6.61	15	7.70	26	5.82	13.717	0.7691	15.585	0.4361	20.383	0.6410
TIB2	21	6.44	15	7.34	26	5.78	14.048	0.6933	15.379	0.4716	20.308	0.6547
TIB3	21	6.88	15	7.05	26	6.33	13.662	0.7818	14.492	0.6416	19.076	0.8927
TIB4	21	9.06	15	9.32	26	9.53	12.987	0.9431	11.653	0.7272	16.667	0.6344
TIB5	20	6.56	12	5.67	26	5.80	9.3572	0.8472	9.4257	0.8424	19.837	0.5630
TIB6	20	4.52	13	4.13	26	4.34	8.4369	0.4296	10.35	0.8451	20.134	0.5124
TIB7	20	6.87	13	7.47	26	7.39	12.84	0.5181	10.331	0.8407	14.883	0.4847
TIB8	20	8.02	13	5.36	26	7.25	6.2911	0.1363	6.5965	0.1819	20.488	0.4553
TIB9	20	7.81	13	5.22	26	6.36	6.9154	0.1984	10.049	0.7743	21.21	0.3519
TIB10	20	7.23	13	3.35	26	6.01	4.1452	0.0285	5.114	0.0743	20.561	0.4443
TIB11	21	7.57	15	7.24	26	7.29	10.596	0.5114	11.342	0.6614	20.448	0.6292
TIB12	21	9.22	15	11.95	26	10.57	13.779	0.7548	13.499	0.8568	17.025	0.7003
TIB13	21	6.14	15	4.73	26	6.64	8.8185	0.2310	8.1638	0.1773	16.15	0.5440
TIB14	21	5.50	15	4.68	26	4.79	10.029	0.4069	13.353	0.8897	22.022	0.3779
TIB15	21	5.95	15	10.49	26	6.73	18.427	0.0840	17.209	0.2134	17.482	0.7878
TIB16	21	6.26	15	11.60	26	6.97	18.329	0.0895	17.099	0.2251	17.315	0.7555
TIB17	21	6.60	15	8.95	26	6.89	14.593	0.5752	15.387	0.4701	17.886	0.8677
TIB18	21	8.20	15	6.81	26	7.30	9.3668	0.3021	11.767	0.7520	19.256	0.8566

Table 5.13 Results of Levene's (median) test for equality of relative variation of PC1 scores among males between the samples. Significant differences ($p < 0.0167$) are in bold. Elements were analyzed using separate PCAs. % Variance represents the percentage of the total variance explained by the first two principal components (additional components were extracted for most elements, but account for < 7% of the total variance).

					Zulu *vs* Kikuyu	**Kikuyu *vs* Ugandan**	**Ugandan *vs* Zulu**
Element	N_Z	N_K	N_U	**% Variance**	**Levene's *p***	**Levene's *p***	**Levene's *p***
PC1							
Humerus	22	13	25	45.16	0.5631	0.5963	0.8890
Ulna	22	15	24	44.79	0.5624	0.3398	0.7504
Radius	16	12	21	48.76	0.1845	0.5816	0.4285
Femur	19	13	25	52.24	0.5123	0.5194	0.9572
Tibia	20	12	26	52.47	0.8694	0.6164	0.6799
PC2							
Humerus	22	13	25	15.21	0.7517	0.5963	0.8318
Ulna	22	15	24	11.38	0.8165	0.5850	0.6582
Radius	16	12	21	17.78	0.6402	0.6862	0.9360
Femur	19	13	25	11.75	0.7959	0.4624	0.5963
Tibia	20	12	26	15.57	0.3905	0.8945	0.3212

Table 5.14 Results of the *t*-test for equality of means and the Fligner-Killeen (FK) test for equality of relative variation in the humerus between the sexes among the Zulu and Kikuyu. Significant differences ($p < 0.05$) are in bold. The table continues on the next page.

Variable	Zulu						Kikuyu					
	♀CV (*N*)	♂CV (*N*)	*t*-test *t*	*p*	FK *T*	*p*	♀CV (*N*)	♂CV (*N*)	*t*-test *t*	*p*	FK *T*	*p*
HUM1	3.34 (19)	6.13 (22)	-5.573	**0.000**	9.3934	**0.048**	7.82 (12)	6.04 (15)	-3.378	**0.002**	12.014	0.411
HUM2	3.19 (19)	6.20 (22)	-5.416	**0.000**	7.6905	**0.015**	7.43 (12)	5.84 (15)	-3.772	**0.001**	11.710	0.479
HUM3	7.55 (19)	7.54 (22)	-4.612	**0.000**	16.595	0.989	8.39 (12)	7.95 (15)	-4.247	**0.000**	9.9353	0.956
HUM4	10.42 (19)	7.46 (22)	-4.546	**0.000**	21.603	0.163	8.01 (12)	8.41 (15)	-3.791	**0.001**	9.7515	0.990
HUM5	5.48 (19)	7.41 (22)	-6.910	**0.000**	11.158	0.137	8.05 (12)	6.03 (13)	-4.378	**0.000**	12.353	0.309
HUM6	4.37 (19)	5.95 (22)	-7.853	**0.000**	11.502	0.164	7.39 (12)	4.12 (13)	-4.510	**0.000**	14.35	0.074
HUM9	14.07 (19)	13.36 (22)	-0.652	0.518	19.194	0.465	14.12 (12)	12.15 (14)	-0.08	0.937	12.725	0.263
HUM11	4.18 (19)	6.50 (22)	-6.728	**0.000**	10.169	0.078	7.53 (12)	5.96 (14)	-4.098	**0.000**	10.658	0.733
HUM12	4.13 (19)	7.40 (22)	-6.300	**0.000**	10.663	0.103	7.37 (12)	6.44 (14)	-4.034	**0.000**	10.149	0.881
HUM13	6.02 (19)	9.54 (22)	-4.645	**0.000**	12.909	0.315	8.70 (12)	8.53 (14)	-4.240	**0.000**	10.298	0.837

Table 5.14 Continued.

Variable	Zulu						Kikuyu					
	♀CV (*N*)	♂CV (*N*)	*t*-test *t*	*p*	FK *T*	*p*	♀CV (*N*)	♂CV (*N*)	*t*-test *t*	*p*	FK *T*	*p*
HUM14	5.78 (19)	8.04 (22)	-4.961	**0.000**	10.494	0.095	9.50 (12)	7.21 (15)	-3.347	**0.003**	12.084	0.398
HUM15	6.04 (19)	7.83 (22)	-4.329	**0.000**	12.902	0.315	10.40 (12)	7.41 (15)	-2.869	**0.008**	12.129	0.389
HUM17	6.47 (19)	8.88 (22)	-4.612	**0.000**	13.274	0.367	7.80 (12)	8.77 (15)	-3.432	**0.002**	9.5064	0.918
HUM18	8.81 (19)	11.43 (22)	-2.430	**0.020**	13.272	0.366	12.31 (12)	10.61 (15)	-3.826	**0.001**	11.369	0.560
HUM19	9.12 (19)	10.72 (22)	-1.275	0.210	16.028	0.886	8.84 (12)	8.96 (15)	-2.697	**0.013**	9.9684	0.946
HUM20	17.07 (19)	22.98 (22)	-3.445	**0.001**	16.193	0.922	11.28 (12)	15.77 (15)	-1.848	0.077	7.4226	0.385
HUM21	8.95 (19)	12.77 (22)	-3.275	**0.002**	12.04	0.214	13.95 (12)	9.56 (15)	-2.025	0.054	12.646	0.293
HUM23	5.68 (19)	8.93 (22)	-4.238	**0.000**	10.397	0.090	8.54 (12)	9.15 (15)	-2.707	**0.012**	8.3028	0.586
HUM24	5.79 (19)	8.54 (22)	-4.611	**0.000**	11.202	0.140	8.92 (12)	9.08 (15)	-2.483	**0.020**	9.0971	0.800
HUM25	6.89 (19)	6.69 (22)	-5.241	**0.000**	18.728	0.547	6.80 (12)	7.49 (15)	-4.538	**0.000**	9.0923	0.799

Table 5.15 Results of the *t*-test for equality of means and the Fligner-Killeen (FK) test for equality of relative variation in the ulna between the sexes among the Zulu and Kikuyu. Significant differences ($p < 0.05$) are in bold. Table continues on next page.

Variable	Zulu						Kikuyu					
	♀CV (*N*)	♂CV (*N*)	*t*-test *t*	*p*	FK *T*	*p*	♀CV (*N*)	♂CV (*N*)	*t*-test *t*	*p*	FK *T*	*p*
ULN1	4.63 (19)	5.65 (22)	-5.653	**0.000**	12.294	0.2406	9.34 (11)	5.64 (14)	-3.727	**0.001**	13.421	0.0744
ULN2	4.35 (19)	5.54 (22)	-5.906	**0.000**	11.287	0.1467	8.75 (11)	5.20 (14)	-3.978	**0.001**	13.251	0.0857
ULN3	10.51 (19)	8.28 (22)	-5.417	**0.000**	21.017	0.2174	9.54 (11)	8.23 (14)	-3.553	**0.002**	9.9379	0.6670
ULN4	7.24 (19)	8.34 (22)	-5.536	**0.000**	14.372	0.5486	9.25 (11)	10.23 (14)	-3.230	**0.004**	8.2751	0.8290
ULN5	5.62 (19)	8.63 (22)	-4.705	**0.000**	13.168	0.3514	6.73 (11)	6.50 (15)	-3.846	**0.001**	10.071	0.6466
ULN6	7.40 (19)	8.53 (22)	-4.598	**0.000**	15.277	0.7262	12.57 (11)	8.34 (15)	-1.930	0.066	12.907	0.1243
ULN7	5.70 (19)	8.45 (22)	-5.212	**0.000**	10.892	0.1187	9.77 (11)	9.21 (15)	-2.436	**0.023**	10.275	0.5918
ULN8	5.58 (19)	8.34 (22)	-3.736	**0.001**	10.712	0.1074	7.89 (11)	6.97 (15)	-2.719	**0.012**	10.366	0.5506
ULN9	5.85 (19)	6.47 (22)	-4.692	**0.000**	14.126	0.5042	6.46 (11)	6.84 (15)	-3.256	**0.003**	8.9785	0.9654
ULN10	5.81 (19)	9.01 (22)	-4.384	**0.000**	12.997	0.3275	6.22 (11)	8.46 (15)	-3.445	**0.002**	7.2829	0.5478

Table 5.15 Continued.

Variable	Zulu						Kikuyu					
	♀CV (*N*)	♂CV (*N*)	*t*-test *t*	*p*	FK *T*	*p*	♀CV (*N*)	♂CV (*N*)	*t*-test *t*	*p*	FK *T*	*p*
ULN11	7.11 (19)	9.38 (22)	-1.685	0.100	12.618	0.2785	9.87 (11)	9.01 (15)	-1.715	0.099	10.786	0.4652
ULN12	3.59 (19)	8.74 (22)	-3.614	**0.001**	7.1178	**0.0093**	11.37 (11)	9.91 (15)	-1.419	0.169	10.421	0.5542
ULN13	3.38 (19)	9.66 (22)	-2.953	**0.005**	5.2339	**0.0018**	9.38 (11)	10.62 (15)	-1.265	0.218	10.537	0.5249
ULN14	5.18 (19)	8.29 (22)	-5.505	**0.000**	10.091	0.0749	7.70 (11)	5.28 (15)	-4.002	**0.001**	8.872	0.9977
ULN15	6.49 (19)	7.66 (22)	-3.450	**0.001**	12.892	0.3134	10.73 (11)	12.33 (15)	-2.909	**0.008**	7.934	0.7236
ULN17	10.33 (19)	14.76 (22)	-2.924	**0.006**	11.647	0.1765	19.45 (11)	14.87 (15)	-1.465	0.156	11.095	0.3966
ULN18	11.24 (19)	10.25 (22)	-2.436	**0.020**	18.448	0.5998	6.90 (11)	10.11 (15)	-3.486	**0.002**	5.6683	0.2244
ULN19	8.60 (19)	8.36 (22)	-4.035	**0.000**	16.66	0.9749	9.35 (11)	9.01 (15)	-3.389	**0.002**	9.9749	0.6729
ULN20	5.64 (19)	11.63 (22)	-4.711	**0.000**	12.123	0.2223	14.12 (11)	4.44 (13)	-4.183	**0.000**	15.81	**0.0052**
ULN21	6.46 (19)	8.60 (22)	-4.417	**0.000**	12.554	0.2699	10.83 (11)	9.18 (15)	-3.094	**0.005**	10.81	0.4590

Table 5.16 Results of the *t*-test for equality of means and the Fligner-Killeen (FK) test for equality of relative variation in the radius between the sexes among the Zulu and Kikuyu. Significant differences ($p < 0.05$) are in bold. Table continues on next page.

Variable	Zulu						Kikuyu					
	♀CV (*N*)	♂CV (*N*)	*t*-test *t*	*p*	FK *T*	*p*	♀CV (*N*)	♂CV (*N*)	*t*-test *t*	*p*	FK *T*	*p*
RAD1	4.21 (19)	6.40 (20)	-5.402	**0.000**	9.9338	0.0623	8.96 (12)	5.97 (15)	-3.824	**0.001**	13.826	0.1375
RAD2	3.98 (19)	6.04 (20)	-6.063	**0.000**	9.7277	0.0545	8.87 (12)	5.51 (14)	-4.231	**0.000**	14.226	0.0923
RAD3	8.95 (19)	10.93 (20)	-3.729	**0.001**	10.634	0.0959	7.85 (12)	10.36 (15)	-4.501	**0.000**	5.6305	0.1267
RAD5	4.39 (17)	6.92 (17)	-6.760	**0.000**	10.158	0.1752	9.73 (11)	5.16 (12)	-3.946	**0.001**	12.751	0.1016
RAD6	4.51 (17)	6.79 (17)	-7.134	**0.000**	20.283	0.0723	8.63 (11)	5.91 (12)	-3.085	**0.006**	12.801	0.0974
RAD7	3.93 (17)	6.75 (16)	-7.512	**0.000**	18.553	0.1134	8.40 (11)	5.40 (12)	-3.810	**0.001**	12.533	0.1217
RAD8	13.60 (19)	12.23 (20)	-0.937	0.355	16.505	0.9967	8.89 (12)	12.52 (15)	-1.925	0.066	9.0163	0.7775
RAD9	10.05 (19)	8.70 (20)	-2.366	**0.023**	19.109	0.4565	11.10 (12)	7.28 (15)	-4.596	**0.000**	14.509	0.0825
RAD10	8.44 (19)	9.15 (20)	-4.118	**0.000**	14.655	0.6019	12.61 (12)	10.97 (15)	-3.578	**0.001**	12.032	0.4088

Table 5.16 Continued.

Variable	Zulu						Kikuyu					
	♀CV (*N*)	♂CV (*N*)	*t*-test *t*	*t*-test *p*	FK *T*	FK *p*	♀CV (*N*)	♂CV (*N*)	*t*-test *t*	*t*-test *p*	FK *T*	FK *p*
RAD13	4.61 (19)	8.50 (20)	-3.692	**0.001**	8.3329	**0.0204**	11.03 (12)	8.12 (14)	-2.439	**0.022**	12.503	0.3005
RAD14	4.50 (19)	7.97 (20)	-4.876	**0.000**	9.6429	0.0515	7.01 (12)	6.96 (14)	-3.035	**0.006**	8.2667	0.5767
RAD15	5.23 (19)	8.18 (20)	-5.025	**0.000**	10.149	0.0708	8.27 (12)	11.47 (15)	-4.240	**0.000**	9.2646	0.8481
RAD16	8.34 (19)	6.96 (20)	-4.788	**0.000**	17.579	0.7567	9.89 (12)	8.54 (15)	-3.638	**0.001**	11.298	0.5781

Table 5.17 Results of the *t*-test for equality of means and the Fligner-Killeen (FK) test for equality of relative variation in the femur between the sexes among the Zulu and Kikuyu. Significant differences ($p < 0.05$) are in bold. Table continues on the next page.

Variable	Zulu						Kikuyu					
	♀CV (*N*)	♂CV (*N*)	*t*-test *t*	*p*	FK *T*	*p*	♀CV (*N*)	♂CV (*N*)	*t*-test *t*	*p*	FK *T*	*p*
FEM1	3.51 (18)	5.49 (20)	-4.722	**0.000**	10.06	0.1121	8.49 (12)	5.66 (15)	-2.597	**0.016**	14.029	0.1188
FEM2	3.45 (18)	5.46 (20)	-4.996	**0.000**	10.16	0.1188	8.67 (12)	5.65 (15)	-2.702	**0.012**	13.85	0.1350
FEM3	11.08 (18)	9.53 (20)	-3.361	**0.002**	16.338	0.8186	5.51 (12)	7.00 (15)	-6.295	**0.000**	7.2232	0.3463
FEM4	5.59 (18)	9.04 (20)	-3.288	**0.002**	8.9239	0.0551	8.55 (12)	5.72 (15)	-3.417	**0.002**	13.509	0.1710
FEM5	6.03 (18)	5.28 (20)	-6.343	**0.000**	15.629	0.9808	7.62 (12)	5.09 (14)	-4.508	**0.000**	14.71	0.0622
FEM6	5.34 (18)	5.17 (20)	-7.452	**0.000**	13.529	0.5592	8.25 (12)	4.87 (15)	-4.529	**0.000**	15.657	**0.0309**
FEM7	5.41 (18)	7.06 (20)	-6.581	**0.000**	10.149	0.1181	8.77 (12)	9.27 (15)	-4.393	**0.000**	10.857	0.6937
FEM8	5.70 (18)	7.79 (20)	-7.520	**0.000**	12.003	0.3050	10.44 (12)	8.95 (15)	-2.644	**0.014**	12.275	0.3545
FEM9	4.13 (18)	7.14 (20)	-5.308	**0.000**	6.5774	**0.0094**	9.47 (12)	3.23 (15)	-4.728	**0.000**	16.977	**0.0082**
FEM10	10.45 (18)	9.40 (20)	-1.303	0.201	15.528	0.9960	8.62 (12)	9.53 (15)	-1.205	0.240	7.1378	0.3305

Table 5.17 Continued.

Variable	Zulu						Kikuyu					
	♀CV (*N*)	♂CV (*N*)	*t*-test *t*	*p*	FK *T*	*p*	♀CV (*N*)	♂CV (*N*)	*t*-test *t*	*p*	FK *T*	*p*
FEM11	9.88 (18)	9.77 (20)	-3.953	**0.000**	16.827	0.7106	11.58 (12)	7.07 (15)	-0.711	0.484	15.72	**0.0291**
FEM12	7.39 (18)	7.66 (20)	-2.654	**0.012**	15.402	0.9668	10.83 (12)	8.38 (15)	-2.598	**0.016**	12.444	0.3283
FEM13	21.29 (18)	21.08 (20)	-1.838	0.074	15.525	0.9952	20.59 (12)	13.09 (15)	-0.863	0.396	14.737	0.0687
FEM14	5.40 (17)	5.13 (20)	-8.085	**0.000**	16.972	0.4842	7.23 (12)	7.69 (14)	-3.072	**0.005**	8.358	0.6004
FEM15	2.94 (18)	6.17 (20)	-7.209	**0.000**	8.3668	**0.0353**	7.59 (12)	5.35 (14)	-3.594	**0.001**	13.05	0.2147
FEM16	4.44 (17)	5.61 (20)	-7.788	**0.000**	12.245	0.4860	6.90 (12)	4.61 (14)	-4.144	**0.000**	13.796	0.1281
FEM17	5.51 (18)	7.39 (20)	-4.364	**0.000**	11.584	0.2505	6.49 (12)	6.17 (15)	-4.738	**0.000**	11.654	0.4919
FEM18	5.32 (18)	7.02 (20)	-3.769	**0.001**	12.189	0.3308	8.05 (12)	7.59 (15)	-3.602	**0.001**	11.277	0.5827

Table 5.18 Results of the *t*-test for equality of means and the Fligner-Killeen (FK) test for equality of relative variation in the tibia between the sexes among the Zulu and Kikuyu. Significant differences ($p < 0.05$) are in bold. Table continues on the next page.

Variable	Zulu						Kikuyu					
	♀CV (*N*)	♂CV (*N*)	*t*-test *t*	*p*	FK *T*	*p*	♀CV (*N*)	♂CV (*N*)	*t*-test *t*	*p*	FK *T*	*p*
TIB1	3.46 (18)	6.61 (21)	-5.334	**0.000**	7.618	**0.0233**	10.37 (12)	7.70 (15)	-2.208	**0.037**	11.392	0.5547
TIB2	3.41 (18)	6.44 (21)	-5.230	**0.000**	8.4485	**0.0421**	10.39 (12)	7.34 (15)	-2.265	**0.032**	12.5	0.3183
TIB3	8.98 (18)	6.88 (21)	-5.886	**0.000**	20.339	0.1741	5.57 (11)	7.05 (15)	-5.673	**0.000**	5.6498	0.2218
TIB4	9.16 (18)	9.06 (21)	-3.685	**0.001**	15.223	0.9203	8.68 (11)	9.32 (15)	-2.590	**0.016**	8.5959	0.9187
TIB5	4.78 (17)	6.56 (20)	-6.854	**0.000**	10.924	0.2771	7.23 (12)	5.67 (12)	-4.278	**0.000**	6.5593	0.2163
TIB6	4.15 (17)	4.52 (20)	-8.890	**0.000**	12.266	0.4898	8.69 (12)	4.13 (13)	-4.023	**0.001**	15.044	**0.0398**
TIB7	4.02 (16)	6.87 (20)	-7.138	**0.000**	8.6676	0.1316	9.39 (12)	7.47 (13)	-2.731	**0.012**	11.797	0.4216
TIB8	6.21 (17)	8.02 (20)	-4.378	**0.000**	11.147	0.3073	11.00 (12)	5.36 (13)	-4.080	**0.000**	14.28	0.0781
TIB9	5.62 (17)	7.81 (20)	-6.676	**0.000**	10.048	0.1784	9.50 (12)	5.22 (13)	-2.730	**0.012**	15.127	**0.0368**
TIB10	5.16 (17)	7.23 (20)	-6.364	**0.000**	10.007	0.1746	8.66 (12)	3.35 (13)	-2.964	**0.007**	14.99	**0.0418**

Table 5.18 Continued.

Variable	Zulu						Kikuyu					
	♀CV (*N*)	♂CV (*N*)	*t*-test *t*	*p*	FK *T*	*p*	♀CV (*N*)	♂CV (*N*)	*t*-test *t*	*p*	FK *T*	*p*
TIB11	8.28 (18)	7.57 (21)	-6.125	**0.000**	17.414	0.5996	7.59 (11)	7.24 (15)	-4.214	**0.000**	10.931	0.4322
TIB12	9.97 (18)	9.22 (21)	-4.165	**0.000**	14.774	0.8195	11.59 (11)	11.95 (15)	-2.620	**0.015**	8.9534	0.9730
TIB13	3.47 (18)	6.14 (21)	-6.807	**0.000**	7.1911	**0.0168**	8.14 (12)	4.73 (15)	-3.848	**0.001**	15.335	**0.0414**
TIB14	3.79 (18)	5.50 (21)	-7.459	**0.000**	11.036	0.1955	6.65 (12)	4.68 (15)	-4.827	**0.000**	11.946	0.4270
TIB15	3.81 (18)	5.95 (21)	-5.880	**0.000**	8.7135	0.0504	10.81 (12)	10.49 (15)	-1.332	0.195	11.185	0.6069
TIB16	4.04 (18)	6.26 (21)	-5.819	**0.000**	9.0024	0.0609	11.03 (12)	11.60 (15)	-1.299	0.206	9.7846	0.9998
TIB17	6.77 (18)	6.60 (21)	-4.986	**0.000**	16.788	0.7292	7.89 (11)	8.95 (15)	-3.139	**0.004**	8.8231	0.9875
TIB18	7.32 (18)	8.20 (21)	-4.878	**0.000**	14.008	0.6551	8.58 (11)	6.81 (15)	-3.452	**0.002**	12.663	0.1485

Table 5.19 Results of *t*-test of equality of means and Levene's (median) test of equal relative variation of PC1 scores between the sexes among the Zulu and Kikuyu. Significant differences ($p < 0.05$) are in bold.

			***t*-test**		**Levene's**
Sample	***N*** ♀	***N*** ♂	***t***	***p***	***p***
Humerus					
Zulu	19	22	-7.491	**0.0000**	**0.0412**
Kikuyu	12	13	-4.654	**0.0000**	0.5412
Ulna					
Zulu	19	22	-6.693	**0.0000**	**0.0423**
Kikuyu	11	13	-4.0126	**0.0006**	0.4269
Radius					
Zulu	17	16	-6.852	**0.0000**	**0.0147**
Kikuyu	11	12	-4.352	**0.0000**	0.1045
Femur					
Zulu	17	19	-6.5985	**0.0000**	0.1716
Kikuyu	12	13	-4.198	**0.0003**	0.1585
Tibia					
Zulu	16	20	-8.0637	**0.0000**	0.1451
Kikuyu	11	12	-4.0469	**0.0006**	0.4219

Table 5.20 Pearson's product-moment correlation between element size (as represented by the geometric mean of all variables for that element) and the PC1-PC3 scores among the Zulu. Significant correlations ($p < 0.05$) are in bold.

Element	*N*	% Variance	r^2	*p*
Humerus				
PC1	41	59.44	0.993	**0.000**
PC2	41	9.71	0.028	0.860
PC3	41	6.47	0.006	0.970
Ulna				
PC1	41	57.48	0.997	**0.000**
PC2	41	7.07	-0.026	0.872
PC3	41	6.34	0.033	0.837
Radius				
PC1	33	63.30	0.978	**0.000**
PC2	33	12.33	0.195	0.277
***PC3**	--	--	--	--
Femur				
PC1	36	67.03	0.991	**0.000**
PC2	36	7.82	0.040	0.815
PC3	36	5.98	-0.049	0.776
Tibia				
PC1	36	77.14	0.999	**0.000**
PC2	36	6.76	-0.030	0.861
***PC3**	--	--	--	--

***** Only two principal components extracted.

Table 5.21 Pearson's product-moment correlation between element size (as represented by the geometric mean of all variables for that element) and the PC1-PC3 scores among the Kikuyu. Significant correlations ($p < 0.05$) are in bold.

Element	*N*	% Variance	r^2	*p*
Humerus				
PC1	25	66.58	0.996	**0.000**
PC2	25	9.82	0.032	0.880
PC3	25	6.83	0.049	0.816
Ulna				
PC1	24	63.57	0.995	**0.000**
PC2	24	8.61	0.051	0.812
PC3	24	5.40	-0.021	0.921
Radius				
PC1	23	69.60	0.996	**0.000**
PC2	23	12.84	0.046	0.834
***PC3**	--	--	--	--
Femur				
PC1	25	67.87	0.996	**0.000**
PC2	25	8.89	0.011	0.958
PC3	25	6.07	0.052	0.805
Tibia				
PC1	23	76.24	0.997	**0.000**
PC2	23	7.66	0.052	0.812
***PC3**	--	--	--	--

***** Only two principal components extracted.

Table 5.22 Results of the Fligner-Killeen (FK) test for equal relative variation in the humerus between the Zulu and Kikuyu mixed-sex samples. Significant differences ($p < 0.05$) are in bold.

Variable	Zulu		Kikuyu		Zulu *vs* Kikuyu FK	
	N	**CV**	***N***	**CV**	***T***	***p***
HUM1	41	6.83	39	7.52	40.528	0.4277
HUM2	41	6.76	39	7.53	41.108	0.3690
HUM3	41	9.27	39	9.76	38.062	0.7301
HUM4	41	10.72	39	9.14	32.787	0.5396
HUM5	41	9.93	37	9.18	31.843	0.6601
HUM6	41	8.56	37	7.51	32.129	0.6987
HUM9	41	13.58	38	13.69	34.189	0.8541
HUM11	41	8.26	38	8.37	36.404	0.8245
HUM12	41	8.86	38	8.57	35.587	0.9426
HUM13	41	10.24	38	9.97	35.913	0.8952
HUM14	41	9.11	39	9.53	39.42	0.5540
HUM15	41	8.59	39	9.31	39.447	0.5507
HUM17	41	9.83	39	9.72	37.087	0.8667
HUM18	41	11.03	39	12.72	40.672	0.4127
HUM19	41	10.13	39	10.57	38.666	0.6493
HUM20	41	23.96	39	15.64	29.706	0.2408
HUM21	41	12.71	39	10.71	32.288	0.4815
HUM23	41	9.27	39	8.58	33.599	0.3207
HUM24	41	9.27	39	8.58	35.119	0.8496
HUM25	41	8.75	38	8.88	30.067	0.9632

Table 5.23 Results of the Fligner-Killeen (FK) test for equal relative variation in the ulna between the Zulu and Kikuyu mixed-sex samples. Significant differences ($p < 0.05$) are in bold.

Variable	Zulu		Kikuyu		Zulu *vs* Kikuyu FK	
	N	**CV**	***N***	**CV**	***T***	***p***
ULN1	41	6.97	37	8.79	41.912	0.1554
ULN2	41	6.88	37	8.52	40.875	0.2195
ULN3	41	12.01	37	10.09	27.949	0.2466
ULN4	41	10.46	37	11.12	36.647	0.6547
ULN5	41	9.24	38	7.96	33.457	0.7505
ULN6	41	9.81	38	11.05	37.2	0.7133
ULN7	41	9.57	38	9.41	34.979	0.9686
ULN8	41	8.4	37	8.1	34.219	0.9992
ULN9	41	7.68	38	8.76	38.909	0.4963
ULN10	41	9.39	38	9.05	37.662	0.6513
ULN11	41	8.68	38	9.28	39.884	0.3904
ULN12	41	8.01	38	10.36	44.778	0.0793
ULN13	41	8.38	38	9.96	38.084	0.5968
ULN14	41	9.38	38	7.78	29.22	0.2740
ULN15	41	8.12	38	13.00	49.534	**0.0086**
ULN17	41	14.4	38	16.53	37.976	0.6104
ULN18	41	11.31	38	10.63	34.015	0.8291
ULN19	41	9.95	38	10.15	36.785	0.7707
ULN20	41	11.82	36	11.28	35.278	0.7066
ULN21	41	9.451	38	10.14	38.553	0.5383

Table 5.24 Results of the Fligner-Killeen (FK) test for equal relative variation in the radius between the Zulu and Kikuyu mixed-sex samples. Significant differences ($p < 0.05$) are in bold.

Variable	Zulu		Kikuyu		Zulu *vs* Kikuyu FK	
	N	**CV**	***N***	**CV**	***T***	***p***
RAD1	39	7.33	39	9.08	43.409	0.1793
RAD2	39	7.30	38	9.08	41.883	0.2114
RAD3	39	11.66	39	11.43	35.812	0.9538
RAD5	34	9.09	35	9.33	30.299	0.8564
RAD6	34	9.26	35	8.69	31.076	0.9787
RAD7	33	9.26	35	8.70	33.08	0.5700
RAD8	39	12.86	39	11.66	30.121	0.2682
RAD9	39	9.88	39	11.83	29.315	0.2092
RAD10	39	10.57	39	12.33	41.598	0.3132
RAD13	39	8.10	38	10.21	44.491	0.0829
RAD14	39	8.43	38	7.71	33.026	0.6922
RAD15	39	9.01	39	12.33	43.753	0.1594
RAD16	39	9.60	39	10.56	30.729	0.3195

Table 5.25 Results of the Fligner-Killeen (FK) test for equal relative variation in the femur between the Zulu and Kikuyu mixed-sex samples. Significant differences ($p < 0.05$) are in bold.

Variable	Zulu		Kikuyu		Zulu *vs* Kikuyu FK	
	N	**CV**	***N***	**CV**	***T***	***p***
FEM1	38	5.94	39	7.47	28.602	0.2232
FEM2	38	6.02	38	7.75	43.983	0.0977
FEM3	38	11.46	39	9.93	41.05	0.2736
FEM4	38	8.75	39	8.62	34.275	0.8698
FEM5	38	8.09	38	8.21	34.068	0.8411
FEM6	38	8.28	39	8.49	34.908	0.9631
FEM7	38	9.41	39	11.12	29.298	0.2763
FEM8	38	10.92	39	10.52	36.471	0.8072
FEM9	38	7.96	39	9.33	28.969	0.2502
FEM10	38	9.97	39	10.69	31.261	0.4691
FEM11	38	11.61	39	8.83	41.95	0.2069
FEM12	38	8.16	39	11.19	24.102	**0.0399**
FEM13	38	22.03	39	15.09	46.834	**0.0298**
FEM14	37	8.74	36	8.51	31.771	0.7864
FEM15	37	7.80	37	7.35	32.565	0.7628
FEM16	37	8.47	36	7.55	29.844	0.5218
FEM17	38	8.10	38	8.29	37.657	0.6370
FEM18	38	7.38	38	8.60	40.084	0.3543

Table 5.26 Results of the Fligner-Killeen (FK) test for equal relative variation in the tibia between the Zulu and Kikuyu mixed-sex samples. Significant differences ($p < 0.05$) are in bold.

Variable	Zulu		Kikuyu		Zulu *vs* Kikuyu FK	
	N	**CV**	***N***	**CV**	***T***	***p***
TIB1	39	7.26	37	8.80	39.961	0.2796
TIB2	39	7.04	37	8.62	39.934	0.2818
TIB3	39	10.67	36	10.13	28.643	0.3872
TIB4	39	10.45	36	9.84	30.038	0.5476
TIB5	37	8.81	34	8.20	30.38	0.8652
TIB6	37	7.76	35	7.93	33.72	0.7710
TIB7	36	9.15	35	9.15	32.76	0.9124
TIB8	37	8.97	34	9.86	36.655	0.2912
TIB9	37	10.47	34	8.07	24.472	0.1857
TIB10	37	9.43	35	7.51	25.194	0.1742
TIB11	39	10.99	36	9.45	28.564	0.3787
TIB12	39	11.30	36	12.10	33.282	0.9908
TIB13	39	7.65	37	7.59	34.622	0.9353
TIB14	39	7.59	37	8.16	37.782	0.5009
TIB15	39	7.09	37	9.80	44.46	0.0543
TIB16	39	7.43	37	10.43	44.046	0.0648
TIB17	39	8.51	36	9.48	38.666	0.3035
TIB18	39	9.90	36	9.11	32.785	0.9344

Table 5.27 Results of Levene's (median) test for equality of relative variation of PC scores between the Zulu and Kikuyu mixed-sex samples. Significant differences ($p < 0.05$) are in bold. Each element is analyzed using a separate PCA; % Variance represents the percentage of the total variance explained by the first two principal components (additional components were extracted in most cases, but account for ≤ 9% of the total variance).

	Zulu *vs* Kikuyu			
Element	**Zulu** ***N***	**Kikuyu** ***N***	**% Variance**	**Levene's test** ***p***
PC1				
Humerus	41	25	60.96	0.8458
Ulna	41	24	58.51	0.4583
Radius	33	23	62.85	0.7334
Femur	36	25	66.15	0.8881
Tibia	36	23	75.59	0.8379
PC2				
Humerus	41	25	9.51	0.7713
Ulna	41	24	7.71	0.6719
Radius	33	23	11.28	0.7237
Femur	36	25	7.88	0.8035
Tibia	36	23	6.53	0.0711

Chapter 6

Morphometric Variation in the Appendicular Skeleton of Prehistoric Humans

Introduction

Goals

The study of skeletal morphometric variability can provide insights into past genetic diversity as well as the evolutionary forces and other influences that have shaped the human lineage. This chapter will assess the morphometric variability of the appendicular skeleton in prehistoric humans, including early *Homo sapiens*, to help elucidate the nature of the biological transition to modernity. As will be discussed below, craniometric studies of early *H. sapiens* fossils and living humans, together with studies of present-day genetic diversity, suggest that the diversity of living populations underestimates the magnitude of variation present among penecontemporaneous humans during the Late Pleistocene. The pattern of past variation could shed light on the processes of human evolution, and has important implications for paleoanthropological studies because many analytical methods rely on a framework of variation equality. This chapter has three main goals. First, to determine whether prehistoric humans from the terminal Pleistocene and early Holocene of Africa exhibit an equal magnitude of variation in the major long bones of appendicular skeleton relative to modern Africans. Since the archaeological samples span several thousand

years, time averaging may influence the level of variation in these samples. Thus, these comparisons permit an assessment of the influence of time on population variability, and indicate whether the level of diversity found in Africans today can be extended into the terminal Pleistocene and early Holocene. Second, this chapter will determine whether samples of early *H. sapiens* fossils from Africa, the Levant, and Europe exhibit an excess of morphometric variation relative to modern Africans, as workers have claimed. Diverse samples of recent and prehistoric Africans, simulating the geographic and temporal breadth of the fossil samples, are used to gain a more reliable assessment of past variability. Third, the magnitude of variability will be compared between an older, Middle Stone Age sample, and a younger, Early Upper Paleolithic sample, providing another view of changes in early *H. sapiens* morphometric diversity in the Late Pleistocene.

Variation in Early *H. sapiens*

In a series of analyses comparing the size and shape of the cranium between humans from across the globe, Howells (1973; 1989; 1995) concluded that living populations are remarkably similar in cranial morphology. As discussed in Chapter 5, this conclusion accords with genetic studies showing that most of human diversity is found within populations and not between populations (e.g., Lewontin, 1972; Relethford, 1994, 1998), and that African populations harbor a greater level of diversity than non-Africans (e.g., Excoffier, 2002). Although the interpretation of modern cranial diversity was the main focus of Howells' work, he extended his modern sample to include some early *H. sapiens*, Neandertals and other archaic Middle Pleistocene hominins. The results indicated that all Neandertal and archaic *Homo* specimens are very distant from any living humans, whether individuals or populations are used. Interestingly, Howells found mixed results among specimens generally accepted as anatomically modern

humans, including those from the European early Upper Paleolithic sites of Mladeč and Predmostí, and the Levantine sites of Skhūl and Qafzeh. Some fossil *H. sapiens*, like Mladeč 1, Predmostí 4, and Qafzeh 6, were reasonably close to at least some living populations, while others such as Predmostí 3 and Skhūl 5 were probabilistically far removed from any modern groups. Based on this, Howells concluded that the cranial homogeneity observed between living populations is a relatively recent phenomenon.

Indirectly, Howells' analyses also hint at the potential for elevated diversity among early *H. sapiens*, since penecontemporaneous specimens from the same or nearby sites often exhibit a different pattern of morphological proximity to living populations. Indeed, paleoanthropologists have long noted the striking level of variation encompassed within the early modern human assemblage, which suggests that the level of morphological variation observed in the crania of living humans likely underestimates the variation present among penecontemporaneous humans during the Pleistocene. For example, McCown and Keith (1939: 13) commented on variation "greater in degree and kind than is to be observed in any local community of modern times" for the Skhūl fossils. They interpreted the cause of this high level of variation as an evolutionary transition or possibly hybridization. Multivariate comparisons of the Skhūl 4 and 9 crania support the initial impression of high variability within this assemblage (Corruccini, 1992).

Fossils from the nearby cave site of Qafzeh, commonly attributed to *H. sapiens*, are also described as exhibiting a substantial amount of individual variation (Vandermeersch, 1981). Vandermeersch's observation received support from a study by van Vark and Schaafsma (1992), who calculated significant differences in inter-individual Mahalanobis squared distances (D^2) between the Qafzeh 6 and 9 fossils based on facial and neurocranial measurements. Furthermore, they found that the average distance between Qafzeh 9 and a recent,

global human sample to be smaller than the average inter-individual distance between modern individuals, which suggests that this fossil represents a modern human. In contrast, the Qafzeh 6 specimen is distantly removed from the modern sample, exhibiting a much greater average distance to modern individuals than the average modern inter-individual distance. At least at Qafzeh, within-sample morphological diversity seems to have been substantial.

The same pattern of relationships for these two fossils was also reported by Kidder and colleagues (Kidder et al., 1992) who applied a similar multivariate approach using a smaller number of cranial measurements and a different global human sample. Again, Qafzeh 9 but not Qafzeh 6 can be accommodated within the modern range of cranial size and shape. Their study also demonstrated that the Skhūl 4 and 5 fossils consistently fall significantly outside the range of modern variation, while the European Upper Paleolithic crania from Mladeč and Cro-Magnon have variable relationships with the modern sample depending on which aspects of cranial size and shape are considered. While these studies did not directly compare levels of variation between prehistoric and living human populations, the results do provide indirect evidence for a high magnitude of variation within the Levatine and European early *H. sapiens* samples.

Similarly, other studies have recognized the heterogeneity of cranial size and shape expressed in the early *H. sapiens*, especially in the larger assemblages recovered from Levantine and European sites, which hints at the potential for increased morphological variability in the cranium of early *H. sapiens* relative to living humans (e.g., Lahr, 1996; Stringer, 1996; Lahr and Foley, 1998; Trinkaus, 2005). Even in Africa, where poor preservation and a low density of sites hampers efforts to study human diversity in the Late Pleistocene, there is some evidence of variability that cannot be explained simply as a function of variation through time or across geographic distances. For example, Member I of the Kibish Formation in southwestern Ethiopia, recently securely dated to ca. 195 ka

BP (McDougall et al., 2005), has yield a pair of fragmentary skulls, Omo 1 and Omo 2, which are dramatically different in their morphology. In fact, the skulls are so divergent morphologically that Omo 1 has been interpreted as a modern *H. sapiens*, while Omo 2 has consistently been interpreted as a more archaic form (e.g., Day, 1969; Smith, 1994; Trinkaus, 2005). However, it is possible that these specimens, which now appear to be approximately contemporaneous, may sample the diversity present in African populations at this time (e.g., Lahr and Foley, 1998). Another Ethiopian fossil, Herto, also appears to add to the diversity of cranial form in Africa during the Late Pleistocene, as it presents yet another unique combination of seemingly modern and archaic features (White et al., 2003).

Crevecoeur and colleagues (2009) recently sought to address the issue of Late Pleistocene variability free of the potential influence that increased temporal depth may impose by studying three approximately contemporaneous early *H. sapiens* fossils: Hofmeyr from South Africa, Nazlet Khater 2 from Egypt, and Peştera cu Oase from Romania. These fossils were compared to a large global sample of modern humans through the multivariate analysis of eight craniofacial dimensions. The D^2 of each fossil to the centroid of the modern sample was computed, and the D^2s of the three fossils were summed. Through bootstrap resampling procedures, they found a low probability ($p = 0.0952$) of sampling a similar sum of distances for any three randomly selected modern humans. Moreover, they obtained a high probability of obtaining an equally high sum of distances when any three specimens were randomly selected from an Upper Paleolithic sample (these distances are also measured from individual UP specimens to the centroid of the modern sample). Based on these results, Crevecoeur et al. concluded that early *H. sapiens* fossils exhibit a greater range of diversity compared to living people, but appear to have equal variability to the Upper Paleolithic humans.

However, their results and the conclusions based on them are problematic. Indeed, the aforementioned study simply demonstrates that one or all of the three early *H. sapiens* specimen(s) is(are) not characterized by the full suite of modern craniofacial morphology present in living people, as has been previously suggested by numerous other studies (e.g., Kidder et al., 1992; van Vark and Schaafsma, 1992; Trinkaus, 2005). In the words of one researcher, these fossils "are 'modern' without being fully modern" (Trinkaus, 2005: 218). In this and other studies that employ the distance from individual fossils to the centroid of the modern sample, the measure of variation is greatly influenced by the morphological similarity between the fossils and modern specimens. A fossil will have a large D^2 to the modern centroid simply by virtue of being outside the modern range of craniofacial variation. If we extend this to three fossils that are known from univariate analyses and observations of non-metric traits to present a mosaic of modern and archaic features (as is the case with the Hofmeyr, Nazlet Khater and Peştera cu Oase fossils, and the majority of fossils that predate the Last Glacial Maximum; see Trinkaus, 2005), each will have a large distance to the modern centroid, and the sum of distances will therefore be quite large. On the other hand, the modern specimens are, by definition, within the modern range of variation, and any three modern individuals will tend to have a low sum of distances to the centroid. This explains why the mean sum of distances (17.67 ± 6.60 s.d) in the resampled modern distribution is much smaller than the mean sum of distances (31.70 ± 11.45 s.d) obtained in the resampled distribution of Upper Paleolithic fossils.

Simply put, the analysis by Crevecoeur et al. (2009) demonstrated that UP fossils, including those from Hofmeyr, Nazlet Khater, and Peştera cu Oase, are more distantly removed from the modern population centroid than any modern human. The distances reported in this study are not the same as inter-individual distances (see van Vark and Schaafsma, 1992), and contrary to their stated aims,

the results presented by Crevecoeur and colleagues do not address differences in the magnitude of variation between the groups. To address this issue, it would be necessary to measure the distance of the early *H. sapiens* fossils to the Upper Paleolithic group centroid, then compare the resultant sum of D^2 to the resampled modern distribution of sums of distances obtained by random sampling of an equal number of modern specimens. However, because many fewer Upper Paleolithic specimens are available than modern humans, the population covariance matrix may not be adequately known (van Vark, 1984; van Vark et al., 1992). Recalling that multivariate studies such as discriminant analysis require that the number of individuals in a sample exceed the number of variables (Quinn and Keough, 2002), this effectively limits the number of measurements that can be analyzed together.

The studies reviewed above provide only indirect evidence for higher variation in Late Pleistocene humans relative to today. Few workers have directly measured the extent of past variation and formally compared it to the magnitude of variation present today. One early exception is the study by van Vark and Schaafsma (1992), which directly tested whether samples from the early and late European Upper Paleolithic were more variable than a global sample of modern humans in facial and neurocranial form. These workers found comparable levels of variation in the neurocranium between the prehistoric and modern humans, but demonstrated that both early and late Upper Paleolithic samples exhibited greater facial variation than modern humans. They argued that the increased temporal depth of the fossil samples alone could not explain the elevated variability in these groups compared to living people on the grounds that this should act to increase variation in all cranial regions uniformily, and not just the face. However, the impact of time on sample variation is complex, with numerous factors potentially influencing the apparent magnitude and pattern of variability, and the *a priori* expectation of a uniform positive linear relationship between

variation and time may not be justified (Plavcan and Cope, 2001). Yet it is clear that the temporal depth, as well as the geographic breadth, of samples must be considered in any study of variability.

A recent study of neurocranial shape variability by Gunz et al. (2009) found that a sample of early *H. sapiens* from Africa and Israel were significantly more variable than a global sample of living humans. Their early *H. sapiens* sample is both geographically and temporally broad, including fossils from East Africa (Omo 2 from Ethiopia and Ngaloba from Laetoli in Tanzania), North Africa (Jebel Irhoud 1 and 2 from Morocco), and from the Near East (Qafzeh 6 and 9, and Skhūl 5). As such, it ranges between approximately 195 to 60 ka BP. The modern reference sample is also geographically broad as it samples individuals from a global distribution of Holocene populations. Gunz and colleagues found elevated variability in the early *H. sapiens* sample compared to modern humans, however, the influence of time on variation in the fossil sample cannot be ruled out because the modern reference lacks any temporal depth. To address the issue that variability increased as a function of the greater temporal depth of the fossil sample, Gunz et al. also compared the variability of the early *H. sapiens* group to that exhibited by other fossil samples that comprise approximately comparable or even greater time spans such as *H. sapiens* from the Upper Paleolithic, Neandertals, and archaic *Homo*. In all cases, the early *H. sapiens* sample was significantly more variable, which suggests that time alone may be insufficient to account for the surplus of variation in the fossil sample. Thus, the study by Gunz and colleagues appears to have documented a true signal for increased morphometric variability in early *H. sapiens* compared to modern humans.

Unfortunately, Gunz et al. (2009) did not compare the variability between the Upper Paleolithic and modern human samples, thus these results are not directly comparable to those reported by van Vark and Schaafsma (1992), who

documented no surplus of variability in the cranial vault between Upper Paleolithic and modern humans. Nonetheless, both studies provide support for increased variation in Late Pleistocene compared to modern *H. sapiens*, albeit in different aspects of cranial anatomy. However, no study has yet addressed the issue of changes in the magnitude of variation in the major long bones of the appendicular skeleton across the transition to modernity. The postcranial skeleton provides the opportunity to study additional lines of evidence that can be used to test the claim for increased relative variation in the Late Pleistocene suggested by cranial studies. Specificially, comparisons of postcranial variation can be used to test the conclusion for higher variability among early *H. sapiens* from Africa and the Levant compared to European Upper Paleolithic put forth by Gunz et al. (2009), and offers potential insights into the evolutionary and historical processes that have shaped the patterning of diversity within our species.

Measurements

This chapter compares the variability of linear measurements recorded from the five major long bones (humerus, ulna, radius, femur, and tibia) between recent and prehistoric humans. For each element, measurements are selected to capture the form of the shaft, articular surfaces, and areas of muscle attachments. All measurements are defined in Appendix 1. Based on the results of the measurement error study conducted in Chapter 2, nine measurements recorded on the long bones are deemed unreliable and are excluded from the analysis.

Skeletal Samples

The results of Chapter 5 demonstrated that the Zulu and Kikuyu, the two known-sex samples available for this study, exhibit equal magnitude of

postcranial variation when the sexes are combined, although some significant differences in variation were found when the sexes where analyzed separately. Therefore, the Zulu sample, which is larger and has a more balanced sex ratio than the Kikuyu sample (Table 6.1), is employed to represent the baseline level of morphometric variation present in the appendicular skeleton of a mixed-sex sample of recent humans from Africa, the geographic source for *H. sapiens* according to genetic and paleontological research (see reviews in Pearson, 2004; Weaver and Roseman, 2008).

The appendicular measurements listed in Appendix 1 were also recorded for three archaeological samples: Khoe-San, Sudanese, and Taforalt (Table 6.1). As described in Chapter 2, the archaeological specimens are sampled from African localities that date from the terminal Pleistocene to historic times, and represent up to roughly 10,000 years of temporal depth. These samples simulate the temporal depth typically encompassed in fossil samples, and help to assess whether variation within a sample increases as a function of time. Although each archaeological sample comprises individuals of both sexes, the exact distribution of sex in these samples is unknown because only a fraction of the individuals could be reliably sexed using the os coxae (see Chapter 4). In addition, a pan-African sample is employed to estimate human morphometric variability on a continent-wide scale since the terminal Pleistocene. The pan-African sample includes all available Zulu, Kikuyu, Khoe-San, Sudanese and Taforalt skeletons (n = 305, Table 6.1).

Morphometrics of the five long bones were also recorded for fossil specimens representing early *H. sapiens* from Africa, the Levant and Europe. The fossils are partitioned *a priori* into two samples (Table 6.1): an earlier Middle Stone Age (MSA) sample comprised of African and Levantine specimens, the majority of which date between approximately 195 to 80 ka BP, and a later sample from the Early Upper Paleolithic (EUP) comprised primarily of European

specimens dated between 38 to 25 ka BP. Details pertaining to the fossil localities and dating are provided in Chapter 2, and sex diagnoses follow the results of Chapter 4. The fossils exhibit differential preservation, such that sample size is not constant for each measurement.

Methods: Testing for Differences in Relative Variation

The methods employed to test for differences in relative morphometric variation are provided below as they pertain to each hypothesis. Multivariate analyses require complete datasets, a requirement which is not satisfied for any element within the MSA and EUP fossil samples due to the differential preservation of specimens. Furthermore, the fossil samples are characterized by small sample sizes, often containing fewer individuals than the total number of measurements available per element. This situation is problematic for multivariate methods such as the PCA employed in Chapter 5 to assess the equality of multivariate variation. While regression techniques can be used to estimate missing data (e.g., Quinn and Keough, 2002), this procedure was not employed here since it may adversely influence the results by underestimating the diversity within samples, if variation was indeed greater in the past. Therefore, differences in relative variation are only assessed using univariate analyses.

Hypothesis 1 (H_1): Recent humans exhibit equal relative variation compared to samples of archaeological origin.

Tests of this hypothesis provide a better understanding of the influence of temporal depth on morphometric variation within a sample, to assess whether samples of archaeological origin may be better suited as reference samples for studies of human fossils which themselves tend to be diachronic. The results will

also indicate whether present-day levels of variation among Africans can be extended into the terminal Pleistocene and early Holocene. To test H_1, the magnitude of morphometric variation in the major long bones from the Zulu, a recent human sample from Africa, is compared to that in three archaeological human samples from Africa: Khoe-San, Sudanese, and Taforalt. These archaeological samples represent up to 10,000 years of temporal depth, and sample human variation across the terminal Pleistocene and Holocene of Africa. The two-tailed Fligner-Killeen (FK) test is employed to test for equality of variation between the Zulu and each archaeological sample in all measurements recorded per element. The FK test is described in detail in Chapter 5 (see also Donnelly and Kramer, 1999). For illustrative purposes, the Kikuyu sample is included in plots of the CV to confirm that it exhibits similar levels of variation to the Zulu sample, but it is not compared to the archaeological samples using the FK test.

The Bonferonni Approximation is used to adjust the probability level when multiple comparisons are made using the same data in order to maintain a familywise probability at 0.05, thus preventing an inflated Type I error rate (Abdi, 2007). The following equation is used to determine the adjusted testwise probability level:

$$\alpha_T = \frac{\alpha_F}{C}$$

where α_T is the probability level per test, α_F is the desired familywise probability level to be maintained across all tests, and C is the number of planned comparisons that are needed to test the hypothesis (Abdi, 2007). For the three planned comparisons needed to test H_1 (i.e., Zulu *vs* Khoe-San, Zulu *vs* Sudanese, and Zulu *vs* Taforalt), 0.5/3 = 0.0167; thus $p < 0.0167$ is the adjusted testwise probability level that preserves a familywise probability of 0.05.

Hypothesis 2 (H_2): The early *H. sapiens* fossil samples (MSA and EUP) each comprise an excess of relative variation compared to a sample of recent humans.

The results of these tests will demonstrate whether human morphometric variation in the appendicular skeleton was greater in the Late Pleistocene compared to modern times, as has been suggested by genetic studies of living populations as well as studies of cranial diversity in the Late Pleistocene. To test H_2, the magnitude of variation in the MSA and EUP fossil samples is compared to that in the Zulu recent human sample. A one-tailed directional FK test is employed because elevated variation in these fossil samples compared to living humans has been postulated. Using Monte Carlo simulation tests under a range of distributions, Donnelly and Kramer (1999) found that the FK test maintains acceptable Type I error rates if sample size is ≥ 7. This restricts the number of univariate comparisons that can be made using the FK test, most notably amongst the MSA fossils which tend to be more poorly preserved than the EUP specimens. However, comparisons of the CV can still be used to suggest trends in the magnitude of variation between the fossils and modern humans. In order to maintain a familywise probability of 0.05, the Bonferonni Approximation (Abdi, 2007) is used to set the level for the testwise probability at 0.025 when two planned comparisons are made (i.e., 0.5/2 = 0.025).

Hypothesis 3 (H_3): The early *H. sapiens* fossil samples (MSA and EUP) each comprise an excess of relative variation compared to a human sample of archaeological origin.

The results of these tests will demonstrate whether human morphometric variation in the appendicular skeleton was greater in the Late Pleistocene

compared to the Holocene and terminal Pleistocene. To test H_3, the magnitude of variation in the MSA and EUP fossil samples is compared to that present in an archaeological human sample spanning the terminal Pleistocene and Holocene of Africa, which helps to address the influence of time on sample variation. If the results of H_1 show equal relative variation between the three archaeological samples compared to the Zulu then only the largest sample (Khoe-San) will be employed to test H_3. Alternatively, if one archaeological sample is found to have excess relative variation compared to the Zulu, then that sample will be employed to test H_3. As with H_2, a one-tailed directional FK test is employed because elevated variation in the fossil samples has been argued, and an adjust testwise probability level of 0.025 is employed in order to maintain a familywise probability of 0.05 over two planned comparisons. Following the recommendations of Donnelly and Kramer (1999), the FK test is employed only when sample size is ≥ 7.

Hypothesis 4 (H_4): The early *H. sapiens* fossil samples (MSA and EUP) each comprise an excess of relative variation compared to a pan-African human sample.

These tests will demonstrate whether morphometric variation in the human appendicular skeleton was greater in the Late Pleistocene compared to the variability documented across Africa from the terminal Pleistocene to the present. To test H_4, the magnitude of variation in the MSA and EUP fossil samples is compared to that present in a human sample spanning most of the African continent (North Africa, East Africa, and South Africa) from the terminal Pleistocene to present day. As with the previous hypothesis, a one-tailed directional FK test is employed to test for elevated variability in the fossil samples. The testwise probability level is adjusted to 0.025 to ensure a

familywise probability of 0.05 across two planned comparisons: MSA *versus* pan-African and EUP *versus* pan-African. As noted above, the FK test is limited to cases in which sample size is ≥ 7 (Donnelly and Kramer, 1999).

Hypothesis 5 (H_5): MSA early *H. sapiens* exhibit an excess of relative variation compared to EUP early *H. sapiens*.

The results of these tests will demonstrate whether early *H. sapiens* from the MSA of Africa and the Levant exhibit elevated morphometric variability relative to early *H. sapiens* from the EUP, as suggested by Gunz et al. (2009) based on studies of cranial vault shape. In addition, because the MSA specimens are sampled over a much large time span than the EUP fossils (see Chapter 2 for details), time averaging in the MSA sample could be expected to inflate variability in this sample. Thus, these tests provide another means of assessing the role of time averaging on sample variation. Unfortunately, the small number of MSA individuals limits the measurements that could be evaluated using the FK test, which requires a minimum of 7 individuals (Donnelly and Kramer, 1999).

Results

Summary statistics for the reference and fossil samples are provided in Appendix 2 in separate tables for each element. The results of tests to assess the equality of relative variation between modern Zulu and archaeological human samples are presented first. Although equality of variation is tested only for the archaeological samples relative to the Zulu, the Kikuyu sample is included in the CV plots as an additional example of variability in a living human population. Following the presentation of H_1 results, comparisons of variability among the early *H. sapiens* fossil samples relative to the Zulu (H_2), archaeological (H_3), and

pan-African (H_4) samples are reported. For each hypothesis, the results are presented separately for each element starting with the upper limb (humerus, ulna and radius), then the lower limb (femur and tibia). Finally, the results of H_5 (MSA versus EUP) are presented.

Equality of Variation Between the Zulu and Archaeological Samples

Figure 6.1 illustrates the level of relative variation in the humerus exhibited by recent and archaeological African samples. Overall, the plot shows a close correspondence between the CVs of the recent samples (Zulu and Kikuyu) and the Khoe-San and Sudanese samples of archaeological origin, although the Zulu and Kikuyu appear to show divergent magnitude of variation in the breadth of the medial dorsal pillar (HUM20). As expected, all samples show a peak in variation for deltoid tuberosity length (HUM9), although variation appears somewhat more elevated among the Khoe-San and Sudanese than the other samples. The null hypothesis of equal relative variation cannot be rejected when either the Khoe-San or Sudanese prehistoric samples are compared to the Zulu using the FK test (Table 6.2). In contrast, Figure 6.1 demonstrates that the Taforalt sample shows a trend of low variation in several measurements of both proximal (HUM5 and 6) and distal articular surfaces (HUM11 to 15) of the humerus, as well as in the length of this element (HUM1-2 and 23-24). As reported in Table 6.2, only maximum and total humeral lengths (HUM1-2) exhibit significantly different levels of variation between the Taforalt and Zulu samples. In both cases, Taforalt exhibits less variation than the Zulu.

As listed in Table 6.3, the results of the FK test cannot reject the null hypothesis of equal relative variation in ulnar measurements between the Zulu and each of the three prehistoric samples. A comparison of the CVs shows a non-significant trend for low variation in most of the ulna dimensions in the Taforalt

sample, the Khoe-San exhibit higher variation in medio-lateral (ML) coronoid width (ULN6), olecranon length (ULN9), and ML diameter of the proximal ulnar shaft, and both modern samples (Zulu and Kikuyu) have increased variation in the position of the brachialis insertion compared to the prehistoric samples.

The results of the FK test for equal relative variation in diverse measurements of the radius are listed in Table 6.4. For all the radial measurements, no significant differences are found between the Zulu and each archaeological African sample. However, a qualitative comparison of CVs shows a (non-significant) trend for a low magnitude of variation in the Taforalt sample compared to the others (Figure 6.3).

CVs for the femoral measurements are illustrated in Figure 6.4. As this figure shows, the Taforalt sample tends to exhibit lower levels of variation than the other samples, although overall the magnitude of variation tracks closely between the modern and prehistoric samples. All samples exhibit elevated variation in gluteal tuberosity breadth (FEM13), as expected for a muscle insertion site. Despite the trend for lower variation in the Taforalt sample, the FK test found no significant differences in variation between any of the archaeological samples and the Zulu recent sample (Table 6.5).

As shown in Figure 6.5, the CVs display a close correspondence across most samples for the majority of tibial measurements, although the Taforalt sample tends to exhibit low levels of variation across the measurements except for TIB15-16 (length of the tibia from the nutrient foramen to the medial malleolus and distal articular surface), where this sample exhibits a substantial peak in variability. Results of the FK test are reported in Table 6.6. They indicate that the Taforalt sample is characterized by significantly lower variation than the Zulu sample in a single dimensions (TIB9: AP diameter of the lateral tibial condyle) despite the trend described above. Equality of variation in the tibia cannot be

rejected for the Zulu *versus* Khoe-San comparison or the Zulu *versus* Sudanese comparison.

Excess Variation in MSA and EUP Fossils Compared to Modern Humans

Based on the results of H_1 described above, which found no support for surplus variation in any of the three archaeological samples compared to the modern Zulu, the Khoe-San sample alone is employed to represent the baseline intra-population variability in prehistoric modern Africans. In addition, variability in the fossil samples is compared to that exhibited by a pan-African sample that captures variation across African populations from the terminal Pleistocene to the present. The pan-African sample combines variation from diverse sources, and helps to simulate the geographic and temporal breadth encompassed in the fossil samples. In sum, the MSA and EUP early *H. sapiens* fossils are compared only to the Khoe-San sample to test H_3, while each is compared to the pan-African to test H_4. To facilitate the visual comparison of CVs between all samples, the CVs for the MSA, EUP, Zulu and Khoe-San samples are plotted together for each element. Similarly, because of the equal variability expressed by the Zulu and Khoe-San, the results for H_2 (fossils *versus* Zulu) and H_3 (fossils *versus* Khoe-San) are presented together for each element, followed by the results for H_4 (fossils *versus* pan-African). As noted above, the MSA sample tends to comprise a small number of poorly preserved specimens; for many measurements, this sample does not reach the minimum number of individuals ($n = 7$) required for a reliable FK test. However, the CVs for the MSA may nonethless suggest trends in variability for measurments that do not meet this requirement.

CVs of the humerus measurements recorded for the MSA and EUP fossil samples and the modern references, depicted in Figure 6.6, demonstrate that both

fossil samples tend to exhibit a higher level of variation than the Zulu and Khoe-San modern humans. The pattern of elevated variability in the Late Pleistocene is less clear when the fossil CVs are compared to those exhibited by the pan-African sample, as shown in Figure 6.7. Using the FK test and an adjusted testwise probability of 0.025, a significant excess of variation is found in a single measurement (HUM15: AP diameter of the capitulum) for the EUP sample compared to the Zulu (Table 6.7). The same result is obtained when variability in the EUP sample is compared to that in the Khoe-San (Table 6.8) and pan-African (Table 6.9) samples. In contrast to the elevated variability demonstrated by the EUP fossils for capitulum AP thickness, the other measurements of the distal humeral articulation (HUM11-13) tend to comprise much lower variation (Figures 6.6 and 6.7). The MSA sample comprised sufficient specimens to permit the FK test for excess relative variation in only four out of twenty humeral measurements. Although none of these exhibits a surplus of variation relative to the Zulu and pan-African samples (Tables 6.7 and 6.9 respectively), the MSA fossils show a significant surplus of variability in the minimum midshaft diameter relative to the Khoe-San (Table 6.8).

Numerous aspects of the distal humerus could be measured on only six MSA fossils, just shy of the minimum required for the FK test. However, as Figures 6.6 and 6.7 illustrate, the MSA sample shows a clear trend towards higher variability in several measurements of the distal humerus (e.g., HUM13: capitulum width, HUM19: olecranon fossa width, HUM21: lateral dorsal pillar width) relative to the Zulu, Khoe-San, and pan-African samples. The strikingly low variation in head DV diameter (HUM6) may be an artifact of the small sample size (n = 3) in the MSA sample. Both the MSA and EUP samples track the modern samples closely in showing low variability of humeral length (HUM1-2), and, as expected, high variability in deltoid tuberosity length (HUM9). Interestingly, all samples exhibit strikingly high variation (CV ranges from 18%

to 24%) in the breadth of the medial dorsal pillar. Recalling the results of Chapter 5, this measurement was found to be highly dimorphic among the Zulu population, with males bearing medial dorsal pillar breadths more than 26% larger than females. In fact, this feature is the most dimorphic variable of the humerus among the Zulu. This sexually dimorphic pattern may account for the high variation documented in this measurement in the other samples as well.

Examining the CVs of the ulnar measurement plotted in Figures 6.8 and 6.9, it is apparent that the MSA sample exhibits a clear trend for higher variability compared to the Zulu, Khoe-San, and pan-African samples, while the EUP appears to track the lower variability in the modern samples more closely, and tends to exhibit less variability than the pan-African group. Of the thirteen measurements (out of twenty possible ulnar variables) with a sufficient number of MSA individuals to allow the FK test, three measurements of the olecranon and trochlear notch (ULN6: maximum ML diameter of the coronoid, ULN9: olecranon length, and ULN11: transverse diameter of the trochlear notch) were found to have excess variation in the MSA sample (Table 6.10). A similar high level of variation in these measurements is found when the MSA sample is compared to the Khoe-San (Table 6.11). This comparison also identifies a significant excess of variation in the MSA sample for two additional measurements: coronoid height (ULN5) and the position of the brachialis insertion (ULN17). The MSA sample also appears to be characterized by higher variation in ulnar midshaft diameters (ULN3-4) relative to the Zulu and Khoe-San (Figure 6.8), although this is a non-significant trend. Compared to the pan-African sample (Table 6.12), the MSA individuals demonstrate a significant surplus of variation in a single dimension (ULN9, olecranon length), while additional measurements (ULN8: olecranon ML breadth, ULN11: transverse diameter of the trochlear notch, ULN12: mid-trochlear notch thickness, and ULN17: position of the brachialis insertion) approach significance, suggesting a

trend for greater variability relative to the pan-African sample (Figure 6.9). For the EUP sample, a surplus of variation relative to the Zulu is identified in three ulnar measurements (Table 6.10): AP thickness of the trochlear notch (ULN13), length of the radial notch (ULN15), and ML diameter of the proximal shaft (ULN19). In contrast, the EUP sample does not comprise excess variation relative to the Khoe-San (Table 6.11) or the pan-African (Table 6.12) samples in any ulnar measurements.

As shown in Figures 6.10 and 6.11, morphometric variability in the radius is frequently greater in the early *H. sapiens* samples than any of the modern reference samples. The MSA sample meets the minimum number of individuals in only three out of the 13 measurements, which limits the statistical assessment of radial variability in these fossils. The FK test supports the presence of significant excess of variation in a single measurement, RAD10 (AP diameter of the neck), for the MSA sample relative to both Zulu and Khoe-San (Tables 6.13 and 6.14 respectively), but this is not supported in the pan-African comparison (Table 6.15). Although increased variability in the other dimensions cannot be directly tested due to the small number of MSA specimens, a clear trend towards elevated variation (i.e., high CV) relative to all modern groups is observed in Figures 6.10 and 6.11 for the following dimensions: RAD6-7: maximum head diameters, and RAD13-14: DV and ML diameters of the distal epiphysis. The very limited variation (CV < 5) observed for the MSA fossils in radial length (RAD1-2) may be an artifact of small sample size, since only three complete radii are available. In the EUP sample, most measurements of the radius can be recorded on a sufficient number of individuals.

The results of the FK test document a significant surplus of variation in the EUP fossils relative to the Zulu (Table 6.13), Khoe-San (Table 6.14), and pan-African (Table 6.15) samples for RAD8 (radial tuberosity length) and RAD13 (DV width of the distal epiphysis), and also find excess variation relative to the

Khoe-San and pan-African humans for RAD5 (max AP head diameter). Elevated variation among the EUP relative to the modern Zulu is suggested for RAD5 (head AP diameter, see also Figure 6.10), and for RAD16 (shaft circumference at the radial tuberosity, see also Figure 6.11) relative to the pan-African sample, although these differences do not quite reach statistical significance.

CVs of the femoral measurements for the MSA, EUP, and modern single-population samples are plotted in Figure 6.12, while Figure 6.13 illustrates the femoral CVs for the fossil and pan-African samples. Overall, variability in both fossil samples seems to correspond to the level of variation exhibited by the modern Zulu, prehistoric Khoe-San, and the mixed population pan-African sample. Due to poor preservation, the MSA sample can be formally compared to the reference samples in only five out of eighteen femoral measurements. Among these, one measurement (FEM12: subtrochanteric shaft ML diameter) exhibits significantly greater variation than the Zulu (Table 6.16), Khoe-San (Table 6.17), and the pan-African (Table 6.18) samples. The MSA fossils appear to comprise a very low level of variation (CV < 5%) in femoral length (FEM1-2), but given the small sample size, diversity in these measurements may not be adequately represented.

In contrast, the EUP sample shows elevated variation in femoral lengths (FEM1-2) compared to the Zulu and Khoe-San (Figure 6.12), but not the pan-African sample (Figure 6.13); these observations are supported by the results of the FK tests (Tables 6.16 to 6.18). In addition to the excess variability documented for femoral lengths relative to both the Zulu and Khoe-San samples, the EUP fossils also exhibit a surplus of variation in biomechanical neck length (FEM9), while excess variability compared to the pan-African humans is documented in subtrochanteric AP diameter (FEM11) only, although variability in midshaft AP diameter (FEM3) approaches significances (Table 6.18). A peak in variability is observed for the EUP sample in gluteal tuberosity breadth (FEM13),

this difference is statistically significant only in comparison to the Khoe-San (Table 6.17).

Variability in the tibial measurements, as captured by the CV, is illustrated in Figures 6.14 and 6.15. Few tibiae are well preserved in the MSA sample; CVs could not be computed for measurements of the tibial plateau (TIB5-10) in this group, and the FK test for excess variability could only be performed for three out of eighteen tibial measurements. The null hypothesis could not be rejected in any of the comparisons of MSA variability to the variability documented in the Zulu (Table 6.19), Khoe-San (Table 6.20), and pan-African (Table 6.21) human samples. Nonetheless, the MSA sample seems to exhibit elevated variability in various measures of tibial length (TIB1-2, TIB15-16) compared to all modern samples (see Figures 6.14 and 6.15), although this apparent surplus of variation may be an artifact of the small number of individuals available.

As shown in the CV plots, the EUP sample appears to show a trend for elevated variability in several tibial dimensions compared to the reference samples. The FK test, performed for fourteen out of eighteen measurements of the tibia available in the EUP sample, rejects the null hypothesis that the EUP fossils have equal or lesser variation than the Zulu for three measurements (Table 6.19): midshaft ML diameter (TIB4), and shaft AP and ML diameters at the nutrient foramen (TIB11-12). In addition, excess variability relative to the Khoe-San for these three measurements, as well as in TIB7 (AP length of the medial condyle) is documented (Table 6.20). The EUP fossils comprise an excess of variation for same three measurements relative to the geographically and temporally diverse pan-African sample (Table 6.21).

Excess Variation in MSA Compared to EUP early *H. sapiens*

The results of the FK test for excess relative variation in the humerus of MSA compared to EUP fossils are reported in Table 6.22. There is no evidence of elevated variability in the MSA sample for the four measurements represented by a sufficient number of specimens in each sample. Excess variability was assessed in thirteen ulnar measurements. As with the humerus, there is no support for elevated variability in the MSA ulna sample compared to the EUP (Table 6.23). Of the three radial measurements which could be tested, one (RAD10: neck AP diameter) exhibited a significant surplus of variability in the MSA sample relative to the EUP sample (Table 6.24). In the lower limb, the FK test was performed on five femoral and three tibial measurements represented by a sufficient number of fossils. Elevated morphometric variability for the MSA sample compared to the EUP sample was found in none of these measurements (Tables 6.25 and 6.26).

Discussion

Variability in the Terminal Pleistocene and Holocene of Africa

The first goal of this chapter was to test for the equality of morphometric variation in the appendicular skeleton between a recent African sample – the Zulu – and several African samples of archaeological origin spanning the terminal Pleistocene and Holocene. Despite a time span of roughly 10,000 years represented by the archaeological samples, none of them is characterized by a greater magnitude of variation than the modern Zulu. Given the large number of individuals available in these samples, especially the Khoe-San and Sudanese where close to 100 individuals were sampled for some measurements, it is likely

that the morphological diversity in these groups is neither inflated nor underestimated, but rather represents an accurate reflection of the variability within them. The results suggest that the level of variation within a sample does not automatically increase simply as a function of time, at least in the last ca. 10,000 years of human history.

Moreover, for a few measurements, the Taforalt sample – which may span 4,000 years or more – exhibits significantly less variability than is documented among Zulu, where individuals likely represent no more than two or three generations. As suggested by Ferembach (1962), based on the high occurrence of ossicles in the neurocranium and specific malformations of the sacrum, the Taforalt specimens appear to sample closely-related individuals from an isolated population. Furthermore, these results suggest that modern levels of morphometric variation in the appendicular skeleton extend into the terminal Pleistocene and earlier parts of the Holocene. Thus, if the diversity observed among living peoples has been reduced due to bottlenecks or other major demographic crises as suggested by studies of modern global diversity (e.g., Ambrose, 1998; Excoffier, 2002; Marth et al., 2003; Manica et al., 2007), then such event(s) seem to have occurred prior to the end of the Pleistocene. Given that the genetic diversity documented outside of Africa often represents a subset of African diversity and that African populations harbor more variability than non-Africans (see review in Excoffier, 2002), the prehistoric African diversity documented here may nonetheless exceed that found in contemporaneous populations outside of Africa.

Variability in Early *H. sapiens* versus Modern Humans

Phenotypes are only partially determined by their genotypes, and skeletal traits almost certainly differ in their heritability, with some being more strongly

influenced by external factors such as environmental or mechanical stimuli than others (Mielke et al., 2006). The size and shape of joints are known to be less influenced by environmental pressures and habitual activities than diaphyses and areas of muscle attachment (e.g., Ruff and Runestad, 1992; Lieberman et al., 2001; Ruff et al., 2006). Accordingly, muscles attachment sites are expected to exhibit consistently high levels of variation across samples, regardless of the age of the specimens. This prediction is supported in the samples studied here, where high variation is documented across all samples in muscle insertions such as the deltoid tuberosity, radial tuberosity, and gluteal tuberosity. Furthermore, because muscle attachments sites tend to be poorly defined and small, especially in more gracile individuals, variability in these dimensions may be inflated due to measurement error. Alternatively, because joints tend to be less plastic than other bony areas, the variability documented in articular surfaces may reflect the underlying genetic variability more directly, and should be less influenced by intra- or inter-observer measurement error. Thus, a surplus of morphometric variation in early *H. sapiens*, especially in joint surfaces, may reflect the genetic diversity represented by the sample, and provides a glimpse into the apportionment of this diversity in the human lineage.

Specifically, the assessment of morphometric variability among early *H. sapiens* undertaken in this chapter provides a better understanding of changes in the magnitude of morphological variation from the Late Pleistocene to the present day. The univariate analyses conducted here support the claim for increased variability in Late Pleistocene humans for some, but not all, aspects of long bone anatomy, as has been suggested for cranial morphology (van Vark and Schaafsma, 1992; Gunz et al., 2009). Both MSA and EUP fossils show a trend for high levels of variation relative to modern and prehistoric Africans, which is consistent with the claim that morphological diversity is reduced in living humans (e.g., Howells, 1989; Lahr, 1996; Stringer, 2002).

In addition, the fossil samples tend to maintain a surplus of morphometric variability relative to a geographically and temporally broad pan-African human sample. By combining two recent African populations and three groups of archaeological origin, the pan-African sample comprises variation from diverse sources. Therefore, the excess of variability documented in the MSA and EUP relative to this diverse African sample for most of the same measurements found to exhibit elevated variation relative to well defined populations (i.e., the Zulu and Khoe-San), provides additional support for a greater magnitude of variation in the Late Pleistocene compared to the present day.

Among the MSA fossils, most of the surplus variation in the upper limb is concentrated on the joint surfaces of the distal humerus, as can be seen clearly on the CV plots (Figures 6.6 and 6.7). Appropriately, the excess variation documented in the MSA distal humerus is matched by elevated variation in several of the proximal ulna measurements. This suggests that diverse morphologies of the elbow seem to have been represented within the MSA human population, as suggested by some multivariate studies of the distal humerus and proximal ulna (Churchill et al., 1996; Yokley and Churchill, 2006).

Among the EUP fossils, most aspects of the distal humerus including epicondylar width, width of the capitulum + trochlea, and width of the capitulum, exhibit variation of a similar magnitude to that expressed by the modern African samples, in stark contrast to the MSA variation in the elbow. However, the EUP do show high variability in the AP thickness of the capitulum relative to all modern groups, along with a trend for elevated variability in the diameter of the radial head. Assuming that the older MSA fossils represent the range of elbow diversity present in the early stages of our species, the pattern of reduced variation in the later EUP fossils may be consistent with events such as a bottleneck or with these individuals stemming from a founding population that preserves only a

portion of the original population diversity in this anatomical region (e.g., Manica et al., 2007; von Cramon-Taubadel and Lycette, 2008).

Importantly, the results demonstrate that a surplus of variation within the MSA and EUP fossil samples is maintained relative to the geographically and temporal broad pan-African sample. This provides clear support for a higher magnitude of morphometric variation in the early human lineage, at least in some aspects of the postcranial skeleton, because variability in the pan-African sample is expected to be substantial, given the multitude of potential influences on morphometric variation within such a diverse sample.

These results are in accordance with the increased variability in neurocranial shape proposed by Gunz et al. (2009) for the MSA sample. Yet in contrast to the results by Gunz et al., this study also found evidence of elevated variability in the EUP fossils relative to the pan-African sample in some joint surfaces and diaphyseal dimensions. Van Vark and Schaafsma (1992) also found evidence of higher levels of variability in the face (but not the neurocranium) of European Upper Paleolithic humans. However, when the magnitude of variation within the MSA is directly compared to that in the EUP sample, only a single measurement shows excess variation for the MSA. Thus, a greater magnitude of variation in African and Levantine early *H. sapiens* compared to European Upper Paleolithic humans, as proposed by Gunz et al. (2009) based on their analysis of cranial vault shape, is not supported here. At least in the appendicular skeleton, there is no evidence that earlier, predominantly African MSA humans were more variable than later, predominantly European UP humans. Rather, this study proposes that samples of early *H. sapiens* from the MSA and EUP had an elevated magnitude of morphometric variability in some, but not all, aspects of the appendicular skeleton.

Interpreting the Elevated Variation in the Past

Overall, the results support claims that human variation, whether genetic or skeletal in expression, was greater in the past compared to today. In the postcranial skeleton, this has been documented in diverse aspects of the joints and diaphyses of the major long bones across early *H. sapiens* from Africa, the Levant, and Europe, while previous work has found evidence of surplus variability in cranial form and shape (van Vark and Schaafsma, 1992; Gunz et al., 2009). Does the pattern of elevated variability in the Late Pleistocene reflect the evolutionary forces acting on early humans, or is the apparent pattern a result of other influences such as the time or geographic breadth of the samples?

As noted above, higher variability among the fossils is maintained even when compared to archaeological and pan-African samples that comprise over 10,000 years, which suggests that time alone may be insufficient to account for the surplus. While the time span covered by the MSA fossils clearly exceeds that represented by any of the archaeological samples employed here, the EUP fossils span roughly the same length of time as the Khoe-San and the pan-African sample. Since none of the archaeological samples exhibited higher levels of variation compared to the modern Zulu, a surplus of variation in the fossil samples likely cannot be explained as a simple accumulation of diversity through time.

Additionally, the MSA fossils are sampled across more than 100 ka, a much longer span of time than the EUP fossils which span a little over 10 ka. If variability accrued linearly through time, one could argue that the MSA sample should exhibit more variation compared to modern humans in more appendicular regions than the EUP sample. This is not the case. Despite marked differences in the temporal depth of the early *H. sapiens* samples studied here, the results demonstrate that both Late Pleistocene groups exhibited a surplus of

morphometric variability compared to the modern humans in some, but not all, aspects of the appendicular skeleton. Importantly, these results demonstrate that variability does not necessarily increase simply as a function of the increased temporal depth covered by a sample. That is, other factors appear to have influenced the high variability observed in the Late Pleistocene of Africa, the Levant, and Europe compared to today.

One explanation for the different pattern observed between the fossil samples may be that the samples differ in the geographical extent they cover. With the exception of Nazlet Khater, the EUP sample is restricted to western and central Europe, while the MSA fossils were drawn from disparate sites in South Africa, East Africa, and the Levant. It would be reasonable to expect a greater range of variation in the sample that covers a broader geographic distance. Yet this does not appear to be the case since both the MSA and EUP fossil samples exhibit elevated variation compared to the pan-African sample that covers an equivalent if not greater geographical area than either fossil sample. Thus, it seems that geographic distance alone also cannot account for the pattern of variability documented here.

This dissertation provides evidence that the sampling issues inherent in paleontological analyses, such as the poor chronological and geographic control of adequately-sized fossil samples, cannot fully account for the surplus of morphometric variability among early *H. sapiens*. Thus, the signal of elevated variability in the past may reflect the evolutionary forces and biological changes that have shaped our species. One potential difference between modern and Late Pleistocene human populations that could account, at least in part, to the overall difference in skeletal variability would be differences in the expression of sexual dimorphism. A change in the degree of dimorphism that characterize modern and prehistoric Africans could contribute to differences in the magnitude of morphometric variability because as a population becomes more dimorphic, the

male and female means diverge, which could result in a higher overall level of variation when the sexes are pooled as they are here.

Elevated variation relative to modern humans, probably due to increased dimorphism in the past, has been documented in the mandibles and molars of early humans recovered from Klasies River, Skhūl and Dolní Věstonice (Royer et al., 2009). For most of the univariate and multivariate analyses in the present chapter, both the MSA and EUP samples comprise individuals of both sexes according to the sexual classification performed in Chapter 4, but unfortunately the small sample sizes available for the fossils do not permit the sexes to be tested separately as was done in Chapter 5 for the recent humans. Yet the unambiguous diagnosis of Omo I as a female (see Chapter 4) suggests that the striking morphological differences between the skull of this fossil and Omo 2 (Day, 1969; Smith, 1994; Trinkaus, 2005), both from Member I of the Kibish Formation in southwestern Ethiopia (McDougall et al., 2005), may reflect greater and/or different patterns of sexual dimorphism in early *H. sapiens* compared to living Africans. However, while sexual dimorphism certainly plays a role in determining levels of sample variability in the past, the results of Chapter 5, which demonstrated significant and consistent directional differences in the variation between individuals of the same sex from different modern populations where the influence of dimorphism is controlled, suggest that higher variation in the Late Pleistocene was not simply a result of greater differences between the sexes. Further work is needed to better understand the influence of sexual dimorphism on skeletal variability in the past.

Recent molecular studies suggest modern diversity reflects a metapopulation or structured model whereby isolation existed, temporarily but likely in a recurrent manner, within the ancestral *H. sapiens* gene pool in Africa during the Pleistocene (Lahr and Foley, 1998; Excoffier, 2002; Watkins, 2003; Forster, 2004; Harding and McVean, 2004; Tiskoff et al., 2009; Wakeley, 2004).

Such structured and temporarily subdivided populations, linked episodically through migration, would each be subject to processes such as local extinctions, group expansion and reduction, and random forces such as drift, leading over time to a decrease in within-population variability (e.g., Harding and McVean, 2004; Wakeley, 2004). From these episodically isolated human groups, separate migrations out of Africa (and likely migrations back to Africa) occurring at different times (Lahr and Foley, 1998; Templeton, 2002; Gunz et al., 2009), and probably using different routes (Mellars, 1996; Disotell, 1999c), led to the spread of *H. sapiens* out of Africa and across more distant regions in Europe and beyond.

Successive periods of rapid climate change on a global scale could have provided a trigger for these iterative dispersals from Africa, or acted as a stimulus for the structured population within Africa (Ambrose, 1998; Lahr and Foley, 1998; Gamble et al., 2004; Carto et al., 2009). For example, the occasional collapse of the thermohaline circulation in the Atlantic Ocean may have caused rapid cooling across northern latitudes along with increasing aridity in Africa (Heinrich, 1988). These Heinrich Events would have caused dramatic climatic shifts on a very rapid timescale (ca. 100 – 500 years), followed by a rapid period of warming (Carto et al., 2009). In addition to a general pattern for increasing aridity in much of the Late Pleistocene, these events likely caused large parts of North, West and East Africa to be unsuitable for human habitation (Carto et al., 2009). Heinrich Events, documented at least eight times during the Late Pleistocene (at ca. 105 ka, 85 ka, 65 ka, 45 ka, 38 ka, 30 ka, 22 ka, and 16 ka BP), or other events such as the ca. 70 ka BP super-eruption of Mount Toba in Sumatra (Ambrose, 1998), could have caused massive population bottlenecks as well as the temporary isolation of a sub-divided population in refugia both within Africa, and later, outside of Africa. The rapid climatic release and warming following these or similar events may have provided the stimulus for repeated human range expansions as well as population growth during the Late Pleistocene, as suggested

by molecular studies (Lahr and Foley, 1998; Excoffier, 2002; Forster, 2004; Gamble et al., 2004; von Cramon-Taubadel and Lycette, 2008; Carto et al., 2009).

In addition, it is important to recall that the *H. sapiens* arriving in Europe did not encounter an empty continent, but rather one already inhabited by Neandertals (Bar-Yosef, 1996; Hoffecker, 1999; Churchill and Smith, 2000). The presence of a native local population that may have been able to interbreed with early *H. sapiens* provides another potential source of variation that might not have been encountered in the MSA populations that remained within Africa (Trinkaus, 2007). Any degree of admixture between these groups, as suggested by the assimilation model (e.g., Smith et al., 2005; Trinkaus, 2005), could contribute to higher variability for the EUP sample compared to the MSA fossils. Although the total morphological pattern of the early *H. sapiens* in Europe is undoubtedly modern in appearance (Trinkaus, 2005), certain anatomical details of cranial form including some development of a suprainiac fossa, occipital bunning, and mid-facial prognathism are argued by some workers to represent some Neandertal contribution to the Upper Paleolithic human gene pool (e.g., Smith et al., 2005).

However, recent advances in radiocarbon calibration in the ca. 50 – 30 ka BP interval suggests a shortened period of roughly 6,000 years for the potential overlap between *H. sapiens* and Neandertals in Europe, with overlap as brief as ca. 1,000 years likely in some regions (Mellars, 2006). Such a reduced timeframe for the co-existence of humans and Neandertals in Europe makes any significant or sustained admixture much less likely. Furthermore, mtDNA extracted from eight Neandertal individuals from across Europe shows that Neandertals cluster together, and falls outside the range of genetic variation documented among modern and Upper Paleolithic Europeans (Krings et al., 1997; Ovchinnikov et al., 2000; Serre et al., 2004). On the other hand, mtDNA from several Upper Paleolithic humans is comfortably accomodated within the modern European range (Serre et al., 2004). Together, these findings provide no support for any

degree of interbreeding between Neandertals and early *H. sapiens*. Still, mtDNA provides only a single view of molecular diversity, and Serre and coworkers caution that a Neandertal contribution of 25% or less to the Upper Paleolithic human gene pool may be undetected based on our present knowledge of genetic diversity in the past. However, the current lack of clear morphological and genetic evidence of admixture between Neandertals and humans combined with a short period of potential overlap does not provide support for anything more than an incidental degree of genetic exchange between the two.

The isolation by distance model posits a gradual reduction of human intra-population diversity with increasing distance from Africa (Harpending and Rogers, 2000; Excoffier, 2002; Betti et al., 2009). This prediction is supported by analyses of mtDNA and Y-chromosome sequences, and across numerous autosomal sequences (see review in Excoffier, 2002). It also receives support from analyses of modern cranial diversity where some, but not all, cranial dimensions also show a gradual decrease in intra-population variability with distance from Africa (Relethford, 1994; Manica et al., 2007; Betti et al., 2009). In a study of 37 cranial measurements, Manica et al. (2007) found that only 12 measurements followed the expectation of decreasing variability with distance from Africa when the measurements were analyzed separately. This underscores the importance of studying a range of skeletal features because traits most likely differ in their heritability and sensitivity to a range of external factors that may also be influencing the phenotypic expression of traits (Mielke et al, 2006). While the present study demonstrates elevated variability in the early human lineage, the results cannot address the predictions of the isolation by distance model because only modern African samples were compared. Additional skeletal samples collected from a worldwide distribution of populations are needed in order to determine whether the appendicular skeleton also shows a gradual decrease in within-population variability with distance from Africa.

In sum, the results presented here support previous claims for elevated variation in early *H. sapiens* from Africa and Eurasia compared to living people (van Vark and Schaafsma, 1992; Gunz, 2009). The elevated variability documented here cannot be fully explained by either the temporal or geographic breadth of the fossil samples, nor does it appear to be solely influenced by greater sexual dimorphism in the past, although this may be a contributing factor. Despite the more fragmentary nature of the MSA compared to the EUP sample, some patterns of variability are apparent for those measurements that can be evaluated in both samples. Elevated variability among the MSA, whether compared to the Zulu, Khoe-San, or pan-African sample, is primarily found in joint surfaces, while the EUP sample shows increased variability predominantly in diaphyseal dimensions such as shaft diameters and circumferences, with fewer joints exhibiting high variation. Moreover, the MSA sample exhibits more instances of elevated variability in the upper limb compared to the lower limb, and in distal limb elements (i.e., ulna, radius, and tibia) compared to proximal limb elements (i.e., humerus and femur). In contrast, the patterning of elevated variation appears to be more randomly distributed in the EUP sample.

These differences suggest that different factors may have influenced the magnitude of morphometric variability in these two fossil samples. As noted above, joints appear to be less sensitive to external stimuli than diaphyseal dimensions, suggesting that the elevated variability of the MSA sample may reflect the greater genetic diversity of this group. In contrast, the EUP fossils show increased variability in both shafts and joints, which might reflect the diversity of environments encountered by these individuals as well as the genetic diversity of the group. Such interpretations remain speculative, but patterns of variability like the ones documented here offer potential insights onto the evolutionary and historical processes that have shaped our species. There is a clear need for a better understanding of the genetic correlates of skeletal traits and

the influence of ecogeography on relative variation. Inasmuch as it is feasible with fossils, it would be prudent to focus on assessing past morphometric variability on the same population-level scale for which it is measured among living people.

Implications for Paleontological Studies

In addition to providing insights on the evolutionary and demographic processes that have shaped the human lineage, this study of variability in the Late Pleistocene has important implications for understanding fossil relationships. Differences in the magnitude and patterning of past variation in a nontrivial issue because variation plays a critical role in many methods employed by paleoanthropologists. For example, the Mahalanobis squared distance (D^2) is a commonly used tool to understand patterns of phenetic relationships between fossils (e.g., Kidder et al., 1992; Pearson, 2000b; Grine et al., 2007; Crevecoeur et al., 2009). However, if the fossil sample exhibits a different pattern of variance and covariance than the extant sample against which it is compared, the resulting D^2 may be biased and should be cautiously interpreted (van Vark, 1984; van Vark and Schaafsma, 1992; Ackermann, 2002, 2003, 2005). The bias arises because methods such as D^2 assume that the samples being compared have an equal covariance or dispersion matrix (Neff and Marcus, 1980; Manly, 1986; Quinn and Keough, 2002). When a small fossil sample is combined with a large extant sample in a multivariate analysis, the underlying matrix primarily reflects the magnitude and pattern of variance and covariance of the extant group (van Vark, 1984).

Although the present study did not specifically test for differences in equality of variances and covariances (as captured in a V/CV matrix) between samples drawn from the Late Pleistocene and more recent times, it did document

an elevated magnitude of variability in the appendicular skeleton of MSA and EUP early *H. sapiens* compared to modern humans. Furthermore, the MSA and EUP samples appear to exhibit unique patterns of variability with different measurements displaying a surplus of variation in each group, although this observation is based solely on univariate results which do not take into account the interconnection between measurements. Other studies (van Vark and Schaafsma, 1992; Gunz, 2009) have also found evidence of elevated variability in various aspects of the skull. Based on these results, it seems unlikely that the assumption of equality of V/CV between these fossil samples and a modern population would be satisfied. If this is the case, then inferences achieved through methods such as the D^2 which rely on an inherent assumption of variation equality between extant and extinct *H. sapiens* should be interpreted with caution. Future research efforts should focus on gaining a better understanding of the ways in which living and past populations differ in both the magnitude and patterning of morphological variation, and how such differences may impact our analytical interpretations.

Conclusions

The results of this chapter support previous claims from craniometric studies that the range of morphological variation exhibited by Africans today and since the terminal Pleistocene underestimates the diversity present within our species during the Late Pleistocene. Thus, any evolutionary or historical processes that have acted to reduce within-population variability in modern humans appears to have occurred between approximately 25 to 14 ka BP. Furthermore, the fact that no archaeological sample exhibited elevated variation compared to recent populations demonstrates that time averaging alone does not necessarily contribute to higher sample variability. In the postcranial skeleton, a

surplus of variation relative to today's baseline level has been documented in numerous articular and diaphyseal dimensions of the major long bones across both older early *H. sapiens* from the MSA of Africa and the Levant, as well as in early Upper Paleolithic humans from Europe and North Africa. The signal of elevated variability is maintained even in comparison to a temporally and geographically broad pan-African sample, and the MSA fossils do not exhibit more variability than the EUP sample, despite being comprised of specimens sampled over more than 100,000 years. These results suggest that the increase in variation is not simply an artifact of sampling.

Furthermore, this dissertation demonstrates that equal variation, whether in the magnitude or patterning of the variation, cannot be assumed between modern populations and samples of past humans. Such variation inequality has critical implications for many commonly used methods in paleoanthropology, and may create unrecognized biases. A global skeletal sample is needed to test wether the appendicular skeleton conforms to the prediction of a gradual decrease in within-population variability with distance from Africa, as predicted by the isolation by distance model. Additional research should focus on expanding our understanding of the ways in which modern and prehistoric human populations differ in both the magnitude and patterning of morphological variation, and on the genetic and ecogeographic correlates of population variability, as this can contribute important insights on interpretations of fossil relationships and the evolutionary and historical processes that have shaped our species.

Figure 6.1 Variation in the humerus measurements* of recent and archaeological African samples. All samples are comprised of males and females.

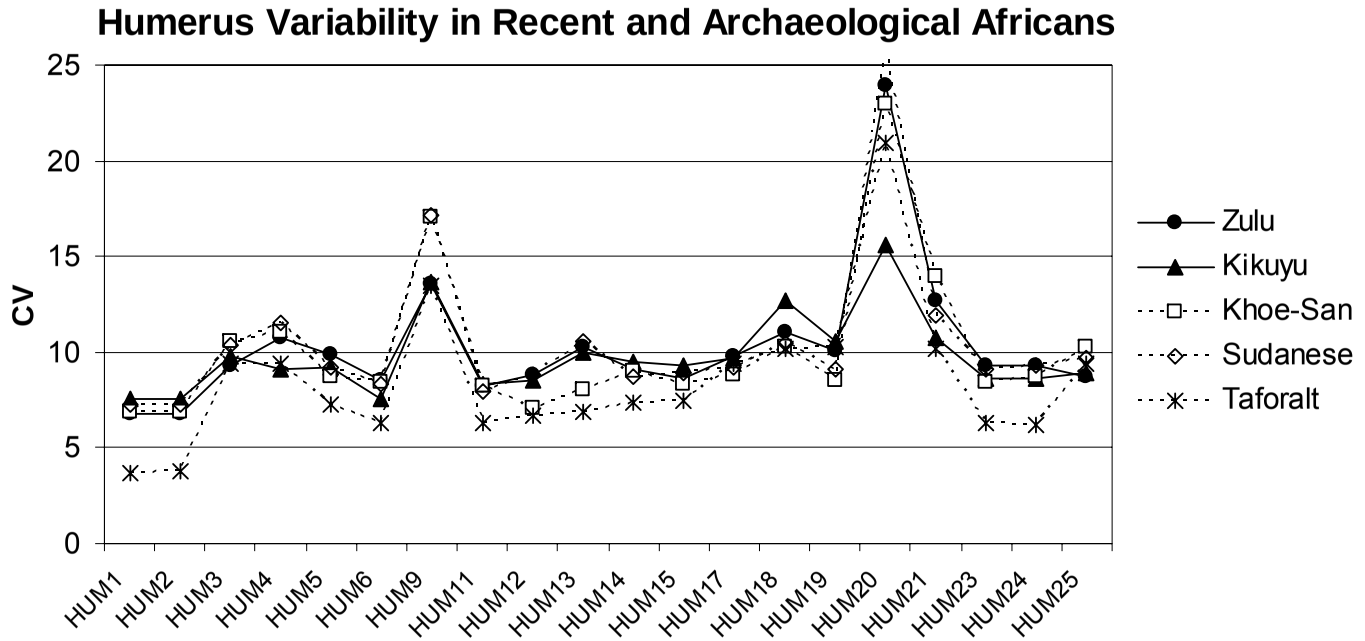

*HUM1: max length, HUM2: total length, HUM3: max midshaft diameter, HUM4: min midshaft diameter, HUM5: head proximo-distal diameter, HUM6: head DV diameter, HUM9: deltoid tuberosity max length, HUM11: epicondylar width, HUM12: capitulum + trochlear width, HUM13: capitulum width, HUM14: capitulum height, HUM15: capitulum AP thickness, HUM17: medial trochlear lip AP diameter, HUM18: min trochlear AP diameter, HUM19: olecranon fossa width, HUM20: medial dorsal pillar breadth, HUM21: lateral dorsal pillar breadth, HUM23: deltoid to capitulum distance, HUM24: deltoid to trochlea distance, HUM25: min shaft circumference.

Figure 6.2 Variation in the ulna measurements* of recent and archaeological African samples. All samples are comprised of males and females.

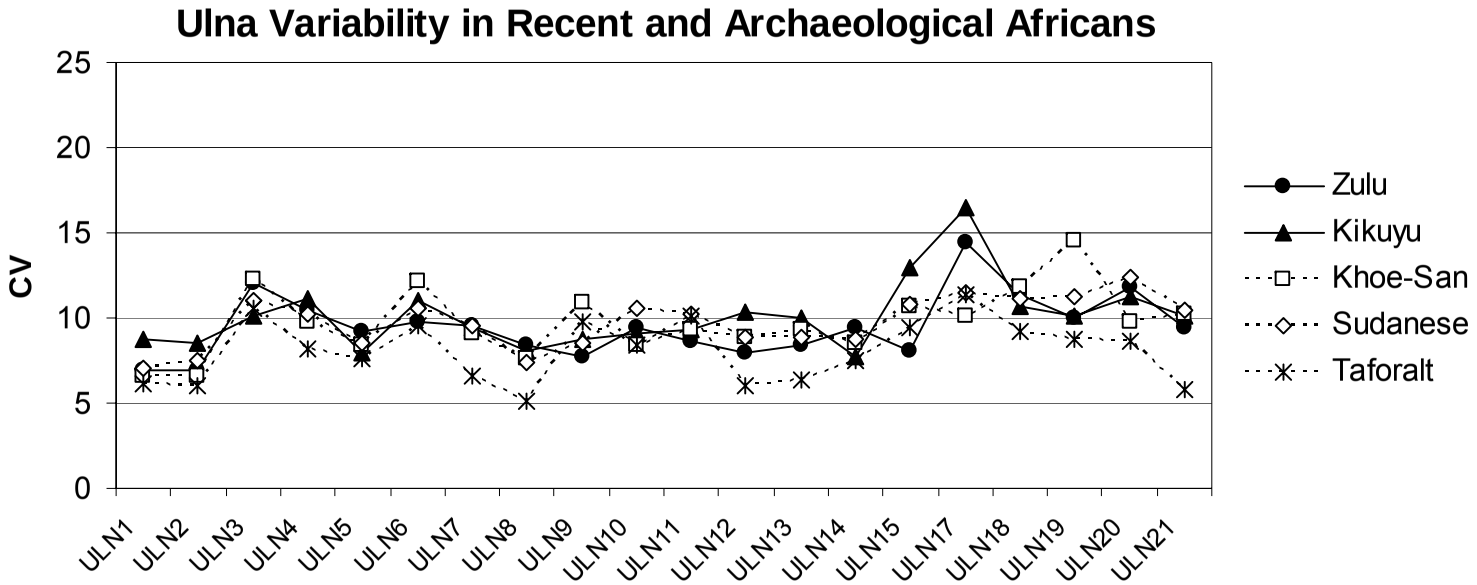

*ULN1: articular length, ULN2: total length, ULN3: max midshaft diameter, ULN4: min midshaft diameter, ULN5: coronoid height, ULN6: max coronoid ML breadth, ULN7: olecranon height, ULN8: olecranon ML breadth, ULN9: olecranon length, ULN10: trochlear notch length, ULN11: trochlear notch transverse breadth, ULN12: mid-trochlear notch thickness, ULN13: trochlear notch AP thickness, ULN14: radial notch position, ULN15: radial notch length, ULN17: brachialis insertion position, ULN18: proximal shaft AP diameter, ULN19: proximal shaft ML diameter, ULN20: distal epiphysis transverse breadth, ULN21: min shaft circumference.

Figure 6.3 Variation in the radius measurements* of recent and archaeological African samples. All samples are comprised of males and females.

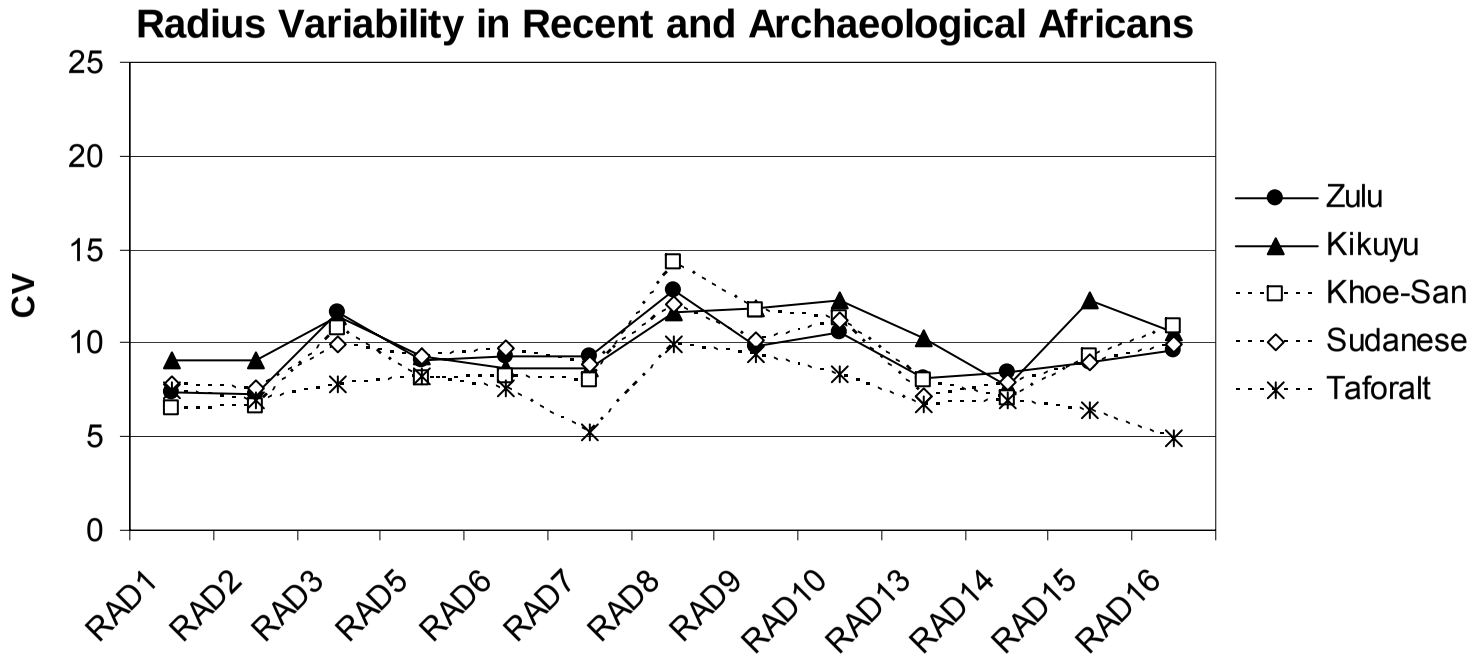

*RAD1: articular length, RAD2: max length, RAD3: max midshaft diameter, RAD5: max head AP diameter, RAD6: max head ML diameter, RAD7: max head diameter, RAD8: radial tuberosity length, RAD9: neck length, RAD10: neck AP diameter, RAD13: distal epiphysis DV breadth, RAD14: distal epiphysis ML breadth, RAD15: min shaft circumference, RAD16: radial tuberosity circumference.

Figure 6.4 Variation in the femur measurements* of recent and archaeological African samples. All samples are comprised of males and females.

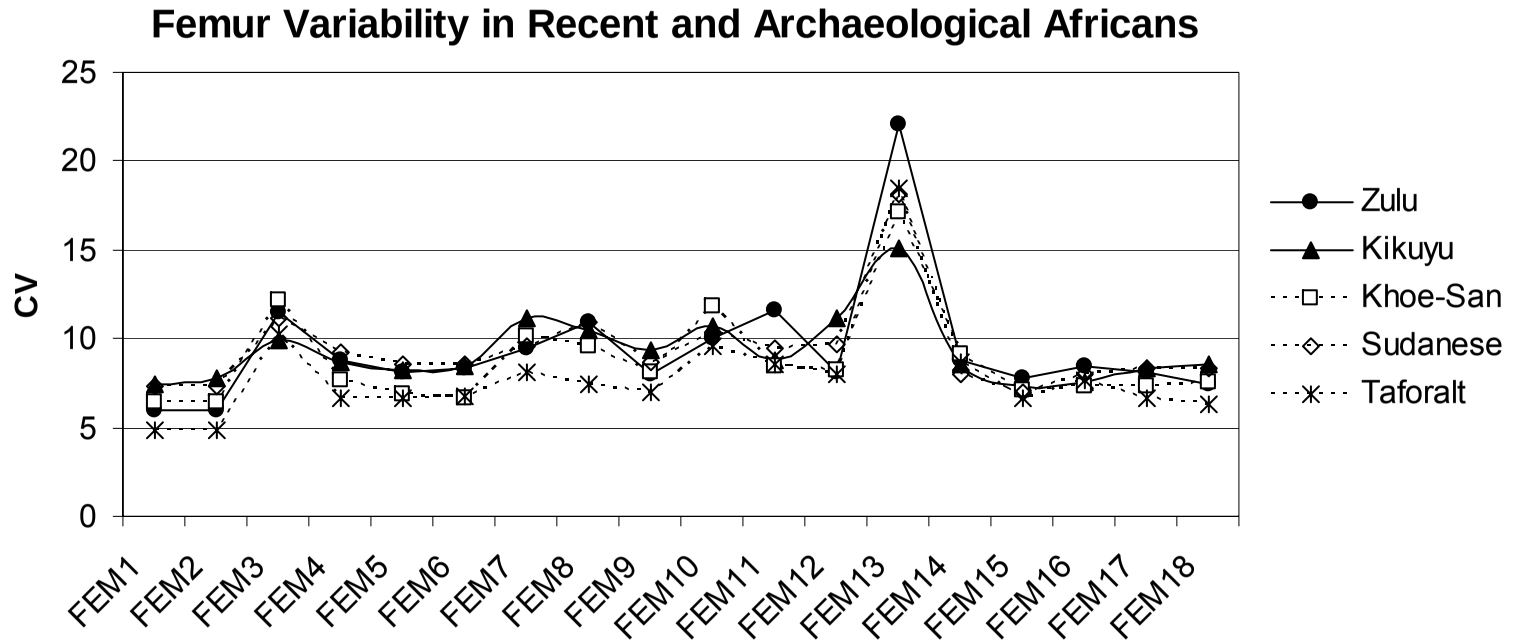

*FEM1: max length, FEM2: bicondylar length, FEM3: midshaft AP diameter, FEM4: midshaft ML diameter, FEM5: vertical head diameter, FEM6: horizontal head diameter, FEM7: min neck height, FEM8: min neck breadth, FEM9: biomechanical neck length, FEM10: neck length, FEM11: subtrochanteric AP shaft diameter, FEM12: subtrochanteric ML shaft diameter, FEM13: gluteal tuberosity breadth, FEM14: patellar notch width, FEM15: biepicondylar breadth, FEM16: max distal articular breadth, FEM17: min shaft circumference, FEM18: subtrochanteric shaft circumference.

Figure 6.5 Variation in the tibia measurements* of recent and archaeological African samples. All samples are comprised of males and females.

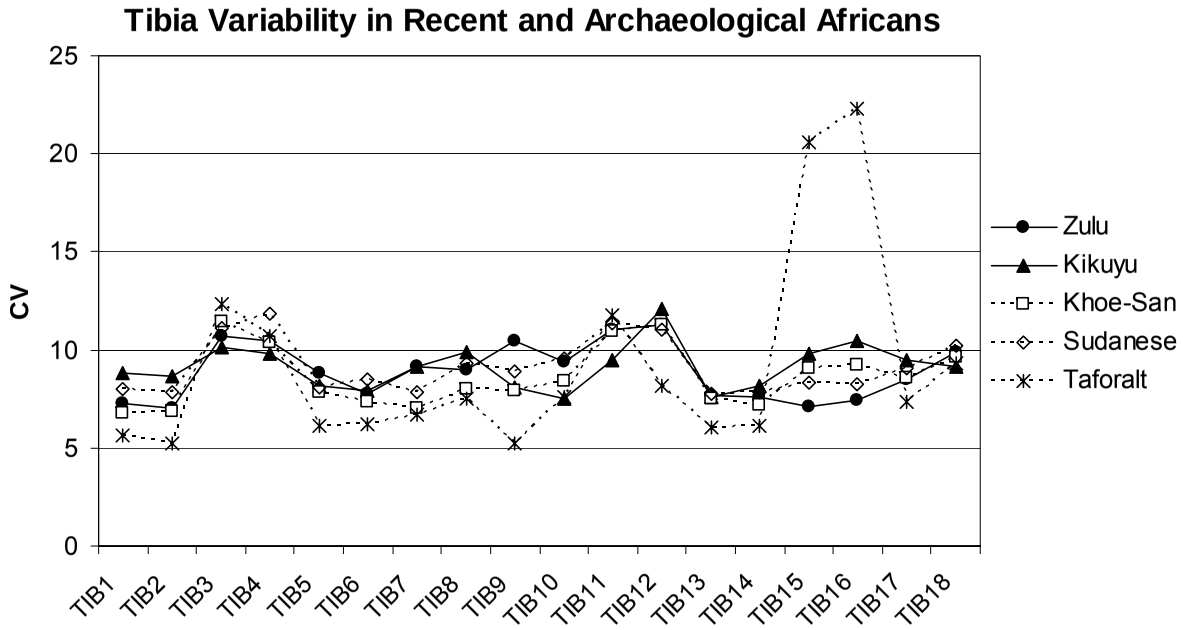

*TIB1: articular length, TIB2: total length, TIB3: midshaft AP diameter, TIB4: midshaft ML diameter, TIB5: proximal epiphysis max length, TIB6: proximal epiphysis max breadth, TIB7: medial condyle AP length, TIB8: medial condyle ML breadth, TIB9: lateral condyle AP length, TIB10: lateral condyle ML breadth, TIB11: shaft AP diameter at nutrient foramen, TIB12: shaft ML diameter at nutrient foramen, TIB13: talar AP length, TIB14: distal epiphysis ML breadth, TIB15: nutrient foramen to medial malleolus distance, TIB16: nutrient foramen to talar articular surface distance, TIB17: min shaft circumference, TIB18: shaft circumference at nutrient foramen.

Figure 6.6 Variation in the humerus measurements of early *H. sapiens* fossils (MSA and EUP samples) compared to samples of modern humans.

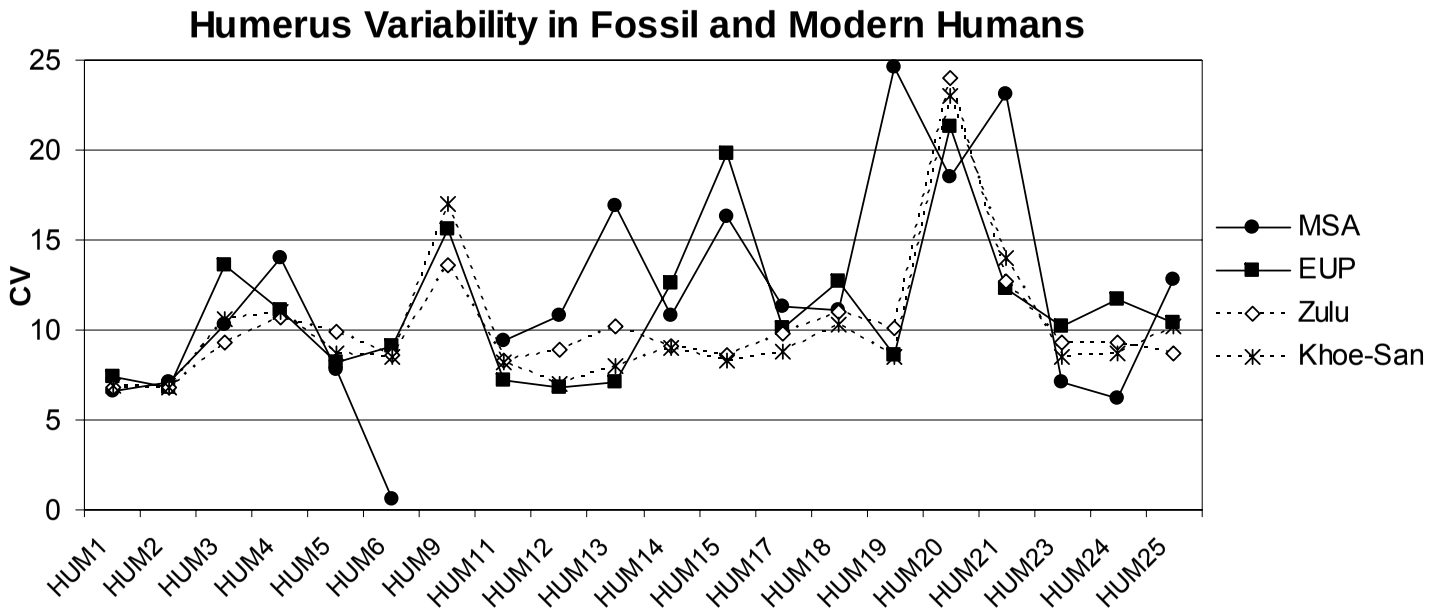

*HUM1: max length, HUM2: total length, HUM3: max midshaft diameter, HUM4: min midshaft diameter, HUM5: head proximo-distal diameter, HUM6: head DV diameter, HUM9: deltoid tuberosity max length, HUM11: epicondylar width, HUM12: capitulum + trochlear width, HUM13: capitulum width, HUM14: capitulum height, HUM15: capitulum AP thickness, HUM17: medial trochlear lip AP diameter, HUM18: min trochlear AP diameter, HUM19: olecranon fossa width, HUM20: medial dorsal pillar breadth, HUM21: lateral dorsal pillar breadth, HUM23: deltoid to capitulum distance, HUM24: deltoid to trochlea distance, HUM25: min shaft circumference.

Figure 6.7 Variation in the humerus measurements of early *H. sapiens* fossils (MSA and EUP samples) compared to the pan-African modern human sample.

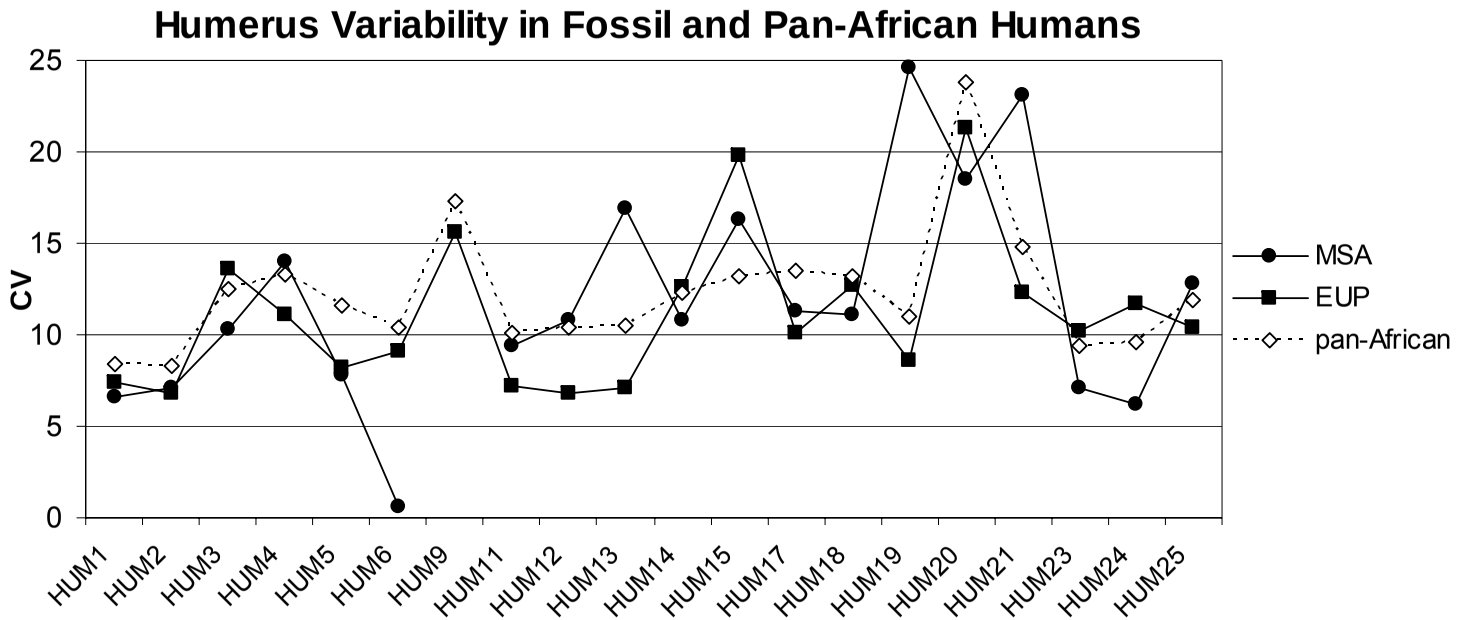

*HUM1: max length, HUM2: total length, HUM3: max midshaft diameter, HUM4: min midshaft diameter, HUM5: head proximo-distal diameter, HUM6: head DV diameter, HUM9: deltoid tuberosity max length, HUM11: epicondylar width, HUM12: capitulum + trochlear width, HUM13: capitulum width, HUM14: capitulum height, HUM15: capitulum AP thickness, HUM17: medial trochlear lip AP diameter, HUM18: min trochlear AP diameter, HUM19: olecranon fossa width, HUM20: medial dorsal pillar breadth, HUM21: lateral dorsal pillar breadth, HUM23: deltoid to capitulum distance, HUM24: deltoid to trochlea distance, HUM25: min shaft circumference.

Figure 6.8 Variation in the ulna measurements* of early *H. sapiens* fossils (MSA and EUP samples) compared to samples of modern humans.

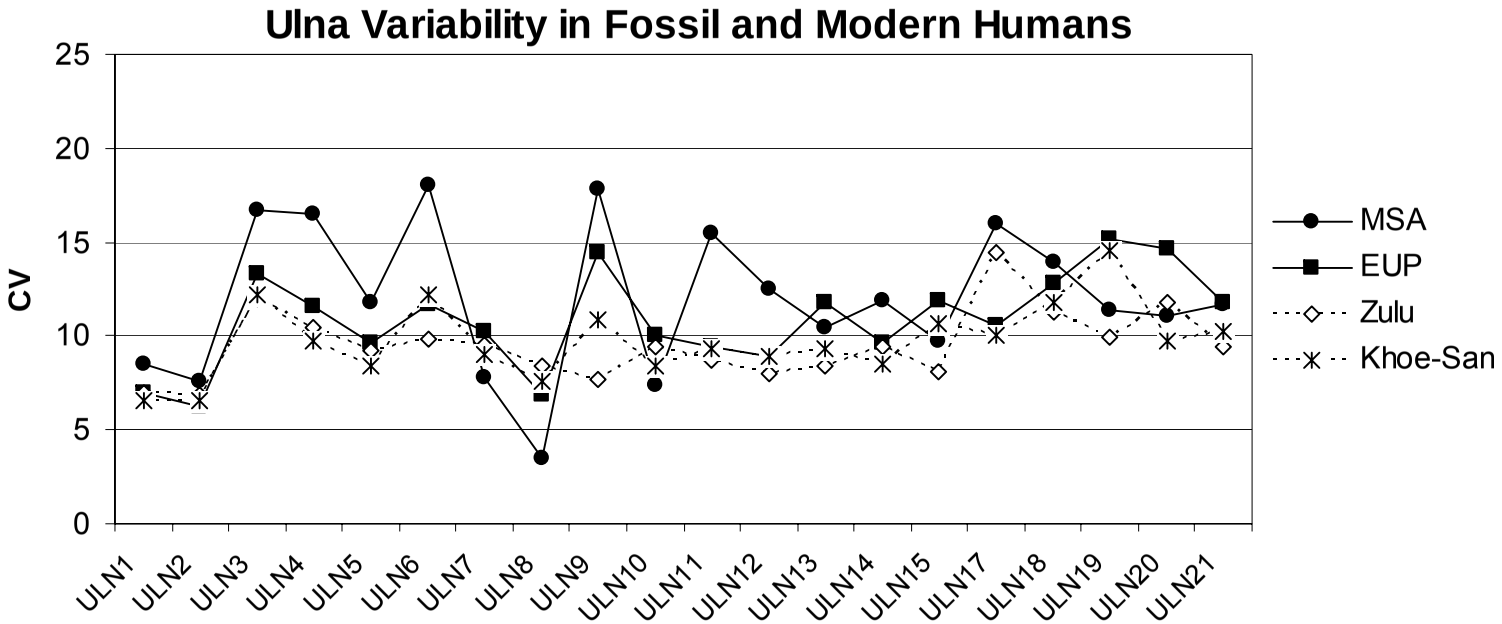

*ULN1: articular length, ULN2: total length, ULN3: max midshaft diameter, ULN4: min midshaft diameter, ULN5: coronoid height, ULN6: max coronoid ML breadth, ULN7: olecranon height, ULN8: olecranon ML breadth, ULN9: olecranon length, ULN10: trochlear notch length, ULN11: trochlear notch transverse breadth, ULN12: mid-trochlear notch thickness, ULN13: trochlear notch AP thickness, ULN14: radial notch position, ULN15: radial notch length, ULN17: brachialis insertion position, ULN18: proximal shaft AP diameter, ULN19: proximal shaft ML diameter, ULN20: distal epiphysis transverse breadth, ULN21: min shaft circumference.

Figure 6.9 Variation in the ulna measurements* of early *H. sapiens* fossils (MSA and EUP samples) compared to the pan-African modern human sample.

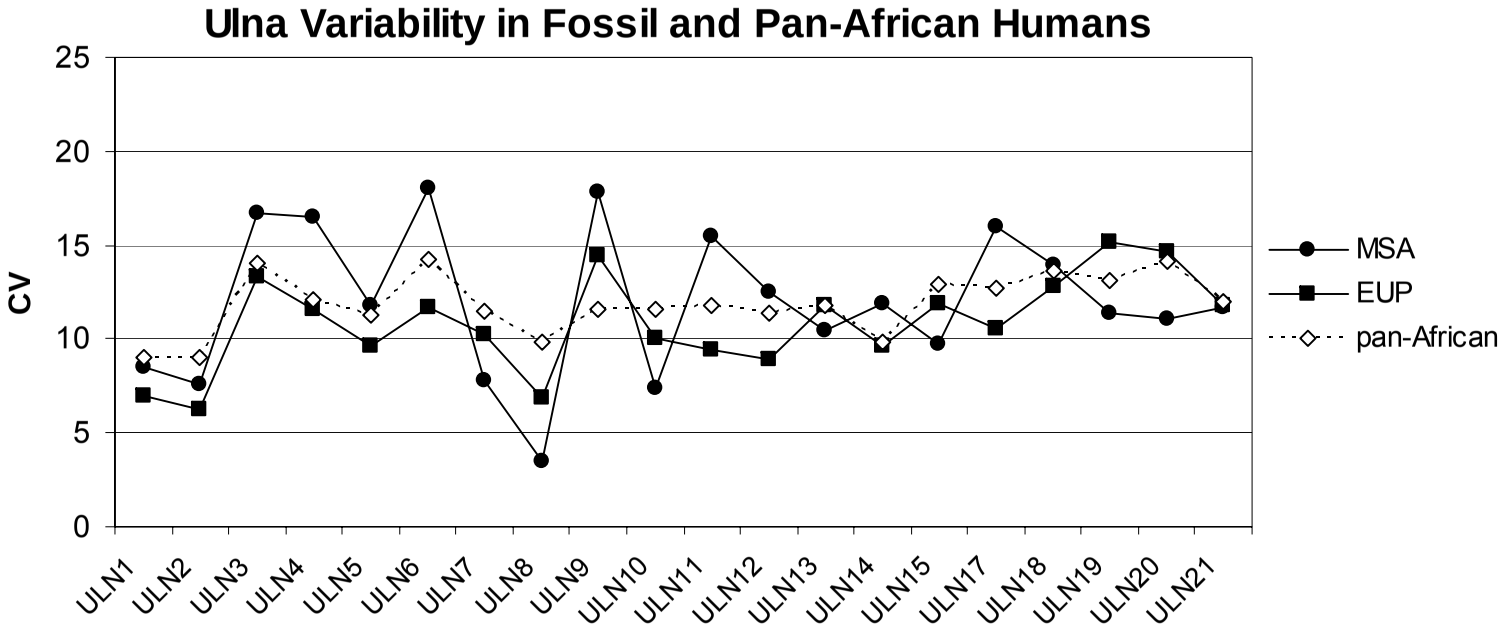

*ULN1: articular length, ULN2: total length, ULN3: max midshaft diameter, ULN4: min midshaft diameter, ULN5: coronoid height, ULN6: max coronoid ML breadth, ULN7: olecranon height, ULN8: olecranon ML breadth, ULN9: olecranon length, ULN10: trochlear notch length, ULN11: trochlear notch transverse breadth, ULN12: mid-trochlear notch thickness, ULN13: trochlear notch AP thickness, ULN14: radial notch position, ULN15: radial notch length, ULN17: brachialis insertion position, ULN18: proximal shaft AP diameter, ULN19: proximal shaft ML diameter, ULN20: distal epiphysis transverse breadth, ULN21: min shaft circumference.

Figure 6.10 Variation in the radius measurements* of early *H. sapiens* fossils (MSA and EUP samples) compared to samples of modern humans.

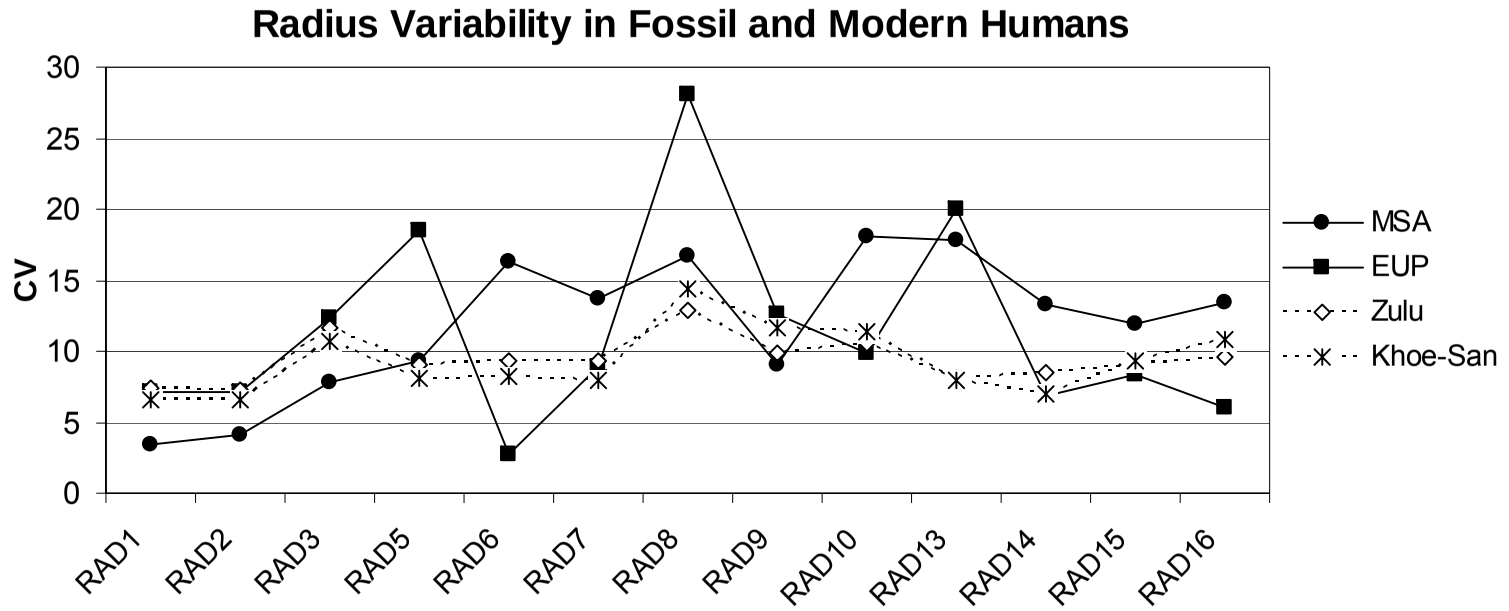

*RAD1: articular length, RAD2: max length, RAD3: max midshaft diameter, RAD5: max head AP diameter, RAD6: max head ML diameter, RAD7: max head diameter, RAD8: radial tuberosity length, RAD9: neck length, RAD10: neck AP diameter, RAD13: distal epiphysis DV breadth, RAD14: distal epiphysis ML breadth, RAD15: min shaft circumference, RAD16: radial tuberosity circumference.

Figure 6.11 Variation in the radius measurements* of early *H. sapiens* fossils (MSA and EUP samples) compared to the pan-African modern human sample.

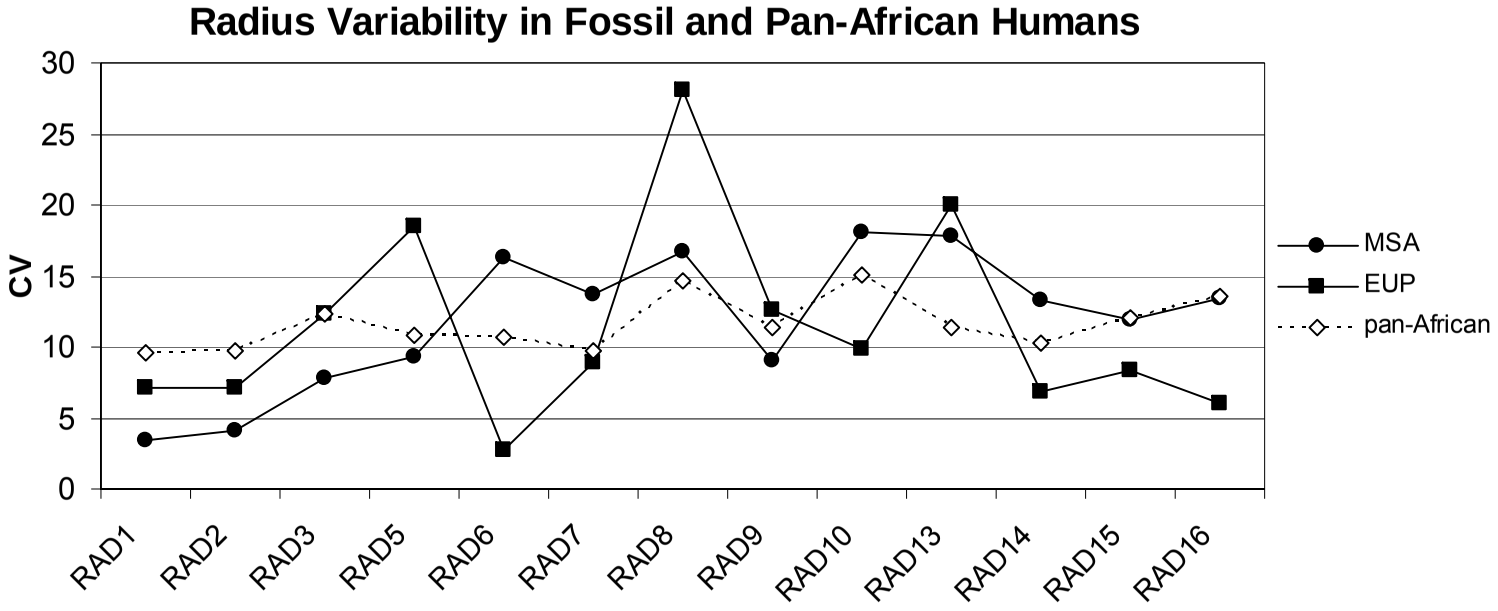

*RAD1: articular length, RAD2: max length, RAD3: max midshaft diameter, RAD5: max head AP diameter, RAD6: max head ML diameter, RAD7: max head diameter, RAD8: radial tuberosity length, RAD9: neck length, RAD10: neck AP diameter, RAD13: distal epiphysis DV breadth, RAD14: distal epiphysis ML breadth, RAD15: min shaft circumference, RAD16: radial tuberosity circumference.

Figure 6.12 Variation in the femur measurements* of early *H. sapiens* fossils (MSA and EUP samples) compared to samples of modern humans.

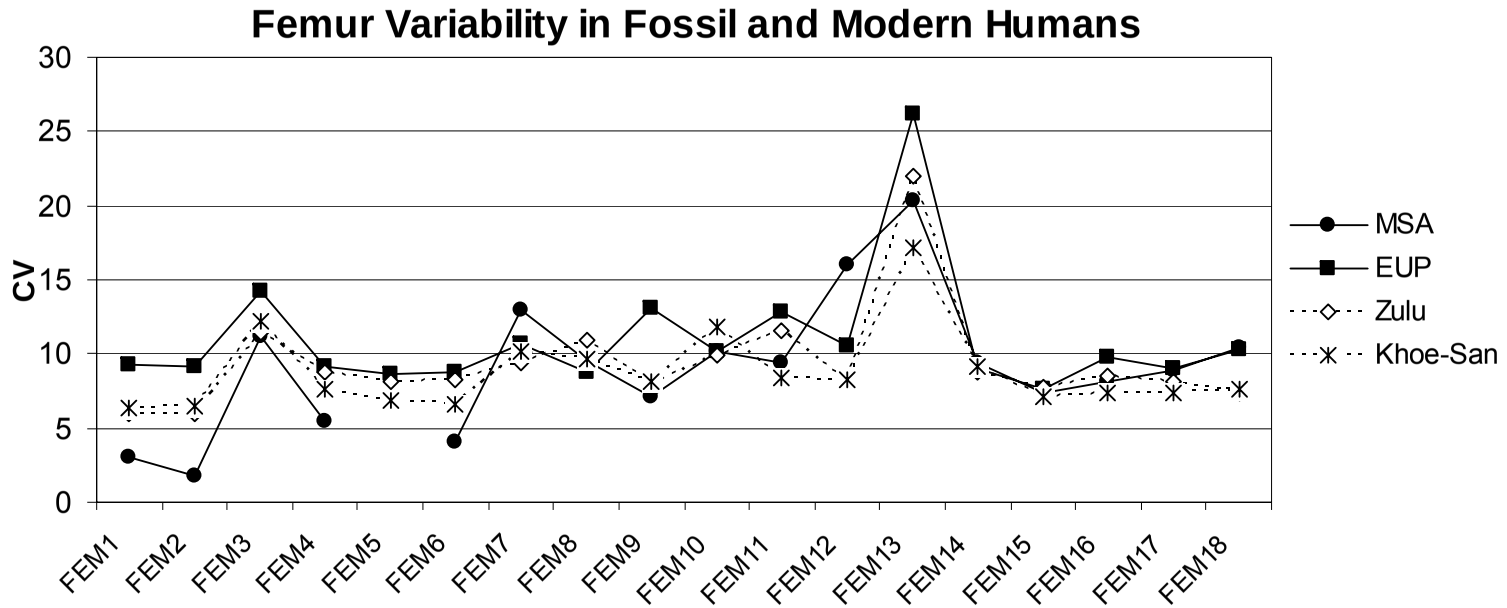

*FEM1: max length, FEM2: bicondylar length, FEM3: midshaft AP diameter, FEM4: midshaft ML diameter, FEM5: vertical head diameter, FEM6: horizontal head diameter, FEM7: min neck height, FEM8: min neck breadth, FEM9: biomechanical neck length, FEM10: neck length, FEM11: subtrochanteric AP shaft diameter, FEM12: subtrochanteric ML shaft diameter, FEM13: gluteal tuberosity breadth, FEM14: patellar notch width, FEM15: biepicondylar breadth, FEM16: max distal articular breadth, FEM17: min shaft circumference, FEM18: subtrochanteric shaft circumference.

Figure 6.13 Variation in the femur measurements* of early *H. sapiens* fossils (MSA and EUP samples) compared to the pan-African modern human sample.

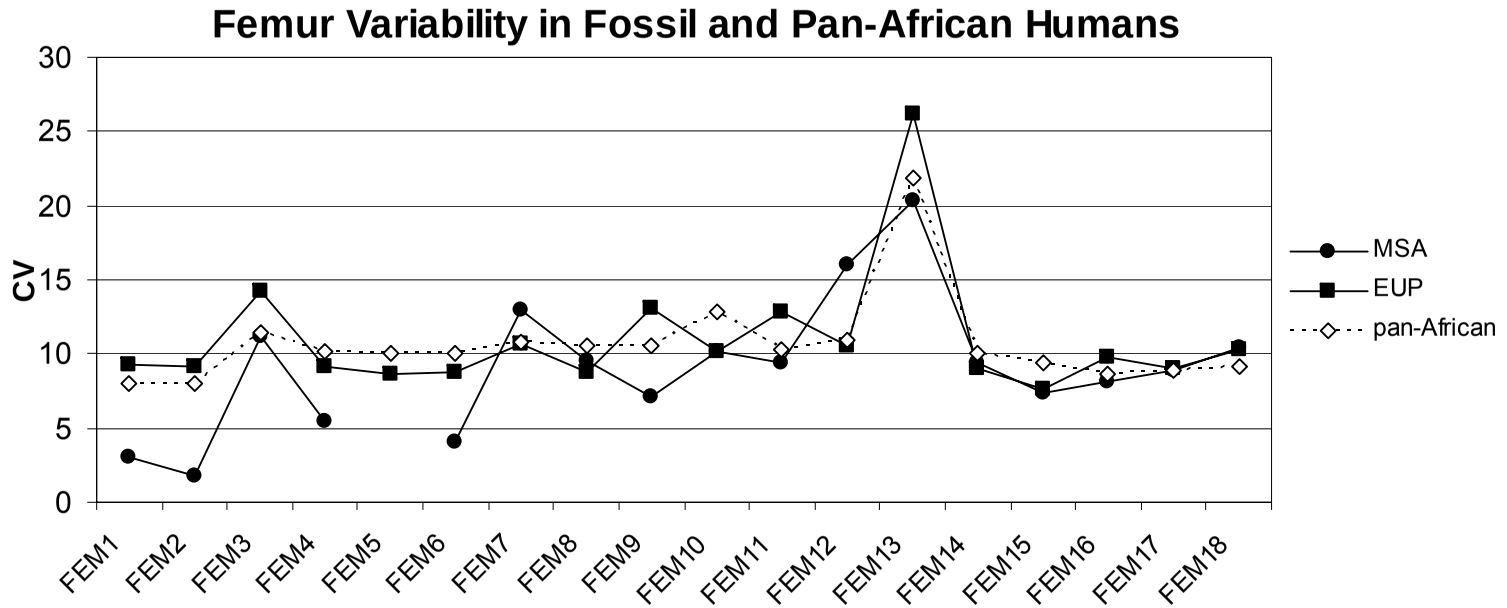

*FEM1: max length, FEM2: bicondylar length, FEM3: midshaft AP diameter, FEM4: midshaft ML diameter, FEM5: vertical head diameter, FEM6: horizontal head diameter, FEM7: min neck height, FEM8: min neck breadth, FEM9: biomechanical neck length, FEM10: neck length, FEM11: subtrochanteric AP shaft diameter, FEM12: subtrochanteric ML shaft diameter, FEM13: gluteal tuberosity breadth, FEM14: patellar notch width, FEM15: biepicondylar breadth, FEM16: max distal articular breadth, FEM17: min shaft circumference, FEM18: subtrochanteric shaft circumference.

Figure 6.14 Variation in the tibia (CV) of early *H. sapiens* fossils (MSA and EUP samples) compared to samples of modern humans.

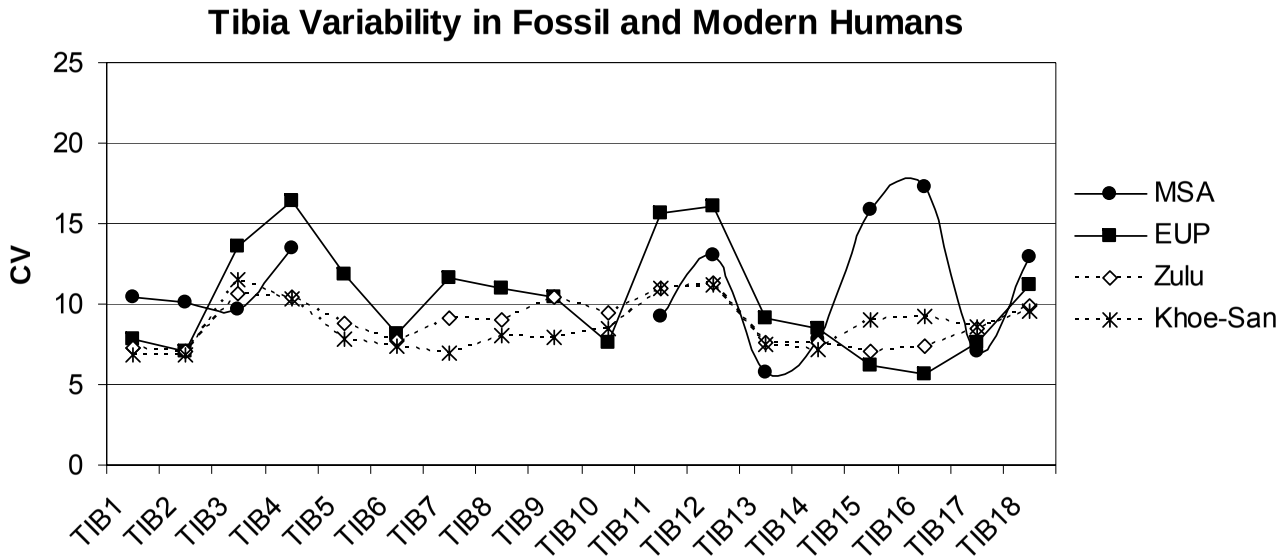

*TIB1: articular length, TIB2: total length, TIB3: midshaft AP diameter, TIB4: midshaft ML diameter, TIB5: proximal epiphysis max length, TIB6: proximal epiphysis max breadth, TIB7: medial condyle AP length, TIB8: medial condyle ML breadth, TIB9: lateral condyle AP length, TIB10: lateral condyle ML breadth, TIB11: shaft AP diameter at nutrient foramen, TIB12: shaft ML diameter at nutrient foramen, TIB13: talar AP length, TIB14: distal epiphysis ML breadth, TIB15: nutrient foramen to medial malleolus distance, TIB16: nutrient foramen to talar articular surface distance, TIB17: min shaft circumference, TIB18: shaft circumference at nutrient foramen.

Figure 6.15 Variation in the tibia (CV) of early *H. sapiens* fossils (MSA and EUP samples) compared to the pan-African modern human sample.

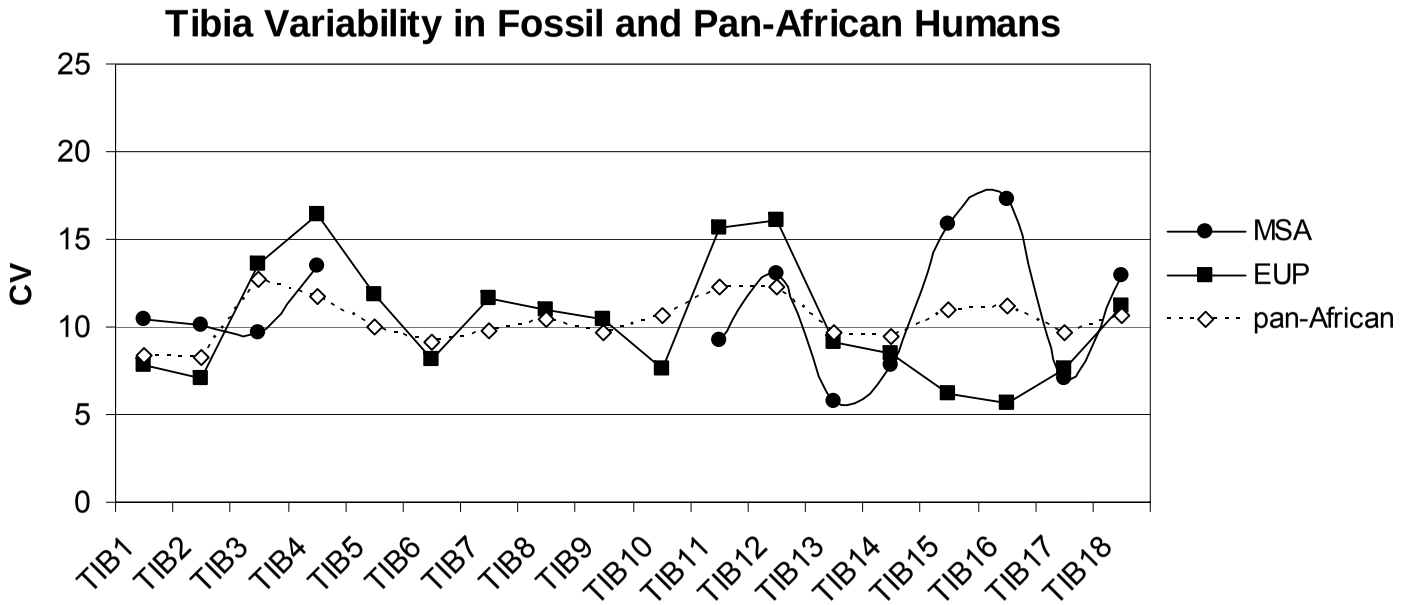

*TIB1: articular length, TIB2: total length, TIB3: midshaft AP diameter, TIB4: midshaft ML diameter, TIB5: proximal epiphysis max length, TIB6: proximal epiphysis max breadth, TIB7: medial condyle AP length, TIB8: medial condyle ML breadth, TIB9: lateral condyle AP length, TIB10: lateral condyle ML breadth, TIB11: shaft AP diameter at nutrient foramen, TIB12: shaft ML diameter at nutrient foramen, TIB13: talar AP length, TIB14: distal epiphysis ML breadth, TIB15: nutrient foramen to medial malleolus distance, TIB16: nutrient foramen to talar articular surface distance, TIB17: min shaft circumference, TIB18: shaft circumference at nutrient foramen.

Table 6.1 Composition of skeletal samples employed in Chapter 6. *N* represents the maximum number of individuals available in each sample; due to differential preservation, fewer individuals are available for some variables.

Sample	Total *N*	Female* *N*	Male* *N*	Indeterminate Sex *N*
Recent				
Zulu	42	20	22	0
Kikuyu	40	12	16	12
Archaeological				
Khoe-San	98	27	21	50
Sudanese	94	21	7	66
Taforalt	31	1	6	24
Pan-African				
Pan- African	305	81	72	152
MSA early *H. sapiens*				
Humerus	11	4	6	1
Ulna	10	4	4	2
Radius	10	4	4	2
Femur	10	3	6	1
Tibia	9	2	6	1
EUP early *H. sapiens*				
Humerus	21	5	13	3
Ulna	20	5	13	2
Radius	20	5	11	4
Femur	24	5	15	4
Tibia	21	5	15	1

* Sex is diagnosed in Chapter 4 (except for the Zulu and Kikuyu, where sex is known from records).

Table 6.2 Results of the Fligner-Killeen (FK) test for equal relative variation in the humerus of archaeological samples compared to the Zulu mixed-sex recent sample. Significant differences ($p < 0.0167$) are in bold. Table continues on the next page.

Variable	Zulu		Khoe-San		Sudanese		Khoe-San *vs* Zulu		Sudanese *vs* Zulu	
							FK		FK	
	N	CV	*N*	CV	*N*	CV	*T*	*p*	*T*	*p*
HUM1	41	6.83	73	6.92	54	7.25	40.252	0.7914	33.711	0.4460
HUM2	41	6.76	73	6.84	52	7.26	39.145	0.4626	33.398	0.4137
HUM3	41	9.27	80	10.56	87	10.41	31.958	0.3157	33.651	0.4569
HUM4	41	10.72	80	11.04	87	11.56	36.435	0.7434	36.146	0.7086
HUM5	41	9.93	72	8.71	55	9.18	46.028	0.2463	41.992	0.5451
HUM6	41	8.56	67	8.47	47	8.38	37.462	0.8739	37.848	0.9510
HUM9	41	13.58	80	17.03	85	17.13	28.835	0.1402	30.264	0.2113
HUM11	41	8.26	80	8.24	65	7.93	38.773	0.9796	40.3	0.7696
HUM12	41	8.86	80	7.04	68	8.78	45.177	0.1404	37.261	0.7852
HUM13	41	10.24	80	8.03	70	10.53	46.19	0.2521	35.665	0.6588
HUM14	41	9.11	78	9.01	68	8.70	39.232	0.9217	39.984	0.8142
HUM15	41	8.59	77	8.31	69	8.87	41.206	0.6888	37.197	0.8396
HUM17	41	9.83	79	8.81	65	9.17	42.713	0.5328	39.306	0.8921
HUM18	41	11.03	80	10.26	76	10.45	42.466	0.5597	40.482	0.7698
HUM19	41	10.13	82	8.55	84	9.12	45.87	0.2762	42.098	0.6052
HUM20	41	23.96	82	23.01	83	25.71	34.411	0.5271	32.304	0.3432
HUM21	41	12.71	81	13.99	78	11.94	32.053	0.1616	38.313	0.9670
HUM23	41	9.27	79	8.47	65	9.15	42.525	0.5517	37.816	0.9202
HUM24	41	9.27	79	8.70	71	9.30	40.833	0.7346	38.8	0.9647
HUM25	41	8.75	82	10.23	87	9.72	24.59	0.3084	28.68	0.7233

Table 6.2 Continued.

Variable	Zulu		Taforalt		Taforalt *vs* Zulu FK	
	N	CV	*N*	CV	*T*	*p*
HUM1	41	6.83	23	3.72	8.5209	**0.0080**
HUM2	41	6.76	23	3.74	8.7667	**0.0094**
HUM3	41	9.27	30	9.36	26.298	0.8182
HUM4	41	10.72	30	9.41	22.859	0.3631
HUM5	41	9.93	25	7.25	13.539	0.0549
HUM6	41	8.56	23	6.33	13.557	0.1191
HUM9	41	13.58	28	13.49	26.846	0.7901
HUM11	41	8.26	27	6.31	18.898	0.2448
HUM12	41	8.86	28	6.64	19.922	0.2561
HUM13	41	10.24	28	6.90	17.626	0.1095
HUM14	41	9.11	28	7.38	20.125	0.2736
HUM15	41	8.59	28	7.46	22.344	0.5185
HUM17	41	9.83	25	9.37	23.189	0.9102
HUM18	41	11.03	28	10.18	24.228	0.7914
HUM19	41	10.13	28	10.26	27.208	0.7351
HUM20	41	23.96	28	20.94	27.058	0.7580
HUM21	41	12.71	27	10.19	20.245	0.3750
HUM23	41	9.27	27	6.26	16.126	0.0834
HUM24	41	9.27	27	6.17	15.196	0.0546
HUM25	41	8.75	29	9.44	27.677	0.7782

Table 6.3 Results of the Fligner-Killeen (FK) test for equal relative variation in the ulna of archaeological samples compared to the Zulu recent sample. Significant differences ($p < 0.0167$) are in bold. Table continues on the next page.

Variable	Zulu		Khoe-San		Sudanese		Khoe-San *vs* Zulu		Sudanese *vs* Zulu	
							FK		FK	
	N	CV	*N*	CV	*N*	CV	*T*	*p*	*T*	*p*
ULN1	41	6.97	65	6.55	51	7.08	43.217	0.4505	39.80	0.7959
ULN2	41	6.88	65	6.55	47	7.45	44.272	0.3567	36.283	0.7408
ULN3	41	12.01	72	12.24	76	11.00	41.001	0.7021	72.496	0.6460
ULN4	41	10.46	72	9.76	76	10.22	41.704	0.6234	39.697	0.8629
ULN5	41	9.24	76	8.41	73	8.52	39.188	0.9242	38.693	0.9806
ULN6	41	9.81	73	12.20	73	10.52	26.668	0.0675	33.922	0.4773
ULN7	41	9.57	75	9.03	69	9.57	40.808	0.7302	37.08	0.8253
ULN8	41	8.40	74	7.59	68	7.34	41.409	0.6602	44.503	0.3460
ULN9	41	7.68	78	10.88	73	8.50	26.995	0.1761	35.652	0.9955
ULN10	41	9.39	77	8.37	71	10.52	40.003	0.8279	30.391	0.2079
ULN11	41	8.68	75	9.28	71	10.21	33.738	0.4607	30.048	0.1894
ULN12	41	8.01	77	8.89	76	8.87	31.974	0.3149	31.993	0.3156
ULN13	41	8.38	77	9.37	70	8.85	31.127	0.2568	35.214	0.6089
ULN14	41	9.38	77	8.49	73	8.73	41.313	0.6768	40.217	0.7957
ULN15	41	8.12	76	10.67	80	10.84	24.632	0.0334	23.189	0.0199
ULN17	41	14.40	78	10.07	79	11.52	53.565	0.0229	47.203	0.1924
ULN18	41	11.31	78	11.77	85	11.14	38.715	0.9842	38.808	0.9810
ULN19	41	9.95	78	14.54	85	11.23	28.752	0.1355	33.633	0.4546
ULN20	41	11.82	59	9.73	49	12.42	40.541	0.2344	33.194	0.9729
ULN21	41	9.451	68	10.21	69	10.50	34.141	0.4961	35.195	0.6062

Table 6.3 Continued.

Variable	Zulu		Taforalt		Taforalt *vs* Zulu FK	
	N	CV	*N*	CV	*T*	*p*
ULN1	41	6.97	23	6.12	15.479	0.2536
ULN2	41	6.88	23	5.98	15.465	0.2521
ULN3	41	12.01	26	10.60	19.675	0.4135
ULN4	41	10.46	26	8.18	17.099	0.1762
ULN5	41	9.24	27	7.66	22.318	0.6439
ULN6	41	9.81	25	9.58	23.546	0.8508
ULN7	41	9.57	27	6.61	15.827	0.0691
ULN8	41	8.40	26	5.13	13.19	0.0304
ULN9	41	7.68	28	9.81	31.984	0.1920
ULN10	41	9.39	26	8.40	24.973	0.7776
ULN11	41	8.68	28	10.14	32.025	0.1892
ULN12	41	8.01	27	6.04	21.21	0.4906
ULN13	41	8.38	27	6.37	20.345	0.3862
ULN14	41	9.38	28	7.55	19.068	0.1907
ULN15	41	8.12	27	9.43	29.141	0.3493
ULN17	41	14.40	27	11.31	18.116	0.1857
ULN18	41	11.31	29	9.25	22.855	0.4665
ULN19	41	9.95	29	8.78	21.479	0.3157
ULN20	41	11.82	26	8.66	19.885	0.4388
ULN21	41	9.451	25	5.76	12.553	0.0332

Table 6.4 Results of the Fligner-Killeen (FK) test for equal relative variation in the radius of archaeological samples compared to the Zulu mixed-sex recent sample. Significant differences ($p < 0.0167$) are in bold. Table continues on the next page.

Variable	Zulu		Khoe-San		Sudanese		Khoe-San *vs* Zulu		Sudanese *vs* Zulu	
							FK		FK	
	N	CV	*N*	CV	*N*	CV	*T*	*p*	*T*	*p*
RAD1	39	7.33	71	6.55	63	7.81	42.334	0.3629	34.844	0.7906
RAD2	39	7.30	69	6.60	57	7.63	42.512	0.3436	35.692	0.9054
RAD3	39	11.66	76	10.74	86	9.89	41.019	0.4939	42.396	0.3886
RAD5	34	9.09	65	8.11	41	9.25	36.79	0.3849	32.743	0.7876
RAD6	34	9.26	65	8.20	47	9.76	36.066	0.4553	30.795	0.9092
RAD7	33	9.26	64	7.96	38	8.83	36.65	0.3051	34.359	0.4276
RAD8	39	12.86	78	14.35	88	12.02	33.212	0.5964	43.382	0.3151
RAD9	39	9.88	77	11.71	76	10.15	30.561	0.3470	35.2	0.8255
RAD10	39	10.57	78	11.36	84	11.21	34.539	0.7457	31.889	0.4648
RAD13	39	8.10	67	8.00	54	7.14	33.406	0.6179	38.479	0.7219
RAD14	39	8.43	67	7.03	58	7.91	43.09	0.2941	38.87	0.6852
RAD15	39	9.01	77	9.31	84	8.95	36.225	0.9501	37.702	0.8774
RAD16	39	9.60	78	10.89	87	9.97	33.883	0.6700	35.197	0.8174

Table 6.4 Continued.

Variable	Zulu		Taforalt		Taforalt *vs* Zulu FK	
	N	CV	*N*	CV	*T*	*p*
RAD1	39	7.33	9	7.48	7.7934	0.9042
RAD2	39	7.30	9	6.94	7.1405	0.9252
RAD3	39	11.66	14	7.77	6.5581	0.1351
RAD5	34	9.09	23	8.24	17.558	0.4859
RAD6	34	9.26	20	7.62	13.899	0.3555
RAD7	33	9.26	8	5.23	3.1788	0.2432
RAD8	39	12.86	24	9.93	14.73	0.1335
RAD9	39	9.88	12	9.44	10.978	0.8340
RAD10	39	10.57	25	8.35	16.172	0.1690
RAD13	39	8.10	26	6.72	19.016	0.3370
RAD14	39	8.43	26	6.94	20.304	0.4907
RAD15	39	9.01	15	6.44	7.9983	0.1848
RAD16	39	9.60	13	4.88	5.6479	0.1248

Table 6.5 Results of the Fligner-Killeen (FK) test for equal relative variation in the femur of archaeological samples compared to the Zulu recent human sample. Significant differences ($p < 0.0167$) are in bold. Table continues on the next page.

Variable	Zulu		Khoe-San		Sudanese		Khoe-San *vs* Zulu		Sudanese *vs* Zulu	
							FK		FK	
	N	CV	*N*	CV	*N*	CV	*T*	*p*	*T*	*p*
FEM1	38	5.94	71	6.41	47	7.31	33.537	0.7429	26.321	0.1138
FEM2	38	6.02	71	6.45	46	7.36	34.068	0.8077	26.085	0.1032
FEM3	38	11.46	72	12.17	79	11.16	31.361	0.5003	35.116	0.9309
FEM4	38	8.75	72	7.61	79	9.22	41.95	0.3139	35.573	0.9875
FEM5	38	8.09	67	6.89	52	8.61	43.666	0.1907	31.503	0.5071
FEM6	38	8.28	69	6.63	56	8.52	47.52	0.0555	32.748	0.6525
FEM7	38	9.41	75	10.16	68	9.56	31.56	0.5212	33.09	0.6907
FEM8	38	10.92	74	9.61	70	10.93	40.738	0.4198	35.97	0.9511
FEM9	38	7.96	69	8.10	53	8.69	34.605	0.8763	29.674	0.3297
FEM10	38	9.97	69	11.77	60	10.33	31.064	0.4696	31.327	0.4924
FEM11	38	11.61	78	8.44	82	9.43	46.475	0.0915	42.788	0.2735
FEM12	38	8.16	78	8.25	82	9.67	34.658	0.8753	27.962	0.2320
FEM13	38	22.03	77	17.11	81	18.17	49.554	0.0295	45.928	0.1128
FEM14	37	8.74	75	9.11	46	7.97	33.563	0.8611	39.327	0.3696
FEM15	37	7.80	70	7.13	39	7.02	39.961	0.3885	38.388	0.4314
FEM16	37	8.47	60	7.36	39	7.95	42.427	0.1856	35.564	0.7967
FEM17	38	8.10	72	7.35	81	8.28	39.259	0.5619	33.617	0.7479
FEM18	38	7.38	78	7.59	82	8.32	33.446	0.7291	29.905	0.3705

Table 6.5 Continued.

Variable	Zulu		Taforalt		Taforalt *vs* Zulu FK	
	N	CV	*N*	CV	*T*	*p*
FEM1	38	5.94	18	4.84	12.186	0.3648
FEM2	38	6.02	18	4.89	12.263	0.3747
FEM3	38	11.46	26	10.28	21.024	0.5908
FEM4	38	8.75	26	6.59	16.042	0.1112
FEM5	38	8.09	19	6.69	12.353	0.2830
FEM6	38	8.28	22	6.81	14.425	0.2327
FEM7	38	9.41	22	8.09	15.929	0.3925
FEM8	38	10.92	22	7.46	12.418	0.1000
FEM9	38	7.96	21	7.02	15.651	0.4744
FEM10	38	9.97	21	9.54	14.951	0.3814
FEM11	38	11.61	25	8.56	17.958	0.3185
FEM12	38	8.16	25	7.98	22.627	0.9960
FEM13	38	22.03	25	18.52	17.218	0.2469
FEM14	37	8.74	20	8.63	15.296	0.5559
FEM15	37	7.80	18	6.69	12.488	0.4041
FEM16	37	8.47	16	7.61	10.562	0.3779
FEM17	38	8.10	26	6.66	20.178	0.4732
FEM18	38	7.38	25	6.25	18.712	0.4033

Table 6.6 Results of the Fligner-Killeen (FK) test for equal relative variation in the tibia of archaeological samples compared to the Zulu mixed-sex recent sample. Significant differences ($p < 0.0167$) are in bold. Table continues on the next page.

Variable	Zulu		Khoe-San		Sudanese		Khoe-San *vs* Zulu FK		Sudanese *vs* Zulu FK	
	N	CV	*N*	CV	*N*	CV	*T*	*p*	*T*	*p*
TIB1	39	7.26	72	6.82	42	8.01	41.405	0.4478	33.003	0.5664
TIB2	39	7.04	70	6.89	41	7.88	39.653	0.6242	33.055	0.5724
TIB3	39	10.67	71	11.47	79	11.15	36.456	0.9857	35.152	0.8177
TIB4	39	10.45	71	10.34	79	11.85	37.575	0.8739	31.018	0.3855
TIB5	37	8.81	65	7.87	33	8.08	38.146	0.5567	27.786	0.6225
TIB6	37	7.76	64	7.39	33	8.51	37.589	0.6169	33.081	0.5814
TIB7	36	9.15	62	6.99	29	7.81	45.515	0.0453	22.161	0.3789
TIB8	37	8.97	64	8.04	29	9.28	37.791	0.5937	28.902	0.6111
TIB9	37	10.47	61	7.95	29	8.91	45.687	0.0630	21.957	0.3580
TIB10	37	9.43	62	8.44	28	9.54	38.642	0.4951	27.745	0.6356
TIB11	39	10.99	73	10.98	78	11.36	36.401	0.9765	35.926	0.9124
TIB12	39	11.30	73	11.24	78	10.99	36.617	0.9966	38.448	0.7795
TIB13	39	7.65	76	7.49	57	7.74	38.464	0.7742	34.93	0.8062
TIB14	39	7.59	72	7.15	52	7.83	39.459	0.6506	34.349	0.7350
TIB15	39	7.09	69	9.04	49	8.30	26.141	0.0984	30.235	0.2950
TIB16	39	7.43	71	9.23	55	8.22	26.634	0.1170	30.971	0.3640
TIB17	39	8.51	72	8.61	78	9.06	36.817	0.9702	34.105	0.6952
TIB18	39	9.90	73	9.61	78	10.22	39.908	0.6027	37.163	0.9352

Table 6.6 Continued.

Variable	Zulu		Taforalt		Taforalt *vs* Zulu FK	
	N	CV	*N*	CV	*T*	*p*
TIB1	39	7.26	22	5.62	13.593	0.1690
TIB2	39	7.04	20	5.24	11.181	0.1230
TIB3	39	10.67	25	12.30	24.286	0.7224
TIB4	39	10.45	25	10.70	22.824	0.9654
TIB5	37	8.81	23	6.10	12.832	0.0808
TIB6	37	7.76	25	6.24	16.996	0.2267
TIB7	36	9.15	23	6.69	13.636	0.1154
TIB8	37	8.97	25	7.50	19.871	0.5571
TIB9	37	10.47	24	5.22	8.0368	**0.0029**
TIB10	37	9.43	25	7.58	16.388	0.1801
TIB11	39	10.99	24	11.74	21.344	0.9450
TIB12	39	11.30	24	8.13	14.179	0.1053
TIB13	39	7.65	22	6.08	13.92	0.1929
TIB14	39	7.59	21	6.16	14.547	0.3344
TIB15	39	7.09	21	20.57	20.107	0.7648
TIB16	39	7.43	20	22.29	17.849	0.4989
TIB17	39	8.51	23	7.39	17.129	0.4317
TIB18	39	9.90	24	9.35	18.346	0.4727

Table 6.7 Results of the Fligner-Killeen (FK) test for excess relative variation in the humerus of the early *H. sapiens* samples compared to the Zulu recent human sample. Significant differences ($p < 0.025$) are in bold.

Variable	MSA		EUP		Zulu		MSA *vs* Zulu FK		EUP *vs* Zulu FK	
	N	CV	*N*	CV	*N*	CV	*T*	*p*	*T*	*p*
HUM1	3	6.60	18	7.42	41	6.83	--	--	18.641	0.2610
HUM2	3	7.01	17	6.76	41	6.76	--	--	16.485	0.3591
HUM3	8	10.31	20	13.65	41	9.27	8.1422	0.2865	20.221	0.2949
HUM4	8	14.02	20	11.10	41	10.72	11.57	0.0405	17.849	0.4984
HUM5	4	7.78	15	8.22	41	9.93	--	--	9.3526	0.1668
HUM6	3	0.56	13	9.12	41	8.56	--	--	14.063	0.2176
HUM9	1	--	8	15.63	41	13.58	--	--	8.9244	0.2024
HUM11	6	9.44	16	7.21	41	8.26	--	--	11.373	0.2506
HUM12	6	10.76	17	6.81	41	8.86	--	--	11.543	0.1986
HUM13	6	16.86	12	7.06	41	10.24	--	--	7.1076	0.1847
HUM14	7	10.78	7	12.56	41	9.11	10.388	0.0377	9.3831	0.0797
HUM15	6	16.34	12	19.76	41	8.59	--	--	23.918	**0.0000**
HUM17	6	11.28	11	10.06	41	9.83	--	--	11.042	0.3060
HUM18	6	11.07	11	12.67	41	11.03	--	--	12.87	0.1476
HUM19	6	24.56	12	8.56	41	10.13	--	--	9.0576	0.3655
HUM20	6	18.48	12	21.29	41	23.96	--	--	12.297	0.2824
HUM21	5	23.08	13	12.34	41	12.71	--	--	13.612	0.2556
HUM23	3	7.15	7	10.20	41	9.27	--	--	6.3166	0.3914
HUM24	3	6.18	6	11.71	41	9.27	--	--	--	--
HUM25	7	12.81	21	10.42	41	8.75	10.085	0.0395	19.087	0.3723

Tables 6.8 Results of the Fligner-Killeen (FK) test for excess relative variation in the humerus of the early *H. sapiens* samples compared to the Khoe-San archaeological human sample. Significant differences ($p < 0.025$) are in bold.

Variable	MSA		EUP		Khoe-San		MSA *vs* Khoe-San FK		EUP *vs* Khoe-San FK	
	N	CV	*N*	CV	*N*	CV	*T*	*p*	*T*	*p*
HUM1	3	6.60	18	7.42	73	6.92	--	--	18.624	0.3062
HUM2	3	7.01	17	6.76	73	6.84	--	--	16.413	0.4030
HUM3	8	10.31	20	13.65	80	10.56	7.0663	0.4525	19.192	0.4231
HUM4	8	14.02	20	11.10	80	11.04	12.982	**0.0241**	17.391	0.4330
HUM5	4	7.78	15	8.22	72	8.71	--	--	12.21	0.3939
HUM6	3	0.56	13	9.12	67	8.47	--	--	12.619	0.3814
HUM9	1	--	8	15.63	80	17.03	--	--	6.2234	0.4423
HUM11	6	9.44	16	7.21	80	8.24	--	--	11.858	0.2879
HUM12	6	10.76	17	6.81	80	7.04	--	--	14.03	0.3887
HUM13	6	16.86	12	7.06	80	8.03	--	--	8.7485	0.3253
HUM14	7	10.78	7	12.56	78	9.01	10.123	0.0683	10.686	0.0466
HUM15	6	16.34	12	19.76	77	8.31	--	--	29.743	**0.0000**
HUM17	6	11.28	11	10.06	79	8.81	--	--	12.211	0.2396
HUM18	6	11.07	11	12.67	80	10.26	--	--	15.288	0.0636
HUM19	6	24.56	12	8.56	82	8.55	--	--	11.753	0.3780
HUM20	6	18.48	12	21.29	82	23.01	--	--	9.8725	0.4334
HUM21	5	23.08	13	12.34	81	13.99	--	--	10.659	0.4195
HUM23	3	7.15	7	10.20	79	8.47	--	--	6.8121	0.3568
HUM24	3	6.18	6	11.71	79	8.70	--	--	--	--
HUM25	7	12.81	21	10.42	82	10.23	9.6489	0.0938	17.687	0.4558

Tables 6.9 Results of the Fligner-Killeen (FK) test for excess relative variation in the humerus of the early *H. sapiens* samples compared to the pan-African human sample. Significant differences ($p < 0.025$) are in bold.

Variable	MSA		EUP		Pan-African		MSA *vs* Pan-African FK		EUP *vs* Pan-African FK	
	N	CV	*N*	CV	*N*	CV	*T*	*p*	*T*	*p*
HUM1	3	6.60	18	7.42	230	8.40	--	--	13.016	0.2456
HUM2	3	7.01	17	6.76	228	8.28	--	--	10.373	0.1514
HUM3	8	10.31	20	13.65	277	12.52	4.8258	0.2790	18.275	0.4716
HUM4	8	14.02	20	11.10	277	13.33	10.159	0.1744	12.936	0.1552
HUM5	4	7.78	15	8.22	230	11.65	--	--	6.3771	0.1292
HUM6	3	0.56	13	9.12	215	10.40	--	--	8.7444	0.2512
HUM9	1	--	8	15.63	272	17.29	--	--	6.0172	0.4031
HUM11	6	9.44	16	7.21	251	10.11	--	--	6.765	0.1137
HUM12	6	10.76	17	6.81	255	10.45	--	--	7.1898	0.1008
HUM13	6	16.86	12	7.06	257	10.49	--	--	4.9129	0.0877
HUM14	7	10.78	7	12.56	254	12.26	5.1634	0.4115	7.0085	0.3644
HUM15	6	16.34	12	19.76	254	13.22	--	--	28.164	**0.0000**
HUM17	6	11.28	11	10.06	249	13.50	--	--	5.7399	0.1628
HUM18	6	11.07	11	12.67	264	13.20	--	--	10.229	0.4608
HUM19	6	24.56	12	8.56	274	11.03	--	--	6.9494	0.1881
HUM20	6	18.48	12	21.29	273	23.80	--	--	10.183	0.4431
HUM21	5	23.08	13	12.34	266	14.78	--	--	9.7764	0.3289
HUM23	3	7.15	7	10.20	251	9.42	--	--	7.9505	0.2615
HUM24	3	6.18	6	11.71	257	9.57	--	--	--	--
HUM25	7	12.81	21	10.42	269	11.94	7.5872	0.3006	13.439	0.1771

Table 6.10 Results of the Fligner-Killeen (FK) test for excess relative variation in the ulna of the early *H. sapiens* samples compared to Zulu recent human samples. Significant differences ($p < 0.025$) are in bold.

Variable	MSA		EUP		Zulu		MSA *vs* Zulu FK		EUP *vs* Zulu FK	
	N	CV	*N*	CV	*N*	CV	*T*	*p*	*T*	*p*
ULN1	5	8.55	17	7.01	41	6.97	--	--	14.089	0.4112
ULN2	5	7.54	17	6.28	41	6.88	--	--	12.062	0.2357
ULN3	5	16.67	14	13.29	41	12.01	--	--	14.064	0.3069
ULN4	5	16.50	14	11.61	41	10.46	--	--	13.881	0.3240
ULN5	9	11.75	14	9.64	41	9.24	11.513	0.0930	13.94	0.3182
ULN6	8	18.03	9	11.67	41	9.81	14.778	**0.0022**	11.444	0.0968
ULN7	8	7.76	17	10.28	41	9.57	4.3506	0.2288	17.17	0.2982
ULN8	7	3.51	13	6.90	41	8.40	1.8305	0.1676	9.1815	0.2889
ULN9	8	17.82	13	14.49	41	7.68	14.668	**0.0025**	17.346	0.0465
ULN10	6	7.36	8	10.03	41	9.39	--	--	6.8607	0.4514
ULN11	8	15.43	8	9.40	41	8.68	16.49	**0.0003**	7.4112	0.3776
ULN12	10	12.47	9	8.93	41	8.01	12.271	0.1149	10.428	0.1661
ULN13	8	10.40	14	11.83	41	8.38	10.54	0.0823	21.318	**0.0076**
ULN14	8	11.92	9	9.60	41	9.38	9.097	0.1860	8.3298	0.3868
ULN15	9	9.77	13	11.93	41	8.12	9.3335	0.2696	18.897	**0.0177**
ULN17	7	15.99	13	10.55	41	14.40	8.3472	0.1527	8.31	0.2132
ULN18	8	13.91	10	12.78	41	11.31	8.8917	0.2056	10.397	0.2670
ULN19	8	11.37	10	15.20	41	9.95	7.98	0.3058	15.63	**0.0126**
ULN20	3	11.08	6	14.69	41	11.82	--	--	--	--
ULN21	6	11.73	10	11.77	41	9.451	--	--	11.53	0.1654

Tables 6.11 Results of the Fligner-Killeen (FK) test for excess relative variation in the ulna of the early *H. sapiens* samples compared to the Khoe-San archaeological human sample. Significant differences ($p < 0.025$) are in bold.

Variable	MSA		EUP		Khoe-San		MSA *vs* Khoe-San FK		EUP *vs* Khoe-San FK	
	N	CV	*N*	CV	*N*	CV	*T*	*p*	*T*	*p*
ULN1	5	8.55	17	7.01	65	6.55	--	--	17.118	0.3373
ULN2	5	7.54	17	6.28	65	6.55	--	--	14.78	0.4589
ULN3	5	16.67	14	13.29	72	12.24	--	--	17.434	0.1133
ULN4	5	16.50	14	11.61	72	9.76	--	--	16.504	0.1621
ULN5	9	11.75	14	9.64	76	8.41	14.326	**0.0235**	16.498	0.1656
ULN6	8	18.03	9	11.67	73	12.20	13.3	**0.0177**	6.864	0.4107
ULN7	8	7.76	17	10.28	75	9.03	4.9917	0.2977	19.271	0.1930
ULN8	7	3.51	13	6.90	74	7.59	1.5104	0.0764	10.584	0.8286
ULN9	8	17.82	13	14.49	78	10.88	13.599	**0.0147**	14.628	0.2187
ULN10	6	7.36	8	10.03	77	8.37	--	--	9.7649	0.1652
ULN11	8	15.43	8	9.40	75	9.28	15.863	**0.0018**	7.0199	0.4561
ULN12	10	12.47	9	8.93	77	8.89	13.269	0.0946	7.5151	0.4859
ULN13	8	10.40	14	11.83	77	9.37	8.0387	0.3339	18.039	0.0908
ULN14	8	11.92	9	9.60	77	8.49	11.245	0.0750	9.6356	0.2766
ULN15	9	9.77	13	11.93	76	10.67	6.2501	0.3409	13.757	0.2856
ULN17	7	15.99	13	10.55	78	10.07	13.688	**0.0035**	11.182	0.4712
ULN18	8	13.91	10	12.78	78	11.77	9.8412	0.1599	10.155	0.3310
ULN19	8	11.37	10	15.20	78	14.54	5.9917	0.4142	12.351	0.1462
ULN20	3	11.08	6	14.69	59	9.73	--	--	--	--
ULN21	6	11.73	10	11.77	68	10.21	--	--	10.531	0.2861

Table 6.12 Results of the Fligner-Killeen (FK) test for excess relative variation in the ulna of the early *H. sapiens* samples compared to the pan-African human sample. Significant differences ($p < 0.025$) are in bold.

Variable	MSA		EUP		Pan-African		MSA *vs* Pan-African FK		EUP *vs* Pan-African FK	
	N	CV	*N*	CV	*N*	CV	*T*	*p*	*T*	*p*
ULN1	5	8.55	17	7.01	217	8.99	--	--	8.7203	0.1757
ULN2	5	7.54	17	6.28	213	9.06	--	--	6.7617	0.0824
ULN3	5	16.67	14	13.29	252	14.01	--	--	10.668	0.3282
ULN4	5	16.50	14	11.61	252	12.07	--	--	11.896	0.4271
ULN5	9	11.75	14	9.64	255	11.25	11.089	0.1922	10.063	0.2831
ULN6	8	18.03	9	11.67	250	14.20	10.835	0.1274	5.5972	0.2724
ULN7	8	7.76	17	10.28	250	11.45	2.821	0.1228	12.385	0.2610
ULN8	7	3.51	13	6.90	246	9.80	0.90425	0.0615	6.5628	0.1244
ULN9	8	17.82	13	14.49	258	11.55	15.58	**0.0063**	16.285	0.1601
ULN10	6	7.36	8	10.03	253	11.61	--	--	4.9933	0.2954
ULN11	8	15.43	8	9.40	253	11.75	11.692	0.0833	4.2473	0.2261
ULN12	10	12.47	9	8.93	259	11.41	14.101	0.0910	4.9911	0.2212
ULN13	8	10.40	14	11.83	253	11.78	5.5023	0.3476	13.775	0.4145
ULN14	8	11.92	9	9.60	257	9.83	9.5267	0.2232	7.8346	0.4982
ULN15	9	9.77	13	11.93	262	12.89	4.1608	0.1609	9.8714	0.3366
ULN17	7	15.99	13	10.55	263	12.682	10.673	0.0699	8.6217	0.2428
ULN18	8	13.91	10	12.78	271	13.65	7.0085	0.4848	7.4836	0.3657
ULN19	8	11.37	10	15.20	271	13.13	5.377	0.3342	11.434	0.2560
ULN20	3	11.08	6	14.69	211	14.18	--	--	--	--
ULN21	6	11.73	10	11.77	241	11.95	--	--	8.1969	0.4363

Table 6.13 Results of the Fligner-Killeen (FK) test for excess relative variation in the radius of the early *H. sapiens* samples compared to Zulu recent human samples. Significant differences ($p < 0.025$) are in bold.

Variable	MSA		EUP		Zulu		MSA *vs* Zulu FK		EUP *vs* Zulu FK	
	N	CV	*N*	CV	*N*	CV	*T*	*p*	*T*	*p*
RAD1	3	3.38	16	7.13	39	7.33	--	--	10.72	0.2005
RAD2	3	4.17	15	7.17	39	7.30	--	--	10.33	0.2369
RAD3	6	7.74	19	12.29	39	11.66	--	--	18.696	0.3342
RAD5	5	9.36	9	18.56	34	9.09	--	--	11.974	0.0609
RAD6	4	16.36	5	2.71	34	9.26	--	--	0.61593	0.1629
RAD7	3	13.72	7	8.84	33	9.26	--	--	5.2221	0.4566
RAD8	7	16.67	17	28.06	39	12.86	8.0756	0.1742	30.547	**0.0000**
RAD9	6	9.06	12	12.55	39	9.88	--	--	13.492	0.1760
RAD10	9	18.15	12	9.90	39	10.57	16.965	**0.0009**	9.8722	0.4572
RAD13	3	17.74	7	20.06	39	8.10	--	--	13.791	**0.0011**
RAD14	3	13.29	10	6.83	39	8.43	--	--	7.3963	0.3813
RAD15	5	11.85	8	8.35	39	9.01	--	--	5.4554	0.3592
RAD16	7	13.41	8	6.01	39	9.60	8.854	0.1097	3.5706	0.1549

Tables 6.14 Results of the Fligner-Killeen (FK) test for excess relative variation in the radius of the early *H. sapiens* samples compared to the Khoe-San archaeological human sample. Significant differences ($p < 0.025$) are in bold.

Variable	MSA		EUP		Khoe-San		MSA *vs* Khoe-San FK		EUP *vs* Khoe-San FK	
	N	CV	*N*	CV	*N*	CV	*T*	*p*	*T*	*p*
RAD1	3	3.38	16	7.13	71	6.55	--	--	15.881	0.3618
RAD2	3	4.17	15	7.17	69	6.60	--	--	15.065	0.3436
RAD3	6	7.74	19	12.29	76	10.74	--	--	21.845	0.1694
RAD5	5	9.36	9	18.56	65	8.11	--	--	14.873	**0.0137**
RAD6	4	16.36	5	2.71	65	8.20	--	--	--	--
RAD7	3	13.72	7	8.84	64	7.96	--	--	6.8844	0.3386
RAD8	7	16.67	17	28.06	78	14.35	7.1735	0.3119	33.217	**0.0000**
RAD9	6	9.06	12	12.55	77	11.71	--	--	11.382	0.4116
RAD10	9	18.15	12	9.90	78	11.36	16.191	**0.0057**	8.7642	0.3270
RAD13	3	17.74	7	20.06	67	8.00	--	--	15.566	**0.0003**
RAD14	3	13.29	10	6.83	67	7.03	--	--	8.9624	0.4533
RAD15	5	11.85	8	8.35	77	9.31	--	--	5.2755	0.3290
RAD16	7	13.41	8	6.01	78	10.89	8.9869	0.1345	3.1786	0.1348

Table 6.15 Results of the Fligner-Killeen (FK) test for excess relative variation in the radius of the early *H. sapiens* samples compared to the pan-African human sample. Significant differences ($p < 0.025$) are in bold.

Variable	MSA		EUP		Pan-African		MSA *vs* Pan-African FK		EUP *vs* Pan-African FK	
	N	CV	*N*	CV	*N*	CV	*T*	*p*	*T*	*p*
RAD1	3	3.38	16	7.13	221	9.61	--	--	6.7186	0.1097
RAD2	3	4.17	15	7.17	212	9.78	--	--	0.33965	0.1930
RAD3	6	7.74	19	12.29	254	12.35	--	--	16.799	0.4367
RAD5	5	9.36	9	18.56	198	10.79	--	--	15.208	**0.0220**
RAD6	4	16.36	5	2.71	201	10.70	--	--	--	--
RAD7	3	13.72	7	8.84	178	9.70	--	--	5.5502	0.4622
RAD8	7	16.67	17	28.06	268	14.64	7.2811	0.3342	43.402	**0.0000**
RAD9	6	9.06	12	12.55	243	11.43	--	--	12.766	0.3240
RAD10	9	18.15	12	9.90	265	15.03	10.606	0.2304	3.975	0.1166
RAD13	3	17.74	7	20.06	224	11.33	--	--	15.144	**0.0020**
RAD14	3	13.29	10	6.83	228	10.24	--	--	4.1888	0.1186
RAD15	5	11.85	8	8.35	254	12.01	--	--	3.5336	0.1692
RAD16	7	13.41	8	6.01	256	13.63	6.2511	0.4552	1.1801	0.0511

Table 6.16 Results of the Fligner-Killeen (FK) test for excess relative variation in the femur of the early *H. sapiens* samples compared to Zulu recent human samples. Significant differences ($p < 0.025$) are in bold.

Variable	MSA		EUP		Zulu		MSA *vs* Zulu FK		EUP *vs* Zulu FK	
	N	CV	*N*	CV	*N*	CV	*T*	*p*	*T*	*p*
FEM1	4	3.11	15	9.26	38	5.94	--	--	22.675	**0.0060**
FEM2	3	1.78	15	9.19	38	6.02	--	--	22.732	**0.0057**
FEM3	7	11.17	22	14.28	38	11.46	6.5554	0.3533	25.535	0.0959
FEM4	7	5.44	22	9.18	38	8.75	2.7811	0.1505	20.312	0.4481
FEM5	2	--	17	8.65	38	8.09	--	--	18.172	0.2128
FEM6	4	4.02	17	8.81	38	8.28	--	--	19.167	0.1483
FEM7	5	12.93	12	10.71	38	9.41	--	--	11.342	0.3749
FEM8	5	9.51	11	8.79	38	10.92	--	--	7.3099	0.2760
FEM9	4	7.18	9	13.15	38	7.96	--	--	16.586	**0.0013**
FEM10	5	10.23	8	10.20	38	9.97	--	--	6.6044	0.4829
FEM11	7	9.39	23	12.85	38	11.61	4.7464	0.3822	24.884	0.1766
FEM12	7	15.99	23	10.61	38	8.16	11.57	**0.0122**	28.001	0.0528
FEM13	4	20.38	17	26.25	38	22.03	--	--	17.323	0.2789
FEM14	5	9.46	9	9.05	37	8.74	--	--	8.8875	0.3121
FEM15	4	7.37	14	7.61	37	7.80	--	--	11.322	0.4154
FEM16	4	8.10	8	9.76	37	8.47	--	--	8.3392	0.2563
FEM17	5	8.92	10	8.99	38	8.10	--	--	10.979	0.2053
FEM18	7	10.37	10	10.27	38	7.38	9.0804	0.0933	14.035	0.0376

Tables 6.17 Results of the Fligner-Killeen (FK) test for excess relative variation in the femur of the early *H. sapiens* samples compared to the Khoe-San archaeological human sample. Significant differences ($p < 0.025$) are in bold.

Variable	MSA		EUP		Khoe-San		MSA *vs* Khoe-San FK		EUP *vs* Khoe-San FK	
	N	**CV**	***N***	**CV**	***N***	**CV**	***T***	***p***	***T***	***p***
FEM1	4	3.11	15	9.26	71	6.41	--	--	23.327	**0.0100**
FEM2	3	1.78	15	9.19	71	6.45	--	--	23.385	**0.0096**
FEM3	7	11.17	22	14.28	72	12.17	5.0454	0.4107	24.459	0.1959
FEM4	7	5.44	22	9.18	72	7.61	2.8898	0.1681	27.759	0.0661
FEM5	2	--	17	8.65	67	6.89	--	--	22.335	0.0575
FEM6	4	4.02	17	8.81	69	6.63	--	--	23.39	0.0360
FEM7	5	12.93	12	10.71	75	10.16	--	--	12.399	0.3127
FEM8	5	9.51	11	8.79	74	9.61	--	--	11.066	0.3406
FEM9	4	7.18	9	13.15	69	8.10	--	--	17.858	**0.0010**
FEM10	5	10.23	8	10.20	69	11.77	--	--	5.6893	0.3793
FEM11	7	9.39	23	12.85	78	8.44	6.9798	0.3354	38.591	**0.0004**
FEM12	7	15.99	23	10.61	78	8.25	13.938	**0.0027**	29.183	0.0622
FEM13	4	20.38	17	26.25	77	17.11	--	--	24.918	**0.0183**
FEM14	5	9.46	9	9.05	75	9.11	--	--	8.3527	0.4147
FEM15	4	7.37	14	7.61	70	7.13	--	--	13.397	0.4044
FEM16	4	8.10	8	9.76	60	7.36	--	--	10.431	0.1074
FEM17	5	8.92	10	8.99	72	7.35	--	--	12.181	0.1532
FEM18	7	10.37	10	10.27	78	7.59	10.944	0.0386	14.312	0.0544

Table 6.18 Results of the Fligner-Killeen (FK) test for excess relative variation in the femur of the early *H. sapiens* samples compared to the pan-African human sample. Significant differences ($p < 0.025$) are in bold.

Variable	MSA		EUP		Pan-African		MSA *vs* Pan-African FK		EUP *vs* Pan-African FK	
	N	CV	*N*	CV	*N*	CV	*T*	*p*	*T*	*p*
FEM1	4	3.11	15	9.26	213	7.97	--	--	19.621	0.1096
FEM2	3	1.78	15	9.19	211	8.05	--	--	18.247	0.1726
FEM3	7	11.17	22	14.28	254	11.46	6.3668	0.4411	30.997	0.0392
FEM4	7	5.44	22	9.18	254	10.136	1.8182	0.1042	18.484	0.3584
FEM5	2	--	17	8.65	214	9.99	--	--	12.831	0.2901
FEM6	4	4.02	17	8.81	224	10.08	--	--	12.331	0.2577
FEM7	5	12.93	12	10.71	242	10.79	--	--	12.42	0.3531
FEM8	5	9.51	11	8.79	243	10.53	--	--	7.4971	0.2882
FEM9	4	7.18	9	13.15	220	10.52	--	--	12.268	0.1148
FEM10	5	10.23	8	10.20	227	12.85	--	--	3.924	0.1988
FEM11	7	9.39	23	12.85	262	10.29	5.4876	0.4506	34.267	**0.0181**
FEM12	7	15.99	23	10.61	262	10.97	13.517	**0.0093**	20.872	0.4511
FEM13	4	20.38	17	26.25	260	21.88	--	--	22.688	0.0899
FEM14	5	9.46	9	9.05	214	10.10	--	--	6.7332	0.3831
FEM15	4	7.37	14	7.61	201	9.39	--	--	8.8801	0.2039
FEM16	4	8.10	8	9.76	188	8.70	--	--	9.3196	0.2342
FEM17	5	8.92	10	8.99	255	8.89	--	--	8.6006	0.4765
FEM18	7	10.37	10	10.27	261	9.15	7.8026	0.2773	11.322	0.2643

Table 6.19 Results of the Fligner-Killeen (FK) test for excess relative variation in the tibia of the early *H. sapiens* samples compared to Zulu recent human samples. Significant differences ($p < 0.025$) are in bold.

Variable	MSA		EUP		Zulu		MSA *vs* Zulu FK		EUP *vs* Zulu FK	
	N	CV	*N*	CV	*N*	CV	*T*	*p*	*T*	*p*
TIB1	4	10.43	10	7.87	39	7.26	--	--	8.8627	0.4384
TIB2	4	10.12	14	7.10	39	7.04	--	--	11.796	0.4637
TIB3	8	9.72	17	13.56	39	10.67	5.4871	0.3637	19.768	0.1185
TIB4	8	13.44	17	16.44	39	10.45	9.8782	0.1195	24.783	**0.0077**
TIB5	1	--	5	11.81	37	8.81	--	--	--	--
TIB6	1	--	13	8.14	37	7.76	--	--	10.95	0.4758
TIB7	2	--	7	11.61	36	9.15	--	--	7.6788	0.2090
TIB8	2	--	8	10.94	37	8.97	--	--	8.9037	0.1969
TIB9	1	--	6	10.44	37	10.47	--	--	--	--
TIB10	1	--	9	7.57	37	9.43	--	--	6.0112	0.3219
TIB11	4	9.25	15	15.60	39	10.99	--	--	22.762	**0.0057**
TIB12	4	13.06	15	16.14	39	11.30	--	--	22.17	**0.0090**
TIB13	7	5.75	17	9.11	39	7.65	3.7543	0.2513	19.237	0.1465
TIB14	6	7.84	17	8.46	39	7.59	--	--	19.667	0.1235
TIB15	3	15.88	5	6.15	39	7.09	--	--	--	--
TIB16	3	17.24	5	5.69	39	7.43	--	--	--	--
TIB17	6	7.07	8	7.60	39	8.51	--	--	5.6293	0.3823
TIB18	4	12.91	7	11.16	39	9.90	--	--	6.9873	0.2970

Tables 6.20 Results of the Fligner-Killeen (FK) test for excess relative variation in the tibia of the early *H. sapiens* samples compared to the Khoe-San archaeological human sample. Significant differences ($p < 0.025$) are in bold.

Variable	MSA		EUP		Khoe-San		MSA *vs* Khoe-San FK		EUP *vs* Khoe-San FK	
	N	CV	*N*	CV	*N*	CV	*T*	*p*	*T*	*p*
TIB1	4	10.43	10	7.87	72	6.82	--	--	11.52	0.2020
TIB2	4	10.12	14	7.10	70	6.89	--	--	13.697	0.3764
TIB3	8	9.72	17	13.56	71	11.47	5.3844	0.3426	21.219	0.0952
TIB4	8	13.44	17	16.44	71	10.34	10.85	0.0911	29.116	**0.0011**
TIB5	1	--	5	11.81	65	7.87	--	--	8.0568	0.0371
TIB6	1	--	13	8.14	64	7.39	--	--	13.029	0.6803
TIB7	2	--	7	11.61	62	6.99	--	--	13.755	**0.0025**
TIB8	2	--	8	10.94	64	8.04	--	--	9.1976	0.2041
TIB9	1	--	6	10.44	61	7.95	--	--	--	--
TIB10	1	--	9	7.57	62	8.44	--	--	5.8591	0.3005
TIB11	4	9.25	15	15.60	73	10.98	--	--	25.55	**0.0023**
TIB12	4	13.06	15	16.14	73	11.24	--	--	25.394	**0.0026**
TIB13	7	5.75	17	9.11	76	7.49	3.0952	0.1868	22.481	0.0588
TIB14	6	7.84	17	8.46	72	7.15	--	--	18.843	0.2171
TIB15	3	15.88	5	6.15	69	9.04	--	--	--	--
TIB16	3	17.24	5	5.69	71	9.23	--	--	--	--
TIB17	6	7.07	8	7.60	72	8.61	--	--	6.1338	0.4334
TIB18	4	12.91	7	11.16	73	9.61	--	--	8.1562	0.2022

Table 6.21 Results of the Fligner-Killeen (FK) test for excess relative variation in the tibia of the early *H. sapiens* samples compared to the pan-African human sample. Significant differences ($p < 0.025$) are in bold.

Variable	MSA		EUP		Pan-African		MSA *vs* Pan-African FK		EUP *vs* Pan-African FK	
	N	CV	*N*	CV	*N*	CV	*T*	*p*	*T*	*p*
TIB1	4	10.43	10	7.87	212	8.34	--	--	7.354	0.3547
TIB2	4	10.12	14	7.10	207	8.21	--	--	9.5106	0.2446
TIB3	8	9.72	17	13.56	250	12.73	4.5092	0.2493	19.323	0.2426
TIB4	8	13.44	17	16.44	250	11.69	9.648	0.2124	31.051	**0.0015**
TIB5	1	--	5	11.81	192	9.96	--	--	--	--
TIB6	1	--	13	8.14	194	9.12	--	--	10.091	0.3565
TIB7	2	--	7	11.61	185	9.75	--	--	8.3073	0.2202
TIB8	2	--	8	10.94	189	10.47	--	--	6.8736	0.4955
TIB9	1	--	6	10.44	185	9.71	--	--	--	--
TIB10	1	--	9	7.57	187	10.64	--	--	4.2352	0.1640
TIB11	4	9.25	15	15.60	250	12.30	--	--	24.841	**0.0113**
TIB12	4	13.06	15	16.14	250	12.25	--	--	24.982	**0.0105**
TIB13	7	5.75	17	9.11	231	9.70	1.8945	0.1079	14.044	0.3751
TIB14	6	7.84	17	8.46	221	9.42	--	--	12.587	0.2740
TIB15	3	15.88	5	6.15	215	10.95	--	--	--	--
TIB16	3	17.24	5	5.69	222	11.24	--	--	--	--
TIB17	6	7.07	8	7.60	248	9.72	--	--	4.2939	0.2299
TIB18	4	12.91	7	11.16	250	10.63	--	--	6.7131	0.3989

Table 6.22 Results of the Fligner-Killeen (FK) test for excess relative variation in the humerus of the MSA early *H. sapiens* sample compared to the EUP early *H. sapiens* sample. Significant differences ($p < 0.025$) are in bold.

Variable	MSA		EUP		MSA *vs* EUP FK	
	N	CV	*N*	CV	*T*	*p*
HUM1	3	6.60	18	7.42	--	--
HUM2	3	7.01	17	6.76	--	--
HUM3	8	10.31	20	13.65	5.7518	0.4212
HUM4	8	14.02	20	11.10	8.9227	0.1417
HUM5	4	7.78	15	8.22	--	--
HUM6	3	0.56	13	9.12	--	--
HUM9	1	--	8	15.63	--	--
HUM11	6	9.44	16	7.21	--	--
HUM12	6	10.76	17	6.81	--	--
HUM13	6	16.86	12	7.06	--	--
HUM14	7	10.78	7	12.56	4.6807	0.4405
HUM15	6	16.34	12	19.76	--	--
HUM17	6	11.28	11	10.06	--	--
HUM18	6	11.07	11	12.67	--	--
HUM19	6	24.56	12	8.56	--	--
HUM20	6	18.48	12	21.29	--	--
HUM21	5	23.08	13	12.34	--	--
HUM23	3	7.15	7	10.20	--	--
HUM24	3	6.18	6	11.71	--	--
HUM25	7	12.81	21	10.42	7.2214	0.2100

Table 6.23 Results of the Fligner-Killeen (FK) test for excess relative variation in the ulna of the MSA early *H. sapiens* sample compared to the EUP early *H. sapiens* sample. Significant differences ($p < 0.025$) are in bold.

Variable	MSA		EUP		MSA *vs* EUP FK	
	N	CV	*N*	CV	*T*	*p*
ULN1	5	8.55	17	7.01	--	--
ULN2	5	7.54	17	6.28	--	--
ULN3	5	16.67	14	13.29	--	--
ULN4	5	16.50	14	11.61	--	--
ULN5	9	11.75	14	9.64	8.9168	0.2102
ULN6	8	18.03	9	11.67	9.1025	0.0499
ULN7	8	7.76	17	10.28	3.0652	0.1910
ULN8	7	3.51	13	6.90	2.4057	0.1821
ULN9	8	17.82	13	14.49	7.4824	0.2607
ULN10	6	7.36	8	10.03	--	--
ULN11	8	15.43	8	9.40	2.6575	0.0415
ULN12	10	12.47	9	8.93	6.1845	0.3754
ULN13	8	10.40	14	11.83	5.0077	0.3140
ULN14	8	11.92	9	9.60	7.275	0.2413
ULN15	9	9.77	13	11.93	5.1722	0.2186
ULN17	7	15.99	13	10.55	9.0714	0.0302
ULN18	8	13.91	10	12.78	6.1395	0.4642
ULN19	8	11.37	10	15.20	5.2371	0.3602
ULN20	3	11.08	6	14.69	--	--
ULN21	6	11.73	10	11.77	--	--

Table 6.24 Results of the Fligner-Killeen (FK) test for excess relative variation in the radius of the MSA early *H. sapiens* sample compared to the EUP early *H. sapiens* sample. Significant differences ($p < 0.025$) are in bold.

Variable	MSA		EUP		MSA *vs* EUP FK	
	N	**CV**	***N***	**CV**	***T***	***p***
RAD1	3	3.38	16	7.13	--	--
RAD2	3	4.17	15	7.17	--	--
RAD3	6	7.74	19	12.29	--	--
RAD5	5	9.36	9	18.56	--	--
RAD6	4	16.36	5	2.71	--	--
RAD7	3	13.72	7	8.84	--	--
RAD8	7	16.67	17	28.06	2.4755	0.1060
RAD9	6	9.06	12	12.55	--	--
RAD10	9	18.15	12	9.90	13.118	**0.0031**
RAD13	3	17.74	7	20.06	--	--
RAD14	3	13.29	10	6.83	--	--
RAD15	5	11.85	8	8.35	--	--
RAD16	7	13.41	8	6.01	7.2427	0.0912

Table 6.25 Results of the Fligner-Killeen (FK) test for excess relative variation in the femur of the MSA early *H. sapiens* sample compared to the EUP early *H. sapiens* sample. Significant differences ($p < 0.025$) are in bold.

Variable	MSA		EUP		MSA *vs* EUP FK	
	N	**CV**	***N***	**CV**	***T***	***p***
FEM1	4	3.11	15	9.26	--	--
FEM2	3	1.78	15	9.19	--	--
FEM3	7	11.17	22	14.28	4.5396	0.3641
FEM4	7	5.44	22	9.18	2.0714	0.1683
FEM5	2	--	17	8.65	--	--
FEM6	4	4.02	17	8.81	--	--
FEM7	5	12.93	12	10.71	--	--
FEM8	5	9.51	11	8.79	--	--
FEM9	4	7.18	9	13.15	--	--
FEM10	5	10.23	8	10.20	--	--
FEM11	7	9.39	23	12.85	2.7941	0.1419
FEM12	7	15.99	23	10.61	8.5584	0.0950
FEM13	4	20.38	17	26.25	--	--
FEM14	5	9.46	9	9.05	--	--
FEM15	4	7.37	14	7.61	--	--
FEM16	4	8.10	8	9.76	--	--
FEM17	5	8.92	10	8.99	--	--
FEM18	7	10.37	10	10.27	4.7282	0.4288

Table 6.26 Results of the Fligner-Killeen (FK) test for excess relative variation in the tibia of the MSA early *H. sapiens* sample compared to the EUP early *H. sapiens* sample. Significant differences ($p < 0.025$) are in bold.

Variable	MSA		EUP		MSA *vs* EUP FK	
	N	**CV**	***N***	**CV**	***T***	***p***
TIB1	4	10.43	10	7.87	--	--
TIB2	4	10.12	14	7.10	--	--
TIB3	8	9.72	17	13.56	3.7553	0.1548
TIB4	8	13.44	17	16.44	4.0099	0.1815
TIB5	1	--	5	11.81	--	--
TIB6	1	--	13	8.14	--	--
TIB7	2	--	7	11.61	--	--
TIB8	2	--	8	10.94	--	--
TIB9	1	--	6	10.44	--	--
TIB10	1	--	9	7.57	--	--
TIB11	4	9.25	15	15.60	--	--
TIB12	4	13.06	15	16.14	--	--
TIB13	7	5.75	17	9.11	3.6047	0.2281
TIB14	6	7.84	17	8.46	--	--
TIB15	3	15.88	5	6.15	--	--
TIB16	3	17.24	5	5.69	--	--
TIB17	6	7.07	8	7.60	--	--
TIB18	4	12.91	7	11.16	--	--

Chapter 7

Summary and Conclusions

Introduction

The study of phenotypic variation can help elucidate the various influences that have shaped modern within-population diversity (Relethford, 1994; Ackermann, 2002; Ackermann and Cheverud, 2002; Gunz et al., 2009), and provides another line of evidence to compliment molecular research on human evolution. Moreover, because modern samples are commonly employed as reference samples to help reconstruct phenetic and taxonomic hominin relationships, and provide a framework for interpreting diversity in the fossil record, our assumptions, implicit or not, regarding skeletal variation today and in the past need to be explicitly tested (Ackermann, 2003). The primary aim of this dissertation has been to contribute to a deeper understanding of intra-population diversity in modern and prehistoric *H. sapiens* by focusing on the magnitude and pattern of variability in the major long bones of the appendicular skeleton.

Classification of Sex Using Fragmentary Os Coxae

In order to understand the relationship between the level of sexual dimorphism and morphometric variability within a skeletal sample, reliable methods are necessary to diagnose sex. In Chapter 3, the accuracy of Bruzek's Visual Method (2002) and Discriminant Function Analysis of the central and

posterior os coxae was tested in order to assess the appropriateness of these methods for classifying sex in modern Africans, and in prehistoric samples where sex is undocumented and preservation is poor. The Visual Method is simple and relatively quick, but the results of Chapter 3 demonstrate that a reliance on non-metric features alone leads to a substantial loss of accuracy in sexing modern Zulu and Kikuyu individuals compared to the morphometric discriminant analysis of partial os coxae in these same populations. The most reliable discriminant function developed for use on the mixed African sample (i.e., Zulu and Kikuyu pooled) achieves an accuracy of 92.8%, compared to only 82.6% using the visual method. The poor performance of the Visual Method in this study may reflect differences in patterns of dimorphism between Africans and the European populations on which the method was developed.

The most effective discriminant function for classify sex in the modern sub-Saharan Africans sampled in this study employs two measurements of the pelvis (width and depth of the sciatic notch), and renders them dimensionless by scaling each measurement using the geometric mean computed from another pair of pelvic measurements (acetabular width and posterior acetabular ischial length) (Darroch and Mosimann, 1985). The resulting sexing function thus emphasizes shape rather than size differences to classify sex. Therefore, this function may be effectively applied to the problem of diagnosing sex from skeletal remains in humans that differ in body size and shape, and that exhibit different levels of postcranial robusticity. Furthermore, because the method requires only four measurements of the pelvis, this approach can be fruitfully applied to paleontological, archaeological and forensic situations where skeletal preservation may be less than ideal. Sliding calipers, a few minutes of time, a basic knowledge of osteology, and access to statistics software are needed to perform this sexing method, making it comparably simple and quick as the Visual Method. Therefore, in accuracy, ease of use, and breadth of applicability, the discriminant

function method developed here is recommended to scoring methods based on non-metric traits for classifying sex from os coxae.

In Chapter 4, the best-performing discriminant functions developed for modern Africans were used to classify sex in the prehistoric human samples from the terminal Pleistocene and early Holocene of Africa (the Khoe-San from South Africa, Epipaleolithic humans from northern Sudan and Taforalt in Morocco). In addition, the discriminant functions developed to diagnose sex in modern Zulu and Kikuyu based on the size and shape of the os coxae were also applied to early *H. sapiens* fossils from the Late Pleistocene of Africa, the Levant, and Europe. For most fossils, an unambiguous signal for the classification of sex was apparent from the results of different discriminant analyses. The morphometric analyses were complimented by a visual assessment of sex based on the majority score of non-metric characters following Bruzek's (2002) method, in order to assess the utility of this method for fossil humans, and provide a tentative diagnosis of sex in cases where the os coxae is too fragmentary for sexing from discrimiant analyses. The morphometric diagnosis of sex was commonly in accordance with the visual determination of sex, despite the results of Chapter 3 which suggest that the latter method may be unreliable in Africans. The congruence of sexing results suggests that a visual, non-metric classification may be reliably employed in early *H. sapiens* when insufficient portions of the os coxae are preserved to allow a more detailed and rigorous morphometric diagnosis.

Importantly, this dissertation provides the first conclusive diagnosis of sex for Omo I, which at ca. 195 ka BP is the earliest *H. sapiens* fossil recovered to date (Day, 1969; McDougall et al., 2005). No analysis had been previously published to determine the sex of this specimen, possibly due to its fragmentary preservation and the lack of pelvis remains, or from observations of its large size and robusticity which may have fostered an informal assumption among some workers that Omo I was male. However, the recent discovery of a partial left os

coxae attributed to Omo I during renewed exploration of the Kibish Formation in southwestern Ethiopia (Pearson et al., 2008b) raised the question of sex. In describing the partial postcranial skeleton of Omo I, Pearson et al. reported a mosaic of male and female features. The male features of the pelvis reflect its large size and marked robusticity, while the female features include a wide sciatic notch and a preauricular sulcus. The results of discriminant analyses of the new fragmentary os coxae in Chapter 4 overwhelmingly classify Omo I as female whether the shape or form of the pelvis is considered. A female diagnosis is also supported by the majority score obtained from non-metric pelvic characters. These results raise the possibility that the marked morphological differences documented in the skulls of Omo I and Omo 2 (Day, 1969; Day and Stringer, 1982; Klein, 1999) may reflect a higher level and different pattern of sexual dimorphism in early *H. sapiens* during the Late Pleistocene, as suggested by the magnitude of size variation in mandibles and molars from Klasies River in South Africa (Royer et al., 2009).

From the consensus diagnosis of sex obtained in Chapter 4, supplemented by the classification of sex proposed by other workers for those specimens that could not be analyzed here due to poor preservation of the os coxae, a substantial portion of the early *H. sapiens* pre-dating 25 ka BP were sexed. Among MSA early *H. sapiens*, four fossils are classified as female (Omo I, Qafzeh 3, Skhūl 2 and 7) and seven as male (Skhūl 3, 4, 5, 6, and 9, Qafzeh 8 and 9), while unassociated postcrania from six localities could not be classified due to poor preservation (AHS tibia, Border Cave humerus, Cave of Hearths radius, Klasies River ulna and radius, KNM-ER 999 femur, and Qafzeh 7 ulna). Among EUP early *H. sapiens*, six fossils are classified as female (Grotte des Enfants 5, Mladeč 21, Gro-Magnon 2, Dolní Věstonice 3, Predmostí 4 and 10) and seventeen as male (Barma Grande 2, Grotte des Enfants 4, Nazlet Khater 2, Paviland 1, Cro-Magnon 1 and 4315, Dolní Věstonice 13, 14, and 16, Pavlol 1, Mladeč 22, Predmostí 1, 3,

9, and 14), while one skeleton (Grotte du Cavillon 1) is diagnosed as indeterminate along with unassociated postcranial remains from Cro-Magnon, Dolní Věstonice, and Mladeč.

In addition, the results of Chapter 4 demonstrate that several early *H. sapiens* individuals are characterized by extreme male or female morphology of the central and posterior os coxae relative to modern sub-Saharan Africans from at least two different populations. This may reflect skeletal differences that have accrued in humans since the Late Pleistocene (Hager, 1989), although not all early *H. sapiens* exhibit atypical pelvis morphology compared to modern Africans. Thus, these results are also suggestive of the greater diversity comprised within early *H. sapiens* populations, since some but not all contemporaneous fossils from the same locality are considered atypical by modern standards.

Appendicular Variation in Recent Sub-Saharan Africans

Chapter 5 of this dissertation contributes a detailed comparison of the level and pattern of morphometric variation in the appendicular skeleton of three modern sub-Saharan human populations, the Zulu from South Africa, the Kikuyu from Kenya, and Nilotic tribes from northern Uganda. The African populations studied here generally exhibit a similar magnitude and pattern of variation. Furthermore, the results of Chapter 6 suggest that populations of prehistoric humans from the terminal Pleistocene and early Holocene of Africa exhibit an equal magnitude of variation in the major long bones of appendicular skeleton relative to modern Africans, despite the fact that these ancient human populations are sampled from archaeological contexts spanning roughly 10,000 years. This demonstrates that the level of phenotypic variability within a sample does not necessarily increase simply as a function of time. Moreover, these results confirm that present-day levels of mophometric diversity also characterized African

populations in the terminal Pleistocene, suggesting that major bottlenecks must have occurred prior to this time (e.g., Manica et al., 2007).

The isolation by distance model, supported by the global patterning of genetic as well as craniometric diversity within modern human populations, predicts that African populations should exhibit greater variability than non-Africans. Further work using a broad distribution of samples from around the globe is needed to test this prediction in the appendicular skeleton. However, given the clear patterning of modern phenotypic diversity, paleoanthropological studies employ caution in the choice of human reference samples because equality of variation cannot be assumed (van Vark, 1984; van Vark and Schaafsma, 1992; Ackermann, 2003, 2005). Minimally, there appears to be dichotomy in the magnitude of variation encompassed by African and non-African populations, and samples drawn from these groups may comprise different baseline measures for current human diversity.

Moreover, the results of Chapter 5 suggest that important differences in phenotypic variability exist among the sexes even within sub-Saharan Africa. While males from three populations were very similar in the magnitude and pattern of postcranial variation, substantially differences were documented between females of the Zulu and Kikuyu tribes. Kikuyu females exhibited a greater magnitude of variation in numerous measurements of the joints and diaphyses of the five major long bones relative to Zulu females. The Kikuyu females also show a trend for greater variation than males from this population, while the opposite is true among the Zulu. Patterns of unequal diversity between the sexes have been identified in studies of mtDNA, which is maternally inherited, and the Y-chromosome, which reflects paternal heritage (Wood et al., 2005; Castri et al., 2009; Coia et al., 2009). Such differences may reflect a sex-bias in demographic processes, including unidirectional migration and/or dispersal that could influence gene flow between groups (Destro-Bisol et al.,

2004). A sex bias might be caused by population-specific sociocultural factors. For example, the elevated variability of Kikuyu females relative to Kikuyu males may reflect a tendency for men from this tribe to marry women from neighboring Bantu tribes or even of non-Bantu origin. The pattern of equal variation in males but not females requires further study across a wider range of populations, although preliminary comparisons suggest that males tend to have more constrained variability than females.

Finally, the results of Chapter 5 demonstrate that although both the Zulu and Kikuyu are characterized by sexual dimorphism on the order of roughly 10% across the five major long bones, only a few cases of dimorphism in variation were documented. Thus, while sexual dimorphism can contribute to the level of phenotypic variability within a population, it is not the only factor involved. As noted above, although dimorphism in variation is not common among either the Zulu or the Kikuyu, the direction of differences presented a clear pattern: in the Zulu, males always exhibit an excess of variation compared to the females, while in the Kikuyu, females always exhibit more variation than the males. This pattern suggests that different factors, likely related to differences in demographic history stemming for the influence of sociocultural factors, have influenced levels of skeletal variation (and presumably genetic variation) in males and females.

Appendicular Variation in Prehistoric Humans

The first goal of Chapter 6 was to test for the equality of morphometric variation in the appendicular skeleton between a recent African sample – the Zulu – and several African samples of archaeological origin spanning the terminal Pleistocene and Holocene. Despite a time span of roughly 10,000 years represented by these samples, none of them is characterized by a greater magnitude of variation than the modern Zulu. Importantly, these results

demonstrate that sample variability does not necessarily increase as a function of the time averaging of the sample. Furthermore, these findings suggest that modern levels of within-population skeletal variability in the appendicular skeleton extend into the terminal Pleistocene and early Holocene in Africa. Thus, if the diversity observed among living peoples has been reduced due to bottlenecks or other major demographic crises, as suggested by studies of modern intra-population diversity on a global scale (e.g., Ambrose, 1998; Excoffier, 2002; Marth et al., 2003; Manica et al., 2007), then such event(s) seem to have occurred prior to the end of the Pleistocene.

In Chapter 6, the magnitude of morphometric variability in the appendicular skeleton of two samples of early *Homo sapiens* was also evaluated: Middle Stone Age specimens from African and the Levant approximately 195 to 60 ka BP, and Early Upper Paleolithic specimens from Egypt and Europe approximately 38 to 25 ka BP. Specifically, the goal of Chapter 6 was to determine whether early *H. sapiens* fossils exhibit an excess of morphometric variation relative to modern humans, as suggested by many workers (Howells, 1989; Lahr, 1996; Trinkaus, 2005; Gunz et al., 2009). This is important because the study of skeletal morphometric variability can provide insights into past genetic diversity and the evolutionary forces and other influences that have shaped the human lineage. The results also have serious implications from a methodological perspective.

In general, the findings from Chapter 6 support craniometric studies which suggest that the range of morphological variation exhibited by modern humans (including populations from the terminal Pleistocene and early Holocene) underestimates the diversity present within our species during the Late Pleistocene. In the postcranial skeleton, a surplus of variation relative to today's baseline level has been documented in numerous articular and diaphyseal dimensions of the major long bones across both older early *H. sapiens* from the

MSA of Africa and the Levant, as well as in early Upper Paleolithic humans from Europe and North Africa. These findings further bracket the timming of events believed to have reduced within-population diversity to between ca. 25 to 14 ka BP.

Furthermore, elevated variability among the MSA and EUP fossil samples is maintained even in comparison to archaeological and pan-African samples that comprise over 10,000 years, providing evidence that the effects of time averaging may be insufficient to account for the increase of within-sample variation. Additionally, if sample variability accrued through time averaging, one would expect that the MSA fossil sample – comprised of specimens spanning more than 100 ka – should exhibit more variation than the EUP fossil sample, which spans a little over 10 ka. This is not the case. Despite marked differences in the temporal depth of the early *H. sapiens* samples studied here, the results demonstrate that both Late Pleistocene groups exhibited a surplus of morphometric variability compared to the modern humans in some, but not all, aspects of the appendicular skeleton, but that neither fossil sample is more variable than the other. Importantly, these findings further demonstrate that within-sample variability does not increase simply as a function of a sample's temporal or geographic depth.

Elevated variability among the MSA, whether compared to the Zulu, Khoe-San, or pan-African sample, is primarily found in joint surfaces, while the EUP sample shows increased variability predominantly in diaphyseal dimensions such as shaft diameters and circumferences, with fewer joints exhibiting high variation. Moreover, the MSA sample exhibits more instances of elevated variability in the upper limb compared to the lower limb, and in distal limb elements (i.e., ulna, radius, and tibia) compared to proximal limb elements (i.e., humerus and femur). In contrast, the patterning of elevated variation appears to be more randomly distributed in the EUP sample. These differences suggest that

different factors may have influenced the magnitude of morphometric variability in these two Late Pleistocene samples.

Since joints appear to be less sensitive to external stimuli than diaphyseal dimensions, the elevated variability of the MSA sample may reflect the greater genetic diversity of this group. In contrast, the EUP fossils show increased variability in both shafts and joints, which might reflect the diversity of environments encountered by these individuals as well as the genetic diversity of the group. A greater expression of sexual dimorphism may also contribute to elevated variability in the Late Pleistocene. Such interpretations will remain speculative until additional research provides a better understanding of the genetic correlates of skeletal traits, as well as the influence of ecogeography on skeletal variability. However, patterns of variability like the ones documented here offer a clear potential for insights onto the evolutionary and historical processes that have shaped our species.

Moreover, these findings demonstrate that equality of phenotypic variation, whether in terms of the magnitude or patterning of the variation, cannot simply be assumed between modern and past human populations, even early representatives of our own species. Although the equality of variance/covariance matrices was not directly tested here, an elevated magnitude of appendicular variability in the past provides preliminary evidence for differences in variation between extant and extinct humans. This may have critical implications for the selection and use of modern analogs in paleoanthropology because many methods rely on the implicit assumption that modern and fossil hominins are characterized by a similar magnitude and pattern of morphological variation. Inequality of variation, as documented here between modern populations and early *H. sapiens* samples, may adversely affect the results and create unrecognized biases in many commonly used methods that rely on covariance matrices such as Canonical Variates Analysis and Mahalanobis (D^2) distances (e.g., Ackermann, 2003).

Conclusions

The focus of this dissertation has been to broaden our knowledge of population-level diversity in modern and prehistoric *H. sapiens* by focusing on the magnitude and pattern of variability in the appendicular skeleton. This endeavor has elucidated some of the factors that have influenced the pattern of modern-day diversity, and has produced results which are generally consistent with prior craniometric and molecular research on the topic. Future research is needed to expanding our understanding of the ways in which modern and prehistoric humans differed in both the magnitude and patterning of phenotypic variation as evinced by different aspects of the skeleton, as this can elucidate the major evolutionary and demographic events that have shaped *H. sapiens* across the transition to modernity.

References Cited

Abdi H. 2007. The Bonferonni and Sidak corrections for multiple comparisons. In: Salkind N, editor. Encyclopedia of Measurement and Statistics. Thousand Oaks, CA: Sage.

Abella Roth E. 1992. Applications of demographic models to paleodemography. In: Saunders SR, and Katzenberg MA, editors. Skeletal Biology of Past Peoples: Research Methods. New York: Wiley-Liss Inc. p 175-188.

Ackermann RR. 1998. A quantitative assessment of variability in the australopithecine, human, chimpanzee, and gorilla face [PhD dissertation]. Saint Louis, Missouri: Washington University. 177 p.

Ackermann RR. 2002. Patterns of covariation in the hominoid craniofacial skeleton: implications for paleoanthropological models. J Hum Evol 42:167-187.

Ackermann RR. 2003. Using extant morphological variation to understand fossil relationships: a cautionary tale. S Afr J Sci 99:255-258.

Ackermann RR. 2005. Variation in Neandertals: a response to Harvati (2003). J Hum Evol 48:643-646.

Ackermann RR, Cheverud JM. 2002. Discerning evolutionary processes in patterns of Tamarin (Genus *Saguinus*) craniofacial variation. Am J Phys Anthropol 117:260-271.

Ackermann RR, Cheverud JM. 2004. Detecting genetic drift versus selection in human evolution. Proc Nat Acad Sci USA 101(52):17946-17951.

Aitken MJ, Valladas H. 1992. Luminescence dating relevant to human origins. Phil Trans Biol Sci B 337:139-144.

Aldhouse-Green S. 2000. Paviland Cave and the "Red Lady". Bristol: Western Academic & Specialist Press Ltd.

Ambrose SH. 1998. Late Pleistocene human population bottlenecks, volcanic winter, and differentiation of modern humans. J Hum Evol 34:623-651.

Arsuaga JL, Carretero J-M. 1994. Multivariate analysis of the sexual dimorphism of the hip bone in a modern human population and early hominids. Am J Phys Anthropol 93:241-257.

Bar-Yosef O. 1996. Modern humans, Neanderthals and the Middle/Upper Paleolithic transition in Western Asia. In: Bar-Yosef O et al., editors. Colloquia of the XIII International Congress of Prehistoric and Protohistoric Sciences. p 175-190.

Bar-Yosef O. 2000. The Middle and Early Upper Paleolithic in southwest Asia and neighboring regions. In: Bar-Yosef O, and Pilbeam D, editors. The Geography of Neandertals and Modern Humans in Europe and the Greater Mediterranean. Cambridge, MA: Peabody Museum of Archaeology and Ethnology. p 107-156.

Beaumont PB, De Villiers H, Vogel JC. 1978. Modern man in sub-Saharan Africa prior to 49,000 years BP: A review and evaluation with particular reference to Border Cave. S Afr J Sci 74:409-419.

Betti L, Balloux F, Amos W, Hanihara T, Manica A. 2009. Distance from Africa, not climate, explains within-population phenotypic diversity in humans. Proc R Soc B 276:809-814.

Bird MI, Fifield LK, Stanos GM, Beaumont PB, Zhou Y, di Tada ML, Hausladen PA. 2003. Radiocarbon dating from 40 to 60 ka BP at Border Cave, South Africa. Quat Sci Rev 22:943-947.

Bisson MS, Tisnerat N, White R. 1996. Radiocarbon dates from the Upper Paleolithic of the Barma Grande. Curr Anthropol 37(1):156-162.

Bonnet C. 1992. Excavations at the Nubian royal town of Kerma: 1975-91. Antiquity 66:611-625.

Bouzouggar A, Barton RNE, Blockley S, Bronk-Ramsey C, Collcutt SN, Gale R, Higham TFG, Humphrey LT, Parfitt SA, Turner E and others. 2008.

Reevaluating the age of the Iberomaurusian in Morocco. Afr Archaeol Rev 25:3-19.

Bräuer G. 1984. A craniological approach to the origin of anatomically modern *Homo sapiens* in Africa and implications for the appearance of modern Europeans. In: Smith FH, and Spencer F, editors. The Origins of Modern Humans: A World Survey of the Fossil Evidence. New York: Alan R. Liss, Inc. p 327-410.

Bräuer G, Rimbach KW. 1990. Late archaic and modern *Homo sapiens* from Europe, Africa, and southwest Asia: Craniometric comparisons and phylogenetic implications. J Hum Evol 19:789-807.

Bräuer G, Singer R. 1996a. The Klasies zygomatic bone: archaic or modern? J Hum Evol 30:161-165.

Bräuer G, Singer R. 1996b. Not outside the modern range. J Hum Evol 30:173-174.

Bräuer G, Yokoyama Y, Falgueres C, Mbua E. 1997. Modern human origins backdated. Nature 386:337-338.

Broca P. 1868. Sure les crânes et les ossements des Eyzies. Bull Soc Anthropol Paris 3:350-392.

Bruzek J. 2002. A method for visual determination of sex, using the human hip bone. Am J Phys Anthropol 117:157-168.

Buikstra JE, Ubelaker DH. 1994. Standards for Data Collection from Human Skeletal Remains. Fayetteville, Arkansas: Arkansas Archeological Survey.

Cann RL, Stoneking M, Wilson AC. 1987. Mitochondrial DNA and human evolution. Nature 325:31-36.

Carto SL, Weaver TD, Hetherington R, Lam YM, Wiebe EC. 2009. Out of Africa and into an ice age: on the role of global climate change in the late Pleistocene migration of early modern humans out of Africa. J Hum Evol 56:139-151.

Castri L, Tofanelli S, Garagnani P, Bini C, Fosella X, Pelotti S, Paoli G, Pettener D, Luiselli D. 2009. mtDNA variability in two Bantu-speaking

populations (Shona and Hutu) from eastern Africa: implications for the peopling and migration patterns in sub-Saharan Africa. Am J Phys Anthropol Early View:xxx-xxx.

Chami FA. 2001. A response to Christopher Ehret's "Bantu Expansions". Int J Afr Hist Stud 34:647-651.

Churchill SE, Formicola V. 1997. A case of marked bilateral asymmetry in the upper limbs of an Upper Palaeolithic male from Barma Grande (Liguria), Italy. Int J Osteoarch 7:18-38.

Churchill SE, Pearson OM, Grine FE, Trinkaus E, Holliday TW. 1996. Morphological affinities of the proximal ulna from Klasies River Mouth Main Site: archaic or modern? J Hum Evol 31:213-237.

Churchill SE, Smith FH. 2000. Makers of the Early Aurignacian of Europe. Yrbk Phys Anthropol 43:61-115.

Coia V, Brisighelli F, Donati F, Pascali V, Boschi I, Luiselli D, Battaggia C, Batini C, Taglioli L, Cruciani F and others. 2009. A multi-perspective view of genetic variation in Cameroon. Am J Phys Anthropol Early View:xxx-xxx.

Coleman WH. 1969. Sex differences in the growth of the human bony pelvis. Am J Phys Anthropol 31:125-151.

Conard NJ, Bolus M. 2003. Radiocarbon dating the appearance of modern humans and timing of cultural innovations in Europe: new results and new challenges. J Hum Evol 44:331-371.

Coon CS. 1962. The Origin of Races. New York: Knopf.

Corruccini RS. 1987. Shape in morphometrics: comparative analyses. Am J Phys Anthropol 73:289-303.

Corruccini RS. 1992. Metrical reconsideration of the Skhūl IV and IX and Border Cave 1 crania in the context of modern human origins. Am J Phys Anthropol 87:433-445.

Crevecoeur I. 2006. Étude anthropologique des restes humains de Nazlet Khater 2 (Paléolithique superieur, Egypte) [Thèse doctorale]. Bordeaux, France: Université Bordeaux I. 466 p.

Crevecoeur I, Villotte S. 2007. The Nazlet Khater 2 palaeopathologies: Correlation with mining activities during the Early Upper Palaeolithic in Egypt. Paleoanthropology Society Annual Meeting (poster session). Philadelphia, PA.

Crevecoeur I, Rougier H, Grine F, Froment A. 2009. Modern human cranial diversity in the Late Pleistocene of Africa and Eurasia: Evidence from Nazlet Khater, Peştera cu Oase, and Hofmeyr. Am J Phys Anthropol Early View:xxx-xxx.

Cox M, Scott A. 1992. Evaluation of the obstetric significance of some pelvic characters in an 18th century British sample of known parity status. Am J Phys Anthropol 89:431-449.

Darroch JN, Mosimann JE. 1985. Canonical and principal components of shape. Biometrika 72(2):241-252.

Day MH. 1969. Omo human skeletal remains. Nature 222:1135-1138.

Day MH, Leakey REF. 1974. New evidence of the genus *Homo* from East Rudolf, Kenya (III). Am J Phys Anthropol 41:367-380.

Day MH, Stringer CB. 1982. A reconsideration of the Omo Kibish remains and the erectus-sapiens transition. In: de Lumley H, editor. L'Homo erectus et la place de l'homme de Tautavel parmi les Hominides fossiles. Nice: Louis-Jean Scientific and Literary Publ. p 814-846.

Deacon HJ, Geleijnse VB. 1988. The stratigraphy and sedimentology of the Main Site sequence, Klasies River, South Africa. S Afri Arch Bull 43:5-14.

de Sonneville-Bordes D. 1960. Le Paléolithique Supérieur en Périgord. Bordeaux: Delmas.

Destro-Bisol G, Donati F, Coia V, Boschi I, Verginelli F, Caglia A, Tofanelli S, Spedini G, Capelli C. 2004. Variation of female and male lineages in sub-Saharan populations: the importance of sociocultural factors. Mol Biol Evol 21:1673-1682.

Disotell TR. 1999a. Human evolution: origins of modern humans still look recent. Curr Biol 9:R647-R650.

Disotell TR. 1999b. Human evolution: sex-specific contributions to genome variation. Curr Biol 9:R29-31.

Disotell TR. 1999c. Human evolution: the southern route to Asia. Curr Biol 9:R925-R928.

Donnelly SM, Kramer A. 1999. Testing for multiple species in fossil samples: an evaluation and comparison of tests for equal relative variation. Am J Phys Anthropol 108:507-529.

Duarte C, Mauricio J, Pattitt PB, Souto P, Trinkaus E, van der Plicht H, Zilhao J. 1999. The early Upper Paleolithic human skeleton from the Abrigo do Lagar Velho (Portugal) and modern human emergence in Iberia. Proc Nat Acad Sci USA 96:7604-7609.

Edgar HJH, Hunley KL. 2009. Race reconciled?: How biological anthropologists view human variation. Am J Phys Anthropol 139:1-4.

Ehret C. 2001. Bantu expansion: re-envisioning a central problem of early African history. Int J Afr Hist Stud 34:5-41.

Eveleth PB. 1975. Differences between ethnic groups in sex dimorphism of adult heights. Ann Hum Biol 2:35-39.

Excoffier L. 2002. Human demographic history: refining the recent African origin model. Curr Op Genet Dev 12:675-682.

Ferembach D. 1962. La Nécropole Epipaleolithique de Taforalt (Maroc Oriental): Étude des squelettes humains. Paris: Centre national de la recherche scientifique en mission universitaire et culturelle française au Maroc.

Ferembach D, Schwidetzky I, Stloukal M. 1980. Recommendations for age and sex diagnoses of skeletons. J Hum Evol 9:517-549.

Formicola V, Pettitt PB, del Lucchese A. 2004. A direct AMS radiocarbon date on the Barma Grande 6 Upper Paleolithic skeleton. Curr Anthropol 45:114-118.

Formicola V, Pontrandolfi A, Svoboda J. 2001. The Upper Paleolithic triple burial of Dolní Věstonice: pathology and funerary behavior. Amer J Archaeol 115:372-379.

Franklin D, O'Higgins P, Oxnard CE. 2008. Sexual dimorphism in the mandible of indigenous South Africans: A geometric morphometric approach. S Afr J Sci 104:101-106.

Frayer DW, Wolpoff MH, Thorne AG, Smith FH, Pope GG. 1993. Theories of modern human origins: the paleontological test. Am Anthropol 95:14-50.

Frisancho AR. 1990. Anthropometric Standards for the Assessment of Growth and Nutrional Status. Ann Arbor: The University of Michigan Press.

Forster P. 2004. Ice ages and the mitochondrial DNA chronology of human dispersals: a review. Philos Trans R Soc Lond B Biol Sci 359:255-264.

Gamble C, Davies W, Pettitt P, Richards M. 2004. Climate change and evolving human diversity in Europe during the last glacial. Phil Trans R Soc Lond B 359:243-254.

Genovés S. 1959. L'estimation des différences sexuelles dans l'os coxal: différences métriques et différences morphologiques. Bull Mem Soc Anthropol Paris 10:3-95.

Goldthorpe JE, Wilson FB. 1960. Tribal Maps of East Africa and Zanzibar. Kampala, Uganda: East African Institute of Social Research.

Gray JP, Wolfe LD. 1980. Height and sexual dimorphism of stature among human societies. Am J Phys Anthropol 53:441-456.

Grine FE, Bailey RM, Harvati K, Nathan RP, Morris AG, Henderson GM, Ribot I, Pike AWG. 2007. Late Pleistocene human skull from Hofmeyr, South Africa, and modern human origins. Science 315:226-229.

Grine FE, Jungers WL, Tobias PV, Pearson OM. 1995. Fossil *Homo* femur from Berg Aukas, northern Namibia. Am J Phys Anthropol 97:151-185.

Grine FE, Pearson OM, Klein RG, Rightmire GP. 1998. Additional human fossils from Klasies River Mouth, South Africa. J Hum Evol 35:95-107.

Grün R, Beaumont PB, Stringer CB. 1990. ESR dating evidence for early modern humans at Border Cave in South Africa. Nature 344:537-539.

Grün R, Stringer C, McDermott F, Nathan R, Porat N, Robertson S, Taylor L, Mortimer G, Eggins S, McCulloch M. 2005. U-series and ESR analyses of bones and teeth relating to the human burials from Skhūl. J Hum Evol 49:316-334.

Gunz P, Bookstein FL, Mitteroecker P, Stadlmayr A, Seidler H, Weber GW. 2009. Early modern human diversity suggests subdivided population structure and a complex out-of-Africa scenario. Proc Nat Acad Sci USA 106:6094-6098.

Hager LD. 1989. The Evolution of Sex Differences in the Hominid Bony Pelvis [PhD dissertation]. Berkeley: University of California at Berkeley. 274 p.

Hager LD. 1996. Sex differences in the sciatic notch of great apes and modern humans. Am J Phys Anthropol 99:287-300.

Hall RL. 1982. Sexual dimorphism for size in seven nineteenth-century northwest coast populations. In: Hall RL, editor. Sexual Dimorphim in *Homo sapiens*: A Question of Size. New York: Praeger. p 231-243.

Hamilton ME. 1982. Sexual dimorphism in skeletal samples. In: Hall RL, editor. Sexual Dimorphism in *Homo sapiens*: A Question of Size. New York: Praeger. p 107-164.

Harding RM, McVean G. 2004. A structured ancestral population for the evolution of modern humans. Curr Op Genet Dev 14:667-674.

Harpending H. 1996. Genetic evidence about the origins of modern humans. In: Bar-Yosef O et al., editors. Colloquia of the XIII International Congress of Prehistoric and Protohistoric Sciences. p 127-131.

Harpending H, Rogers A. 2000. Genetic perspectives on human origins and differentiation. Ann Rev Geno Hum Genet 1:361-385.

Harvati K. 2003. The Neanderthal taxonomic position: models of intra- and inter-specific craniofacial variation. J Hum Evol 44:107-132.

Heinrich H. 1988. Origin and consequences of cyclic ice rafting in the Northeast Atlantic Ocean during the past 130,000 years. Quat Res 29:142-152.

Henry-Gambier D. 2002. Les fossiles de Cro-Magnon (Les Eyzies-de-Tayac, Dordogne): nouvelles données sur leur position chronologique et leur attribution culturelle. Bull Mem Soc Anthropol Paris 14:89-112.

Hiernaux J. 1968. La diversité humaine en Afrique subsaharienne: Recherches biologiques. Brussels: Éditions de l'Institut de Sociologie de l'Université libre de Bruxelles.

Hoffecker JF. 1999. Neanderthals and modern humans in Eastern Europe. Evol Anthropol 7(4):129-141.

Holcomb SMC, Konigsberg LW. 1995. Statistical study of sexual dimorphism in the human fetal sciatic notch. Am J Phys Anthropol 97:113-125.

Holliday TW. 1997. Body proportions in Late Pleistocene Europe and modern human origins. J Hum Evol 32:423-447.

Holliday TW. 1999. Qafzeh-Skhūl, West Asian "Neandertals" and modern human origins. J Hum Evol 36:A7-8.

Holliday TW. 2002. Body size and postcranial robusticity of European Upper Paleolithic hominins. J Hum Evol 43:513-528.

Houghton P. 1974. The relationship of the pre-auricular groove of the ilium to pregnancy. Am J Phys Anthropol 41:381-390.

Howells WW. 1973. Cranial Variation in Man: A Study by Multivariate Analysis of Patterns of Difference Among Recent Human Populations. Cambridge, MA: Harvard University Press.

Howells WW. 1989. Skull Shapes and the Map: Craniometric Analyses in the Dispersion of Modern *Homo*. Cambridge: Harvard University Press.

Howells WW. 1995. Who's who in skulls: ethnic identification of crania from measurements. Papers of the Peabody Museum of Archaeology and Ethnology, Harvard University 82:1-108.

Humphrey LT, Dean MC, Stringer CB. 1999. Morphological variation in great ape and modern human mandibles. J Anat 195:491-513.

Iscan MY, Derrick K. 1984. Determination of sex from the sacroiliac joint: a visual assessment technique. FL Sci 47:94-98.

Jelínek J. 1987. A new Paleolithic triple-burial find. Anthropologie; venoveno fysicke historicke a ethnicke anthropologii 25:189-190.

Jungers WL, Falsetti AB, Wall CE. 1995. Shape, relative size, and size-adjustments in morphometrics. Yrbk Phys Anthropol 38:137-161.

Kelley J, Xu Q. 1991. Extreme sexual dimorphism in a Miocene hominoid. Nature 352:151-153.

Kidder JH, Jantz RL, Smith FH. 1992. Defining modern humans: a multivariate approach. In: Bräuer G, and Smith FH, editors. Continuity or Replacement: Controversies in *Homo sapiens* Evolution. Rotterdam: A.A. Balkema. p 157-177.

Klein RG. 1999. The Human Career. Chicago: University of Chicago Press.

Krings M, Stone A, Schmitz RW, Krainitzki H, Stoneking M, Paabo S. 1997. Neandertal DNA sequences and the origin of modern humans. Cell 90:19-30.

Lahr MM. 1994. The Multiregional Model of modern human origins: a reassessment of its morphological basis. J Hum Evol 26:23-56.

Lahr MM. 1996. The Evolution of Modern Human Diversity: A Study of Cranial Variation. Cambridge: Cambridge University Press.

Lahr MM, Foley RA. 1998. Towards a theory of modern human origins: geography, demography, and diversity in recent human evolution. Yrbk Phys Anthropol 41:137-176.

Lam YM, Pearson OM, Smith CM. 1996. Chin morphology and sexual dimorphism in the fossil hominid mandible sample from Klasies River Mouth. Am J Phys Anthropol 100:545-557.

Lartet L. 1868. Une sépulture des Troglodytes du Périgord (cânes des Eyzies). Bull Soc Anthropol Paris 3:335-349.

Lazorthes G, Lhés A. 1939. La grande échancrure sciatique: étude de la morphologie et de ses caractères sexuels. Arch Anat Histol Embryol de Strasbourg 27:143-170.

Leakey REF. 1969. Early *Homo sapiens* Remains from the Omo River Region of South-west Ethiopia. Nature 222:1132-1133.

Leutenegger W. 1982. Sexual dimorphism in nonhuman primates. In: Hall RL, editor. Sexual Dimorphism in *Homo sapiens*: A Question of Size. New York: Praeger. p 11-36.

Lewontin RC. 1966. On the measurement of relative variability. Syst Zool 15(2):141-142.

Lewontin RC. 1972. The apportionment of human diversity. In: Dobzhansky T, Hecht MK, and Steere WC, editors. Evolutionary Biology. New York: Appleton Century Crofts. p 381-398.

Lieberman DE, Devlin MJ, Pearson OM. 2001. Articular area responses to mechanical loading: effects of exercise, age, and skeletal location. Am J Phys Anthropol 116:266-277.

Lockwood CA, Richmond BG, Jungers WL, Kimbel WH. 1996. Randomization procedures and sexual dimorphism in *Australopithecus afarensis*. J Hum Evol 31:537-548.

Lovell NC. 1989. Test of Phenice's method for determining sex from the os pubis. Am J Phys Anthropol 79:117-120.

MacLaughlin SM, Bruce MF. 1986a. Population variation in sexual dimorphism in the human innominate. Hum Evol 1:221-231.

MacLaughlin SM, Bruce MF. 1986b. The sciatic notch/acetabular index as a discriminator of sex in European skeletal remains. J For Sci 31:1380-1390.

MacLaughlin SM, Bruce MF. 1990. The accuracy of sex identification in European skeletal remains using the Phenice characters. J For Sci 35:1384-1392.

Manica A, Amos W, Balloux F, Hanihara T. 2007. The effect of ancient population bottlenecks on human phenotypic variation. Nature 448:346-348.

Manly BFJ. 1986. Multivariate Statistical Methods: A Primer. London: Chapman and Hall.

Mariotti V, Bonfiglioli B, Facchini F, Condemi S, Belcastro MG. 2009. Funerary practices of the Iberomaurusian population of Taforalt (Tafoughalt; Morocco, 11-12,000 BP): new hypotheses based on a grave by grave skeletal inventory and evidence of deliberate human modification of the remains. J Hum Evol 56:340-354.

Marth G, Schuler G, Yeh R, Davenport R, Agarwala R, Church D, Wheelan S, Baker J, Ward M, Kholodov M and others. 2003. Sequence variations in the public domain genome data reflect a bottlenecked population history. Proc Nat Acad Sci USA 100:376-381.

Matiegka J. 1934. L'homme fossile de Predmosti en Moravie (Tchecoslovaquie): partie I, les crânes (traduction française). Prague: Academie Technique des Sciences et des Arts.

Matiegka J. 1938. L'homme fossile de Predmosti en Moravie (Tchecoslovaquie), partie 2. Prague: Academie Technique des Sciences et des Arts

McCown TD. 1937. Mugharet Es-Skhūl: Description and Excavations. In: Garrod DAE, and Bate DMA, editors. The Stone Age of Mount Carmel: Excavations at the Wady El-Mughara. Oxford: Clarendon. p 91-107.

McCown TD, Keith A. 1939. The Stone Age of Mount Carmel: The Fossil Human Remains From The Levalloiso-Mousterian. Oxford: Clarendon Press.

McDermott F, Grün R, Stringer CB, Hawkesworth CJ. 1993. Mass-spectrometric U-series dates for Israeli Neanderthal/early modern hominid sites. Nature 363:252-255.

McDougall I, Brown FH, Fleagle JG. 2005. Stratigraphic placement and age of modern humans from Kibish, Ethiopia. Nature 433:733-736.

Mellars PA. 1996. Models for the dispersal of anatomically modern populations arcross Europe: theoretical and archaeological perspectives. In: Bar-Yosef O, et al., editors. Colloquia of the XIII International Congress of Prehistoric and Protohistoric Sciences. p 225-235.

Mellars PA. 2006. A new radiocarbon revolution and the dispersal of modern humans in Eurasia. Nature 439:931-935.

Mercier N, Valladas H, Bar-Yosef O, Vandermeersch B, Stringer CB, Joron JL. 1993. Thermoluminescence date for the Mousterian burial site of Es-Skhūl, Mt. Carmel. J Arch Sci 20:169-174.

Mielke JH, Konigsberg LW, Relethford JH. 2006. Human Biological Variation. New York: Oxford University Press.

Millard AR. 2008. A critique of the chronometric evidence for hominid fossils: I. Africa and the Near East 500-50 ka. J Hum Evol 54:848-874.

Milner GR, Wood JW, Boldsen JL. 2000. Paleodemography. In: Katzenberg MA, and Saunders SR, editors. Biological Anthropology of the Human Skeleton. New York: Wiley-Liss. p 467-497.

Morris AG. 1992a. Biological relationships between Upper Pleistocene and Holocene populations in southern Africa. In: Bräuer G, and Smith F, editors. Continuity or Replacement: Controversies in *Homo sapiens* Evolution. Rotterdam: A.A. Balkema. p 131-143.

Morris AG. 1992b. The Skeletons of Contact: A Study of Protohistoric Burials from the Lower Orange River Valley, South Africa. Johannesburg: Witwatersrand University Press.

Mosimann JE. 1970. Size allometry: size and shape variables with characterizations of the log-normal and gamma distributions. J Am Stat Assoc 56:930-945.

Murail P, Bruzek J, Braga J. 1999. A new approach to sexual diagnosis in past populations: Practical adjustments from van Vark's procedure. Int J Osteoarch 9:39-53.

Murail P, Bruzek J, Houet F, Cunha E. 2005. DSP: A tool for probabilistic sex diagnosis using worldwise variability in hip-bone measurements. Bull Mem Soc Anthropol Paris 17:167-176.

Mussi M. 1986. On the chronology of the burials found in the Grimaldi caves. Anthropol Contemp 9:95-104.

Neff NA, Marcus LF. 1980. A Survey of Multivariate Methods for Systematics. New York: American Association of Mammalogists.

Novotný V. 1986. Sex determination of the pelvic bone: A system approach. Anthropologie (Brno) 24:197-206.

Nurse GT, Weiner JS, Jenkins T. 1985. The Peoples of Southern Africa and Their Affinities. Oxford: Clarendon Press.

O'Higgins P, Moore WJ, Johnson DR, McAndrew TJ, Flinn RM. 1990. Patterns of cranial sexual dimorphism in certain groups of extant hominoids. J Zool Lond 222:399-420.

Oschinsky L. 1954. The Racial Affinities of the Baganda and Other Bantu Tribes of British East Africa. Cambridge: W. Heffer & Sons Ltd.

Ovchinnikov IV, Gotherstrom A, Romanova GP, Kharitonov VM, Liden K, Goodwin W. 2000. Molecular analysis of Neanderthal DNA from the northern caucasus. Nature 404:490-493.

Oxnard CE. 1987. Fossils, Teeth and Sex: New Perspectives on Human Evolution. Seattle: University of Washington Press.

Patriquin ML, Loth SR, Steyn M. 2003. Sexually dimorphic pelvis morphology in South African whites and blacks. Homo 53(3):255-262.

Pearson OM. 1997. Postcranial Morphology and the Origin of Modern Humans [PhD dissertation]. Stony Brook: SUNY at Stony Brook. 783 p.

Pearson OM. 2000a. Activity, climate, and postcranial robusticity: implications for modern human origins and scenarios of adaptive change. Curr Anthropol 41:569-607.

Pearson OM. 2000b. Postcranial remains and the origin of modern humans. Evol Anthropol 9:229-247.

Pearson OM. 2004. Has the combination of genetic and fossil evidence solved the riddle of modern human origins? Evol Anthropol 13:145-159.

Pearson O, Churchill SE, Grine F, Trinkaus E, Holliday TW. 1998. Multivariate analyses of the hominid ulna from Klasies River Mouth. J Hum Evol 34:653-656.

Pearson OM, Fleagle JG, Grine FE, Royer DF. 2008a. Further new hominin fossils from the Kibish Formation, southwestern Ethiopia. J Hum Evol 55:444-447.

Pearson OM, Grine FE. 1997. Re-analysis of the hominid radii from Cave of Hearths and Klasies River Mouth, South Africa. J Hum Evol 32:577-592.

Pearson OM, Royer DF, Grine FE, Fleagle JG. 2008b. A description of the Omo I postcranial skeleton, including newly discovered fossils. J Hum Evol 55:421-437.

Pereira L, Gusmao L, Alves C, Amorim A, Prata M. 2002. Bantu and European Y-lineages in sub-Saharan Africa. Ann Hum Genet 66:369-378.

Petersen HC. 2000. On statistical methods for comparison of intrasample morphometric variability: Zalavar revisited. Am J Phys Anthropol 113:79-84.

Pettitt PB. 2000. The Paviland radiocarbon dating programme: reconstructing the chronology of faunal communities, carnivore activity and human occupation. In: Aldhouse-Green S, editor. Paviland Cave and the "Red Lady". Bristol: Western Academic & Specialist Press Limited. p 63-71.

Pfeiffer S, Sealy J. 2006. Body size among Holocene foragers of the Cape ecozone, southern Africa. Am J Phys Anthropol 129:1-11.

Phenice TW. 1969. A newly developed visual method of sexing the os pubis. Am J Phys Anthropol 30:297-301.

Pietrusewsky M. 2000. Metric analysis of skeletal remains: methods and applications. In: Katzenberg MA, and Saunders SR, editors. Biological Anthropology of the Human Skeleton. New York: Wiley-Liss. p 375-415.

Pinhasi R, Semal P. 2000. The position of the Nazlet Khater specimen among prehistoric and modern African and Levantine populations. J Hum Evol 39:269-288.

Plavcan JM, Cope DA. 2001. Metric variation and species recognition in the fossil record. Evol Anthropol 10:204-222.

Polly PD. 1998. Variability in mammalian dentitions: size-related bias in the coefficient of variation. Biol J Linn Soc 64:83-99.

Quinn GP, Keough MJ. 2002. Experimental Design and Data Analysis for Biologists. Cambridge: Cambridge University Press.

Quintana-Murci L, Quacha H, Harmanta C, Luca F, Massonnet B, Patin E, Sica L, Mouguiama-Daoudad P, Comas D, Tzur S and others. 2008. Maternal traces of deep common ancestry and asymmetric gene flow between Pygmy hunter-gatherers and Bantu-speaking farmers. Proc Nat Acad Sci USA 105:1596-1601.

Reisner GA. 1923. Excavations at Kerma I-III/IV-V. Cambridge: Peabody Museum of Harvard University.

Reitz EJ, Wing ES. 1999. Zooarchaeology. Cambridge: Cambridge University Press.

Relethford JH. 1994. Craniometric variation among modern human populations. Am J Phys Anthropol 95:53-62.

Relethford JH. 1998. Genetics of modern human origins and diversity. Ann Rev Anthropol 27:1-23.

Relethford JH. 1999. Models, predictions, and the fossil record of modern human origins. Evol Anthropol 8:7-10.

Relethford JH. 2001. Ancient DNA and the origin of modern humans. Proc Nat Acad Sci USA 98(2):390-391.

Relethford JH. 2009. Race and global patterns of phenotypic variation. Am J Phys Anthropol 139:16-22.

Relethford JH, Harpending H. 1994. Craniometric variation, genetic theory, and modern human origins. Am J Phys Anthropol 95:249-270.

Relethford JH, Jorde LB. 1999. Genetic evidence for larger African population size during recent human evolution. Am J Phys Anthropol 108:251-260.

Richman EA, Michel ME, Schulter-Ellis FP, Corruccini RS. 1979. Determination of sex by discriminant function analysis of postcranial skeletal measurements. J For Sci 24:159-167.

Richmond BG, Jungers WL. 1995. Size variation and sexual dimorphism in *Australopithecus afarensis* and living hominoids. J Hum Evol 29:229-245.

Richtsmeier JT, Cheverud JM, Lele S. 1992. Advances in anthropological morphometrics. Ann Rev Anthropol 21:283-305.

Rightmire GP. 1979. Implications of Border Cave skeletal remains for later Pleistocene human evolution. Curr Anthropol 20:23-26.

Rightmire GP. 1984. *Homo sapiens* in Sub-Saharan Africa. In: Spencer F, and Smith FH, editors. The Origins of Modern Humans: A World Survey of the Fossil Evidence. New York: Liss, Inc. p 295-325.

Rightmire GP. 1989. Middle Stone Age humans from eastern and southern Africa. In: Mellars P, and Stringer CB, editors. The Human Revolution. Edinburgh: Edinburh University Press. p 109-122.

Rightmire GP, Deacon HJ. 1991. Comparative studies of Late Pleistocene human remains from Klasies River Mouth, South Africa. J Hum Evol 20:131-156.

Rightmire GP, Deacon HJ, Schwartz JH, Tattersall I. 2006. Human foot bones from Klasies River main site, South Africa. J Hum Evol 50:96-103.

Rivière ME. 1872. Sur le squelette humain trouvé dans les cavernes des Baoussé-Roussé (Italie), dites grottes de Menton, le 26 mars 1872. Comptes rendus 74:1204-1207.

Rogers T, Saunders S. 1994. Accuracy of sex determination using morphological traits of the human pelvis. J For Sci 39:1047-1056.

Rose, MD. 1984. A hominine hip bone, KNM-ER 3228, from East Lake Turkana, Kenya. Am J Phys Anthropol 63:371-378.

Rougier H, Milota S, Rodrigo R, Gherase M, Sarcina L, Moldovan O, Zilhao J, Constantin S, Franciscus RG, Zollikofer C and others. 2007. Pestera cu Oase 2 and the cranial morphology of early modern Europeans. Proc Nat Acad Sci USA 104(4):1165-1170.

Royer DF, Lockwood CA, Scott JE, Grine FE. 2009. Size variation in early human mandibles and molars from Klasies River, South Africa: comparison with other Middle and Late Pleistocene assemblages and with modern humans. Am J Phys Anthropol Early View:xxx-xxx.

Ruff CB. 1991. Climate and body shape in hominid evolution. J Hum Evol 21:81-105.

Ruff CB. 1994. Morphological adaptation to climate in modern and fossil hominids. Yrbk Phys Anthropol 37:65-107.

Ruff CB. 2000. Body size, body shape, and long bone strength in modern humans. J Hum Evol 38:269-290.

Ruff CB, Holt BM, Trinkaus E. 2006. Who's afraid of the big bad Wolff?: "Wolff's Law" and bone functional adaptation. Am J Phys Anthropol 129:484-498.

Ruff CB, Runestad JA. 1992. Primate limb bone structural adaptations. Ann Rev Anthropol 21:433-459.

Ruff CB, Trinkaus E, Holliday TW. 1997. Body mass and encephalization in Pleistocene Homo. Nature 387:173-176.

Ruff CB, Trinkaus E, Walker A, Spencer Larsen C. 1993. Postcranial robusticity in *Homo* I: Temporal trends and mechanical interpretation. Am J Phys Anthropol 91:21-53.

Safont S, Malgosa A, Subira ME. 2000. Sex assessment on the basis of long bone circumference. Am J Phys Anthropol 113:317-328.

Satta Y, Takahata N. 2002. Out of Africa with regional interbreeding? Modern human origins. BioEssays 24:871-875.

Scheuer L. 2002. Application of osteology to forensic medicine. Clin Anat 15:297-312.

Schmitt LH. 1995. Using within-populational variability to measure environmental optimality and adaptability. In: Boyce AJ, and Reynolds V, editors. Human Populations: Diversity and Adaptation. Oxford: Oxford University Press. p 106-121.

Schulter-Ellis FP, Schmidt DJ, Hayek LA, Craig J. 1983. Determination of sex with a discriminant analysis of new pelvic bone measurements (part 1). J For Sci 28:169-180.

Schwarcz HP, Grün R, Vandermeersch B, Bar-Yosef O, Valladas H, Tchernov E. 1988. ESR dates for the hominid burial site of Qafzeh in Israel. J Hum Evol 17:733-737.

Schwartz JH, Tattersall I. 2000. The human chin revisited: what is it and who has it? J Hum Evol 38:367-409.

Serre D, Langaney A, Chech M, Teschler-Nicola M, Paunovic M, Mennecier P, Hofreiter M, Possnert G, Paabo S. 2004. No evidence of Neandertal mtDNA contribution to early modern humans. PLoS Biol 2:313-317.

Shackleton NJ. 1982. Stratigraphy and chronology of the KRM deposits: oxygen isotope evidence. In: Singer R, and Wymer J, editors. The Middle Stone Age at Klasies River Mouth in South Africa. Chicago: University of Chicago Press. p 194-199.

Simpson GG, Roe A, Lewontin RC. 1960. Quantitative Zoology. New York: Harcout Brace & World Inc.

Singer R, Wymer J. 1982. The Middle Stone Age at Klasies River Mouth in South Africa. Chicago: University of Chicago Press.

Singh S, Potturi BR. 1978. Greater sciatic notch in sex determination. J Anat 125:619-624.

Sládek V, Trinkaus E, Hillson SW, Holliday TW, editors. 2000. The People of the Pavlovian: Skeletal Catalogue and Osteometrics of the Gravettian Fossil Hominids from Dolní Věstonice and Pavlov. Brno: Academy of Sciences of the Czech Republic. 244 p.

Smith FH. 1992. Models and realities in modern human origins: the African fossil evidence. Phil Trans R Soc Lond B 337:243-250.

Smith FH. 1994. Samples, Species, and Speculations in the Study of Modern Human Origins. In: Nitecki MH, and Nitecki DV, editors. Origins of Anatomically Modern Humans. New York: Plenum Press. p 227-249.

Smith FH. 2006. Assimilation and modern human origins in the African peripheries (abstract). African Genesis: A Symposium on Hominid Evolution in Africa. Johannesburg, South Africa. p 40.

Smith FH, Jankovic I, Karavancic I. 2005. The assimilation model, modern human origins in Europe, and the extinction of Neandertals. Quat Intern 137:7-19.

Sokal RR, Rohlf FJ. 1995. Biometry: The Principles and Practice of Statistics in Biological Research. New York: W.H. Freeman and Co.

Steyn M, Pretorius E, Hutten L. 2004. Geometric morphometric analysis of the greater sciatic notch in South Africans. Homo 54(3):197-206.

Stone AC. 2000. Ancient DNA from skeletal remains. In: Katzenberg MA, and Saunders SR, editors. Biological Anthropology of the Human Skeleton. New York: Wiley-Liss. p 351-371.

Stringer CB. 1994. Out of Africa - a personal history. In: Nitecki MH, and Nitecki DV, editors. Origins of Anatomically Modern Humans. New York: Plenum Press. p 149-172.

Stringer CB. 1996. Current issues in modern human origins. In: Meikle WE, Howell FC, and Jablonski NG, editors. Contemporary Issues in Human Evolution. San Francisco: California Academy of Sciences. p 115-134.

Stringer CB. 2000. Coasting out of Africa. Nature 405:24-27.

Stringer CB. 2002. Modern human origins: progress and prospects. Phil Trans R Soc Lond B 357:563-579.

Stringer CB, Andrews P. 1988. Genetic and fossil evidence for the origin of modern humans. Science 239:1263-1268.

Stringer CB, Grün R, Schwarcz HP, Goldberg P. 1989. ESR dates for the hominid burial site of Es Skhūl in Israel. Nature 338:756-758.

Stringer CB, Hublin JJ, Vandermeesch B. 1984. The origin of anatomically modern humans in western Europe. In: Smith FH, and Spencer F, editors. The Origins of Modern Humans: A World Survey of the Fossil Evidence. New York: Alan R. Liss, Inc. p 51-135.

Stynder D. 2006. A quantitative assessment of variation in Holocene Khoesan crania from South Africa's western, south-western, southern and south-eastern coasts and coastal forelands [PhD dissertation]. Cape Town: University of Cape Town.

Suchey JM, Wiseley DV, Green RF, Noguchi TT. 1979. Analysis of the dorsal pitting on the os pubis in an extensive sample of modern American females. Am J Phys Anthropol 51:517-540.

Svoboda J. 2000. The depositional context of th Early Upper Paleolithic human fossils from the Koneprusy (Zlaty kun) and Mladeč Caves, Czech Republic. J Hum Evol 38:523-536.

Svoboda J, Klima B, Jarosava L, Skrdla P. 2000. The Gravettian in Moravia: climate, behaviour and technological complexity. In: Roebroeks W, Mussi M, Svoboda J, and Fennema K, editors. Hunters of the Golden Age: The mid-Upper Palaeolithic of Eurasia, 30,000 to 20,000 BP. Leiden: Leiden University Press. p 197-217.

Svoboda JA, van der Plicht J, Kuzelka V. 2002. Upper Palaeolithic and Mesolithic human fossils from Moravia and Bohemia (Czech Republic): some new ^{14}C dates. Antiquity 76(294):957-962.

Tague R. 1989. Variation in pelvic size between males and females. Am J Phys Anthropol 80:59-71.

Takahashi H. 2006. Curvature of the greater sciatic notch in sexing the human pelvis. Anthropol Sci 114:187-191.

Taylor JV, DiBennardo R. 1984. Discriminant function analysis of the central portion of the innominate. Am J Phys Anthropol 64:315-320.

Tchernov A. 1992. Biochronology, paleoecology, and dispersal events of hominids in the southern Levant. In: Akazawa T, Aoki K, and Kimura T, editors. The Evolution and Dispersal of Modern Humans in Asia. Tokyo: Hokusen-sha Publ. Co. p 149-188.

Templeton AR. 1993. The "Eve" hypothesis: a genetic critique and reanalysis. Am Anthropol 95(1):51-72.

Templeton AR. 2002. Out of Africa again and again. Nature 416:45-51.

Teschler-Nicola M. 2007. Early Modern Humans at the Moravian Gate: the Mladeč Caves and their Remains. New York: Springer.

Thieme FP, Schull WJ. 1957. Sex determination from the skeleton. Hum Biol 29:242-273.

Thoma A. 1984. Morphology and affinities of the Nazlet Khater man. J Hum Evol 13:287-296.

Thorne AG, Wolpoff MH. 2003 The multiregional evolution of humans. Scientific American:46-53.

Tobias PV. 1957. Bushmen of the Kalahari. Man 36:1-8.

Tobias PV. 1971. Human skeletal remains from the Cave of Hearths, Makapansgat, Northern Transvaal. Am J Phys Anthropol 34:335-368.

Tobias PV. 1975. Anthropometry among disadvantaged peoples: studies in southern Africa. In: Watts ES, Johnston FE, and Lasker GW, editors. Biosocial Interrelations in Population Adaptation. The Hague: Mouton Publ. p 287-305.

Trinkaus E. 1983. Neandertal postcrania and the adaptive shift to modern humans. In: Trinkaus E, editor. The Mousterian Legacy: Human Biocultural

Change in the Upper Pleistocene. Oxford: BAR International Series 164. p 165-200.

Trinkaus E. 1984. Western Asia. In: Smith FH, and Spencer F, editors. The Origins of Modern Humans: A World Survey of the Fossil Evidence. New York: Alan R. Liss, Inc. p 251-293.

Trinkaus E. 1992. Morphological contrasts between the Near Eastern Qafzeh-Skhūl and late archaic human samples: grounds for a behavioral difference? In: Akazawa T, Aoki K, and Kimura T, editors. The Evolution and Dispersal of Modern Humans in Asia. Tokyo: Hokusen-Sha Publ. Co. p 277-294.

Trinkaus E. 1993a. Femoral neck-shaft angles of the Qafzeh-Skhūl early modern humans, and activity levels among immature Near Eastern Middle Paleolithic hominids. J Hum Evol 25:393-416.

Trinkaus E. 1993b. A note on the KNM-ER 999 hominid femur. J Hum Evol 24:493-505.

Trinkaus E. 2000. Late Pleistocene and Holocene human remains from Paviland Cave. In: Aldhouse-Green S, editor. Paviland Cave and the "Red Lady". Bristol: Western Academic & Specialist Press Limited. p 141-199.

Trinkaus E. 2005. Early modern humans. Ann Rev Anthropol 34:207-230.

Trinkaus E. 2007. European early modern humans and the fate of Neandertals. Proc Nat Acad Sci USA 104:7367-7372.

Trinkaus E, Jelínek J. 1997. Human remains from the Moravian Gravettian: the Dolní Věstonice 3 postcrania. J Hum Evol 33:33-82.

Trinkaus E, Milota S, Rodrigo R, Mircea G, Moldovan O. 2003. Early modern human cranial remains from the Pestera cu Oase, Romania. J Hum Evol 45:245-253.

Trinkaus E, Svoboda J, West DL, Sládek V, Hillson SW, Drozdova E, Fisakova M. 2000. Human remains from the Moravian Gravettian: morphology and taphonomy of isolated elements from the Dolní Věstonice II site. J Arch Sci 27:1115-1132.

Turbon D, Perez-Perze A, Stringer C. 1997. A multivariate analysis of Pleistocene hominids: testing hypotheses of European origins. J Hum Evol 32:449-468.

Ulijaszek SJ, Lourie JA. 1994. Intra- and inter-observer error in anthropometric measurement. In: Ulijaszek SJ, and Mascie-Taylor CGN, editors. Anthropometry: the individual and the population. Cambridge: Cambridge University Press. p 30-55.

Ullrich H. 1975. Estimation of fertility by means of pregnancy and childbirth alterations at the pubis, ilium, and the sacrum. Ossa 2:23-29.

Valladas H, Reyss JL, Joron JL, Valladas G, Bar-Yosef O, Vandermeersch B. 1988. Thermoluminescence dating of Mousterian 'Proto-Cro-Magnon' remains from Israel and the origin of modern man. Nature 331:614-616.

Vallois HV, Billy G. 1965. Nouvelles recherches sur les hommes fossiles de l'abri de Cro-Magnon. Anthropologie 69:47-74.

Van Gerven DP. 1972. The contribution of size and shape variation to patterns of sexual dimorphism of the human femur. Am J Phys Anthropol 37:49-60.

Van Valen L. 1978. The statistics of variation. Evol Theory 4:33-43.

van Vark GN. 1984. On the determination of hominid affinities. In: van Vark GN, and Howells WW, editors. Multivariate Statistical Methods in Physical Anthropology. Dordrecht: Reidel Publ. Co. p 323-349.

van Vark GN, Bilsborough A, Henke W. 1992. Affinities of European Upper Palaeolithic *Homo sapiens* and later human evolution. J Hum Evol 23:401-417.

van Vark GN, Schaafsma W. 1992. Advances in the Quantitative Analysis of Skeletal Morphology. In: Saunders SR, and Katzenberg MA, editors. Skeletal Biology of Past Peoples: Research Methods. New York: Wiley-Liss, Inc. p 225-257.

van Vark GN, van der Sman PGM. 1982. New discrimination and classification techniques in anthropological practice. Z Morph Anthropol 73:21-36.

van Vark GN, van der Sman PGM, Dijkema J, Buikstra JE. 1989. Some multivariate tests for differences in sexual dimorphism between human populations. Ann Hum Biol 16:301-310.

Vandermeersch B. 1981. Les Hommes Fossiles de Qafzeh (Israel). Paris: CNRS.

Vandermeersch B. 1992. The Near Eastern hominids and the origins of modern humans in Eurasia. In: Akazawa T, Aoki K, and Kimura T, editors. The Evolution and Dispersal of Modern Humans in Asia. Tokyo: Hokusen-sha Publ. Co. p 29-38.

Vermeersch PM, Paulissen E, Gijselings G, Otte M, Thoma A, van Peer P, Lauwers R. 1984. 33,000-yr old chert mining site and related *Homo* in the Egyptian Nile Valley. Nature 309:342-344.

Verneau R. 1908. L'Homme de la Barma-Grande (Baousse-Rousse). Menton: Imprimerie Colombani.

Villeneuve L. 1906. Les Grottes de Grimaldi (Baousee-Rousse): Historique et Description. Monaco: Imprimerie de Monaco.

Vlcek E. 1967. Morphological relations of the fossil human types Brno and Cro-Magnon in the European Late Pleistocene. Folia Morph 15:214-221.

von Cramon-Taubadel N, Lycette SJ. 2008. Human cranial variation fits iterative founder effect model with African origins. Am J Phys Anthropol 136:108-113.

Wakeley J. 2004. Metapopulation models for historical inference. Mol Ecol 13:865-875.

Waldron T. 1987. The relative survival of the human skeleton: Implications for palaeopathology. In: Boddington A, Garland AN, and Janaway RC, editors. Death, Decay and Reconstruction. Manchester: Manchester University Press. p 55-64.

Walker PL. 2005. Greater sciatic notch morphology: sex, age, and population differences. Am J Phys Anthropol 127:385-391.

Walter RC, Buffler R, Bruggemann J, Guillaume M, Berhe S, Negassi B, Libsekal Y, Cheng H, Edwards R, Cosel R and others. 2000. Early human

occupation of the Red Sea coast of Eritrea during the last interglacial. Nature 405:65-69.

Washburn SL. 1948. Sex differences in the pubic bone. Am J Phys Anthropol 6:199-207.

Washburn SL. 1949. Sex differences in the pubic bone of Bantu and Bushmen. Am J Phys Anthropol 7:425-433.

Watkins WS, Rogers AR, Ostler CT, Wooding S, Bamshad MJ, Brassington A-M, Carroll ML, Nguyen SV, Walker JA, Prasad BVR, Reddy PG, Das PK, Batzer MA, Jorde LB. 2003. Genetic variation among world populations: inferences from 100 Alu insertion polymorphisms. Genome Res 13:1607-1618.

Weaver TD, Roseman CC. 2008. New developments in the genetic evidence for modern human origins. Evol Anthropol 17:69-80.

Weisheit LE. 1997. Metric and Non-Metric Methods of Sex Determination in the Human Pelvis [M.A. thesis]. Stony Brook: SUNY Stony Brook. 75 p.

Weisl H. 1954. The ligaments of the sacro-iliac joint examined with particular reference to their function. Acta Anat 20:201-213.

Weiss KM. 1972. On the systemic bias in skeletal sexing. Am J Phys Anthropol 37:239-249.

Wendorf F, editor. 1968a. The Prehistory of Ancient Nubia. Dallas: Southern Methodist University Press.

Wendorf F. 1968b. Site 117: a Nubian Final Paleolithic graveyard near Jebel Sahaba, Sudan. In: Wendorf F, editor. The Prehistory of Ancient Nubia. Dallas: Southern Methodist University Press. p 954-995.

White TD, Asfaw B, DeGusta D, Gilbert H, Richards GD, Suwa G, Howell FC. 2003. Pleistocene *Homo sapiens* from Middle Awash, Ethiopia. Nature 423:742-747.

White TD, Folkens PA. 2000. Human Osteology. San Diego: Academic Press.

Wild EM, Teschler-Nicola M, Kutschera W, Steier P, Trinkaus E, Wanek W. 2005. First direct dating of Early Upper Paleolithic human remains from Mladeč. Nature 435:332-335.

Wolfe LD, Gray JP. 1982. A cross-cultural investigation into the sexual dimorphism of stature. In: Hall RL, editor. Sexual Dimorphism in *Homo sapiens*: A Question of Size. New York: Praeger Publishers. p 197-230.

Wolpoff MH, Caspari R. 1996. The modernity mess. J Hum Evol 30:167-172.

Wolpoff MH, Hawks JD, Caspari R. 2000. Multiregional, not multiple origins. Am J Phys Anthropol 112:129-136.

Wolpoff MH, Lee S-H. 2001. The Late Pleistocene human species of Israel. Bull Mem Soc Anthropol Paris 13(3-4):291-310.

Wolpoff MH, Thorne AG, Smith FH, Frayer DW, Pope GG. 1994. Multiregional evolution: a world-wide source for modern human populations. In: Nitecki MH, and Nitecki DV, editors. Origins of Anatomically Modern Humans. New York: Plenum Press. p 175-199.

Wood B, Li Y, Willoughby C. 1991. Intraspecific variation and sexual dimorphism in cranial and dental variables among higher primates and their bearing on the hominid fossil record. J Anat 174:185-205.

Wood E, Stover D, Ehret C, Destro-Bisol G, Spedini G, McLeod H, Louie L, Bamshad M, Strassmann B, Soodyall H et al. 2005. Contrasting patterns of Y chromosome and mtDNA variation in Africa: evidence for sex-biased demographic processes. Eur J Hum Genet 13:867-876.

Yokley TR, Churchill SE. 2006. Archaic and modern human distal humeral morphology. J Hum Evol 51:603-616.

Zhivotovsky LA, Rosenberg NA, Feldman MW. 2003. Features of evolution and expansion of modern humans inferred from genomewide microsatellite markers. Amer J Hum Genet 72:1171-1186.

Appendix 1

Measurement List and Data Collection Protocols

Unless otherwise indicated, all measurements are taken using digital sliding calipers. M-# following a definition refers to its Martin number (Martin and Saller, 1956; Bräuer, 1988).

Abbreviations: AP = anterior-posterior, ML = medial-lateral, SI = superior-inferior, PD = proximal-distal, * = variable eliminated from study due to high intra-observer measurement error (see Chapter 2).

The Humerus

HUM1	Maximum length of the humerus. Distance from the highest point of the humeral head to the most inferior point on the trochlea. Taken with an osteometric board. (M-1)
HUM2	Total length of the humerus. Distance from the highest point on the humeral head to the lower point on the capitulum. Taken with an osteometric board. (M-2)
HUM3	Maximum mid-shaft diameter of the humerus. Midshaft position determined by halving HUM1.
HUM4	Minimum mid-shaft diameter of the humerus. Midshaft position determined by halving HUM1.
HUM5	Maximum SI diameter of the humeral head.
HUM6	Maximum AP diameter of the humeral head.
HUM7*	Intertubercular sulcus width. Measured as the minimum distance between the internal crests of the greater and lesser tubercles.

HUM8*	Maximum width of the pectoralis major attachment site.
HUM9	Maximum length of the deltoid tuberosity. Measured parallel to the tuberosity's long axis.
HUM10*	Maximum width of the deltoid tuberosity. Measurement perpendicular to HUM9.
HUM11	Maximum ML epicondylar width. Measured in anterior view. (M-4a)
HUM12	Maximum ML width of the capitulum and trochlea. Measured in anterior view, including only articular surfaces. (M-12)
HUM13	Maximum ML width of the capitulum. Measured in anterior view from the gutter separating the capitulum and the trochlea to the most lateral point on the capitulum.
HUM14	Maximum PD height of the capitulum. Measured perpendicular to HUM13, including only the articular surface.
HUM15	Maximum AP thickness of the capitulum. Includes articular and non-articular bone.
HUM16*	Maximum ML width of the trochlea. Measured in posterior view.
HUM17	AP thickness of the medial trochlear lip.
HUM18	Minimum AP thickness of the trochlea. Usually coincides with mid-trochlea.
HUM19	Olecranon fossa width. Measured as the maximum distance between the medial and lateral edges of the fossa.
HUM20	Medial dorsal pillar width. Measured as the minimum distance between the medial border of the medial pillar and the medial margin of the olecranon fossa.
HUM21	Lateral dorsal pillar width. Measured as the minimum distance between the lateral border of the lateral pillar and the lateral margin of the olecranon fossa.

HUM22* Medial epicondyle thickness. Measured as the greatest AP distance of the medial epicondyle.

HUM23 Deltoid-capitulum distance. Measured as the distance from the inferior border of the deltoid tuberosity to the inferior-most point on the capitulum. Taken with a measuring tape.

HUM24 Deltoid-trochlea distance. Measured as the distance from the inferior border of the deltoid tuberosity to the inferior-most point on the trochlea. Taken with a measuring tape.

HUM25 Minimum shaft circumference of the humerus. Taken with a measuring tape.

The Ulna

ULN1 Ulna articular length. Measured as the distance from the middle of the trochlear notch to the distal-most point on the ulna. Taken with a measuring tape. (M-2a)

ULN2 Maximum length of the ulna. Measured excluding the styloid process. Taken with an osteometric board.

ULN3 Maximum mid-shaft diameter. Mid-shaft determined by halving HUM 1.

ULN4 Minimum mid-shaft diameter. Mid-shaft determined by halving ULN1. (M-3a)

ULN5 Coronoid height. Distance from the posterior surface of the shaft to the tip of the coronoid process, measured perpendicular to the long axis of the shaft.

ULN6 Maximum ML coronoid width. Measured just before the coronoid process joints the ulnar shaft.

ULN7 Olecranon height. Distance from the tip of the olecranon process to the posterior side of the shaft, measured perpendicular to the long axis of the shaft.

ULN8	Olecranon ML width. Maximum width of the olecranon process, measuring in the ML plane. (M-6)
ULN9	Olecranon length. Distance from the middle of the trochlear notch to the most proximal point of the olecranon process, measured parallel to the long axis of the shaft.
ULN10	Trochlear notch length. Distance between the tip of the olecranon process to the tip of the coronoid process.
ULN11	Trochlear notch width. Measured as the minimum ML width of the trochlear notch.
ULN12	Mid-trochlear notch thickness. The AP thickness measured from the mid-trochlear notch articular surface to the posterior aspect of the shaft.
ULN13	Minimum trochlear notch thickness. The minimum AP thickness measured from the articular surface of the notch to the posterior aspect of the shaft; this may coincide with ULN12.
ULN14	Radial notch position. Distance from the proximal-most point on the olecranon process to the distal border of the radial notch, measured parallel to the long axis of the shaft.
ULN15	Radial notch length. Maximum distance between the anterior and posterior borders of the radial notch, measured with caliper tips parallel to the notch sides.
ULN16*	Radial notch width. Maximum distance between the proximal and distal borders of the radial notch.
ULN17	Brachialis insertion position. Distance from the midpoint of the trochlear notch to the middle of the rugosity marking the brachialis attachment site.
ULN18	Ulna proximal shaft AP diameter. Measured at the distal border of the rugosity marking the brachialis insertion.

ULN19 Ulna proximal shaft ML diameter. Measured at the distal border of the rugosity marking the brachialis insertion, perpendicular to ULN18.

ULN20 Maximum diameter of the distal epiphysis. Measured excluding the styloid process, in a plane perpendicular to the long axis of the shaft.

ULN21 Minimum ulna shaft circumference. Taken with a measuring tape.

The Radius

RAD1 Articular length of the radius. Distance from the middle of the fovea of the head to the middle of the carpal articular surface. Taken with a measuring tape. (M-2)

RAD2 Maximum length of the radius. Distance from the proximal surface of the rim of the head to the distal-most point on the styloid process. (M-1)

RAD3 Maximum mid-shaft diameter of the radius. Mid-shaft determined by halving RAD1. (M-4)

RAD4* Minimum mid-shaft diameter of the radius. Mid-shaft determined by halving RAD1.

RAD5 Maximum AP diameter of the head.

RAD6 Maximum ML diameter of the head, measured perpendicular to RAD5.

RAD7 Maximum diameter of the head, measured in any plane.

RAD8 Radial tuberosity length. PD length of the radial tuberosity, measured from the most proximal point where the tuberosity begins to swell or displays a roughened area to the distal most point of pronounced relief. Taken parallel to the long axis of the radial shaft.

RAD9 Neck length. Distance from the center of the proximal articular surface of the radial head to the center of the raised surface of the radial tuberosity.

RAD10 Neck AP diameter. Measured midway between the distal edge of the radial head and the proximal border of the radial tuberosity.

RAD11* Neck ML diameter. Transverse diameter of the neck, measured at the same level as RAD10.

RAD12* Radial tuberosity breadth. Maximum transverse diameter across the radial tuberosity. Measured across the medial- and lateral-most extent of the swelling.

RAD13 Distal epiphysis AP diameter. Maximum AP diameter of the distal articular surface, including dorsal spines.

RAD14 Distal epiphysis ML diameter. Maximum transverse diameter of the distal articular surface, measured from the edge of the ulnar notch to the lateral-most point on the styloid process.

RAD15 Minimum shaft circumference. Taken with a tape measure.

RAD16 Radial tuberosity circumference. Shaft circumference measured at the mid-point of the radial tuberosity. Taken with a tape measure.

The Os Coxae

PEL1 Acetabular width. Horizontal diameter measured from posterior rim of the acetabulum to the anterior rim, following the horizontal plane when the os coxae is held in anatomical position (generally, this is parallel to the superior pubic ramus).

PEL2 Ischium length. Distance from the most anterior and inferior point of the ischial tuberosity to the nearest point on the acetabular rim. Taken in the vertical plane when the os coxae is held in anatomical position.

PEL3 Post-acetabular ischial length. Distance from the most anterior and inferior point of the ischial tuberosity to the furthest point on the

	acetabular rim. This projects PEL2 superiorly to include the vertical height of the acetabulum.
PEL4*	Acetabulum height. Vertical diameter measured from inferior rim of the acetabulum to the superiro rim, following the vertical plane employed in PEL2 and PEL3 (generally, this is parallel to the long axis of the ischium).
PEL5	Ischium depth. Distance from the most inferior point inside the obturator foramen to the furthest point along the ischial tuberosity.
PEL6	Ischial tuberosity maximum width. Measured across the outer lips of the ischial tuberosity regardless of the position at which these points occur along the tuberosity.
PEL7	Ischial body thickness. The ML distance from the ischial rim of the acetabulum to the mid-point of the anterior portion of the sciatic notch, measured in posterior view.
PEL8	Iliac tubercle thickness. Measured at the point of maximum thickness.
PEL9	Sciatic notch width. Measured from the base of the posterior inferior iliac spine to the base of the ischial spine. This distance spans the open end of the notch, but excludes the ischial and iliac spines because these are frequently broken.
PEL10	Sciatic notch depth. Distance from the base of the posterior inferior iliac spine to the anterior border of the notch. Taken perpendicular to the anterior border of the notch, using the small arms of the calipers. Also called sciatic notch height.
PEL11	Average sciatic notch angle (degrees). Measured from photographs using Sigma Scan Pro 5.0©, following the photographic protocol outlined below. In Sigma Scan, points are marked at the base of the ischial spine (A), base of the posterior inferior iliac spine (B), and the apex (i.e., deepest part) of the sciatic notch (C) in order to measure the angle between lines extending from A and B. The angle is measured three times per specimen, and the average is employed.

The Femur

FEM1	Maximum femoral length. Maximum PD length of the femur, measured from the superior-most point on the head to the inferior-most point of the medial condyle ('straight length'). Taken with an osteometric board.
FEM2	Bicondylar length. Measured from the superior-most point on the femoral head to a line tangent to the inferior-most points on the two distal condyles. Taken with an osteometric board.
FEM3	Midshaft AP diameter. Mid-shaft determined by halving FEM1.
FEM4	Midshaft ML diameter. Measured perpendicular to FEM3.
FEM5	Vertical head diameter. The maximum SI diameter of the femoral head.
FEM6	Horizontal head diameter. The maximum transverse diameter of the femoral head.
FEM7	Minimum neck height. Measured perpendicular to the long axis of the femoral neck.
FEM8	Minimum neck breadth. Measured in a plane perpendicular to FEM7.
FEM9	Biomechanical neck length. The horizontal distance from the medial-most point on the head to the lateral-most point on the greater trochanter.
FEM10	Neck length. The shortest distance from the base of the lesser trochanter to the articular rim of the femoral head.
FEM11	Subtrochanteric AP shaft diameter. Measured immediately below the lesser trochanter.
FEM12	Subtrochanteric ML shaft diameter. Measured perpendicular to FEM12.

FEM13 Gluteal tuberosity breadth. Maximum breadth of the gluteal tuberosity, measured perpendicular to the long axis of the shaft.

FEM14 Patella notch width. Maximum ML width of the patellar notch, measured in anterior view.

FEM15 Biepicondylar breadth. Maximum ML breadth of the distal femur, measured across both epicondyles.

FEM16 Maximum distal articular breadth. Maximum breadth across the distal articular of both condyles.

FEM17 Minimum shaft circumference. Taken with a tape measure.

FEM18 Subtrochanteric shaft circumference. Measured immediately below the lesser trochanter. Taken with a tape measure.

The Tibia

TIB1 Articular length of the tibia. Distance from the middle of the medial condyle to the middle of the talar trochlear articular surface. Taken with a tape measure. (M-2)

TIB2 Total length of the tibia. Distance from the middle of the medial condyle to the inferior-most point on the medial malleolus. Taken with a tape measure. (M-1b)

TIB3 Mid-shaft AP diameter. Mid-point determined by halving TIB1.

TIB4 Mid-shaft ML diameter. Measured perpendicular to TIB3.

TIB5 Proximal epiphysis maximum length. Maximum AP diameter across the proximal condyles.

TIB6 Proximal epiphysis maximum breadth. Maximum ML diameter across the proximal condyles. (M-3)

TIB7 Medial condyle AP diameter. Maximum AP diameter across the articular surface of the medial condyle.

TIB8 Medial condyle ML diameter. Maximum ML diameter across the articular surface of the medial condyle.

TIB9 Lateral condyle AP diameter. Maximum AP diameter across the articular surface of the lateral condyle.

TIB10 Lateral condyle ML diameter. Maximum ML diameter across the articular surface of the lateral condyle.

TIB11 AP proximal shaft diameter. Measured at the level of the nutrient foramen. (M-8a)

TIB12 ML proximal shaft diameter. Measured at the level of the nutrient foramen, perpendicular to TIB11. (M-9a)

TIB13 Talar AP diameter. Maximum AP diameter of the distal tibia, including non-articular surfaces.

TIB14 Talar ML diameter. Distance from the most indented part of the fibular notch to the medial-most aspect of the medial malleolus.

TIB15 Nutrient foramen length. Distance from the nutrient foramen to the inferior tip of the medial malleolus. Taken with a tape measure.

TIB16 Nutrient foramen articular length. Distance from the nutrient foramen to the middle of the talar articular surface. Taken with a tape measure.

TIB17 Minimum shaft circumference. Taken with a tape measure.

TIB18 Nutrient foramen shaft circumference. Taken with a tape measure.

Photographic Protocol for the Os Coxae

One angular variable (PEL11, average sciatic notch angle) and three non-metric characters of the os coxae are recorded from photographs. To ensure consistency in data collection, a strict photographic protocol was followed. The four step protocol is described below.

1. Place the external aspect of the os coxae flat on a hard surface, orienting the bone such that the ischial spine, posterior inferior iliac spine and apex of the sciatic notch form a single plane that is perpendicular to the observer. In this position, the ischial tuberosity lies flat on the surface, and the auricular surface is visible.

2. Select the macro setting on the digital camera, and center the lens on the sciatic notch.

3. Position a small bubble level on the back of the camera to ensure that the lens is parallel to the surface.

4. Take two photographs per specimen, positioning the camera as close to the specimen as possible while capturing the required anatomical features in views A and B:

    A. Internal aspect of the os coxae showing the full extent of the auricular surface and sciatic notch, including the ischial spine (or its base, if broken).

    B. Close up of the sciatic notch, including the apex of the notch, the posterior inferior iliac spine, and the ischial spine (or its base, if broken).

Appendix 2

Summary Statistics for the Skeletal Samples

All measurements are in millimeters unless otherwise noted. Details pertaining to the composition of each sample are provided in Chapter 2.

Abbreviations:

n = sample size

X = mean

s.d. = standard deviation

Sex: B = both sexes, F = female, M = male

EUP = early Upper Paleolithic early *H. sapiens*
(see Chapter 2 for a list of specimens included in this sample)

MSA = Middle Stone Age early *H. sapiens*
(see Chapter 2 for a list of specimens included in this sample)

Table A2-1. Univariate summary statistics of the humerus.

		HUM1			HUM2			HUM3		
	sex	***n***	***X***	**± s.d.**	***n***	***X***	**± s.d.**	***n***	***X***	**± s.d.**
Recent										
Zulu	B	41	308.16	21.05	41	304.62	20.58	41	20.36	1.89
	F	19	293.26	9.80	19	290.29	9.27	19	19.17	1.44
	M	22	321.02	19.68	22	317.00	19.67	22	21.40	1.60
Kikuyu	B	39	314.19	23.63	39	309.58	23.30	39	20.33	1.98
	F	12	296.21	23.15	12	290.79	21.61	12	18.59	1.56
	M	15	322.37	19.48	15	318.20	18.59	15	21.43	1.70
Ugandan	M	25	331.04	19.29	25	326.52	19.17	25	21.22	2.07
Archaeological										
Khoe-San	B	73	284.55	19.68	73	282.64	19.34	80	17.20	1.82
Sudanese	B	54	318.40	23.07	52	315.28	22.88	87	19.62	2.04
Taforalt	B	23	324.63	12.08	23	322.17	12.06	30	21.43	2.01
Fossil										
EUP	B	18	338.50	25.10	17	337.70	22.84	20	22.23	3.04
MSA	B	3	347.83	22.97	3	340.17	23.86	8	21.58	2.22

Table A2-1. Continued.

	sex	HUM4 *n*	HUM4 *X*	HUM4 ± s.d.	HUM5 *n*	HUM5 *X*	HUM5 ± s.d.	HUM6 *n*	HUM6 *X*	HUM6 ± s.d.
Recent										
Zulu	B	41	17.15	1.84	41	40.85	4.06	41	38.83	3.32
	F	19	16.00	1.67	19	37.65	2.06	19	36.07	1.58
	M	22	18.14	1.35	22	43.62	3.23	22	41.22	2.45
Kikuyu	B	39	16.27	1.49	37	40.94	3.76	37	38.40	2.88
	F	12	15.04	1.20	12	37.68	3.03	12	36.22	2.67
	M	15	17.05	1.43	13	42.59	2.57	13	40.19	1.65
Ugandan	M	25	16.83	1.72	25	42.67	2.96	25	39.59	2.90
Archaeological										
Khoe-San	B	80	13.96	1.54	72	36.66	3.19	67	35.27	2.99
Sudanese	B	87	15.81	1.82	55	42.47	3.90	50	39.30	3.22
Taforalt	B	30	17.51	1.65	25	46.29	3.36	23	46.29	2.78
Fossil										
EUP	B	20	17.83	1.98	15	48.16	3.96	13	43.29	3.96
MSA	B	8	17.17	2.41	4	47.16	3.67	3	41.73	0.23

Table A2-1. Continued.

	sex	HUM9 *n*	HUM9 *X*	HUM9 ± s.d.	HUM11 *n*	HUM11 *X*	HUM11 ± s.d.	HUM12 *n*	HUM12 *X*	HUM12 ± s.d.
Recent										
Zulu	B	41	64.86	8.81	41	58.70	4.85	41	42.58	3.77
	F	19	63.89	8.99	19	54.92	2.30	19	39.73	1.64
	M	22	65.70	8.78	22	61.96	4.03	22	45.04	3.33
Kikuyu	B	38	65.13	8.91	38	56.77	4.75	38	41.18	3.53
	F	12	66.50	9.39	12	53.06	3.99	12	38.47	2.81
	M	14	66.29	8.05	14	59.09	3.52	14	42.52	2.74
Ugandan	M	25	59.26	11.64	25	59.99	3.62	25	43.07	2.67
Archaeological										
Khoe-San	B	80	55.83	9.51	80	52.01	4.28	80	37.83	2.66
Sudanese	B	85	65.94	11.30	65	59.16	4.69	68	41.94	3.68
Taforalt	B	28	68.14	9.19	27	62.45	3.94	29	46.87	3.09
Fossil										
EUP	B	8	68.57	10.72	16	61.89	4.47	17	44.99	3.06
MSA	B	1	--	--	6	61.91	5.84	6	46.44	5.00

Table A2-1. Continued.

	sex	HUM13			HUM14			HUM15		
		n	*X*	± s.d.	*n*	*X*	± s.d.	*n*	*X*	± s.d.
Recent										
Zulu	B	41	17.37	1.78	41	19.64	1.79	41	25.94	2.23
	F	19	16.24	0.98	19	18.46	1.07	19	24.59	1.49
	M	22	18.35	1.75	22	20.66	1.66	22	27.10	2.12
Kikuyu	B	38	17.54	1.75	39	19.62	1.87	39	26.82	2.50
	F	12	16.16	1.41	12	18.23	1.73	12	25.09	2.61
	M	14	18.68	1.59	15	20.24	1.46	15	27.75	2.06
Ugandan	M	25	18.16	1.49	25	20.49	1.75	25	26.84	2.38
Archaeological										
Khoe-San	B	80	15.92	1.28	78	17.49	1.58	77	23.84	1.98
Sudanese	B	70	17.44	1.83	68	20.87	1.82	69	28.69	2.54
Taforalt	B	29	18.34	1.26	29	22.61	1.66	28	32.52	2.42
Fossil										
EUP	B	12	18.25	1.29	7	21.89	2.75	12	27.22	5.38
MSA	B	6	19.66	3.31	7	19.65	2.12	6	26.25	4.29

Table A2-1. Continued.

	sex	HUM17			HUM18			HUM19		
		n	*X*	± s.d.	*n*	*X*	± s.d.	*n*	*X*	± s.d.
Recent										
Zulu	B	41	24.95	2.45	41	15.88	1.75	41	25.64	2.60
	F	19	23.41	1.51	19	15.21	1.34	19	25.09	2.29
	M	22	26.29	2.33	22	16.47	1.88	22	26.12	2.80
Kikuyu	B	39	23.99	2.33	39	15.50	1.97	39	24.67	2.61
	F	12	22.27	1.74	12	13.89	1.71	12	23.13	2.04
	M	15	24.68	2.17	15	16.45	1.75	15	25.56	2.29
Ugandan	M	25	26.15	1.87	25	16.27	1.83	25	26.11	1.82
Archaeological										
Khoe-San	B	79	20.88	1.84	80	14.07	1.44	82	23.32	1.98
Sudanese	B	65	24.50	2.25	76	15.93	1.67	84	25.16	2.30
Taforalt	B	27	28.52	2.75	30	18.04	1.78	28	28.24	2.90
Fossil										
EUP	B	11	27.29	2.75	11	18.63	2.36	12	25.42	2.18
MSA	B	6	23.96	2.70	6	15.54	1.72	6	25.79	6.33

Table A2-1. Continued.

	sex	HUM20			HUM21			HUM23		
		n	*X*	± s.d.	*n*	*X*	± s.d.	*n*	*X*	± s.d.
Recent										
Zulu	B	41	9.51	2.28	41	16.68	2.12	41	147.26	13.66
	F	19	8.34	1.42	19	15.63	1.40	19	139.11	7.90
	M	22	10.52	2.42	22	17.58	2.24	22	154.30	13.78
Kikuyu	B	39	9.89	1.55	39	16.62	1.78	39	151.03	12.95
	F	12	9.25	1.04	12	15.85	2.21	12	143.00	12.22
	M	15	10.40	1.64	15	17.24	1.65	15	154.63	14.15
Ugandan	M	25	10.07	1.56	25	17.80	2.01	25	164.40	9.78
Archaeological										
Khoe-San	B	82	8.06	1.85	81	13.91	1.94	79	138.90	11.76
Sudanese	B	83	8.56	2.19	78	16.72	1.99	65	152.32	13.94
Taforalt	B	28	8.64	1.81	27	17.33	1.77	27	152.69	9.56
Fossil										
EUP	B	12	10.23	2.18	13	17.87	2.20	7	153.64	15.68
MSA	B	6	11.67	2.16	5	17.96	4.15	3	185.67	13.28

Table A2-1. Continued.

	sex	HUM24 *n*	HUM24 *X*	HUM24 ± s.d.	HUM25 *n*	HUM25 *X*	HUM25 ± s.d.
Recent							
Zulu	B	41	150.44	13.95	41	60.79	5.32
	F	19	141.63	8.19	19	57.16	3.94
	M	22	158.05	13.50	22	63.93	4.28
Kikuyu	B	39	155.01	13.31	38	58.92	5.23
	F	12	147.25	13.13	12	54.46	3.70
	M	15	158.37	14.38	15	62.33	4.67
Ugandan	M	25	168.34	9.54	25	61.32	4.69
Archaeological							
Khoe-San	B	79	140.98	12.26	82	51.05	5.23
Sudanese	B	71	154.60	14.38	87	57.12	5.55
Taforalt	B	27	155.07	9.57	29	62.24	5.87
Fossil							
EUP	B	6	156.83	18.37	21	63.40	6.60
MSA	B	3	183.83	11.36	7	61.00	7.82

Table A2-2. Univariate summary statistics of the ulna.

		ULN1			ULN2			ULN3		
	sex	***n***	***X***	**± s.d.**	***n***	***X***	**± s.d.**	***n***	***X***	**± s.d.**
Recent										
Zulu	B	41	239.46	16.69	41	257.80	17.74	41	15.32	1.84
	F	19	227.63	10.54	19	244.92	10.67	19	14.05	1.48
	M	22	249.68	14.11	22	268.93	14.89	22	16.42	1.36
Kikuyu	B	37	246.41	21.67	37	264.09	22.49	37	14.90	1.50
	F	11	230.59	21.55	11	247.05	21.63	11	13.71	1.31
	M	14	257.29	14.51	14	275.61	14.34	14	15.59	1.28
Ugandan	B	30	262.28	15.59	30	280.52	15.67	30	15.42	1.59
	F	4	258.00	24.33	4	276.25	24.77	4	14.58	1.45
	M	24	263.71	14.69	24	281.94	14.75	24	15.67	1.58
Archaeological										
Khoe-San	B	65	220.05	14.41	65	234.85	15.38	72	12.24	1.50
Sudanese	B	51	252.29	17.87	47	269.05	20.05	76	13.75	1.51
Taforalt	B	23	250.24	15.33	23	268.96	16.08	26	14.68	1.56
Fossil										
EUP	B	17	256.29	17.96	17	281.94	17.70	14	16.67	2.21
MSA	B	5	252.40	21.59	5	267.20	20.16	5	14.72	2.45

Table A2-2. Continued.

	sex	ULN4			ULN5			ULN6		
		n	*X*	± s.d.	*n*	*X*	± s.d.	*n*	*X*	± s.d.
Recent										
Zulu	B	41	11.98	1.25	41	33.47	3.09	41	23.79	2.33
	F	19	11.10	0.80	19	31.53	1.77	19	22.35	1.64
	M	22	12.75	1.06	22	35.15	3.03	22	25.04	2.14
Kikuyu	B	37	11.38	1.27	38	32.34	2.57	38	21.30	2.35
	F	11	10.51	0.97	11	30.34	2.04	11	19.95	2.51
	M	14	11.94	1.22	15	33.52	2.18	15	21.49	1.79
Ugandan	M	24	11.86	1.00	24	34.15	2.76	24	22.85	2.20
Archaeological										
Khoe-San	B	72	10.02	0.98	76	28.12	2.37	73	18.59	2.27
Sudanese	B	76	11.16	1.14	73	31.76	2.71	73	22.14	2.33
Taforalt	B	26	11.97	0.98	27	35.09	2.69	25	23.78	2.28
Fossil										
EUP	B	14	13.49	1.57	14	35.91	3.46	9	24.21	2.83
MSA	B	5	12.22	2.02	9	29.83	3.51	8	19.82	3.57

Table A2-2. Continued.

	sex	ULN7 *n*	ULN7 *X*	ULN7 ± s.d.	ULN8 *n*	ULN8 *X*	ULN8 ± s.d.	ULN9 *n*	ULN9 *X*	ULN9 ± s.d.
Recent										
Zulu	B	41	21.51	2.06	41	25.60	2.15	41	21.46	1.65
	F	19	20.12	1.15	19	24.44	1.36	19	20.42	1.19
	M*	22	22.71	1.92	22	26.61	2.22	22	22.37	1.45
Kikuyu	B	38	20.83	1.96	37	25.42	2.06	38	21.02	1.84
	F	11	19.66	1.92	11	24.32	1.92	11	19.69	1.27
	M	15	21.54	1.98	14	26.37	1.84	15	21.46	1.47
Ugandan	B	30	21.56	1.91	30	26.09	1.72	30	21.18	2.05
	F	4	21.28	2.31	4	25.71	1.75	4	20.33	2.10
	M	24	21.82	1.76	24	26.29	1.68	24	21.43	2.02
Archaeological										
Khoe-San	B	75	20.50	1.85	74	22.85	1.73	78	17.80	1.94
Sudanese	B	69	23.31	2.23	68	25.90	1.90	73	19.51	1.66
Taforalt	B	27	25.07	1.66	26	27.85	1.43	28	20.44	2.00
Fossil										
EUP	B	17	24.09	2.48	13	27.75	1.91	13	20.37	2.95
MSA	B	8	23.76	1.84	7	26.28	0.92	8	19.50	3.47

Table A2-2. Continued.

	sex	ULN10			ULN11			ULN12		
		n	***X***	**± s.d.**	***n***	***X***	**± s.d.**	***n***	***X***	**± s.d.**
Recent										
Zulu	B	41	23.39	2.20	41	19.18	1.66	41	18.68	1.50
	F	19	22.08	1.28	19	18.70	1.33	19	17.89	0.64
	M	22	24.53	2.21	22	19.59	1.84	22	19.36	1.69
Kikuyu	B	38	23.03	2.08	38	19.63	1.82	38	18.22	1.89
	F	11	21.38	1.33	11	18.91	1.87	11	17.39	1.98
	M	15	23.80	2.01	15	20.15	1.82	15	18.42	1.83
Ugandan	B	30	22.87	2.40	30	19.27	1.84	30	18.58	1.76
	F	4	22.53	1.71	4	18.62	1.45	4	17.68	1.75
	M	24	23.30	2.22	24	19.48	1.93	24	18.94	1.63
Archaeological										
Khoe-San	B	77	20.29	1.70	75	16.89	1.57	77	16.56	1.47
Sudanese	B	71	22.65	2.38	71	19.19	1.96	76	18.69	1.66
Taforalt	B	26	25.28	2.12	28	20.72	2.10	27	21.23	1.28
Fossil										
EUP	B	8	23.47	2.35	8	19.84	1.86	9	21.82	1.95
MSA	B	6	22.25	1.64	8	19.30	2.98	10	18.97	2.36

Table A2-2. Continued.

	sex	ULN13			ULN14			ULN15		
		n	*X*	± s.d.	*n*	*X*	± s.d.	*n*	*X*	± s.d.
Recent										
Zulu	B	41	16.64	1.39	41	38.55	3.61	41	19.59	1.59
	F	19	16.00	0.54	19	36.06	1.87	19	18.77	1.22
	M	22	17.19	1.66	22	40.71	3.38	22	20.29	1.55
Kikuyu	B	38	16.05	1.60	38	39.11	3.04	38	18.88	2.45
	F	11	15.50	1.45	11	36.57	2.82	11	17.24	1.85
	M	15	16.29	1.73	15	40.58	2.14	15	19.77	2.44
Ugandan	M	24	16.99	1.34	24	41.07	2.67	24	19.30	1.58
Archaeological										
Khoe-San	B	77	15.13	1.42	77	35.61	3.02	76	16.07	1.71
Sudanese	B	70	17.31	1.53	73	39.86	3.48	80	18.72	2.03
Taforalt	B	27	19.46	1.24	28	40.94	3.09	27	18.82	1.78
Fossil										
EUP	B	14	18.41	2.18	9	42.96	4.12	13	19.09	2.28
MSA	B	8	17.92	1.86	8	39.58	4.72	9	16.75	1.64

Table A2-2. Continued.

	sex	ULN17			ULN18			ULN19		
		n	*X*	± s.d.	*n*	*X*	± s.d.	*n*	*X*	± s.d.
Recent										
Zulu	B	41	30.53	4.40	41	17.84	2.02	41	15.16	1.51
	F	19	28.53	2.95	19	17.08	1.92	19	14.29	1.23
	M	22	32.25	4.76	22	18.51	1.90	22	15.91	1.33
Kikuyu	B	38	33.19	5.49	38	16.69	1.77	38	14.98	1.52
	F	11	31.21	6.07	11	15.51	1.07	11	13.86	1.30
	M	15	34.30	5.10	15	17.60	1.78	15	15.64	1.41
Ugandan	M	24	32.82	3.39	24	17.25	2.26	24	15.86	1.42
Archaeological										
Khoe-San	B	78	32.67	3.29	78	14.53	1.71	78	12.80	1.86
Sudanese	B	79	33.35	3.84	85	15.82	1.76	85	13.95	1.57
Taforalt	B	27	31.80	3.60	29	18.20	1.68	29	14.74	1.29
Fossil										
EUP	B	13	33.26	3.51	10	19.00	2.43	10	17.33	2.63
MSA	B	7	32.80	5.25	8	15.72	2.19	8	14.66	1.67

Table A2-2. Continued.

	sex	ULN20 *n*	ULN20 *X*	ULN20 ± s.d.	ULN21 *n*	ULN21 *X*	ULN21 ± s.d.
Recent							
Zulu	B	41	16.53	1.95	41	35.54	3.36
	F	19	15.32	0.86	19	33.47	2.16
	M	22	17.57	2.04	22	37.32	3.21
Kikuyu	B	36	16.14	1.82	38	33.89	3.44
	F	11	14.64	2.07	11	31.55	3.42
	M	13	17.20	0.76	15	35.63	3.27
Ugandan	M	24	16.97	1.75	23	35.89	3.05
Archaeological							
Khoe-San	B	59	13.56	1.32	68	29.85	3.05
Sudanese	B	50	16.57	2.06	69	34.88	3.66
Taforalt	B	29	17.49	1.59	26	35.75	2.27
Fossil							
EUP	B	6	18.69	2.75	10	37.85	4.45
MSA	B	4	16.42	2.45	6	35.08	4.12

Table A2-3. Univariate summary statistics of the radius.

		RAD1			RAD2			RAD3		
	sex	***n***	***X***	**± s.d.**	***n***	***X***	**± s.d.**	***n***	***X***	**± s.d.**
Recent										
Zulu	B	39	226.99	16.63	39	236.99	17.31	39	14.08	1.64
	F	19	215.82	9.09	19	224.63	8.95	19	13.22	1.18
	M	20	237.60	15.22	20	248.73	15.02	20	14.88	1.63
Kikuyu	B	39	236.86	21.50	38	244.54	22.22	39	14.06	1.61
	F	12	221.75	19.87	12	228.17	20.25	12	12.86	1.01
	M	15	247.03	14.74	14	256.82	14.16	15	15.18	1.57
Ugandan	M	23	253.67	13.53	23	263.20	14.08	23	14.36	1.50
Archaeological										
Khoe-San	B	71	208.27	13.64	69	216.80	14.31	76	12.08	1.30
Sudanese	B	63	239.63	18.71	57	253.20	19.32	86	13.41	1.33
Taforalt	B	18	241.14	19.26	17	253.82	19.45	26	14.97	1.18
Fossil										
EUP	B	16	247.38	17.64	15	262.77	18.85	19	15.57	1.91
MSA	B	3	252.00	8.53	3	260.50	10.85	6	14.57	1.13

Table A2-3. Continued.

	sex	RAD5 *n*	RAD5 *X*	RAD5 ± s.d.	RAD6 *n*	RAD6 *X*	RAD6 ± s.d.	RAD7 *n*	RAD7 *X*	RAD7 ± s.d.
Recent										
Zulu	B	34	21.62	1.97	34	21.20	1.96	33	21.92	2.03
	F	17	20.14	0.88	17	19.70	0.89	17	20.37	0.80
	M	17	23.10	1.60	17	22.70	1.54	16	23.56	1.59
Kikuyu	B	35	21.31	1.99	35	21.03	1.83	35	21.70	1.89
	F	11	19.64	1.91	11	19.78	1.71	11	20.15	1.69
	M	12	22.18	1.14	12	21.70	1.28	12	22.45	1.21
Ugandan	M	21	22.42	1.42	22	21.85	1.17	21	22.73	1.37
Archaeological										
Khoe-San	B	65	19.63	1.59	65	19.44	1.59	64	19.91	1.59
Sudanese	B	41	21.44	1.98	47	21.22	2.07	38	21.79	1.92
Taforalt	B	23	24.08	1.99	20	23.96	1.83	18	24.83	2.02
Fossil										
EUP	B	9	21.97	4.08	5	22.95	0.62	7	22.87	2.02
MSA	B	5	21.33	2.00	4	21.65	3.54	3	21.45	2.94

Table A2-3. Continued.

	sex	RAD8 *n*	RAD8 *X*	RAD8 ± s.d.	RAD9 *n*	RAD9 *X*	RAD9 ± s.d.	RAD10 *n*	RAD10 *X*	RAD10 ± s.d.
Recent										
Zulu	B	39	29.19	3.76	39	32.45	3.21	39	13.19	1.39
	F	19	28.64	3.90	19	31.29	3.14	19	12.40	1.05
	M	20	29.72	3.64	20	33.56	2.92	20	13.94	1.28
Kikuyu	B	39	25.92	3.02	39	33.02	3.91	39	13.42	1.65
	F	12	24.96	2.22	12	29.65	3.29	12	12.15	1.53
	M	15	27.07	3.39	15	34.77	2.53	15	14.31	1.57
Ugandan	M	23	24.67	2.47	23	34.61	3.68	23	13.21	1.43
Archaeological										
Khoe-San	B	78	26.81	3.85	77	31.34	3.67	78	10.59	1.20
Sudanese	B	88	30.92	3.72	76	34.40	3.49	84	13.03	1.46
Taforalt	B	24	31.23	3.10	24	35.26	3.06	25	14.18	1.18
Fossil										
EUP	B	17	28.48	7.99	12	36.12	4.53	12	14.09	1.39
MSA	B	7	30.17	5.03	6	35.41	3.21	9	12.92	2.34

Table A2-3. Continued.

	sex	RAD13			RAD14			RAD15		
		n	*X*	± s.d.	*n*	*X*	± s.d.	*n*	*X*	± s.d.
Recent										
Zulu	B	39	24.71	2.00	39	29.03	2.45	39	39.49	3.56
	F	19	23.67	1.09	19	27.49	1.24	19	37.21	1.95
	M	20	25.70	2.18	20	30.49	2.43	20	41.65	3.41
Kikuyu	B	38	22.31	2.28	38	27.96	2.16	39	39.55	4.88
	F	12	20.84	2.30	12	26.35	1.85	12	36.13	2.99
	M	14	22.83	1.85	14	28.67	2.00	15	42.50	4.87
Ugandan	M	23	22.35	3.90	23	29.04	1.88	23	40.43	3.27
Archaeological										
Khoe-San	B	67	20.65	1.65	67	25.74	1.81	77	32.99	3.07
Sudanese	B	55	23.09	1.76	59	28.90	2.28	84	37.56	3.36
Taforalt	B	26	26.13	1.75	26	32.10	2.23	26	40.13	2.71
Fossil										
EUP	B	7	28.59	5.74	10	30.55	2.09	8	43.56	3.64
MSA	B	3	22.56	4.00	3	29.41	3.91	5	40.20	4.76

Table A2-3. Continued.

	sex	RAD16 *n*	*X*	± s.d.
Recent				
Zulu	B	39	49.71	4.77
	F	19	46.68	3.89
	M	20	52.58	3.66
Kikuyu	B	39	50.10	5.29
	F	12	46.17	4.56
	M	15	52.70	4.50
Ugandan	M	23	49.46	4.89
Archaeological				
Khoe-San	B	78	39.95	4.35
Sudanese	B	87	48.33	4.82
Taforalt	B	25	51.86	3.50
Fossil				
EUP	B	8	53.31	3.21
MSA	B	7	50.86	6.82

Table A2-4. Univariate summary statistics of the os coxae.

		PEL1			PEL2			PEL3		
	sex	***n***	***X***	**± s.d.**	***n***	***X***	**± s.d.**	***n***	***X***	**± s.d.**
Recent										
Zulu	B	42	50.76	3.97	42	48.75	4.27	42	98.59	7.40
	F	20	47.74	2.93	20	46.52	2.84	20	93.48	4.22
	M	22	53.50	2.53	22	50.78	4.38	22	103.24	6.57
Kikuyu	B	40	50.50	4.01	39	49.15	3.93	39	99.34	7.71
	F	12	48.31	3.94	12	46.17	3.48	12	93.82	7.24
	M	16	51.50	3.37	15	50.94	3.60	15	102.67	5.72
Ugandan	M	25	51.89	3.59	25	49.12	3.82	25	99.66	5.93
Archaeological										
Khoe-San	B	57	47.45	3.35	54	45.49	3.60	54	93.34	6.54
Sudanese	B	39	49.98	4.21	38	49.47	3.79	38	100.76	7.49
Taforalt	B	12	58.41	3.49	19	54.96	4.47	17	113.66	7.41
Fossil										
EUP	B	10	52.36	5.01	6	55.27	5.86	6	109.47	9.81
MSA	B	4	51.69	3.01	4	52.94	3.63	4	106.58	5.72

Table A2-4. Continued.

	sex	PEL5			PEL6			PEL7		
		n	*X*	± s.d.	*n*	*X*	± s.d.	*n*	*X*	± s.d.
Recent										
Zulu	B	42	28.70	2.55	42	28.11	2.69	42	33.75	3.04
	F	20	27.50	1.65	20	26.77	2.29	20	31.70	1.87
	M	22	29.79	2.77	22	29.32	2.49	22	35.62	2.69
Kikuyu	B	39	29.44	2.42	39	28.35	2.35	40	33.87	2.35
	F	12	28.21	2.02	12	28.53	2.36	12	31.67	3.36
	M	15	29.71	2.29	15	28.26	2.25	16	34.89	2.24
Ugandan	M	25	29.32	2.19	25	29.27	2.35	25	34.57	3.07
Archaeological										
Khoe-San	B	60	26.82	2.47	64	26.69	2.83	66	31.40	2.45
Sudanese	B	45	32.18	3.14	55	28.55	3.13	56	36.58	4.20
Taforalt	B	25	35.33	2.42	24	33.07	2.84	22	40.04	2.78
Fossil										
EUP	B	9	33.10	5.32	12	30.94	4.21	11	38.96	3.76
MSA	B	4	30.01	2.67	4	28.32	2.74	5	36.38	1.58

Table A2-4. Continued.

	sex	PEL8 *n*	PEL8 *X*	PEL8 ± s.d.	PEL9 *n*	PEL9 *X*	PEL9 ± s.d.	PEL10 *n*	PEL10 *X*	PEL10 ± s.d.
Recent										
Zulu	B	42	17.24	2.63	42	37.05	5.71	42	34.08	5.70
	F	20	16.07	1.95	20	40.91	4.49	20	37.83	5.08
	M	22	18.30	2.76	22	33.54	4.30	22	30.68	3.81
Kikuyu	B	40	16.03	1.89	40	35.75	4.59	39	34.63	4.74
	F	12	15.38	2.25	12	37.64	5.01	12	36.42	4.72
	M	16	15.86	1.44	16	34.21	3.77	15	32.74	3.08
Ugandan	M	25	17.58	2.56	25	35.10	4.41	25	32.05	3.22
Archaeological										
Khoe-San	B	64	15.88	2.08	65	35.31	5.34	66	34.22	5.70
Sudanese	B	46	17.82	2.89	47	38.75	5.21	47	37.63	6.03
Taforalt	B	19	20.81	2.87	17	39.07	4.65	16	38.29	4.05
Fossil										
EUP	B	9	19.16	3.17	9	37.65	2.94	8	35.39	4.15
MSA	B	4	19.25	3.87	4	39.02	6.03	4	31.75	8.57

Table A2-4. Continued.

	sex	PEL11 (degree) *n*	*X*	± s.d.
Recent				
Zulu	B	42	77.30	11.20
	F	20	85.83	7.87
	M	22	69.55	7.53
Kikuyu	B	39	77.35	9.04
	F	12	84.43	7.98
	M	15	72.62	6.25
Ugandan	M	25	70.84	8.92
Archaeological				
Khoe-San	B	65	81.94	9.59
Sudanese	B	47	77.15	10.87
Taforalt	B	19	67.48	9.36
Fossil				
EUP	B	9	71.43	12.47
MSA	B	4	83.69	14.80

Table A2-5. Univariate summary statistics of the femur.

		FEM1			FEM2			FEM3		
	sex	***n***	***X***	**± s.d.**	***n***	***X***	**± s.d.**	***n***	***X***	**± s.d.**
Recent										
Zulu	B	38	437.42	25.96	38	433.80	26.12	38	27.88	3.19
	F	18	420.75	14.78	18	416.44	14.35	18	26.32	2.91
	M	20	452.43	24.84	20	449.43	24.53	20	29.30	2.79
Kikuyu	B	39	441.96	33.02	38	438.20	33.97	39	27.86	2.77
	F	12	420.42	35.70	12	416.17	36.08	12	25.26	1.39
	M	15	450.33	25.47	15	447.40	25.26	15	29.51	2.06
Ugandan	M	26	473.77	22.25	26	469.35	21.73	26	29.01	2.67
Archaeological										
Khoe-San	B	71	410.39	26.31	71	407.04	26.24	72	27.40	3.33
Sudanese	B	47	454.93	33.26	46	451.63	33.23	79	28.38	3.17
Taforalt	B	18	465.81	22.55	18	461.42	22.56	26	30.11	3.09
Fossil										
EUP	B	15	457.90	42.42	15	454.70	41.78	22	31.90	4.55
MSA	B	4	489.38	15.21	3	490.83	8.75	7	34.13	3.81

Table A2-5. Continued.

	sex	FEM4			FEM5			FEM6		
		n	*X*	± s.d.	*n*	*X*	± s.d.	*n*	*X*	± s.d.
Recent										
Zulu	B	38	26.06	2.28	38	42.48	3.44	38	42.34	3.51
	F	18	24.90	1.39	18	39.88	2.40	18	39.50	2.11
	M	20	27.09	2.45	20	44.83	2.37	20	44.83	2.37
Kikuyu	B	39	24.88	2.14	38	42.04	3.45	39	42.06	3.57
	F	12	23.59	2.02	12	39.01	2.97	12	38.89	3.21
	M	15	25.91	1.48	14	43.55	2.22	15	43.51	2.12
Ugandan	M	26	24.93	2.12	26	43.53	2.86	26	43.64	2.85
Archaeological										
Khoe-San	B	72	22.83	1.74	67	39.01	2.69	69	39.00	2.59
Sudanese	B	79	25.49	2.35	52	42.85	3.69	56	43.08	3.67
Taforalt	B	26	27.17	1.79	19	48.72	3.26	22	48.58	3.31
Fossil										
EUP	B	22	27.51	2.53	17	46.86	4.05	17	46.40	4.09
MSA	B	7	28.03	1.52	2	47.65	1.32	4	46.94	1.89

Table A2-5. Continued.

	sex	FEM7 *n*	FEM7 *X*	FEM7 ± s.d.	FEM8 *n*	FEM8 *X*	FEM8 ± s.d.	FEM9 *n*	FEM9 *X*	FEM9 ± s.d.
Recent										
Zulu	B	38	28.89	2.72	38	23.97	2.62	38	84.72	6.74
	F	18	26.81	1.45	18	21.87	1.25	18	80.10	3.31
	M	20	30.77	2.17	20	25.85	2.01	20	88.87	6.35
Kikuyu	B	39	29.77	3.31	39	24.76	2.60	39	83.08	7.76
	F	12	27.09	2.38	12	23.12	2.41	12	76.54	7.25
	M	15	31.54	2.93	15	25.50	2.28	15	86.06	2.78
Ugandan	M	26	30.45	2.79	26	25.94	2.77	26	84.61	5.53
Archaeological										
Khoe-San	B	75	26.67	2.71	74	23.34	2.24	69	77.37	6.27
Sudanese	B	68	28.50	2.72	70	24.09	2.63	53	85.08	7.39
Taforalt	B	22	30.47	2.47	22	25.84	1.93	21	96.71	6.79
Fossil										
EUP	B	12	33.09	3.55	11	25.32	2.23	9	94.01	12.37
MSA	B	5	32.43	4.19	5	28.91	2.75	4	93.61	6.73

Table A2-5. Continued.

	sex	FEM10			FEM11			FEM12		
		n	*X*	± s.d.	*n*	*X*	± s.d.	*n*	*X*	± s.d.
Recent										
Zulu	B	38	45.86	4.57	38	27.85	3.23	38	29.80	2.43
	F	18	44.89	4.69	18	26.00	2.57	18	28.78	2.13
	M	20	46.74	4.40	20	29.51	2.88	20	30.73	2.35
Kikuyu	B	39	47.86	5.12	39	27.83	2.46	39	29.45	3.29
	F	12	46.00	3.97	12	27.23	3.15	12	27.86	3.02
	M	15	48.06	4.58	15	27.82	1.97	15	30.56	2.56
Ugandan	M	26	49.65	5.21	26	27.83	2.81	26	28.36	2.69
Archaeological										
Khoe-San	B	69	41.03	4.83	78	25.57	2.16	78	26.20	2.16
Sudanese	B	60	45.35	4.69	84	25.28	2.38	84	28.74	2.76
Taforalt	B	21	52.04	4.97	25	27.46	2.35	25	31.79	2.54
Fossil										
EUP	B	8	53.21	5.43	23	26.49	3.40	23	34.61	3.67
MSA	B	5	52.64	5.38	7	30.03	2.82	7	33.78	5.40

Table A2-5. Continued.

	sex	FEM13			FEM14			FEM15		
		n	*X*	± s.d.	*n*	*X*	± s.d.	*n*	*X*	± s.d.
Recent										
Zulu	B	38	14.48	3.19	37	37.57	3.29	37	75.28	5.87
	F	18	13.44	2.86	17	34.74	1.88	18	70.71	2.08
	M	20	15.41	3.25	20	39.98	2.05	19	79.61	4.92
Kikuyu	B	39	10.16	1.53	36	38.67	3.29	37	74.19	5.45
	F	12	9.80	2.02	12	36.63	2.65	12	69.94	5.31
	M	15	10.24	1.34	14	40.12	3.09	14	76.51	4.10
Ugandan	M	26	10.02	2.87	25	38.77	2.88	26	76.41	3.67
Archaeological										
Khoe-San	B	77	11.34	1.94	75	34.95	3.19	70	68.28	4.87
Sudanese	B	83	11.78	2.12	46	35.83	2.85	39	75.12	5.28
Taforalt	B	25	14.06	2.60	21	41.10	3.46	19	83.60	5.44
Fossil										
EUP	B	17	11.31	2.97	9	41.77	3.78	14	82.13	6.25
MSA	B	4	10.15	2.07	5	42.38	4.01	4	78.54	5.79

Table A2-5. Continued.

	sex	FEM16 *n*	FEM16 *X*	FEM16 ± s.d.	FEM17 *n*	FEM17 *X*	FEM17 ± s.d.	FEM18 *n*	FEM18 *X*	FEM18 ± s.d.
Recent										
Zulu	B	37	70.96	6.01	38	83.26	6.74	38	89.51	6.61
	F	17	65.84	2.93	18	79.17	4.36	18	85.86	4.57
	M	20	75.31	4.22	20	86.95	6.43	20	92.80	6.51
Kikuyu	B	36	69.27	5.23	38	80.58	6.68	38	88.21	7.59
	F	12	65.04	4.49	12	75.58	4.91	12	82.63	6.65
	M	14	71.33	3.29	15	84.77	5.23	15	91.93	6.98
Ugandan	M	25	71.89	3.54	26	83.02	6.63	26	89.33	6.22
Archaeological										
Khoe-San	B	60	66.26	4.88	72	75.65	5.56	78	79.98	6.07
Sudanese	B	39	69.22	5.51	82	81.71	6.73	84	86.09	7.15
Taforalt	B	17	76.71	5.75	26	86.38	5.76	25	92.32	5.77
Fossil										
EUP	B	8	77.54	7.57	10	92.70	8.33	10	97.70	10.03
MSA	B	4	74.10	6.00	5	96.20	8.58	7	103.1	10.69

Table A2-6. Univariate summary statistics of the tibia.

	sex	TIB1 *n*	TIB1 *X*	TIB1 ± s.d.	TIB2 *n*	TIB2 *X*	TIB2 ± s.d.	TIB3 *n*	TIB3 *X*	TIB3 ± s.d.
Recent										
Zulu	B	39	349.03	25.33	39	360.95	25.40	39	29.52	3.15
	F	18	331.25	11.47	18	343.28	11.72	18	27.19	2.44
	M	21	364.26	24.07	21	376.10	24.22	21	31.52	2.17
Kikuyu	B	37	357.38	31.44	37	369.35	31.83	36	30.03	3.04
	F	12	340.58	35.33	12	352.08	36.57	11	27.28	1.52
	M	15	366.43	28.20	15	378.97	27.81	15	31.60	2.23
Ugandan	M	26	380.81	22.17	26	392.75	22.71	26	29.93	1.90
Archaeological										
Khoe-San	B	72	329.58	22.46	70	340.84	23.47	71	27.57	3.16
Sudanese	B	42	360.99	28.93	41	372.24	29.33	79	28.13	3.14
Taforalt	B	22	360.95	20.29	20	373.25	19.56	25	33.75	4.15
Fossil										
EUP	B	10	375.00	29.51	14	387.82	27.55	17	33.25	4.51
MSA	B	4	392.50	40.94	4	406.13	41.11	8	34.44	3.35

Table A2-6. Continued.

	sex	TIB4			TIB5			TIB6		
		n	*X*	± s.d.	*n*	*X*	± s.d.	*n*	*X*	± s.d.
Recent										
Zulu	B	39	21.56	2.25	37	49.59	4.37	37	72.02	5.59
	F	18	20.34	1.86	17	46.10	2.20	17	67.05	2.78
	M	21	22.61	2.05	20	52.56	3.45	20	76.24	3.45
Kikuyu	B	36	21.55	2.12	34	48.79	4.00	35	70.59	5.60
	F	11	20.45	1.77	12	45.52	3.29	12	65.96	5.73
	M	15	22.40	2.09	12	50.91	2.88	13	73.25	3.02
Ugandan	M	26	21.72	2.07	26	50.34	2.92	26	72.59	3.15
Archaeological										
Khoe-San	B	71	19.11	1.98	65	44.61	3.51	64	66.26	4.90
Sudanese	B	79	20.50	2.43	33	49.76	4.02	33	70.33	5.98
Taforalt	B	25	20.73	2.22	23	53.56	3.27	25	77.71	4.85
Fossil										
EUP	B	17	21.78	3.58	5	53.35	6.30	13	77.93	6.34
MSA	B	8	23.98	3.22	1	--	--	1	--	--

Table A2-6. Continued.

	sex	TIB7 *n*	TIB7 *X*	TIB7 ± s.d.	TIB8 *n*	TIB8 *X*	TIB8 ± s.d.	TIB9 *n*	TIB9 *X*	TIB9 ± s.d.
Recent										
Zulu	B	36	44.71	4.09	37	29.83	2.68	37	39.15	4.10
	F	16	41.27	1.66	17	28.14	1.75	17	35.88	2.02
	M	20	47.47	3.26	20	31.26	2.51	20	41.93	3.27
Kikuyu	B	35	44.80	4.10	34	29.25	2.88	34	38.70	3.12
	F	12	42.12	3.95	12	26.99	2.97	12	36.47	3.46
	M	13	46.08	3.44	13	30.79	1.65	13	39.48	2.06
Ugandan	M	26	45.66	3.38	26	29.85	2.17	26	40.91	2.60
Archaeological										
Khoe-San	B	62	41.40	2.90	64	28.99	2.33	61	36.23	2.88
Sudanese	B	29	45.23	3.53	29	29.27	2.72	29	39.28	3.50
Taforalt	B	23	49.47	3.31	25	34.52	2.59	24	42.29	2.21
Fossil										
EUP	B	7	49.36	5.73	8	32.97	3.61	6	44.13	4.60
MSA	B	2	45.14	7.35	2	32.57	2.14	1	--	--

Table A2-6. Continued.

	sex	TIB10			TIB11			TIB12		
		n	*X*	± s.d.	*n*	*X*	± s.d.	*n*	*X*	± s.d.
Recent										
Zulu	B	37	31.13	2.94	39	33.66	3.70	39	23.76	2.68
	F	17	28.83	1.49	18	30.87	2.55	18	22.18	2.21
	M	20	33.08	2.39	21	36.05	2.73	21	25.11	2.32
Kikuyu	B	35	29.41	2.21	36	34.10	3.22	36	23.80	2.88
	F	12	28.15	2.44	11	31.35	2.38	11	22.16	2.57
	M	13	30.32	1.01	15	35.36	2.56	15	24.90	2.98
Ugandan	M	26	31.33	1.88	26	34.70	2.53	26	24.71	2.61
Archaeological										
Khoe-San	B	62	28.57	2.41	73	30.94	3.40	73	20.66	2.32
Sudanese	B	28	30.31	2.89	78	32.37	3.68	78	22.10	2.43
Taforalt	B	25	34.64	2.63	24	37.48	4.40	24	22.44	1.82
Fossil										
EUP	B	9	34.89	2.64	15	40.33	6.29	15	24.39	3.94
MSA	B	1	--	--	4	38.67	3.58	4	25.03	3.27

Table A2-6. Continued.

	sex	TIB13 *n*	TIB13 *X*	TIB13 ± s.d.	TIB14 *n*	TIB14 *X*	TIB14 ± s.d.	TIB15 *n*	TIB15 *X*	TIB15 ± s.d.
Recent										
Zulu	B	39	36.75	2.81	39	41.90	3.18	39	256.08	18.15
	F	18	34.54	1.20	18	39.28	1.49	18	242.69	9.24
	M	21	38.64	2.37	21	44.14	2.43	21	267.55	15.93
Kikuyu	B	37	36.43	2.77	37	41.47	3.38	37	259.42	25.42
	F	12	34.11	2.78	12	38.54	2.56	12	249.54	26.97
	M	15	37.47	1.77	15	42.77	2.00	15	263.10	27.60
Ugandan	M	26	37.76	2.51	26	41.52	1.99	26	276.60	18.62
Archaeological										
Khoe-San	B	76	32.49	2.44	72	37.57	2.69	69	239.63	21.66
Sudanese	B	57	36.22	2.80	52	41.59	3.26	49	263.88	21.90
Taforalt	B	22	39.33	2.39	21	45.04	2.77	21	248.80	51.18
Fossil										
EUP	B	17	40.44	3.68	17	48.41	4.10	5	282.90	17.41
MSA	B	7	37.77	2.17	6	43.83	3.44	3	266.33	42.29

Table A2-6. Continued.

	sex	TIB16			TIB17			TIB18		
		n	*X*	± s.d.	*n*	*X*	± s.d.	*n*	*X*	± s.d.
Recent										
Zulu	B	39	244.64	18.18	39	73.35	6.24	39	91.46	9.06
	F	18	231.31	9.34	18	69.14	4.68	18	85.47	6.26
	M	21	256.07	16.02	21	76.95	5.08	21	96.60	7.92
Kikuyu	B	37	247.45	25.81	36	74.26	7.04	36	89.35	8.14
	F	12	237.54	26.19	11	69.18	5.46	11	83.36	7.16
	M	15	251.03	29.11	15	77.17	6.91	15	92.37	6.29
Ugandan	M	26	265.17	18.49	26	74.67	5.14	26	93.50	6.83
Archaeological										
Khoe-San	B	71	229.01	21.13	72	66.90	5.76	73	82.71	7.95
Sudanese	B	55	251.44	20.66	78	70.20	6.36	78	86.92	8.89
Taforalt	B	20	236.43	52.69	23	75.57	5.58	24	94.69	8.85
Fossil										
EUP	B	5	272.20	15.49	8	86.44	6.57	7	108.14	12.07
MSA	B	3	256.50	44.21	6	82.17	5.81	4	99.25	12.82